

**INVESTIGATION OF THE SIMULTANEOUS UREA
HYDROLYSIS AND DENITRIFICATION ACTIVITY OF
BIOGRANULES UNDER VARIOUS ENVIRONMENTAL
CONDITIONS AND THEIR COMPARISON WITH THE
INHERENTLY PRESENT PURE CULTURES**

**BİYOGRANÜLLERİN SİMÜLTANE ÜRE HİDROLİZİ VE
DENİTRİFİKASYON AKTİVİTELERİNİN FARKLI
ORTAM KOŞULLARINDA İNCELENMESİ VE
İÇERİĞİNDEKİ SAF KÜLTÜRLERLE KIYASLANMASI**

MEVLÜT SOLUK

ASSOC. PROF. DR. YUSUF ÇAĞATAY ERŞAN

Supervisor

Submitted to

Graduate School of Science and Engineering of Hacettepe University

as a Partial Fulfillment to the Requirements

for the Award of the Degree of Master of Science

in Environmental Engineering

June 2024

To My Dear Family and My Eternal and Inspirational Love...

ABSTRACT

INVESTIGATION OF THE SIMULTANEOUS UREA HYDROLYSIS AND DENITRIFICATION ACTIVITY OF BIOGRANULES UNDER VARIOUS ENVIRONMENTAL CONDITIONS AND THEIR COMPARISON WITH THE INHERENTLY PRESENT PURE CULTURES

Mevlüt SOLUK

Master of Science, Department of Environmental Engineering

Supervisor: Assoc. Prof. Dr. Yusuf Çağatay ERŞAN

June 2024, 225 pages

In microbially induced calcium carbonate precipitation (MICP) related studies, urea hydrolysis and denitrification metabolisms have been prevalently investigated. Furthermore, studies were mostly conducted by using axenic cultures, and biomineralization performances were determined only through a single metabolic pathway. Several constraints were detected in MICP applications due to the limits of the exploited metabolic pathway and the axenic cultures. Recently, researchers presented a way to overcome the reported limitations in MICP applications by combining the aforementioned metabolic pathways in non-axenic granulated cultures. Yet, MICP performance of these non-axenic granulated cultures and their advantages over axenic cultures under different environmental conditions still remain unknown. Therefore, the objective of this thesis study was to investigate granular cultures, capable of conducting

simultaneous urea hydrolysis and nitrate reduction, under various environmental conditions and compare its biomineralization performance with the axenic cultures. Biogranules were compared with ureolytic *Sporosarcina pasteurii* DSM 33 and denitrifying *Pseudomonas aeruginosa* as well as with the axenic cultures isolated from the biogranules. The study compared how MICP performance of axenic and non-axenic cultures depended on changes in the following parameters: (i) yeast extract concentration (0.05-5.00 g.L⁻¹), (ii) dehydration stress (wet/dry), (iii) salinity (35 g.L⁻¹, 1 g.L⁻¹ and 0.02 g.L⁻¹ NaCl), (iv) temperature (10°C, 22°C, 45°C), and (v) dissolved oxygen concentration (<0.2 mg.L⁻¹, 1.3 mg.L⁻¹, 4.8 mg.L⁻¹). Results indicated that wet biogranules had higher biomineralization performance than axenic cultures in all tests. Biogranules' MICP performance appeared to be less dependent on the presence of yeast extract, and biogranules could be dried and resuscitated without any problem. Wet biogranules and *S. pasteurii* totally precipitated dissolved calcium as CaCO₃ (0.65 g CaCO₃) in the environment under three different oxygenic conditions and three different temperatures. Moreover, wet biogranules and *S. pasteurii* totally precipitated dissolved calcium as CaCO₃ (0.65 g CaCO₃) in the environment under fresh water and rainwater conditions except for marine water conditions. In marine water conditions, wet biogranules were superior to *S. pasteurii* in terms of biomineralization performance. Wet biogranules precipitated 0.62±0.01 g CaCO₃, while *S. pasteurii* precipitated 0.57±0.03 g CaCO₃.

According to these results, it was revealed that wet biogranules could simply adapt to changes in environmental conditions. Dried biogranules could resuscitate under all tested conditions and induced calcium carbonate precipitation. Consequently, this thesis study revealed that the non-axenic biogranules capable of urea hydrolysis and denitrification were superior to axenic cultures for MICP applications, and they were more resilient to the changes in environmental conditions making them more suitable for MICP applications.

Keywords: biomineralization, dissolved oxygen, MICP, *Pseudomonas aeruginosa*, salinity, *Sporosarcina pasteurii*, temperature, yeast extract

ÖZET

BİYOGRANÜLLERİN SİMÜLTANE ÜRE HİDROLİZİ VE DENİTRİFİKASYON AKTİVİTELERİNİN FARKLI ORTAM KOŞULLARINDA İNCELENMESİ VE İÇERİĞİNDEKİ SAF KÜLTÜRLERLE KIYASLANMASI

Mevlüt SOLUK

Yüksek Lisans, Çevre Mühendisliği Bölümü

Tez Danışmanı: Doç. Dr. Yusuf Çağatay ERŞAN

Haziran 2024, 225 sayfa

Mikrobiyal olarak indüklenen kalsiyum karbonat çökmesi (MICP) ile ilgili çalışmalarda üre hidrolizi ve nitrat indirgenmesi metabolizmaları yaygın olarak araştırılmaktadır. Ayrıca çalışmalar çoğunlukla aksenik kültürlerle yürütülmüş olup biyomineralizasyon performansları yalnızca tek bir metabolik yol üzerinden belirlenmiştir. Kullanılan metabolik yolun ve aksenik kültürlerin sınırları nedeniyle MICP uygulamalarında çeşitli kısıtlar tespit edilmiştir. Son zamanlarda, araştırmacılar, bu kısıtların bahsi geçen metabolik yolların aksenik olmayan granüle kültürlerde birleştirilmesi ile aşılabileceğini göstermiştir. Ancak, bu aksenik olmayan granüle kültürlerin farklı çevresel koşullar altında MICP performansı ve aksenik kültürlerle kıyasla avantajları hala bilinmemektedir. Bu nedenle, bu tez çalışmasının amacı eş zamanlı üre hidrolizi ve nitrat indirgenmesi yapabilen granüle kültürlerin farklı çevresel koşullarda incelenmesi ve aksenik kültürlerle

biyomineralizasyon performansının kıyaslanması olmuştur. Biyogranüller, ürolitik *Sporosarcina pasteurii* DSM 33, denitrifikasyon yapan *Pseudomonas aeruginosa* ve aynı zamanda biyogranüllerden izole edilen aksenik kültürlerle kıyaslanmıştır. Bu çalışmada, aksenik ve aksenik olmayan kültürlerin biyomineralizasyon performansının şu koşullara bağlı olarak nasıl değiştiği kıyaslanmıştır: (i) maya özütü konsantrasyonu (0.05-5 g.L⁻¹), (ii) dehidrasyon stresi (ıslak/kuru), (iii) tuzluluk (35 g.L⁻¹, 1 g.L⁻¹ ve 0.02 g.L⁻¹ NaCl), (iv) sıcaklık (10°C, 22°C, 45°C) ve (v) çözülmüş oksijen konsantrasyonu (<0.2 mg.L⁻¹, 1.3 mg.L⁻¹, 4.8 mg.L⁻¹). Sonuçlar ıslak biyogranüllerin tüm testlerde aksenik kültürlerden daha yüksek biyomineralizasyon performansına sahip olduğunu göstermiştir. Biyogranüllerin biyomineralizasyon performansının maya özütü varlığına daha az bağımlı olduğu ve biyogranüllerin herhangi bir problem olmadan kurutulabildiği ve yeniden canlandırılabilirdiği ortaya çıkmıştır. Islak biyogranüller ve *S. pasteurii* üç farklı oksijenik koşulda ve üç farklı sıcaklıkta ortamdaki çözülmüş kalsiyumu tamamen CaCO₃ olarak çöktürmüştür (0.65 g CaCO₃). Buna ek olarak, ıslak biyogranüller ve *S. pasteurii*, deniz suyu koşulu hariç tatlı su ve yağmur suyu koşullarında ortamdaki çözülmüş kalsiyumu tamamen CaCO₃ olarak çöktürmüştür (0.65 g CaCO₃). Islak biyogranüller, biyomineralizasyon performansı açısından deniz suyu koşulunda *S. pasteurii*'ye üstünlük sağlamıştır. Islak biyogranüller 0.62±0.01 g CaCO₃ çöktürürken, *S. pasteurii* 0.57±0.03 g CaCO₃ çöktürmüştür.

Bu sonuçlara göre ıslak biyogranüllerin çevresel koşullardaki değişimlere kolayca uyum sağlayabildiği ortaya çıkarılmıştır. Kurutulan biyogranüller ise tüm ortam koşullarında yeniden canlanabilmiş ve kalsiyum karbonat çökmesini tetiklemiştir. Sonuç olarak, bu tez çalışması, üre hidrolizi ve denitrifikasyon yapabilen aksenik olmayan biyogranüllerin MICP uygulamaları için aksenik kültürlerle üstünlük sağladığını ve biyogranüllerin MICP uygulamalarına daha elverişli hale getiren çevresel koşullardaki değişimlere karşı daha dirençli olduğunu ortaya çıkarmıştır.

Anahtar kelimeler: biyomineralizasyon, çözülmüş oksijen, maya özütü, MICP, *Pseudomonas aeruginosa*, *Sporosarcina pasteurii*, sıcaklık, tuzluluk

ACKNOWLEDGEMENTS

I am thankful that this thesis allows me to express gratitude the many incredible people who supported and encouraged me during preparation of this master's thesis.

First of all, I would like to deeply express gratitude to my thesis supervisor Assoc. Prof. Dr. Yusuf Çağatay ERŞAN who supported me always with his valuable ideas and comments, respectable contributions, motivational and patient attitude under all circumstances during my thesis study. He also allowed me to increase my desires and ambitions for research. Thanks to his valuable knowledge, he always enabled me to look at my studies and research from different perspectives. Thank you for everything.

My master's thesis was supported by The Scientific and Technological Research Council of Türkiye (TÜBİTAK) under the project no 120Y291. I would like to express my gratitude to TÜBİTAK for allowing me to perform my studies as a project assistant.

I would like to express gratitude to the master's thesis committee members Prof. Dr. Ayşenur UĞURLU, Prof. Dr. Selim SANİN, Prof. Dr. Merih AYDINALP KÖKSAL, Assoc. Prof. Dr. Yasemin Dilşad YILMAZEL TOKEL for their respectable and beneficial contributions and comments.

I would like to also thank Assoc. Prof. Dr. Zeynep BAŞARAN BUNDUR and Assoc. Prof. Dr. Yusuf Doruk ARACAGÖK for their support to provide axenic cultures used in this study.

I would like to also thank to Beyza KARDOĞAN for her supportive attitude and friendship, and assistance to me for laboratory studies. In addition, I would like to thank to Lab-Mine team members with whom we had an enjoyable time.

I would like to express warmest gratitude to my family for their unrequited support, patience, encouragement under any circumstances. They were forever by my side.

I would also like to express my deepest gratitude to my beloved wife, Berfin BOĞAZKAYA SOLUK, who has been with me my whole life and supported me under all circumstances. She always motivated and encouraged me in good times and bad times.

TABLE OF CONTENTS

ABSTRACT	i
ÖZET.....	iii
ACKNOWLEDGEMENTS	v
TABLE OF CONTENTS	vi
LIST OF TABLES	x
LIST OF FIGURES.....	xii
SYMBOLS AND ABBREVIATIONS	xviii
1. INTRODUCTION.....	1
2. LITERATURE REVIEW	4
2.1. Biomineralization	4
2.2. Microbial-Induced Calcium Carbonate (CaCO ₃) Precipitation (MICP)	6
2.3. Metabolic Pathways Employed in MICP Applications.....	7
2.4. MICP Applications.....	10
2.4.1. Merits and Demerits of Metabolic Pathways Employed in MICP Applications	11
2.4.2. Urea Hydrolysis and Ureolytic Bacteria in MICP Applications.....	13
2.4.3. Denitrification (Complete Nitrate Reduction) and Denitrifiers in MICP Applications	19
2.5. Axenic and Non-Axenic Cultures Used in MICP	23
2.5.1. Axenic Cultures (Pure Cultures) and Their Drawbacks	23
2.5.2. Non-Axenic Cultures (Mixed Cultures).....	25
2.5.2.1. Biogranulation and Biogranules.....	28
2.6. Selecting An Appropriate MICP Approach According to The Required or Target Conditions.....	30
2.7. Parameters Affecting Efficiency of MICP and Its Applications	33
2.7.1. Microbial Species and Microbial Biomass Concentration.....	33
2.7.2. Enzymatic Activity of MICP Mediated Bacteria.....	34

2.7.3.	Ambient Temperature and Salinity.....	34
2.7.4.	pH.....	35
2.7.5.	Influence of Available Ca ²⁺ Source.....	36
2.8.	The Scope and Goal of The Thesis Study.....	36
3.	MATERIALS AND METHODS.....	39
3.1.	Operation Details of The SBR Reactor Produced Biogranules	39
3.2.	Effect of Yeast Extract (YE) on Bacterial Growth, Dehydration, and Resuscitation of Biogranules	41
3.3.	Isolation of Inherently Present Bacteria from Biogranules.....	43
3.4.	Selection of Appropriate Strains Showing Decent Microbial Activity (Urea Hydrolysis and Nitrate Reduction)	44
3.5.	Determination of 16S rRNA Gene Sequencing for Isolates	45
3.6.	Cultivation of Reference Ureolytic Strain (<i>Sporosarcina pasteurii</i> DSM 33) ...	46
3.7.	Cultivation of Reference Nitrate Reducing Strain (<i>Pseudomonas aeruginosa</i>). 46	
3.8.	Growth Curve Experiments for Isolates (WB1, WC2X, YB1, YC2), <i>Sporosarcina pasteurii</i> , and <i>Pseudomonas aeruginosa</i>	47
3.9.	Preparation of Experimental Setup for Calcium Carbonate Precipitation Test Under Various Environmental Conditions.....	48
3.9.1.	Oxygen	50
3.9.1.1.	Assessment of Growth and Microbial Activity of <i>S. pasteurii</i> Under Anoxic Conditions.....	51
3.9.2.	Temperature.....	52
3.9.3.	Salinity.....	53
3.10.	Analytical and Experimental Methods	53
3.10.1.	TAN Measurement	53
3.10.2.	NO ₃ -N and NO ₂ -N Measurements	54
3.10.3.	TSS and VSS Measurement	54
3.10.4.	Ca ²⁺ Measurement	54
3.10.5.	CaCO ₃ Measurement	55
3.10.6.	Dissolved Oxygen (DO) and pH Measurements	56
4.	RESULTS AND DISCUSSION	57
4.1.	Effect of Yeast Extract (YE) on Bacterial Growth onto Solid Medium	57

4.2. Testing Biogranules for Their Resistance to Drying and The Resuscitation Performance of Inherently Present Bacteria.....	58
4.3. Isolation of Pure Cultures and Their Selection Based on Microbial Performance	61
4.3.1. The First Phase of The Isolation Process	61
4.3.2. The Second Phase of The Isolation Process	62
4.3.3. The Third Phase of The Isolation Process	64
4.3.4. The Fourth Phase of The Isolation Process.....	65
4.4. Determination of 16S rRNA Gene Sequencing for Axenic Strains (Isolates)	66
4.5. Microbial Growth Characteristics of Isolated Cultures.....	68
4.6. Assessment of Ureolytic Reference Strain (<i>Sporosarcina pasteurii</i> DSM 33)...	70
4.7. Nitrate-Reducing Axenic Strain (<i>Pseudomonas aeruginosa</i>)	73
4.8. Calcium Carbonate Precipitation with Biogranules and Axenic Cultures at Different Dissolved Oxygen (DO) Concentrations	75
4.8.1. Comparison of Urea Hydrolysis Activities at Different DO Concentrations	76
4.8.2. Nitrate Reduction Activities at Different DO Concentrations	85
4.8.3. Changes in Dissolved Ca ²⁺ Concentration at Different DO Concentrations	94
4.8.4. Comparison of CaCO ₃ Precipitation Activities at Different DO Concentrations	98
4.9. Calcium Carbonate Precipitation with Biogranules and Axenic Cultures at Different Ambient Temperature	103
4.9.1. Comparison of Urea Hydrolysis Activities at Different Ambient Temperatures.....	104
4.9.2. Nitrate Reduction Activities at Different Ambient Temperatures	110
4.9.3. Changes in Dissolved Ca ²⁺ Concentration at Different Ambient Temperatures.....	121
4.9.4. Comparison of CaCO ₃ Precipitation Activities at Different Ambient Temperatures.....	123
4.10. Calcium Carbonate Precipitation with Biogranules and Axenic Cultures at Different Salt Concentrations	129

4.10.1. Comparison of Urea Hydrolysis Activities at Different Salt Concentrations	130
4.10.2. Nitrate Reduction Activities at Different Salt Concentrations	135
4.10.3. Changes in Dissolved Ca ²⁺ Concentration at Different Salt Concentrations	145
4.10.4. Comparison of CaCO ₃ Precipitation Activities at Different Salt Concentrations	148
4.11. Analysis and Comparison of Microbial Activities of Biogranules and Axenic Cultures Under Varying Environmental Conditions	153
5. CONCLUSION	156
6. REFERENCES	159
APPENDIX	189
ANNEX 1 – Publications Derived from The Thesis (Conference Paper)	189
ANNEX 2 – Thesis Originality Report	190
CURRICULUM VITAE	191

LIST OF TABLES

Table 2-1. Metabolic pathways in MICP (redrafted after [63])	8
Table 2-2. Different types of bacteria used in different MICP applications	10
Table 2-3. Metabolic by-products and drawbacks of various metabolic pathways employed in MICP applications (redrafted after [29]).....	12
Table 3-1. The composition of the nutrient solution used for biogranules cultivation in the SBR	39
Table 3-2. Summary of operational parameters of biogranule production reactor	40
Table 3-3. The chemical ingredients of the solid-nutrient medium containing powder agar	42
Table 3-4. Composition of the biomineralization solution for tests under various environmental conditions	50
Table 4-1. TAN measurement of samples obtained in the second phase.....	63
Table 4-2. TAN measurement results of isolates obtained after the third phase	65
Table 4-3. Potential species of isolates according to 16s rRNA gene analysis.....	66
Table 4-4. Specific urea hydrolysis activity at different DO concentrations	84
Table 4-5. Specific NO ₃ -N reducing, NO ₂ -N accumulation, and denitrification activity at aerobic conditions	88
Table 4-6. Specific NO ₃ -N reducing, NO ₂ -N accumulation, and denitrification activity at microaerobic condition.....	91
Table 4-7. Specific NO ₃ -N reducing, NO ₂ -N accumulation, and denitrification activity at anoxic condition	94
Table 4-8. Specific CaCO ₃ precipitation at different DO concentrations	101
Table 4-9. Comparison of the amount of precipitated CaCO ₃ and the precipitated dissolved calcium concentration at different DO concentrations.....	102
Table 4-10. Specific urea hydrolysis activity at different temperatures	109
Table 4-11. Specific NO ₃ -N reducing, NO ₂ -N accumulation, and denitrification activity at 10°C.....	113
Table 4-12. Specific NO ₃ -N reducing, NO ₂ -N accumulation, and denitrification activity at 22°C.....	116
Table 4-13. Specific NO ₃ -N reducing, NO ₂ -N accumulation, and denitrification activity at 45°C.....	120

Table 4-14. Specific CaCO ₃ precipitation at different ambient temperature.....	126
Table 4-15. Comparison of the amount of precipitated CaCO ₃ and the precipitated dissolved calcium concentration at different ambient temperatures.....	128
Table 4-16. Specific urea hydrolysis activity at different salinity concentrations (marine water (35 g.L ⁻¹ NaCl), drinking water, urban runoff, groundwater (1 g.L ⁻¹ NaCl), rainwater (0.02 g.L ⁻¹ NaCl).....	134
Table 4-17. Specific NO ₃ -N reducing, NO ₂ -N accumulation, and denitrification activity at marine water condition	138
Table 4-18. Specific NO ₃ -N reducing, NO ₂ -N accumulation, and denitrification activity at 1 g.L ⁻¹ NaCl condition	141
Table 4-19. Specific NO ₃ -N reducing, NO ₂ -N accumulation, and denitrification activity at rainwater condition	145
Table 4-20. Specific CaCO ₃ precipitation at different salt concentrations.....	151
Table 4-21. Comparison of the amount of precipitated CaCO ₃ and the precipitated dissolved calcium concentration at different salt concentrations	152

LIST OF FIGURES

Figure 2-1. Schematic representation of urea hydrolysis by ureolytic bacteria (redrafted after [79]).....	14
Figure 2-2. Schematic representation of denitrification mechanism (redrafted after [63])	20
Figure 2-3. Various biogranules utilized in wastewater treatment and recovery of resources; (a) methanogenic biogranules, (b) hydrogenic biogranules, (c) aerobic biogranules, (d) ammonium oxidizing biogranules, (e) aerobic biogranules (replicated from [189])	29
Figure 2-4. Selecting an appropriate MICP approach according to the required or target conditions (redrafted after [14])	32
Figure 3-1. Representative micrographs of biogranules used in this thesis study	41
Figure 3-2. <i>Sporosarcina pasteurii</i> (DSM 33) (ureolytic axenic strain) colonies on agar medium.....	46
Figure 3-3. <i>Pseudomonas aeruginosa</i> (nitrate-reducing axenic strain) colonies on agar medium.....	47
Figure 3-4. Batches in biomineralization test under different dissolved oxygen concentrations, (a) aerobic, (b) microaerobic, (c) anoxic	51
Figure 3-5. <i>S. pasteurii</i> growth and tested under anoxic conditions	52
Figure 3-6. Calibration curve of standard calcium solutions	55
Figure 3-7. The schematic representation of CO ₂ volume exchange method [166]	56
Figure 4-1. Bacterial growth of 0.2 ml biogranule in different solid medium for 11 days (a) solid medium no containing YE, (b) solid medium containing YE.....	58
Figure 4-2. Change in the growth of biogranules dried at 60°C on agar solid medium in the absence of YE (a) 1 st day, (b) at the end of the 11 th day	59
Figure 4-3. Change in the growth of biogranules dried at 60°C on agar solid medium in the presence of YE (a) 1 st day, (b) at the end of the 11 th day	59
Figure 4-4. Bacterial growth on the solid medium at the end of the 11 th day; (a) in the absence of YE, (b) in the presence of YE	60
Figure 4-5. Dried biogranules into small pieces and growing them in solid medium containing or without YE	62
Figure 4-6. Samples transferred and grown in (a) 0.1 L and (b) 1 L	62

Figure 4-7. Grown in the first phase (a) W1, (b) Y1, (c) Different colonies formed by Y2 cultures on solid medium.....	63
Figure 4-8. Isolates (axenic cultures) obtained from biogranules at the end of the third phase	64
Figure 4-9. Dominant species resuscitated from dried biogranules.....	68
Figure 4-10. Growth related turbidity change during cultivation of axenic cultures; (a) t=0 h; (b) t=48 h	69
Figure 4-11. Growth curves of isolated strains in a minimal nutrient solution enriched with 5 g.L ⁻¹ YE	70
Figure 4-12. First and last hour images of the growth curve experiment performed at different YE concentrations (0.05 g.L ⁻¹ , 0.5 g.L ⁻¹ , 5 g.L ⁻¹)	71
Figure 4-13. Growth curves for <i>S pasteurii</i> (DSM 33) at different YE concentrations (0.05 g.L ⁻¹ , 0.5 g.L ⁻¹ , 5 g.L ⁻¹)	72
Figure 4-14. Urea hydrolysis of <i>S pasteurii</i> (DSM 33) at different YE concentrations (0.05 g.L ⁻¹ , 0.5 g.L ⁻¹ , 5 g.L ⁻¹)	73
Figure 4-15. First and last hour images of the growth curve experiment for <i>P. aeruginosa</i> performed at different YE concentrations (0.05 g.L ⁻¹ , 0.5 g.L ⁻¹ , 5 g.L ⁻¹).....	74
Figure 4-16. Growth curves for <i>Pseudomonas aeruginosa</i> at different YE concentrations (0.05 g.L ⁻¹ , 0.5 g.L ⁻¹ , 5 g.L ⁻¹).....	75
Figure 4-17. pH values at different DO concentrations; (a, b) aerobic, (c, d) microaerobic, (e, f) anoxic	76
Figure 4-18. Urea hydrolysis results of wet and dried biogranules, and <i>S. pasteurii</i> in biomineralization medium with 0.05 g.L ⁻¹ YE and 4.8 mg.L ⁻¹ DO concentration (aerobic conditions); (a) TAN results, (b) hydrolyzed urea.....	77
Figure 4-19. Urea hydrolysis activities of axenic strains (WB1, YB1, YC2) in biomineralization medium with 0.05 g.L ⁻¹ YE and 4.8 mg.L ⁻¹ DO concentration (aerobic conditions); (a) TAN results, (b) hydrolyzed urea.....	78
Figure 4-20. Urea hydrolysis results of wet and dried biogranules, and <i>S. pasteurii</i> in biomineralization medium with 0.05 g.L ⁻¹ YE and 1.3 mg.L ⁻¹ DO concentration (microaerobic conditions); (a) TAN results, (b) hydrolyzed urea	79
Figure 4-21. Urea hydrolysis activities of axenic strains (WB1, YB1, YC2) in biomineralization medium with 0.05 g.L ⁻¹ YE and 1.3 mg.L ⁻¹ DO concentration (microaerobic conditions); (a) TAN results, (b) hydrolyzed urea	80

Figure 4-22. Urea hydrolysis results of wet and dried biogranules, and <i>S. pasteurii</i> in biomineralization medium with 0.05 g.L ⁻¹ YE and <0.2 mg.L ⁻¹ DO concentration (anoxic conditions); (a) TAN results, (b) hydrolyzed urea	80
Figure 4-23. Urea hydrolysis activities of axenic strains (WB1, YB1, YC2) in biomineralization medium with 0.05 g.L ⁻¹ YE and <0.2 mg.L ⁻¹ DO concentration (anoxic conditions); (a) TAN results, (b) hydrolyzed urea	81
Figure 4-24. Nitrate reduction and nitrite measurements under aerobic condition, (a) wet biogranules, (b) dried biogranules, (c) <i>S. pasteurii</i> , (d) <i>P. aeruginosa</i>	86
Figure 4-25. Nitrate reduction and nitrite measurements under aerobic condition, (a) WB1, (b) WC2X, (c) YB1, (d) YC2	87
Figure 4-26. Nitrate reduction and nitrite measurements under microaerobic condition, (a) wet biogranules, (b) dried biogranules, (c) <i>S. pasteurii</i> , (d) <i>P. aeruginosa</i>	89
Figure 4-27. Nitrate reduction and nitrite measurements under microaerobic condition, (a) WB1, (b) WC2X, (c) YB1, (d) YC2.....	90
Figure 4-28. Nitrate reduction and nitrite measurements under anoxic condition, (a) wet biogranules, (b) dried biogranules, (c) <i>S. pasteurii</i> , (d) <i>P. aeruginosa</i>	92
Figure 4-29. Nitrate reduction and nitrite measurements under anoxic condition, (a) WB1, (b) WC2X, (c) YB1, (d) YC2.....	93
Figure 4-30. Dissolved calcium concentration results at the end of the second and sixth days under aerobic condition; (a) biogranules, <i>S. pasteurii</i> , and <i>P. aeruginosa</i> , (b) isolates.....	95
Figure 4-31. Dissolved calcium concentration results at the end of the second and sixth days under microaerobic condition; (a) biogranules, <i>S. pasteurii</i> , and <i>P. aeruginosa</i> , (b) isolates	96
Figure 4-32. Dissolved calcium concentration results at the end of the second and sixth days under anoxic conditions; (a) biogranules, <i>S. pasteurii</i> , and <i>P. aeruginosa</i> , (b) isolates.....	97
Figure 4-33. CaCO ₃ precipitation under aerobic conditions; (a) biogranules, <i>S. pasteurii</i> , and <i>P. aeruginosa</i> , (b) isolates	98
Figure 4-34. CaCO ₃ precipitation under microaerobic conditions; (a) biogranules, <i>S. pasteurii</i> , and <i>P. aeruginosa</i> , (b) isolates.....	99
Figure 4-35. CaCO ₃ precipitation under anoxic conditions; (a) biogranules, <i>S. pasteurii</i> , and <i>P. aeruginosa</i> , (b) isolates	99

Figure 4-36. pH values at different temperatures; (a, b) 10°C, (c, d) 22°C, (e, f) 45°C	104
Figure 4-37. Urea hydrolysis results of wet and dried biogranules, and <i>S. pasteurii</i> in biomineralization medium with 0.05 g.L ⁻¹ YE and at 10°C; (a) TAN results, (b) hydrolyzed urea.....	105
Figure 4-38. Urea hydrolysis results of axenic strains (WB1, YB1, YC2) in biomineralization medium with 0.05 g.L ⁻¹ YE and at 10°C; (a) TAN results, (b) hydrolyzed urea.....	105
Figure 4-39. Urea hydrolysis results of wet and dried biogranules, and <i>S. pasteurii</i> in biomineralization medium with 0.05 g.L ⁻¹ YE and at 22°C; (a) TAN results, (b) hydrolyzed urea.....	106
Figure 4-40. Urea hydrolysis results of axenic strains (WB1, YB1, YC2) in biomineralization medium with 0.05 g.L ⁻¹ YE and at 22°C; (a) TAN results, (b) hydrolyzed urea.....	106
Figure 4-41. Urea hydrolysis results of wet and dried biogranules, and <i>S. pasteurii</i> in biomineralization medium with 0.05 g.L ⁻¹ YE and at 45°C; (a) TAN results, (b) hydrolyzed urea.....	108
Figure 4-42. Urea hydrolysis results of axenic strains (WB1, YB1, YC2) in biomineralization medium with 0.05 g.L ⁻¹ YE and at 45°C; (a) TAN results, (b) hydrolyzed urea.....	108
Figure 4-43. Nitrate reduction and nitrite measurements at 10°C, (a) wet biogranules, (b) dried biogranules, (c) <i>S. pasteurii</i> , (d) <i>P. aeruginosa</i>	111
Figure 4-44. Nitrate reduction and nitrite measurements at 10°C, (a) WB1, (b) WC2X, (c) YB1, (d) YC2.....	112
Figure 4-45. Nitrate reduction and nitrite measurements at 22°C, (a) wet biogranules, (b) dried biogranules, (c) <i>S. pasteurii</i> , (d) <i>P. aeruginosa</i>	114
Figure 4-46. Nitrate reduction and nitrite measurements at 22°C, (a) WB1, (b) WC2X, (c) YB1, (d) YC2.....	115
Figure 4-47. Nitrate reduction and nitrite measurements at 45°C, (a) wet biogranules, (b) dried biogranules, (c) <i>S. pasteurii</i> , (d) <i>P. aeruginosa</i>	118
Figure 4-48. Nitrate reduction and nitrite measurements at 45°C, (a) WB1, (b) WC2X, (c) YB1, (d) YC2.....	119
Figure 4-49. Dissolved calcium concentration results at the end of the second and sixth days at 10°C; (a) biogranules, <i>S. pasteurii</i> , and <i>P. aeruginosa</i> , (b) isolates.....	121

Figure 4-50. Dissolved calcium concentration results at the end of the second and sixth days at 22°C; (a) biogranules, <i>S. pasteurii</i> , and <i>P. aeruginosa</i> , (b) isolates	122
Figure 4-51. Dissolved calcium concentration results at the end of the second and sixth days at 45°C; (a) biogranules, <i>S. pasteurii</i> , and <i>P. aeruginosa</i> , (b) isolates	123
Figure 4-52. CaCO ₃ precipitation at 10°C; (a) biogranules, <i>S. pasteurii</i> , and <i>P. aeruginosa</i> , (b) isolates	124
Figure 4-53. CaCO ₃ precipitation at 22°C; (a) biogranules, <i>S. pasteurii</i> , and <i>P. aeruginosa</i> , (b) isolates	124
Figure 4-54. CaCO ₃ precipitation at 45°C; (a) biogranules, <i>S. pasteurii</i> , and <i>P. aeruginosa</i> , (b) isolates	124
Figure 4-55. pH values at different salinity conditions; (a, b) marine water conditions, (c, d) 1 g.L ⁻¹ NaCl, (e, f) rainwater conditions	129
Figure 4-56. Urea hydrolysis activities of wet and dried biogranules and <i>S. pasteurii</i> in biomineralization medium with 0.05 g.L ⁻¹ YE and 35 g.L ⁻¹ NaCl concentration (marine water conditions); (a) TAN results, (b) hydrolyzed urea.....	130
Figure 4-57. Urea hydrolysis activities of axenic strains (WB1, YB1, YC2) in biomineralization medium with 0.05 g.L ⁻¹ YE and 35 g.L ⁻¹ NaCl concentration (marine water conditions); (a) TAN results, (b) hydrolyzed urea.....	131
Figure 4-58. Urea hydrolysis activities of wet and dried biogranules and <i>S. pasteurii</i> in biomineralization medium with 0.05 g.L ⁻¹ YE and 1 g.L ⁻¹ NaCl concentration (tap water, urban runoff); (a) TAN results, (b) hydrolyzed urea.....	131
Figure 4-59. Urea hydrolysis activities of axenic strains (WB1, YB1, YC2) in biomineralization medium with 0.05 g.L ⁻¹ YE and 1 g.L ⁻¹ NaCl concentration (tap water, urban runoff conditions); (a) TAN results, (b) hydrolyzed urea	132
Figure 4-60. Urea hydrolysis activities of wet and dried biogranules and <i>S. pasteurii</i> in biomineralization medium with 0.05 g.L ⁻¹ YE and 0.02 g.L ⁻¹ NaCl concentration (rainwater conditions); (a) TAN results, (b) hydrolyzed urea.....	132
Figure 4-61. Urea hydrolysis activities of axenic strains (WB1, YB1, YC2) in biomineralization medium with 0.05 g.L ⁻¹ YE and 0.02 g.L ⁻¹ NaCl concentration (rainwater conditions); (a) TAN results, (b) hydrolyzed urea.....	133
Figure 4-62. Nitrate reduction and nitrite measurements at marine water, (a) wet biogranules, (b) dried biogranules, (c) <i>S. pasteurii</i> , (d) <i>P. aeruginosa</i>	136

Figure 4-63. Nitrate reduction and nitrite measurements at marine water, (a) WB1, (b) WC2X, (c) YB1, (d) YC2.....	137
Figure 4-64. Nitrate reduction and nitrite measurements at 1 g.L ⁻¹ NaCl, (a) wet biogranules, (b) dried biogranules, (c) <i>S. pasteurii</i> , (d) <i>P. aeruginosa</i>	139
Figure 4-65. Nitrate reduction and nitrite measurements at 1 g.L ⁻¹ NaCl, (a) WB1, (b) WC2X, (c) YB1, (d) YC2.....	140
Figure 4-66. Nitrate reduction and nitrite measurements at rainwater, (a) wet biogranules, (b) dried biogranules, (c) <i>S. pasteurii</i> , (d) <i>P. aeruginosa</i>	143
Figure 4-67. Nitrate reduction and nitrite measurements at rainwater, (a) WB1, (b) WC2X, (c) YB1, (d) YC2.....	144
Figure 4-68. Dissolved calcium concentration results at the end of the second and sixth days under marine water condition; (a) biogranules, <i>S. pasteurii</i> , and <i>P. aeruginosa</i> , (b) isolates.....	146
Figure 4-69. Dissolved calcium concentration results at the end of the second and sixth days at 1 g.L ⁻¹ NaCl; (a) biogranules, <i>S. pasteurii</i> , and <i>P. aeruginosa</i> , (b) isolates	147
Figure 4-70. Dissolved calcium concentration results at the end of the second and sixth days under rainwater condition; (a) biogranules, <i>S. pasteurii</i> , and <i>P. aeruginosa</i> , (b) isolates	148
Figure 4-71. CaCO ₃ Precipitation at 35 g.L ⁻¹ NaCl (marine water conditions); (a) biogranules, <i>S. pasteurii</i> , and <i>P. aeruginosa</i> , (b) isolates.....	149
Figure 4-72. CaCO ₃ precipitation at 1 g.L ⁻¹ NaCl (tap water/groundwater condition); (a) biogranules, <i>S. pasteurii</i> , and <i>P. aeruginosa</i> , (b) isolates.....	149
Figure 4-73. CaCO ₃ precipitation at 0.02 g.L ⁻¹ NaCl (rainwater condition); (a) biogranules, <i>S. pasteurii</i> , and <i>P. aeruginosa</i> , (b) isolates.....	149
Figure 4-74. Comparison of urea hydrolysis of biogranules and axenic cultures under varying environmental conditions	154
Figure 4-75. Comparison of denitrification rate of biogranules and axenic cultures under varying environmental conditions	155

SYMBOLS AND ABBREVIATIONS

AAS	Atomic absorption spectrometer
ACDC	Active compact denitrifying core
BCM	Biologically controlled mineralization
BIM	Biologically induced mineralization
CA	Carbonic anhydrase
CDW	Cell dry weight
CERUP	Cyclic enriched ureolytic powder
CFU	Colony forming unit
CO ₂	Carbon dioxide
DO	Dissolved oxygen
EPS	Extracellular polymeric substances
H ₂ CO ₃	Carbonic acid
HCO ₃ ⁻	Bicarbonates
MICP	Microbial induced calcium carbonate precipitation
NCBI	National Center for Biotechnology Information
NH ₃ ⁺	Ammonia
NH ₄ ⁺	Ammonium
NO ₂ ⁻	Nitrite
NO ₂ -N	Nitrite nitrogen
NO ₃ ⁻	Nitrate
NO ₃ -N	Nitrate nitrogen
NO _x -N	Nitrate and nitrite nitrogen
OD	Optical density
ppm	Parts per million

rpm	Revolution rate per minute
rRNA	Ribosomal RNA
SBR	Sequencing batch reactor
SE	Soybean extract
SiO _x	Silicates
SO ₄ ²⁻	Sulfate
SRB	Sulfate-reducing bacteria
TAN	Total ammonium nitrogen
TSS	Total suspended solids
VSS	Volatile suspended solids
YE	Yeast extract

1. INTRODUCTION

At the beginning of the 21st century, revolution of traditional or fossil economy to green economy has been gaining significance to cope with climate change impacts and reduce anthropogenic carbon emissions. Moreover, concerns about climate change impacts and global environmental issues and their negative effects on ecosystems have also accelerated a transition to sustainable and eco-friendly economy [1,2], because reliance on fossil-based economy is not a sustainable way in the long term. In recent years, the transition from fossil economy to bioeconomy has become inevitable because of increase in carbon emissions and climate change impacts [3].

In order to accelerate and contribute to transition to bioeconomy, a number of legal frameworks and strategies were developed in our country and in the world [4]. In the Twelfth Development Plan of Türkiye, transition of green economy with low carbon have been aimed with using sustainable and biotechnological solutions. In the European Union (EU) Green Deal and the EU's Bioeconomy Strategy, bioeconomy has been adopted to mitigate climate change impacts and reduce carbon footprint [4]. Globally, the United Nations (UN) Sustainable Development Goals has supported also transition to sustainable bioeconomy with targets and actions. These frameworks and strategies which are considered as leverages have promoted notable transition. However, the transition to bioeconomy requires substantial actions for many industries, especially carbon and energy intensive industries such as cement, iron-steel, and chemical [4]. Considering all these strategies, the role of bioeconomy in industry should be increased to achieve circular industry and reduce dependency of fossil fuel sources [4].

In this transition period, where the fossil economy has phased out and the foundations of bioeconomy era have been laid, integration of microorganism-based solutions into the industry and research and development of novel eco-friendly approaches play a pivotal role [5]. In addition, many countries have already investigated sustainable and environmentally friendly approaches because conventional methods in fossil economy have commonly carbon and energy-intensive and harmful to the environment [1,3,5,6].

Microbial induced calcium carbonate precipitation (MICP) has been offered as one of the prominent approaches which could renovate traditional economy to sustainable bioeconomy by replacing chemical agents with bacteria [5]. MICP has contributed to reducing carbon emissions by decreasing chemical consumption which were used in some applications and extending lifespan of some materials [5,7,8]. Moreover, MICP has also contributed to reducing carbon footprint by working compatible with nature and considering as a carbon sink because of precipitation of CaCO_3 . MICP has frequently studied by scientists and engineers for the last years, especially for the last two decades [9]. In literature, it has been stated that MICP offers innovative solutions to solve various engineering problems (especially in environmental engineering) that stem from predominantly anthropogenic activities [9]. MICP applications in environmental engineering are pivotal to solve environmental problems such as carbon emissions, soil, and water pollution (contaminated by heavy metals), soil erosion etc. Research has demonstrated that with MICP, chemical consumption can be reduced, ecosystems can be protected, autonomous systems can be developed, resources can be recovered, and carbon footprint can be reduced [5,8,10,11].

Many of the recently proposed bio-based approaches such as biocementation, bioremediation, biocrusting, bioclogging, bioagglomeration, biogrouts, biocoating, carbon capture and storage are based on MICP [1,3,6,12–20]. Studies have been performed at lab and pilot scale for these applications [1,17,21]. However, further experimental studies and efforts are needed for optimization. When these applications can be used for a purpose under controlled conditions, it will be possible to offer sustainable solutions to many environmental, structural, and geotechnical problems [1,5,15,17,18].

MICP has been governed by numerous metabolic pathways. These metabolic pathways can be listed as urea hydrolysis, nitrate reduction (denitrification), aerobic respiration (aerobic oxidation), sulfate reduction, iron reduction, photosynthesis, ammonification, methane oxidation, etc. [22,23]. MICP contains comprehensive biogeochemical reactions and processes [24]. In nature and controlled conditions where free calcium ions are available, CaCO_3 precipitation is observed and deposited as a result of MICP via metabolic pathways.

MICP strictly relied on some parameters which include both biotic and abiotic factors. These parameters are type and concentration of microorganisms, nucleation sites of microorganisms, enzymatic activity of microorganism, pH, temperature, salinity, calcium sources [1,5,10,17,19]. MICP is primarily governed by using these effective parameters. Furthermore, studies on these effective parameters need to be increased. Accordingly, biogranules which were biomineralization-oriented was produced to enhance efficiency of MICP applications (Kardogan, 2024). These biogranules needed to be investigated comprehensively.

Within the scope of this thesis study, biomineralization-oriented biogranules were investigated at different environmental conditions. Biogranules were tested to determine their resuscitation performance and resistance to dehydration stress in the presence and absence of YE. These biogranules were compared to isolated strains (isolated inherently present bacteria in biogranules) and reference ureolytic and nitrate reducing axenic cultures (*Sporosarcina pasteurii* DSM 33 and *Pseudomonas aeruginosa*) in terms of biomineralization performance and microbial activity under different environmental conditions (different dissolved oxygen concentrations, temperatures, and salt concentrations).

2. LITERATURE REVIEW

2.1. Biomineralization

Recently, biomineralization studies have gaining great momentum, particularly in the last two decades, and have become a popular research area. Microorganism-mineral contact results in a phenomenon known as biomineralization process [25]. In literature, biomineralization have defined as the processes of conversion into inorganic mineral derivatives in which living organisms, especially bacteria, take an active role in biomineralization [26].

Using a variety of metabolic pathways, microorganisms produce a wide range of different sorts of minerals in varying sizes and forms [27,28]. In nature, biological and chemical processes that contribute to biomineralization evolve on their own. The intricate process of biomineralization takes place in both prokaryotic and eukaryotic species [29]. Biomineralization emerges via a series of complicated reactions belonging to various metabolic pathways [26]. The common feature of whole biological mineralization processes is that ions need to be removed from the medium and transported to the mineralization zone where they will accumulate. In literature, it has been stated that biomineralization forms mineral-like inorganic substances both inside and outside of microorganisms [30]. Biomediated-minerals differ in structure, composition, and morphology depending on the kind of microorganisms [31].

There are multiple kinds of living organisms, especially bacteria, in nature that stimulate to biomineralization, and these microorganisms can form biomediated-minerals [32]. Over 60 different biominerals produced by these microorganisms have been identified [33]. Examples of these minerals are silicates (SiO_x), carbonates (CO_3^{2-}), calcium phosphates ($\text{Ca}_3(\text{PO}_4)_2$) [33]. These minerals can form structural features of living organisms such as shells and bones in mammals and birds for millions of years, at that contributing to the hardening of their tissues [25,34]. Organisms have produced mineralized skeletons owing to calcification and silicification process for millions of years [35]. Depending on microorganism species, accumulation of calcium or silica salts in tissues are carried out by microorganisms. In literature, it is defined that calcium carbonates and calcium phosphates produced as a result of these processes are usually

crystalline, and silica organisms (sponges, diatoms) are popularly non-crystalline minerals [35].

Mineralization can be classified into different categories based on processes responsible for creating necessary conditions to form mineral, crystal morphology, and microbial growth [30]. In the literature, biomineralization has been investigated in two divided categories [36,37]. Biologically controlled mineralization (BCM) takes place when some parameters which are crystal structure, composition, and bacterial growth are totally governed by the certain microorganisms [33]. Independent of environment in which it lives, organism creates minerals which is distinctive to its own species. Biologically induced mineralization occurs when metabolic activity of bacteria creates biochemical conditions which are suitable for biomineral formation [33]. Calcareous or siliceous stromatolites are examples of biologically induced mineralization process. Calcium carbonate (CaCO_3) is one of the most prominent biomineralization agents employed in BIM process [36,38]. This type of biomineralization stands for biomineral formation that is not vigorously controlled by cellular processes so that this can lead to uncommon crystal morphologies [33,39].

CaCO_3 is the primary and most important carbonate found in biominerals. The most common CaCO_3 polymorphs in biomineralization are calcite and aragonite, yet metastable vaterite and amorphous CaCO_3 are also produced as byproducts in biomineralization process [31]. Some biominerals also contain a mixture of these CaCO_3 polymorphs. CaCO_3 polymorphs are much more common in marine environments, but they are also abundant in freshwater and terrestrial organisms [26].

Dissolved calcium (Ca^{2+}) in aquatic environments could precipitate in many forms such as calcium carbonate (CaCO_3), hydroxyapatite ($\text{Ca}_5\text{OH}(\text{PO}_4)_3$), calcium phosphate ($\text{Ca}_3(\text{PO}_4)_2$), carbonate-apatite ($\text{Ca}_5(\text{PO}_4)_3\text{CO}_3$). It is known that these sediment minerals are main components of coral reefs, bones, teeth, and fish scales vertebrate skeleton, and eggshells [34,40]. Precipitation and dissolution reactions depend on the solubility coefficient (K_{sp}) of the compounds. Although this coefficient for CaCO_3 changes according to different environmental conditions, it is determined as 4.8×10^{-9} at 25°C

[34,41,42]. Accordingly, solubility of CaCO_3 in water is quite low, and increase in the concentration of CO_3^{2-} in the environment in which Ca^{2+} ions are available can trigger CaCO_3 formation (Equation 1).

$$K_{sp} = [\text{Ca}^{2+}][\text{CO}_3^{2-}] = 4.8 \times 10^{-9} \quad (\text{Equation 1})$$

2.2. Microbial-Induced Calcium Carbonate (CaCO_3) Precipitation (MICP)

One of the most abundant minerals on Earth, calcium-containing minerals account for 4% of the weight of the crust of the earth [43]. These calcium-containing minerals constitute 50% of the total amount of biominerals and organo-minerals [27]. Due to several essential functions in the metabolic mechanism of microorganisms, Ca^{2+} serves as the primary ion in biominerals and organo-minerals [26,36,43]. Calcium carbonate precipitation via microorganisms was referred to as microbial-induced calcium carbonate precipitation (MICP).

MICP is defined as bacteria-mediated biomineralization approach. MICP consists of a widespread biogeochemical process. MICP happens in various habitats such as soil, freshwater bodies, marine water sediments, caves, subsurface, and even hypersaline environments [23,32,43,44]. Biogeochemical processes in MICP result from metabolic interactions and activities among microorganisms, organic/inorganic substances which are existing in the environment.

MICP has been increasing in popularity on account of its numerous versatile applications in civil, environmental, and geotechnical engineering. In the 19th century, MICP was initially reported by Murray, Irvine and Steinmann associated with urea hydrolysis in marine microbial consortia. The first study that comprehensively proved relationship between microbial activity and CaCO_3 precipitation was published by Nadson [45,46]. It could be indicated that all microorganisms and their microbial activities led to an increase in concentration of dissolved inorganic carbon (DIC) which could trigger MICP [47]. When considering the historical development of MICP, it was probably first used in geotechnical applications (contaminant removal from contaminated groundwater) by *S.*

pasteurii in 1995 [48]. It was reported in the literature that many microorganisms could induce CaCO₃ precipitation via different metabolic pathways and microbial activities [26].

According to literature, it was reported that various factors such as type of microorganism, dissolved calcium ions (Ca²⁺) concentration and inorganic carbon, presence of nucleation regions, and pH of the medium affected MICP performances [20,27,42,49,50]. These factors did not only affect CaCO₃ precipitation rate, but also have significant effects on the morphology of CaCO₃ minerals [20,39,51,52].

It was stated that there were six calcium carbonate polymorphs encountered in MICP applications: calcite, vaterite, ikaite, aragonite, mono-hydrocalcite and amorphous calcium carbonate (ACC) [37,52,53]. It was reported that aragonite often formed via biomineralization processes [54]. This indicated that biominerals had different properties and different appearances. In literature, while the most common polymorphs in MICP are calcite and vaterite, ikaite and ACC are very rarely observed [31,38,53].

2.3. Metabolic Pathways Employed in MICP Applications

MICP occurred by various metabolic activities of many different types of microorganisms. These metabolic pathways are classified into two groups: (i) autotrophic, and (ii) heterotrophic [55–57]. While photosynthesis and methane oxidation occur via autotrophic metabolic pathways, urea hydrolysis, denitrification, sulfur reduction, iron reduction, and ammonification are carried out heterotrophic metabolic pathways [58–62]. For instance, bacterial species involved in autotrophic CO₃²⁻ production obtain carbon from gaseous carbon dioxide (CO₂) or dissolved CO₂. In this process, photoautotrophs utilize the energy obtained from sunlight and inorganic components as a source [61].

These metabolic pathways involve a series of reactions and have a complex structure. Bacteria secrete various enzymes, such as urease, carbonic anhydrase, nitrate reductase, nitrite reductase, methanol dehydrogenase through these metabolic pathways and ensure

CaCO₃ precipitation. The aforementioned metabolic pathways are preferred in MICP applications depending on the purpose of MICP and the type of microorganism. Table 2-1 presents the reactions which are specific to metabolic pathways and the bacteria used in these metabolic pathways.

Table 2-1. Metabolic pathways in MICP (redrafted after [63])

Metabolic Pathways	Microorganism's type	Consecutive Reactions
Photosynthesis [58,61,63,64]	Cyanobacteria Algae	$2\text{HCO}_3^- + \text{Ca}^{2+} \rightarrow \text{CH}_2\text{O} + \text{CaCO}_3 + \text{O}_2$
Urea Hydrolysis [27,65–68]	Ureolytic Bacteria (<i>S. pasteurii</i> , <i>B. megaterium</i> , <i>B. cereus</i>)	$\text{CO}(\text{NH}_2)_2 + \text{H}_2\text{O} \rightarrow \text{NH}_2\text{COOH} + \text{NH}_3$ $\text{NH}_2\text{COOH} + \text{H}_2\text{O} \rightarrow \text{NH}_3 + \text{H}_2\text{CO}_3$ $\text{H}_2\text{CO}_3 \rightarrow \text{HCO}_3^- + \text{H}^+$ $2\text{NH}_3 + 2\text{H}_2\text{O} \rightarrow 2\text{NH}_4^+ + 2\text{OH}^-$ $\text{HCO}_3^- + \text{H}^+ + 2\text{NH}_4^+ + 2\text{OH}^- \rightarrow \text{CO}_3^{2-} + 2\text{NH}_4^+ + 2\text{H}_2\text{O}$ $\text{CO}_3^{2-} + \text{Ca}^{2+} \rightarrow \text{CaCO}_3$
Aerobic Oxidation [69,70]	Aerobic heterotrophs	$\text{Ca}(\text{C}_3\text{H}_5\text{O}_3)_2 + 6\text{O}_2 \rightarrow \text{Ca}^{2+} + 4\text{CO}_2 + 2\text{HCO}_3^- + 4\text{H}_2\text{O}$ $4\text{CO}_2 + 2\text{HCO}_3^- + 6\text{Ca}(\text{OH})_2 \rightarrow 6\text{CaCO}_3 + 6\text{H}_2\text{O} + 2\text{OH}^-$
Ammonification [61,65,67]	Myxobacteria, (<i>Myxococcus xanthus</i>)	$\text{Aminoacids} + \text{O}_2 \rightarrow \text{CO}_2 + \text{H}_2\text{O}$ $\text{NH}_3 + \text{H}_2\text{O} \rightarrow \text{NH}_4^+ + \text{OH}^-$ $\text{OH}^- + \text{CO}_2 \rightarrow \text{HCO}_3^-$ $\text{Ca}^{2+} + \text{HCO}_3^- + \text{OH}^- \rightarrow \text{CaCO}_3 + \text{H}_2\text{O}$
Methane Oxidation [29,58,61]	Methanotrophs (<i>Methylomonas</i> , <i>Methylomicrobium</i> , <i>Methylohalobius</i>)	$\text{CH}_4 + \text{O}_2 \xrightarrow[\text{NAD}^+]{\text{Methane Mono-Oxygease, NADH+H}^+} \text{CH}_3\text{OH} + \text{H}_2\text{O}$ $\text{CH}_3\text{OH} \xrightarrow[\text{PQQ} \rightarrow \text{PQQH}_2]{\text{Methanol Dehydrogenase}} \text{CHOH}$ $\text{CHOH} + \text{H}_2\text{O} \xrightarrow[\text{NAD}^+ \rightarrow \text{NADH+H}^+]{\text{Formaaldehyde Dehydrogenase}} \text{HCOO}^- + \text{H}^+$

Metabolic Pathways	Microorganism's type	Consecutive Reactions
		$\text{HCOO}^- + \text{H}_2\text{O} \leftrightarrow \text{HCOOH} + \text{OH}^-$ $\text{HCOOH} \rightarrow \text{CO}_2$ $\text{Ca}^{2+} + \text{CO}_2 + 2\text{OH}^- \leftrightarrow \text{CaCO}_3 + \text{H}_2\text{O}$
Sulphate Reduction [59,71,72]	Sulphate reducing bacteria (SRB) (<i>Desulfovibrio</i> sp., <i>D. desulfuricans</i>)	$\text{CaSO}_4 + 2\text{CH}_2\text{O} + \text{OH}^- \rightarrow \text{CaCO}_3 + \text{H}_2\text{O} + 2\text{CO}_2 + \text{HS}^-$
Iron Reduction [10,73]	Iron reducing bacteria	$\text{C}_2\text{H}_3\text{O}_2^- + 8\text{Fe}(\text{OH})_3 + 6\text{HCO}_3^- + 7\text{H}^+ \rightarrow 8\text{FeCO}_3 + 20\text{H}_2\text{O}$
Nitrate Reduction [22,71,74]	Denitrifiers or nitrate reducing bacteria	$2\text{HCOO}^- + 2\text{NO}_3^- + 2\text{H}^+ \rightarrow 2\text{CO}_2 + 2\text{H}_2\text{O} + 2\text{NO}_2^-$ $\text{HCOO}^- + 2\text{NO}_2^- + 3\text{H}^+ \rightarrow \text{CO}_2 + 2\text{NO} + 2\text{H}_2\text{O}$ $\text{HCOO}^- + 2\text{NO} + \text{H}^+ \rightarrow \text{CO}_2 + \text{N}_2\text{O} + \text{H}_2\text{O}$ $\text{HCOO}^- + \text{N}_2\text{O} + \text{H}^+ \rightarrow \text{CO}_2 + \text{N}_2 + \text{H}_2\text{O}$ $\text{CO}_2 + 2\text{OH}^- \rightarrow \text{CO}_3^{2-} + \text{H}_2\text{O}$ $\text{CO}_3^{2-} + \text{Ca}^{2+} \leftrightarrow \text{CaCO}_3$

According to literature, it was stated that the most preferred and researched metabolic pathways for the MICP concept were photosynthesis, urea hydrolysis, denitrification, and sulfate reduction metabolic pathway. In nature, the most common metabolic pathway was photosynthesis. According to the literature, approximately 70% of the Earth's rocks (containing CO_3^{2-}) were formed by cyanobacteria [64]. It was also reported that different minerals containing CaCO_3 minerals were precipitated via photosynthesis in several environments such as seawater, freshwater bodies, hot springs, etc. [29,61,64].

The most researched and used metabolic pathway for MICP applications is urea hydrolysis [9,63]. In the literature, ureolytic axenic cultures and non-axenic cultures via urea hydrolysis were frequently tested in MICP applications [33,75]. However, in recent years, studies on MICP applications via denitrification have accelerated. Denitrification, which is preferred as an alternative metabolic pathway to urea hydrolysis, has advantages

such as occur under anoxic conditions, having no toxic byproducts, and not need any external alkalinity.

In MICP, microbial activity increases alkalinity and generates CO₂ or HCO₃⁻ ions which enables CO₃²⁻ ions production [48]. During photosynthetic process, alkalinity rises depending on the alteration of HCO₃⁻/OH⁻ concentration [48]. During methane oxidation, it leads to increase in alkalinity in environment [44,76]. In sulfate reduction, sulfate-reducing bacteria (SRB) also produce alkalinity which are depending on SO₄²⁻ reduction and using up organic acids in environments [59,72]. Dissimilar to other metabolic pathways, during aerobic respiration, merely CO₂ is produced and does not generate alkalinity [48]. This indicates that aerobic oxidation metabolic pathway depends on external alkalinity in MICP applications. MICP via denitrification and urea hydrolysis do not rely on any external alkalinity because both denitrification and urea hydrolysis produce enough alkalinity to raise pH of the environment [63].

2.4. MICP Applications

MICP, which offers revolutionary and environmentally friendly biotechnological applications thanks to its wide range of usage areas and applications, has gained increasing momentum in recent decades. Under favor of its environmentally friendly and groundbreaking usage areas, it has become significant to many scientists working in biomineralization. MICP applications, which normally studied in the literature, are core of biomineralization studies [9,61,62,67]. Considering above this, MICP applications, which used for numerous engineering studies and applications in the literature, described broadly in Table 2-2.

Table 2-2. Different types of bacteria used in different MICP applications

Types of bacteria	MICP applications	Metabolic pathways
<ul style="list-style-type: none"> • <i>S. pasteurii</i> • <i>B. sphaericus</i> • <i>B. megaterium</i> • <i>B. cohnii</i> 	<ul style="list-style-type: none"> • Soil stabilization • Erosion control • Mitigation of soil liquefaction • Soil strengthening 	<ul style="list-style-type: none"> • Urea Hydrolysis [30,33,58,71,77–84]

Types of bacteria	MICP applications	Metabolic pathways
<ul style="list-style-type: none"> • <i>B. subtilis</i> • <i>B. cereus</i> • <i>Lysinibacillus sphaericus</i> • <i>Sporosarcina koreensis</i> • <i>Kocuria flava</i> 	<ul style="list-style-type: none"> • Crack-healing activity • Historical building restoration • Heavy metal removal (Cu^{2+}, Zn^{2+}, Cd^{2+}, Pb^{2+}, Ni^{2+}, Co^{2+}) • Water absorption • Porosity, and permeability 	
<ul style="list-style-type: none"> • <i>Chlorella vulgaris</i> • <i>Spirulina platensis</i> • <i>Chlorella</i> sp. • Cyanobacteria and diatoms 	<ul style="list-style-type: none"> • CO_2 storage • CO_2 sequestration 	<ul style="list-style-type: none"> • Photosynthesis [28,61,85–88]
<ul style="list-style-type: none"> • <i>P. aeruginosa</i> • <i>Diaphorobacter nitroreducens</i>, • ACDC • <i>P. denitrificans</i> • <i>Castellaniella denitrificans</i> 	<ul style="list-style-type: none"> • Crack-healing activity • Self-healing concrete • Preventing corrosion • Enhanced-oil recovery 	<ul style="list-style-type: none"> • Denitrification [48,71,87,89–96]
<ul style="list-style-type: none"> • <i>Desulfovibrio desulfuricans</i> 	<ul style="list-style-type: none"> • Steel bar corrosion • Carbon steel pipe corrosion prevention 	<ul style="list-style-type: none"> • Sulphate reduction [58,72,97]
<ul style="list-style-type: none"> • <i>Myxococcus xanthus</i> • <i>Stenotrophomonas rhizophila</i> 	<ul style="list-style-type: none"> • Limestone restoration • Water absorption • Porosity, and permeability 	<ul style="list-style-type: none"> • Ammonification

2.4.1. Merits and Demerits of Metabolic Pathways Employed in MICP Applications

While the aforementioned metabolic pathways used in MICP applications are triggered by bacteria, some metabolic by-products are formed (resulting from successive reactions). These metabolic byproducts were summarized in Table 2-3. Although these metabolic byproducts have some advantages, they also have disadvantages. Some drawbacks associated with metabolic pathways in MICP applications commonly based on production of byproducts during metabolic reactions, contributing to limitations in MICP applications [5]. These metabolic by-products, which pose a greater risk to aquatic or marine habitats, are stated as a disadvantage in MICP applications [5,48,98].

In photosynthesis, CH₂O (formaldehyde) which pose a risk to human health can be produced as metabolic byproducts [29]. In urea hydrolysis and ammonification, NH₄⁺ and NH₃⁺ are produced during enzymatic reactions. These byproducts are harmful chemicals, and toxic to marine habitats and human health. NH₄⁺ and NH₃⁺ production is considered as significant drawback of urea hydrolysis [5,99]. In sulphate reduction and methane oxidation, H₂S (hydrogen sulfide) are produced as byproduct [61]. It is toxic and malodorous gas even at low concentrations. In nitrate reduction, NO, NO₂⁻, N₂O can be produced [29]. These have toxic effects on human health, aquatic habitats, agriculture. However, it is also possible to effectively utilize the resulting intermediate products. For example, ammonium ions produced as a result of urea hydrolysis can be employed to generate biofuel or capture CO₂ with the help of bacteria [100]. On the other hand, NO₂⁻ ions accumulated in the environment during partial denitrification are also exploited to prevent corrosion [74,89]. In addition, N₂ (biogenic gas) accumulated in the environment by reducing nitrate and nitrite to N₂ could also be used to increase soil stiffness, reduce hydraulic conductivity of soil, and mitigate soil liquefaction [63,94,101]. To sum up, these metabolic pathways have both advantages and disadvantages. It is also possible to gain advantages in more than one area by using these metabolic pathways together, that is, by engendered a synergistic microbial environment approach with the help of biostimulation, bioaugmentation, biogranulation, etc. [20,48]. When using a microbial community in which both urea hydrolysis and denitrification take place simultaneously in MICP applications, it is possible to reach high biomineralization performance by minimizing disadvantages of both metabolic pathways.

Table 2-3. Metabolic by-products and drawbacks of various metabolic pathways employed in MICP applications (redrafted after [29])

Metabolic Pathways	Metabolic by-products at the end of the reactions	Risks
Photosynthesis	O ₂ and CH ₂ O (formaldehyde)	Posing a risk to health (CH ₂ O)
Urea Hydrolysis	NH ₄ ⁺ and NH ₃ ⁺ production	Toxic to marine or aquatic ecosystems [98,99]

Metabolic Pathways	Metabolic by-products at the end of the reactions	Risks
Ammonification	NH_3^+ production	Toxic gas [61]
Sulphate reduction	CO_2 and H_2S	Toxic and malodorous gas [61]
Nitrate reduction	NO , NO_2^- , N_2O production (intermediate products)	Deleterious products to aquatic habitats, agriculture, and the atmosphere
Methane oxidation	H_2S	Toxic and malodorous gas [61]

2.4.2. Urea Hydrolysis and Ureolytic Bacteria in MICP Applications

Urea hydrolysis, major metabolic pathway, is one of the most prominent metabolic pathways predominantly opted for MICP applications [9,75,102]. Urea hydrolysis is orientated by urease enzyme secreted by specific bacteria, thus initiating a series of reactions [33]. Urea hydrolysis involves irreversible reactions mentioned above (Table 2-1), which occur gradually [29,103]. Schematic representation and reactions of urea hydrolysis by ureolytic bacteria are given in Figure 2-1.

The urea molecule has been hydrolyzed to NH_3^+ and NH_2COOH by using urease enzyme secreted by bacteria. Then, carbamate (NH_2COOH) spontaneously converts into NH_3^+ and H_2CO_3 substances in aqueous environment. As seen in the above-mentioned reactions (Table 2-1), H_2CO_3 is transformed into HCO_3^- by using carbonic anhydrase enzyme, and then NH_4^+ and OH^- accumulate in the environment by ammonia hydrolysis [1]. In consequence of cascade reactions of urea hydrolysis, ammonium (NH_4^+) accumulation in the environment lead pH to increase in the microbial environment. Through the elevated pH of the environment, HCO_3^- ions also convert into CO_3^{2-} ions [77]. Since extracellular surface of microorganisms is negatively charged, Ca^{2+} are attached to microbial cells. In the presence of sufficient dissolved Ca^{2+} around microorganisms, it combines with CO_3^{2-}

and Ca^{2+} , and at end of the reaction, CaCO_3 crystals are formed and thus precipitate in the environment as CaCO_3 crystals or minerals [27,68,80].

During urea hydrolysis, two moles of ammonium are released as a result of hydrolysis of one mole of urea. Ammonium is also produced as a reactions' by-product. Under alkaline conditions, ammonium converts to ammonia and both by-products possess toxicity for aquatic species [29,104].

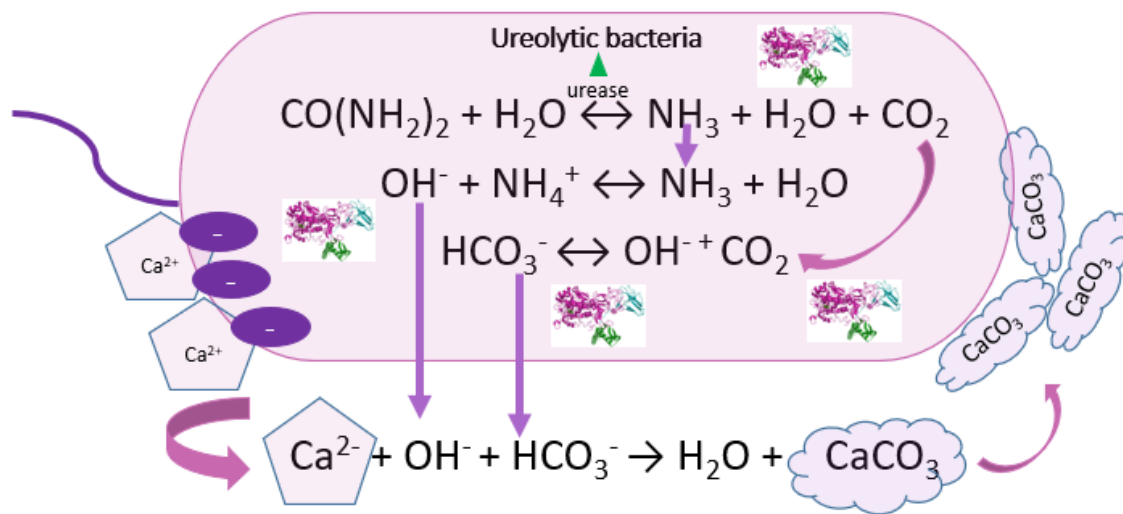


Figure 2-1. Schematic representation of urea hydrolysis by ureolytic bacteria (redrafted after [79])

Urea hydrolysis and ureolytic bacteria are used in many MICP studies in the literature [75]. Bacteria generated enzyme urease, which hydrolyzes urea, are often used in MICP applications to facilitate CaCO_3 precipitation in soil, sediments, aquatic environments, or construction materials [105]. CaCO_3 precipitation triggered by urea hydrolysis also has several applications such as soil or ground improvement, bioremediation, self-healing cracks, groundwater treatment, and biocement production [48,94,106–111].

It was stated that MICP via urea hydrolysis could be used to enhance characteristics of soil or ground. By injection bacteria that can trigger CaCO_3 precipitation into the soil (biostimulation or bioaugmentation), strengthening and stabilizing the soil, increasing the

load-carrying capacity, and reducing erosion are possible with MICP [20,48]. Among different MICP metabolic pathways, urea hydrolysis by urease-positive bacteria had maximum microbial activity (up to 90%) and higher CaCO₃ precipitation when compared to other metabolic pathways [102].

Various axenic strains with high urea hydrolysis activity have been described in the literature, such as *Sporosarcina pasteurii*, *Lysinibacillus sphaericus*, *Bacillus cereus*, *Bacillus megaterium*, *Bacillus cohnii*, *Bacillus thuringiensis*, *Bacillus subtilis*, and *Bacillus alkalinitriculus*. They have been identified as the most widely used non-pathogenic axenic culture that can tolerate extreme environmental conditions [33,49,68,79,83,108,112–116].

In the literature, *Sporosarcina pasteurii* (priorly denominated as *B. pasteurii*) is one of the urease positive bacteria and enzyme-secreting bacteria most frequently and efficiently used in MICP applications [48,75,117–120]. *S. pasteurii* is described as a non-pathogenic soil borne bacteria, alkaliphilic, aerobic, and capable of spore formation [68,121,122]. It is known for its robust urease activity and ability to precipitate CaCO₃ in various environments [123,124]. It is the most routinely utilized species for biomineralization and MICP applications because of its high intercellular microbial activity (high rate of hydrolyzed urea) and its alkaliphilic nature [33,48,79,118,125,126].

In the literature, it was reported that ureolytic axenic cultures (*B. sphaericus* LMG22557 and *Sporosarcina pasteurii* DSM33) had the highest calcium carbonate precipitation performance. These axenic cultures could have approximately 0.4 g CaCO₃ · h⁻¹ · g CDW⁻¹ [127]. *Bacillus* sp. MCP11 also hydrolyzed urea with suitable growth conditions around pH 9, thus being able to tolerate severe environmental conditions [128].

MICP, mostly driven through urea hydrolysis, offers an innovative bioremediation method to remove heavy metal ions. Heavy metals including Hg²⁺, Pb²⁺, Cd²⁺, Co²⁺ and Zn²⁺ could be removed from contaminated environment via MICP [48,67]. Although high concentrations of divalent heavy metal ions could hinder microbial activity of urease-

positive bacteria, it was stated that the MICP approach gives positive results even at high-concentration heavy metal solutions. For example, in the literature, 97% of Cu^{2+} was removed using *Kocuria flava* in MICP with an initial concentration of 1000 ppm [67]. It was reported that in the MICP application triggered by *B. cereus*, the amount of Cr^{2+} in the contaminated soil was significantly reduced, and 99.95% of the Cd^{2+} was removed by using *Lysinibacillus sphaericus* [61]. In another study, using *S. pasteurii*, it was stated that 95% of Sr^{2+} was removed from the environment within 24 hours at an initial concentration of approximately 90 ppm.

A hydrogel encapsulation approach for *B. sphaericus* endospores was suggested in the literature to achieve self-healing concrete. It was demonstrated that this method can maintain the viability of endospores within the concrete and that bacteria could heal cracks on their own [129,130].

Silva et al. developed Cyclic Enriched Ureolytic Powder or CERUP involving urease-positive bacteria (non-axenic ureolytic microbial consortia) to reduce product cost of concrete that heals itself via urea hydrolysis [127]. CERUP consisted of a bacterial community that was capable of germination of spores but was not axenic. In the conducted tests, it was stated that cracks with approximately 400 μm width in concrete containing CERUP were completely healed in 28 days.

Bacillus is a type of bacteria that has a rod-shaped which is recognized as bacilli, and they are known for being gram-positive (dense peptidoglycan structure in their cell wall layer) and endospore formation [131,132]. Sporulation of the bacteria cell pertains to the metamorphosis of a vegetative cell into an endospore [132]. These genera belong to the *Bacillaceae* family [133,134]. Their morphology can vary from species to species. According to the literature, the size of *Bacillus* species typically ranges from 0.5 to 5.0 μm depending on the family or species [61]. It was stated in the literature that their spores were resistant to harsh environmental conditions, osmotic stress, and heat, etc. [131] Their endospore formation ability allows *Bacillus* sp. to survive or endure in adverse/harsh environmental conditions, radiation, osmotic stress, heat, desiccation, and chemical resistance [131,132,135]. The formation of endospores is an essential factor in the ability

of *Bacillus* species to remain alive and persist in unbearable environments [131,136]. *Bacillus* species are either obligate aerobes or facultative anaerobes. Since most *Bacillus* species are aerobic that is, they necessitate oxygen to proliferate and perform metabolic activities [61,132]. Certain species, on the other hand, are facultative anaerobes, which means that, in response to O₂ availability, they may alternate between aerobic and anaerobic metabolism [133,134]. Many ecosystems, including soil, water, air, and animal gastrointestinal tracts, are frequently host to *Bacillus* species [132,133]. These microorganisms are essential to the nutrient cycles in soil ecosystems. Many species of *Bacillus* are benign or even beneficial, although some are opportunistic pathogens that may infect humans and animals [133,134,137]. To give an example, anthrax is brought about by *Bacillus anthracis*, and food poisoning can be caused by certain strains of *Bacillus cereus* [131].

Given that flagella are present, many *Bacillus* species are motile. Their ability to migrate promptly allows them to colonize a variety of environments and migrate toward a variety of growth and survival-promoting conditions [133,134,137]. *Bacillus* species are utilized in a variety of fields such as medicine, pharmaceuticals, agriculture, and industry due to their diverse or multiple physiological characteristics and their capacity to generate numerous enzymes, antibiotics, and other compounds [131,132].

In recent years, *Bacillus* species have been commonly investigated for their potential applications in MICP because they can produce urease enzyme, which is the main element for CaCO₃ precipitation via MICP [136]. *Bacillus* species are frequently used in MICP applications due to the abovementioned properties. *Bacillus* species frequently used in MICP applications are summarized below: *Bacillus sphaericus*, urease positive bacteria, was researched and used in MICP applications [123]. *B. sphaericus*, similar to *S. pasteurii*, has high urease enzyme activity and precipitates CaCO₃ [82,138]. According to the literature, *B. sphaericus* has been studied for areas such as soil amendment and bioremediation applications.

Bacillus pseudofirmus, similar to other *Bacillus* species, is a ureolytic bacteria that can survive in severe environments such as extremely elevated pH and high saline medium

and have urease activity. Its ability to secrete urease enzyme even under these conditions makes it advantageous for MICP applications, especially in harsh environmental conditions such as saline soils or highly alkaline environments [56]. *B. subtilis*, *B. cohnii* and *B. megaterium* are also described ureolytic bacteria because of capable of high amount of urea hydrolyzed. [139,140]. It has been researched for their potential in MICP applications, especially in soil stabilization and biocement production [141–144]. It is a highly tolerant bacterium that can adapt to and thrive in harsh and diverse environmental conditions [136,144]. *Bacillus* species mentioned above are just some examples of ureolytic bacteria that have been investigated for their potential in MICP. The performance of bacteria due to their metabolic activities and MICP applications depends on various factors such as urease activity, adaptation and tolerance to harsh environmental conditions, and ease to cultivation [127,131].

Overall, *Bacillus* species have significant role to offer eco-friendly and promising sustainable approaches to numerous MICP applications [82,109,136,145–147]. According to the literature, *Bacillus* sp. is effectively utilized in several MICP applications, such as soil improvement and stabilization, bioremediation, self-healing concrete, carbon sequestration, dust, and erosion control [60,61,129,148,149].

Although urea hydrolysis has been studied intensively due to its efficiency, it has some disadvantages. Due to reaction rate of urea hydrolysis, CaCO_3 minerals that rapidly precipitate around bacteria cause an inhibition effect on microbial activity [1,33]. This eventually terminates microbial activity [33]. Additionally, since urease-positive bacteria are mostly aerobic or facultative anaerobic, microbial activity is negatively affected in environments where oxygen is limited [121,150].

Due to such disadvantages, an alternative metabolic pathway to urea hydrolysis was required in MICP applications. MICP performance of ureolytic axenic strains directly depends on dissolved oxygen (DO) concentration and yeast extract (YE). This indicates that alternative metabolic pathways to urea hydrolysis should be investigated, especially in MICP applications including soil and ground improvement and self-healing cracks.

Ongoing and future studies are crucial to understand the role of urea hydrolysis and ureolytic bacteria on MICP (particularly *Bacillus* sp.), to optimize MICP techniques, and to exploit their potential in various engineering and environmental applications.

2.4.3. Denitrification (Complete Nitrate Reduction) and Denitrifiers in MICP Applications

Denitrifying microorganisms are extensively spread in a variety of habitats and can be found in enormous numbers in nature [93,151]. The literature highlighted that such organisms could reach a population number of roughly 10^6 microorganisms per gram of soil [63]. Denitrifying bacteria account for from 1% to 5% of the soil microbial consortia and around 20% of the whole microorganism consortia that could thrive in anoxic environments [63].

As far as is known that denitrification is a significant process in nitrogen cycling in nature, which takes place in the absence of available O_2 . This process is also notable in applications involving MICP. In this process, several nitrate-reducing bacteria employ NO_3^- as an alternative electron acceptor for anoxic respiration [48]. Schematic representation and reactions of denitrification by denitrifying bacteria are given in Figure 2-2. A sequence or consecutive of chemical reactions is performed by denitrifying microbes, which secrete multiple enzymes (Table 2-1). The process involves enzymatically reducing nitrate (NO_3^-) to nitrite (NO_2^-) by using NO_3^- reductase enzyme. NO_2^- can further reduce to NO by utilizing NO_2^- reductase enzyme. NO is then reduced to N_2O by using the NO reductase enzyme. Ultimately, N_2O can reduce to inert nitrogen gas (N_2) by using the N_2O reductase enzyme, accomplishing the denitrification metabolic pathways. N_2 is subsequently released into the atmosphere [62,94].

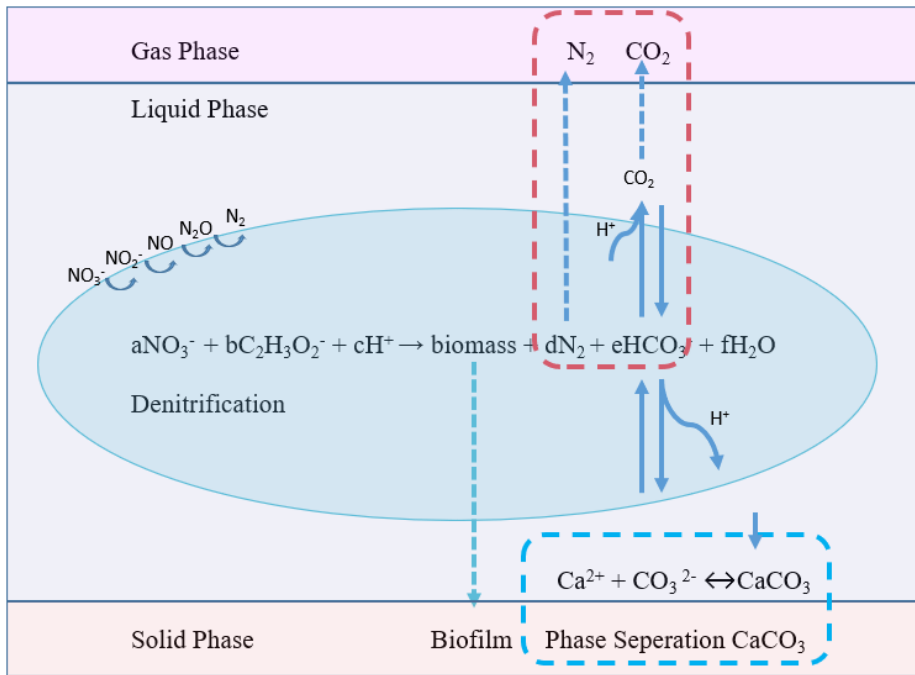


Figure 2-2. Schematic representation of denitrification mechanism (redrafted after [63])

Biologically, nitrate reduction occurs during the metabolic respiration of organic substances by using NO_3^- which is utilized as an electron acceptor. In this process, NO_3^- is used instead of oxygen. Metabolic reduction of NO_3^- produces carbonate and bicarbonate ions to form alkalinity, which are required for $CaCO_3$ formation [71]. In the presence of available Ca^{2+} ions in the medium, reduction of NO_3^- together with the produced CO_3^{2-} and HCO_3^- ions provides $CaCO_3$ precipitation [94].

In recent years, denitrification have been considered as an alternative metabolic pathway to urea hydrolysis. MICP via denitrification is considered an environmentally friendly and promising metabolic pathway [63]. In order to find a way, some researchers have investigated denitrifying bacteria and nitrate reduction metabolic pathway as alternative to urea hydrolysis in biomineralization applications such as ground improvement, calcium removal from industrial wastewater, soil stabilization, and microbial self-healing bio-concrete [94,99,152,153].

Nitrate-reducing bacteria could prevent corrosion in steel-reinforced concrete by simultaneously creating NO_2^- and triggering $CaCO_3$ formation [29,74]. It leads to heal

cracks in concrete. Bacteria such as *Pseudomonas aeruginosa*, *Pseudomonas denitrificans*, *Castellaniella denitrificans*, *Diaphorobacter nitroreducens* could be given as examples of nitrate-reducing bacteria [23,63]. It was reported that nitrate-reducing bacteria (*D. nitroreducens* or *P. aeruginosa*) could precipitate CaCO₃ even under minimal nutrient conditions [29,74].

The first research of MICP via nitrate reduction were performed to improve soil and sand. The maximum CaCO₃ precipitation efficiency reported among the studies (10.6 g CaCO₃.g⁻¹ NO₃-N) was accomplished via the denitrification efficiency of *P. denitrificans* at nutrient-rich environments. By nitrate reduction, the highest CaCO₃ formation rate of 18 g CaCO₃.h⁻¹ was stated for *C. denitrificans* with nutrient-rich solution. It was recommended to utilize more appropriate strains at higher inoculum rate to rise CaCO₃ precipitation rate. In experiments conducted with *D. nitroreducens* and *P. aeruginosa*, 14.1 and 18.9 g CaCO₃.g⁻¹ NO₃-N performance were obtained, respectively [69,152,154].

Pseudomonas aeruginosa was well-known for its metabolic versatility and environmental adaptability [49]. *Pseudomonas aeruginosa* is an opportunistic pathogen that primarily infects individuals with compromised immune systems [155,156]. Its host range includes humans, animals, and plants. *P. aeruginosa* represents Biosafety Level 2 Criteria, posing a moderate risk to humans and the environment [155].

P. aeruginosa is found almost all over the place in nature and may be present at a diversity habitat or ecosystem, such as soil, freshwater, plants, and animals. It grows relatively better in humid environments. *P. aeruginosa*, also known as the hospital microbe, is frequently found in hospital environments [155]. *P. aeruginosa* can form resistant biofilm from the extracellular polymeric substances (EPS) [157]. Biofilms make bacteria more resistant to host immune defenses and antibiotics [156]. *P. aeruginosa* generates biofilm formation depending on population density [156]. This allows synergistic behavior between bacterial cells.

Despite its moderate pathogenic potential, *P. aeruginosa* is used in MICP applications via nitrate reduction [74,154,158]. *P. aeruginosa* has high NO_3^- reducing ability. In this way, it can trigger high levels of CaCO_3 precipitation. According to some studies, *P. aeruginosa* was tested together with *D. nitroreducens* for biomineralization applications through nitrate reduction, and it was revealed that its biomineralization performance was similar or better than *D. nitroreducens* [91,153,159–163]. Additionally, it was reported that denitrifying dried granules could be used in self-healing concrete applications in MICP. Ersan et al. developed non-axenic granules, a compact community of denitrifying bacteria, labeled the "active compact denitrifying core" (ACDC) [69,154]. ACDC mainly consisted of a nitrate-reducing microbial community. It was reported that healing rate reached 90% after 28 days by using ACDC.

However, during incomplete microbial nitrate reduction, harmful intermediates including NO^{2-} , NO^- , and N_2O could be produced. Therefore, similar to urea hydrolysis, denitrification has both advantages and disadvantages. In literature, it was stated that nitrate-reducing bacteria had a slower reaction rate compared to ureolytic bacteria in terms of CaCO_3 precipitation [151]. It was reported in the literature that MICP via denitrification lasted 50 to 1000 times slower than urea hydrolysis [152]. This situation provided advantages in terms of stability of microbial activity, continuity, and homogeneity of MICP [151,152]. Although this made it potentially advantageous over urea hydrolysis in the long term, it was stated that it had a disadvantage due to the longer application period [123,164].

Denitrification metabolic pathways could also produce its alkalinity. Thus, it eliminates the necessity for any external alkalinity and produces non-toxic (unless accumulated in the environments), and chemically inert N_2 [165]. In comparison with other metabolic pathways, denitrification has such advantages. Dissimilar to urea hydrolysis, nitrate reduction does not require oxygen, so that it can enable biomineralization in environments where oxygen access is limited or impossible [48]. Since nitrate-reducing bacteria could use NO_3^- as an electron acceptor in its place of O_2 , it could be used efficiently in biomineralization applications without oxygen or with limited access to oxygen [99]. Since nitrate reduction process has such an advantage, it can be considered as an

alternative metabolic pathway to urea hydrolysis. Although byproduct N_2 is not very harmful, the byproduct during MICP via nitrate reduction, namely NO_2^- and N_2O , may be detrimental to the medium, especially the marine environment, and is toxic to marine species.

Nitrate was reduced even under minimal nutrient conditions. Nitrate-reducing bacteria or denitrifying axenic strains can substitute aerobic axenic strains and ureolytic axenic strains as they require O_2 and a nutrient-rich environment for germination or growth. This was an advantage compared to urea hydrolysis because ureolytic axenic cultures efficiently precipitated $CaCO_3$ at nutrient-rich conditions [152]. Nevertheless, $CaCO_3$ precipitation efficiency is quite low compared to urea hydrolysis. In addition, if there is a high concentration of NO_3^- in the environment, it can inhibit bacterial growth.

One of another benefit of nitrate reduction over urea hydrolysis is accumulation of NO_2^- through reduction of nitrate. This leads to achieve corrosion prevention and self-healing cracks in concrete by utilizing nitrate-reducing axenic strains that accumulate NO_2^- during NO_3^- reduction [29,74].

Overall, nitrate reduction metabolic pathway can hold potential to alternative metabolic pathway to urea hydrolysis. But further efforts are needed to optimize and understand completely conceptual mechanisms of nitrate reduction.

2.5. Axenic and Non-Axenic Cultures Used in MICP

2.5.1. Axenic Cultures (Pure Cultures) and Their Drawbacks

Cultures containing single-type colonies or single-type microorganisms are called axenic cultures. Axenic cultures are also referred to as pure cultures in microbiology. It is mostly utilized in MICP applications or studies that require use of axenic culture when investigating issues such as the characteristics, physiology, morphology, and metabolism of a specific microorganism. Obtaining axenic or pure cultures requires a thorough sterilization process to prevent contamination from the environment. Researchers have

studied with axenic cultures to observe the characteristics and behavior of single types of microorganisms under certain conditions. Studying the dynamic behavior of axenic cultures was easier than non-axenic cultures. Because non-axenic cultures containing more than one type of microorganisms represented a complex system.

Many limitations which required to be eliminated were identified for axenic cultures in MICP applications. These limitations related to axenic cultures in MICP applications were commonly identified as high production and cultivation cost, high sensitivity to nutrient-rich medium, cost of aseptic conditions [127,166]. Growing axenic culture without any contamination requires strictly controlled sterilization processes [51,127,167,168]. Additionally, there are differences in the growth medium of pure cultures compared to non-pure cultures. The growing environment of axenic cultures requires a nutrient-rich medium. Therefore, cultivation of axenic cultures or the ability to test them without any contamination of their purity in studies is required higher production costs compared to non-axenic cultures [51,127,167–169].

It was reported that using only axenic cultures significantly increased production and application costs and hindered MICP applications [169]. For instance, Silva et al. reported that costs of aseptic conditions were added to nutrients costs such as yeast extract (YE) and soybean extract (SE) used during production of axenic cultures. It was also reported that total production costs might reach up to 2000 Euro per kg of bacteria [169,170]. Therefore, if non-axenic bacterial cultures were used in MICP applications, total costs can be reduced by 40 times per kg of bacteria [127,169,170]. In addition, non-axenic cultures are also a reduced amount of cost to produce on an industrial scale [51,169].

S. pasteurii and *B. sphaericus*, axenic ureolytic cultures performed extensively in MICP, have some disadvantages. These disadvantages are high cost of nutrient-rich solutions and maintaining aseptic conditions used in production and application of these cultures [116,171,172]. It was reported that both cultures had high sensitivity to YE, and in the absence of YE, microbial processes such as growth, enzyme production, and spore germination were retarded or did not occur at all. The fact that YE or similar micro-nutrient is essential for use of these cultures in MICP applications causes undesirable

results in MICP applications [127,152,166]. For example, it was reported that if YE was added to the concrete mixture with *Bacillus sphaericus* in self-healing bioconcrete applications, setting time of concrete mixture was prolonged, porosity of hardened concrete increased, and its strength decreased [116,171]. In addition to these drawbacks, micronutrients such as YE significantly were increased cost of nutrient solutions [169,173,174]. In addition, since use of axenic cultures is based on a single metabolic pathway, its use in MICP applications is limited.

Propagating axenic cultures and maintaining their sterility is both costly and requires extra labor. Especially for slow-growing microorganisms, this process is more costly and requires intensive labor. Reliance of axenic cultures on nutrient-rich medium, sterile conditions, labor costs were disadvantage over non-axenic cultures. Further efforts and research have been needed to eliminate their drawbacks and to optimize to enhance biomineralization performances.

2.5.2. Non-Axenic Cultures (Mixed Cultures)

Non-axenic cultures are also referred as mixed cultures in microbiology. Non-axenic cultures (mixed cultures) represent cultures containing more than one type or strain of microorganisms. Non-axenic cultures are mostly based on study of microbial interactions between different types of microorganisms. Non-axenic cultures are used to generate microbial synergy (bacteria support and increase each other's development and proliferation) between target microorganism species for a specific purpose and are isolated from habitats that are complex in nature and contain many different types of microorganisms. Axenic and non-axenic cultures are of great importance in the literature depending on their intended use. Both types of cultures are widely used and are important for microbiological and biotechnological research. Axenic cultures and non-axenic cultures have both advantages and disadvantages depending on their intended use [169].

On the other hand, it was stated that through non-axenic cultures, multiple metabolic pathways offered by microbial consortia could be efficiently utilized in different fields such as wastewater treatment, bioremediation, environmental biotechnology, bioenergy

production and multiple MICP applications [175]. In the literature, it was reported that mixed cultures could be higher metabolic activity and higher biomineralization efficiency compared to axenic cultures in MICP applications [176,177].

Research on MICP has been increasing day by day as it gives promising results in research on many applications. Until the last decades, axenic cultures were mostly used in MICP applications. In addition, MICP was examined through a single metabolic pathway. In the last decade, non-axenic culture, especially biogranule production studies have been conducted for MICP applications [96,178–181]. However, although all these studies investigated the production of non-axenic biogranules for MICP applications, MICP was achieved through a single metabolic pathway in all these studies [89,96,127,159,178,180,181].

Non-axenic granular cultures have some advantages compared to axenic cultures. In the literature, these advantages were described as cost-effective, resist to severe environmental conditions and aggressive agents, versatility in applications, and ease of cultivation [127,182,183]. One of the most important advantages of non-axenic granular cultures is that, due to their compact spherical structure, both aerobic, anoxic, and anaerobic conditions could be provided simultaneously in biogranules [184–187]. In addition, compact form of non-axenic granular cultures protected cultures against harsh environmental conditions, deprivation of micronutrients and this made non-axenic granular cultures easier stored at dried form and practicality [183].

One of the advantages of non-axenic cultures was also environmentally friendly due to releasing lower CO₂ emissions compared to axenic cultures [127,166]. Production and cultivation of both non-axenic cultures and axenic cultures needed for energy, nutrient sources, chemical consumption, selecting optimum conditions etc. Therefore, they had directly or indirectly CO₂ emissions. Yet, non-axenic cultures had lower CO₂ emissions [127,166]. For instance, Silva et al. revealed that the CERUP production (mixed ureolytic culture) caused to less amount of carbon emissions when compared to ureolytic axenic strains such as *B. sphaericus* and *B. cohnii* [127]. CERUP production resulted in 2.7- and

40-times lower CO₂ emissions compared to *B. sphaericus* and *B. cohnii*, respectively [127]. This could pave the way for using non-axenic cultures in MICP applications.

ACDC, non-axenic nitrate reducing granular culture, was developed in order to use MICP applications [153]. It was reported that ACDC had some advantages over axenic cultures [153]. The production and cultivation process of ACDC was conducted under minimal nutrient conditions. ACDC was developed as self-protected granular culture [153]. Due to its self-protected granular culture, ACDC did not require extra protective layer or encapsulation methods. Encapsulation was essential to bacteria to resist harsh environments including highly alkali environment [11,76,129]. But ACDC could resuscitate and withstand severe environmental conditions for a long time in self-healing concrete applications without encapsulation [153]. Therefore, the fact that ACDC did not need encapsulation or protective layer made ACDC easier to apply in MICP. This was an advantage over axenic cultures. Another advantage of ACDC over axenic cultures was cost-effective because ACDC did not need any extra nutrients, protection layer [153]. De Vrieze et al. reported that non-axenic cultures could be produced with a highly stable microbial community and protected against invasive species by adjusting growth or environmental conditions, and enriching nutrient solution [188].

In the literature, it was reported that complementary metabolisms of denitrification and urea hydrolysis increased biomineralization efficiency. It was concluded that *B. sphaericus* LMG 22257 and *R. eutropha* H16 could perform both hydrolyzing urea and reducing nitrate [99]. Therefore, the importance of using simultaneously two metabolic pathways together has revealed. By using non-axenic cultures and granular cultures, it became possible to use two metabolic pathways simultaneously in MICP applications. This situation led to both decrease in costs and an increase biomineralization performances in MICP applications. It was demonstrated that the limitations related to microbial activity and biomineralization capacity could be overcome by combining two different metabolic pathways associated with biomineralization in non-axenic biogranules.

Due to the aforementioned disadvantages, the need to use more than one metabolic pathway simultaneously in MICP applications has emerged. Therefore, the significance of non-axenic granular cultures has increased. With the common use of non-axenic cultures in MICP applications, the aforementioned drawbacks could be eliminated. Non-axenic cultures bear potential to contribute to prevalence of MICP applications in environmental, civil, and geotechnical engineering.

2.5.2.1. Biogranulation and Biogranules

Biogranules, which represent structures formed by bacterial cells gathering, represent the process called biogranulation. Biogranulation process was first studied and reported anaerobically [189]. It has been used in industrial wastewater treatment because high amounts of biomass can be operated by using anaerobic biogranules, thus allowing the treatment of wastewater containing high pollution load [189]. Biogranulation essentially involves microbial communities that have a range of biological, physical, and chemical activities.

Biogranulation process, which was fundamentally enhanced for wastewater treatment, contains anaerobic or aerobic biogranulation phases [175,186,190]. Therefore, biogranules are often categorized as aerobic and anaerobic biogranules [175,191].

Extracellular polymers (EPS) secreted by bacteria during biogranule formation cause changes on the surfaces of the negatively charged cell membrane of bacteria, allowing bacteria to form biofilms [189]. The extracellular polymers contained in biogranules ensure that bacteria inside biogranules are more resilient to inhibitory environments and shock loading than flocs or axenic cultures [189]. Biogranules have higher settling ability compared to traditional microbial flocs. At the same time, since biogranules have a more regular and dense structure than microbial flocs, they allow a larger number of bacteria to be kept together in a smaller volume [189]. Additionally, biogranules have higher toxicity resistance than microbial flocs and pure cultures [189].

Another advantage of biogranules is that they can simultaneously carry out various metabolic pathways thanks to different microbial communities. In this way, production of more than one microbial enzyme can be triggered by more than one metabolic pathway. Thus, biogranules can have a wider range of utilizes than axenic cultures. It was stated in the literature that there were various biogranules including methanogenic, hydrogenic, aerobic, anaerobic ammonium oxidizing and aerobic photo-biogranules [189]. Figure 2-3 presented biogranules used for resource recovery in the treatment of wastewater with different pollution loads.

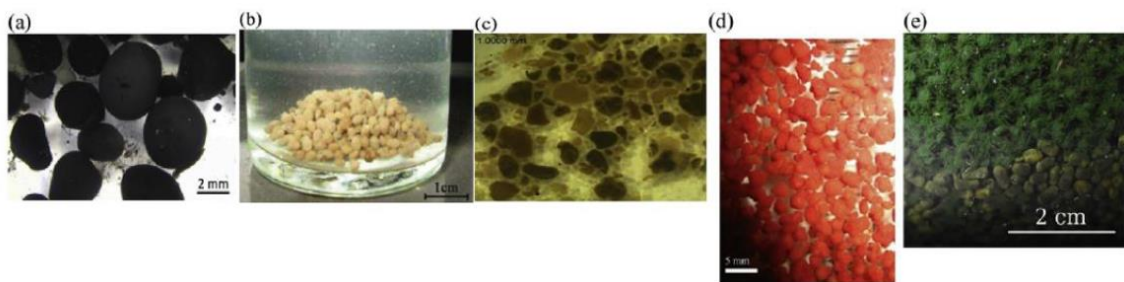


Figure 2-3. Various biogranules utilized in wastewater treatment and recovery of resources; (a) methanogenic biogranules, (b) hydrogenic biogranules, (c) aerobic biogranules, (d) ammonium oxidizing biogranules, (e) aerobic biogranules (replicated from [189])

As seen Figure 2-3, each biogranules has different microbial consortia depending on the metabolic activities. Therefore, biogranules may have different shapes, colors, and sizes due to microbial communities and their formation mechanisms. Considering the advantages and areas of use mentioned above, anaerobic, and aerobic biogranulation was considered as an innovative process technology over traditional activated sludge in biological nutrient removal systems (even in wastewater with high pollution load) in environmental engineering applications [190,192–196].

The production of biogranules for MICP applications was first developed by Ersan et al. in 2015 [153]. In this study, it was reported that denitrifying biogranules called non-axenic active compact denitrifying core (ACDC) were produced. It was reported that by adding dried biogranules into concrete mixture, bioconcrete could be developed to use

self-healing concrete cracks [153]. Sonmez et al. revealed that denitrifying biogranules could be used to improve recycled aggregates in terms of surface characteristics [159]. Song and Chetty et al produced non-axenic sulfate-reducing biogranules and reported that if these biogranules were added to concrete mixture in wet form, sulfate-induced concrete corrosion (sewer corrosion preventing) could be prevented, and self-healing bio-concrete can be obtained [96,176]. Granulation technology described for wastewater treatment sludge can be exploited to produce non-axenic microbial granules suitable for use in MICP applications.

In this way, biogranules can achieve MICP via urea hydrolysis and denitrification simultaneously and enable to increase biomineralization capacity. Both ureolytic bacteria and nitrate-reducing bacteria are effective in MICP studies and applications. Further efforts associated with biogranules are needed to use in MICP applications. In particular, studies on biogranules under severe environments including high-alkali medium and too low or high temperatures should be increased.

2.6. Selecting An Appropriate MICP Approach According to The Required or Target Conditions

Real-time and in-situ biotechnological applications in MICP driven by diverse and intricate metabolic pathways should be accurately determined. In order to achieve higher efficiency via MICP, a step-by-step manual approach including MICP application preference mentioned below [14]. Deciding on which metabolic pathway and under which conditions MICP application will be carried out is important to achieve efficient CaCO_3 precipitation [14]. It is possible to obtain an efficient CaCO_3 precipitate with the correct use of the approach mentioned in Figure 2-4.

To design an effective MICP protocol, determining parameters such as application type, metabolic pathway, bacterial species, and environmental conditions is of critical importance [14]. It is possible to apply the correct method with the approach depicted in Figure 2-4. These factors should be selected according to the chosen application criteria to achieve the target efficiency. However, other factors including environmental

conditions and characteristics of the target medium should also be considered before applying the procedure. In order to conduct a MICP procedure, three features must be essentially considered: (i) defining surroundings and application environment characteristics, (ii) defining the application goal, and (iii) defining and selecting the most appropriate application methods. A recommended procedure for creating an efficient MICP way offers illustrations of how efficient MICP procedure is performed. As illustrated in the diagram (Figure 2-4), the selection of microorganisms for MICP is affected by numerous parameters such as oxygenic conditions, temperature, exposure to chemicals. For instance, bacteria selection will vary depending upon oxygenic conditions which are aerobic, anaerobic, or anoxic. The approach in the scheme should be considered for the use of different types of bacteria such as *S. pasteurii*, *B. thuringiensis*, *P. aeruginosa*, *P. fluorescens*, *B. sphaericus*, *P. denitrificans*, *B. megaterium*, and *D. bacillus* which were frequently used in MICP applications in the literature [14]. MICP has a numerous application in geotechnical engineering, environmental engineering, and civil engineering, and ongoing research is performed rigorously [68,138,197].

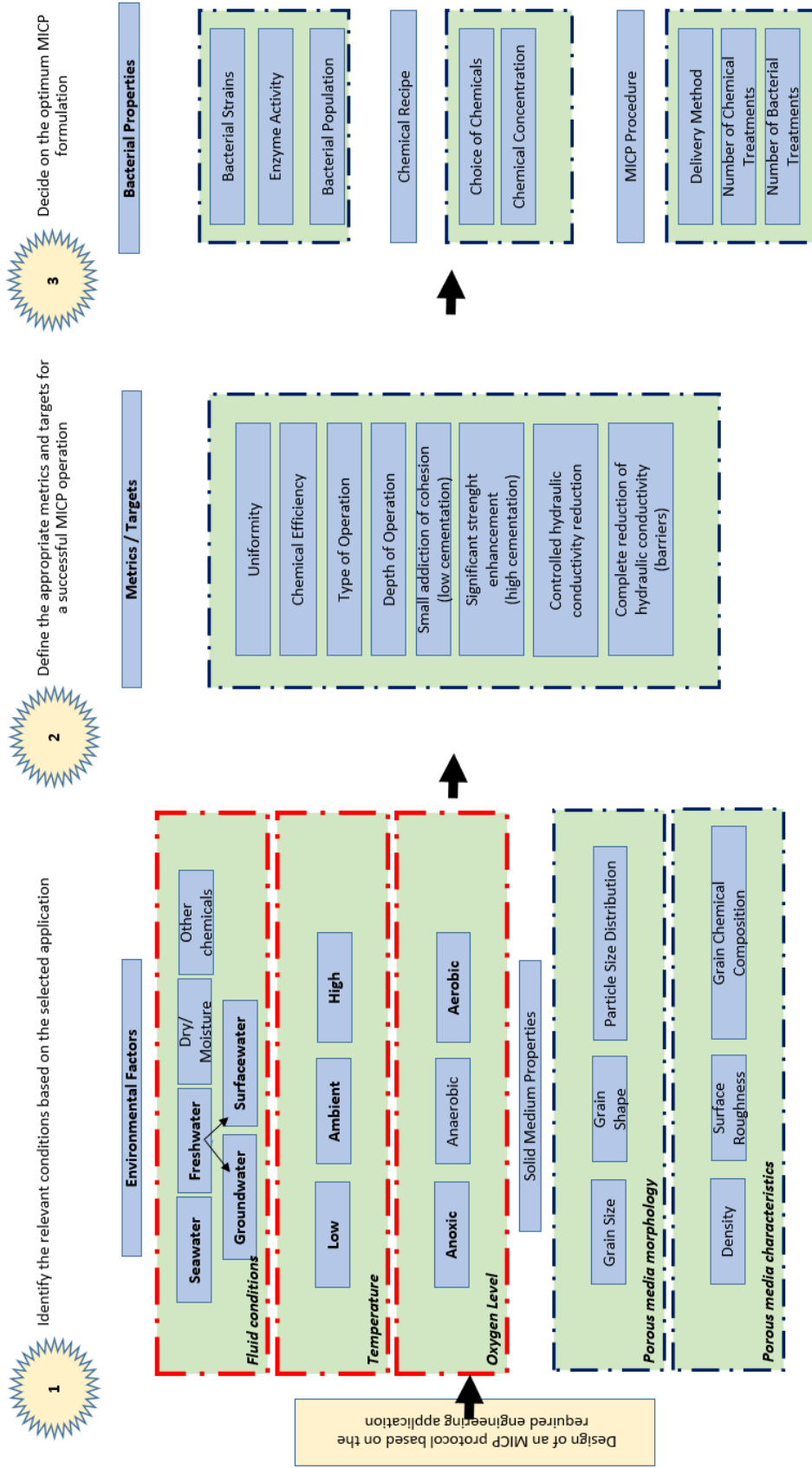


Figure 2-4. Selecting an appropriate MICP approach according to the required or target conditions (redrafted after [14])

2.7. Parameters Affecting Efficiency of MICP and Its Applications

MICP involves very complex biological and chemical reactions. Many biotic and abiotic parameters directly affect MICP. MICP is principally influenced by following crucial parameters: [61,136,198–200]

- (i) microbial species and microbial biomass concentration,
- (ii) enzymatic activity of MICP mediated bacteria,
- (iii) ambient temperature and salinity,
- (iv) pH,
- (v) influence of available Ca^{2+}

2.7.1. Microbial Species and Microbial Biomass Concentration

Different bacterial species and different microbial concentrations (biomass) were used by researchers in MICP studies. Microbial activities of bacteria species vary depending on the metabolic pathways. In addition, CaCO_3 precipitation rate is affected by microbial activity of bacteria and metabolic pathway [121]. It was emphasized in the literature that microorganisms with high urea hydrolysis activity provoked higher CaCO_3 precipitation [200]. Therefore, it was highlighted that bacterial species was a prominent factor in MICP applications. In addition to type of bacteria, bacterial concentration or number of microbial cells are among factors that affect CaCO_3 precipitation [121,198]. The type of bacteria also affects crystalline structure and morphology of CaCO_3 [39].

In some experiments with *S. pasteurii*, Mitchell et al. reported that higher bacteria concentrations lead to larger crystal structures and formation of more insoluble crystals [123]. It was also checked by Harkes et al. that as increasing bacteria concentrations, microbial activity and urea hydrolysis rate also increases [201]. Another study stated that there was increase in CaCO_3 precipitation by 30% when microorganisms' population was raised from 10^6 CFU/ml to 10^8 CFU/ml [149].

It was stated by Tourney et al. that bacterial density and secretion of microbial EPS influenced morphology and crystal structure of CaCO_3 minerals [202]. For example, EPS can hinder aragonite formation and trigger calcite formation [31,202]. It was also tested in another study that concentration of bacterial solution strongly affects CaCO_3 minerals morphology [25]. These minerals may vary depending on bacterial biomass or bacterial concentration [40,203]. The precipitation of most CaCO_3 crystals was sphere-shaped under dense bacterial concentrations. It was reported that at less intense bacterial solution concentration, a bit amount of minerals has asymmetrical forms, while others have regular cuboids-shape [31].

2.7.2. Enzymatic Activity of MICP Mediated Bacteria

It is depended on catalysis of organic or inorganic components by a wide variety of enzymes secreted by microorganisms during the MICP process. Each metabolic pathway is driven by secretion of different enzymes. For example, urea hydrolysis, which is metabolic pathway frequently used in the literature, is initiated by urease enzyme secreted by bacteria [105]. As in urea hydrolysis, reactions during nitrate reduction are carried out by enzymes [103]. Dissimilar to partial denitrification, enzymes such as NO_2^- reductase and N_2O reductase are also secreted in complete denitrification. If bacteria only secreted NO_3^- reductase enzyme, complete denitrification did not occur and NO_2^- accumulation occurs in the environment.

As is known, enzymes directly are affected by temperature [121,198]. Enzymes are sensitive to temperature exposure and are active at optimum ambient temperature for bacteria. If temperature is too high or low, enzymes will not function effectively. In addition, dissolved oxygen (DO) is also significant parameter in terms of enzymes production. For instance, it was revealed that production of urease enzyme mostly relied on aerobic conditions [123,150].

2.7.3. Ambient Temperature and Salinity

Fluctuations in environmental or ambient temperature directly affect microbial growth and metabolic activities. Therefore, ambient temperature affects type and morphology of

precipitated CaCO₃ crystals by affecting CaCO₃ precipitation rate and efficiency [199]. Microbial activity occurs at a higher rate at optimum temperature where bacteria have highest growth rate. It was reported that a positive correlation was obtained between temperature and microbial activity (mostly in urea hydrolysis), which varied depending on temperature [122,200]. According to the literature, it was stated that calcium carbonate minerals precipitated at higher rate at 20-30°C through urea hydrolysis, while precipitation rate significantly decreased at 10-15°C [204].

Salinity is also among the factors affecting MICP. In the literature, salt concentration, especially in soil and marine environment, significantly affects microbial activity and CaCO₃ precipitation [108,135,205–207]. The sensitivity of bacteria to salinity varies from species to species and salt concentrations [108,205,207]. While some bacteria have low CaCO₃ precipitation efficiency and rate in tests conducted at high salt concentrations, some bacteria can also achieve microbial activity and precipitate CaCO₃ even at high salt concentrations (marine water and hypersaline environments) [32,113,205,208]. It was reported in the literature that *S. pasteurii* could also precipitate CaCO₃ at high-salt concentrations (0.5-5% w/v) [113,208]. In addition, since *Bacillus* species have ability to adapt to a high saline environment, they can have CaCO₃ precipitation performance [51,209,210].

2.7.4. pH

pH of medium has a significant role for metabolic activity of bacteria and CaCO₃ precipitation via MICP. Studies carried out at different pH values for MICP applications enable introduction and implementation of this environmentally friendly approach [198–200]. Most of ureolytic microorganisms normally tested in MICP applications are appropriate for highly alkaline medium [77,136]. For instance, optimum pH value for *Bacillus* species to effectively precipitate CaCO₃ in MICP applications is approximately 9 [61,121].

In the literature, *S. pasteurii* was tested at different pH values [122]. It was stated that *S. pasteurii*'s microbial activity and CaCO₃ precipitation efficiency increased when ambient

pH was gradually elevated from 7 to 9.8 [9,121,122]. According to the literature, it was stated that the highest cell number of *S. pasteurii* could be reached when pH value was 8.6 [211]. It was stated that as pH value increases higher than 8.6, the number of bacterial cells gradually decreases [211].

It was also stated that extremely high pH could damage bacterial cells and inhibit or limit their enzymatic and metabolic activities. Therefore, in MICP applications such as self-healing concrete and biocement production where surroundings were extremely alkaline (pH 12-13), an encapsulation process in a protective material for bacteria might be required [76,129,146]. Most CaCO₃ precipitations occurred at highly alkaline conditions such as 8.5-9.5 of pH [61]. It was stated in the literature that when pH decreased, dissolution instead of precipitation occurs for CO₃²⁻ ions [33].

2.7.5. Influence of Available Ca²⁺ Source

The presence of Ca²⁺ in the environment is among the factors affecting CaCO₃ precipitation in MICP applications. It affects MICP and precipitated CaCO₃ morphology [30,31]. In addition, dissolved calcium concentration in the environment also affects microbial activity [26,33,39,212]. Another important issue is chemical components containing calcium source [49,213]. It was stated in the literature that Ca²⁺ supplies including CaCl₂, CaC₄H₆O₄, Ca(NO₃)₂ had an effect on crystal type of precipitated CaCO₃ in MICP [214].

2.8. The Scope and Goal of The Thesis Study

In recent years, studies on biogranule production and their testing for MICP applications have been commonly performed by Ersan, Sonmez, Sekercioglu, Ozbay and Kardogan [154,159,183,215,216]. In addition, Sekercioglu (2022), Ozbay (2023) and Kardogan (2024) carried out studies on production and applications of biogranules capable of simultaneous urea hydrolysis and denitrification [215]. Some preliminary findings showed that biogranules could outperform axenic cultures in MICP applications. It was also speculated that biogranules could eliminate the limitations occurring in different environmental conditions due to the sensitivity of axenic cultures. To the best of our

knowledge, no thorough or detailed study has been performed to reveal MICP performance of biogranules under varying environmental conditions. In addition, to confirm biogranules' advantages, it is necessary to assess the microbial activity and related MICP performance of biogranules with respect to two aspects: (i) the activity of inherently present axenic cultures, (ii) the activity of commonly investigated reference cultures. Therefore, it was planned to contribute to these deficiencies within the scope of this study. In addition, it would be possible to overcome some of the aforementioned drawbacks associated with axenic cultures in MICP applications and obtain higher efficiency in MICP applications. Therefore, it was expected to shed light on the research gaps and further needs in the literature by comparing biogranules with (i) inherently present axenic cultures and (ii) reference axenic cultures under different environmental conditions. In this study, biogranules produced by Kardogan (2024) were further tested in both wet and dried forms. Biogranules' adaptability to different environmental conditions and applicability to MICP according to changing environmental conditions were investigated.

Biogranules, pure cultures isolated from biogranules, ureolytic axenic strain (*Sporosarcina pasteurii* DSM 33), and nitrate-reducing axenic strain (*Pseudomonas aeruginosa*) were compared among each other under various environmental conditions in terms of biomineralization performances, urea hydrolysis and nitrate reduction activities. This study also had a unique importance in terms of determining the activities of pure cultures isolated from biogranules.

Comparisons were made based on microbial activities and total amount of precipitated CaCO_3 (i.e., biomineralization performance). The following were targets to be met in this respect:

- Determination of the effect of YE on microbial growth, resuscitation, and microbial activity of biogranules and the pure cultures
- Determination of biogranules' resistance to dehydration stress (wet/dry) and their resuscitation performance
- Comparison of the urea hydrolysis and nitrate reduction activities of biogranules with axenic cultures isolated from biogranules, as well as with two reference

axenic cultures each one representing a single metabolic pathway: (i) *Sporosarcina pasteurii* DSM 33 for urea hydrolysis pathway and (ii) *Pseudomonas aeruginosa* for nitrate reduction pathway

- Comparison of the calcium carbonate precipitation performance of biogranules with the isolated axenic cultures, and reference cultures, *Sporosarcina pasteurii* DSM 33, and *Pseudomonas aeruginosa*, at various environmental conditions (i.e., different dissolved oxygen, temperature, and salinity conditions)

3. MATERIALS AND METHODS

3.1. Operation Details of The SBR Reactor Produced Biogranules

Granular culture and biogranules, which were simultaneously capable of both urea hydrolysis and denitrification, were produced within the scope of the study conducted by Kardogan (2024). A sequencing batch reactor (SBR) with a 76 cm effective-height and a 4.5 cm diameter was operated to cultivate biogranules. The effective volume of this reactor was 1.2 L. In the scope of this thesis, previously produced biogranules were used in experiments. The hydraulic retention time (HRT) in SBR which produced biogranules was adjusted to 12 hours. During the operation of this reactor, four batch cycles were used day-to-day with each cycle consisting of three main periods: (i) a fill and draw period under anoxic conditions lasting two hours, (ii) a follow-up anoxic period with intermittent mixing lasting one hour, and (iii) an aerobic period lasting three hours. During the fill and draw period, this reactor was fed with a nutrient solution given in Table 3-1 at a rate of 5 ml.min⁻¹ for 120 minutes. In aeration period, the reactor content was aerated by using a time-adjusted aquarium air pump. The pH range of the nutrient solution was set to 9.8-10 to select alkali-tolerant microorganisms. Operational parameters of the biogranule production reactor were summarized in Table 3-2.

Table 3-1. The composition of the nutrient solution used for biogranules cultivation in the SBR

Chemicals	Concentration
Sodium nitrate (NaNO ₃)	1.1 g.L ⁻¹
Sodium formate (NaHCOO)	2.2 g.L ⁻¹
Yeast extract (YE)	0.05 g.L ⁻¹
Urea (CH ₄ N ₂ O)	1 g.L ⁻¹
Magnesium sulfate heptahydrate (MgSO ₄ .7H ₂ O)	0.09 g.L ⁻¹
Monopotassium phosphate (KH ₂ PO ₄)	0.01 g.L ⁻¹
Sodium chloride (NaCl)	0.5 g.L ⁻¹
Methanol (CH ₃ OH)	0.8 ml.L ⁻¹

Samples were taken on a routine weekly basis during operation of biogranules reactor. The pH, dissolved oxygen (DO), and total ammonium nitrogen (TAN), TSS, and VSS of biogranules used in the tests were measured regularly, at the end of both anoxic and aerobic periods and in the nutrient solution to monitor microbial activity and granulation. While the reactor was operated at completely mixed batch mode, a sample was taken from the reactor and examined under a light microscope to detect granules and flocs and determine size distribution of the agglomerates.

Table 3-2. Summary of operational parameters of biogranule production reactor

Parameters	Values of biogranule production reactor
Feed pH	9.8-10
Anoxic pH	9.1±0.2
Aerobic pH	9.1±0.2
Organic loading rate	2.9 g.COD. L ⁻¹ .d ⁻¹
NO ₃ -N loading rate	0.38 g NO ₃ -N.L ⁻¹ .d ⁻¹
Urea loading rate	2 g Urea.L ⁻¹ .d ⁻¹
Hydraulic retention time	12 h
VSS/TSS ratio	0.60
Anoxic period	180 min
Aerobic period	180 min
SVI ₃₀ /SVI ₅ ratio	0.80
Nutrient flow rate	5 ml.min ⁻¹

Representative micrographs of the biogranules utilized in this thesis were presented in Figure 3-1.

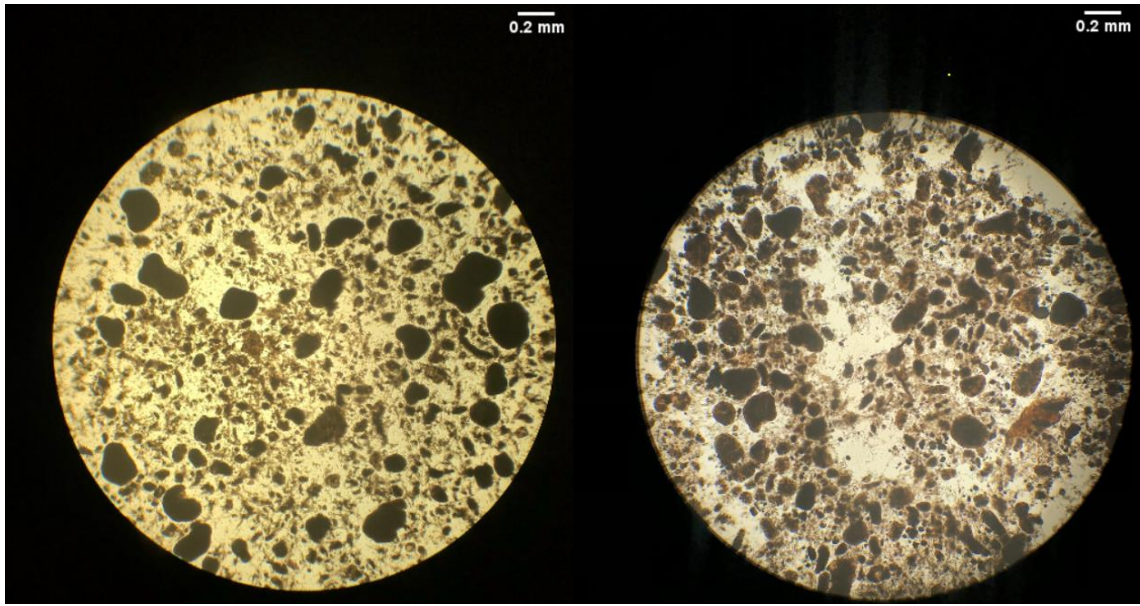


Figure 3-1. Representative micrographs of biogranules used in this thesis study

Size distribution analysis was performed by analyzing different micrographs of the harvested biogranules (randomly selected different micrographs and performed at least 10 size measurements on each selected micrograph by using ImageJ 1.53 image processing software). Approximately 90% of biogranules used in the tests were larger than 200 μm . Approximately 65% of biogranules were in the range of 200-300 μm .

3.2. Effect of Yeast Extract (YE) on Bacterial Growth, Dehydration, and Resuscitation of Biogranules

A solid-nutrient medium containing agar was prepared to use in the experiments. The solid-nutrient medium content was given in Table 3-3. The solid-nutrient medium was prepared in two types (YE containing and without YE). In order to ensure sterile conditions during the experiments, nutrient media, all glassware, and tools were autoclaved at 1 bar and 121°C for 20 minutes by using Nuve OT 40 L (Ankara, Türkiye) autoclave. Inoculations and sample taken were conducted in Nuve MN 120 (Ankara, Türkiye) laminar flow cabinet.

During the sterilization of media, non-autoclavable chemicals (2 $\text{g}\cdot\text{L}^{-1}$ $\text{CH}_4\text{N}_2\text{O}$ (urea), 0.09 $\text{g}\cdot\text{L}^{-1}$ $\text{MgSO}_4\cdot 7\text{H}_2\text{O}$, and 0.01 $\text{g}\cdot\text{L}^{-1}$ KH_2PO_4) were added using a sterile syringe filter

in the laminar flow cabinet. After preparation of the agar plates, one plate was separated to check possible contamination. The separated plate was left open in the laminar flow cabinet for one hour and then incubated at 28°C for 72 hours. This procedure was repeated during the preparation of each series of agar plates.

Table 3-3. The chemical ingredients of the solid-nutrient medium containing powder agar

Chemicals	Concentration
Pure powder agar	15 g.L ⁻¹
Sodium nitrate (NaNO ₃)	0.6 g.L ⁻¹
Sodium formate (NaHCOO)	6 g.L ⁻¹
Yeast extract (YE)	0.1 g.L ⁻¹
Urea (CH ₄ N ₂ O)	2 g.L ⁻¹
Magnesium sulfate heptahydrate (MgSO ₄ .7H ₂ O)	0.09 g.L ⁻¹
Monopotassium phosphate (KH ₂ PO ₄)	0.01 g.L ⁻¹

In order to observe YE effects on dehydration and resuscitation, wet and dried biogranules were tested in the presence and absence of YE. Mixed liquor sample was taken from the biogranules production reactor. The liquid sample (0.2 ml) was spread on agar plates via a sterile glass rod. The growth of bacteria present in wet biogranules were also tested in the presence and absence of YE. Mixed liquor sample taken from the biogranules reactor was used to inoculate agar plates via steak plate method.

Mixed liquor sample (25 ml) was taken from the biogranule production reactor, and this sample was dried in a drying oven at 60°C for 24 hours. Biogranules were cut into small pieces following drying process. After being cut into tiny pieces, dried biogranules were spread in pieces (fragment) onto solid-nutrient medium (medium content was given in Table 3-3) with and without 0.1 g.L⁻¹ YE.

These experiments lasted for 11 days. All agar plates were incubated at a 28°C in the incubator. After the incubation, growth was checked. All experiments were meticulously conducted in the laboratory. While carrying out the experiments, to prevent any contamination or cross-contamination, there was great attention to the sterilization of laboratory equipment, chemicals, and the environments where the experiments were carried out. In case of any contamination, the experiments were repeated.

3.3. Isolation of Inherently Present Bacteria from Biogranules

In order to isolate strains from the biogranules, the mixed liquor sample (25 ml) was taken from the biogranules production reactor. This sample was dried according to the aforementioned biogranule drying process (at 60°C, for 24 hours). In isolation process, only dried biogranules was used. The dried tiny biogranule pieces placed under sterile conditions on agar plates with and without 0.1 g.L⁻¹ YE concentration. The inoculated agar plates were incubated at 28°C for 72 hours.

At the end of the incubation period, a sterile inoculating loop was used to take samples from the bacterial growth area around biogranule pieces. These samples were added into fresh liquid nutrient medium (10 ml) and further incubated at 28°C for 72 hours. The fresh liquid medium had same composition with feed solution used for the biogranule production reactor (Table 3-1). Samples taken from the agar plates were named as Y and W, respectively. Y represented sample taken from agar plates containing YE. Dissimilar to Y, W represented sample taken from agar plate free YE.

At the end of 72 hours, grown liquid Y (Y1, and Y2) and W (W1) cultures were pasteurized at 80°C for 30 minutes and diluted by 10 times with the addition of sterile fresh medium. Same procedure was repeated until 1 L of liquid culture was achieved. In order to eliminate potential vegetative bacteria, obtained liquid cultures were pasteurized at 80°C for 30 minutes. Following pasteurization process, these samples were kept active by replacing 90% of the liquid with fresh sterile nutrient solution in every 72 hours. This cycle was repeated three times.

After pasteurization cycle, the treated grown samples were spread to the solid medium via streak plate technique. These inoculated solid mediums were incubated at 28°C for 72 hours. At the end of the incubation period, three distinct colony types were observed on each agar plate.

The distinct colonies were inoculated in the fresh sterile nutrient solution. These inoculated solutions were incubated again at 28°C for 72 hours. At the end of the first phase of the isolation, nine inoculated samples were obtained. Three of the nine samples were originating from the inoculum taken from agar plates without YE and thus named as WA, WB, and WC. The remaining six samples were originating from the inoculum taken from agar plates including 0.1 g.L⁻¹ YE and thus named as Y1A, Y1B, Y1C, Y2A, Y2B, Y2C.

3.4. Selection of Appropriate Strains Showing Decent Microbial Activity (Urea Hydrolysis and Nitrate Reduction)

Obtained cultures (WB1, WC2, YB1, and YC2) were incubated at 28°C for 72 hours in the fresh liquid nutrient medium enriched with 2 g.L⁻¹ YE. YE was provided to cultivate all cultures in a shorter term, so that the total experimental period could be shortened. At the end of the incubation period, samples were taken from the incubated culture solutions and analyzed for the production of total ammonium nitrogen (TAN) to determine the amount of hydrolyzed urea. TAN results of cultures were compared among each other.

Before the isolates (WB1, WC2, YB1, and YC2) were used in further experiments, their purity was checked for cultivation by streak plate method. These processes were repeated for all isolates. The obtained isolates were grown in Schott bottles (0.25 L, 0.5 L, and 1 L), and were incubated at 28°C in the fresh liquid nutrient medium enriched with 2 g.L⁻¹ YE, and 10 g.L⁻¹ urea for further tests.

TAN measurements of isolates demonstrating colony growth similar to *Bacillus* genus were compared with each other, and three different isolates with the highest urea hydrolysis activity (WB1, YB1, YC2) were selected to be employed in subsequent

experiments. At the same time, WC2 isolate, which had a different type of colony formation than other selected isolates, was also selected to be employed in further experiments. In total, four isolates (WB1, WC2X, YB1, and YC2) were tested.

3.5. Determination of 16S rRNA Gene Sequencing for Isolates

Isolated strains were identified upon 16s rRNA gene amplification analysis. EurX GeneMATRIX Bacterial & Yeast DNA isolation kit (Poland) was utilized for bacterial species determination and DNA isolation. This gene sequencing analysis procedure was given step by step below:

- Spectrophotometric measurement was conducted on the Thermo Scientific Nanodrop 2000 (USA) equipment to check DNAs' purity.
- The PCR study amplified aimed gene sites for species determination with 27F–1492R primers as universal primers. The primer sequences and PCR conditions were as follows:
5' AGAGTTTGATCMTGGCTCAG 3' (27F),
5' TACGGYTACCTTGTTACGACTT (1492R).
- A one-step PCR process was conducted to amplify the about 1470 base area. The PCR reaction was conducted with Solis Biodyne-FIREPol® DNA Polymerase (Estonia).
- In the PCR purification phase, MAGBIO "HighPrep™ PCR Clean-up System" (AC-60005) purification kit was used.
- For Sanger Sequencing samples, the ABI 3730XL Sanger sequencer (Applied Biosystems, Foster City, CA) and the BigDye Terminator v3.1 Cycle Sequencing Kit were used at the Macrogen Netherlands laboratory (Applied Biosystems, Foster City, CA).
- The CAP contig assembly algorithm was used within the BioEdit software to analyze the results obtained with the 27F and 1492R primers. Species determinations at the strain level were prepared according to the most similar species in the National Center for Biotechnology Information (NCBI) database.

3.6. Cultivation of Reference Ureolytic Strain (*Sporosarcina pasteurii* DSM 33)

Sporosarcina pasteurii (DSM 33) is a ureolytic axenic strain mostly used in MICP applications [217]. In literature, many studies revealed that *S. pasteurii* had high urea hydrolysis activity and high calcium carbonate precipitation yield in MICP applications [67,217,218]. Therefore, *S. pasteurii* (ureolytic axenic culture) was used as a reference ureolytic strain. *S. pasteurii* DSM 33 was provided from a stock culture. Lyophilized *S. pasteurii* DSM 33 culture was resuscitated and transferred in 10 ml liquid nutrient medium enriched with 10 g.L⁻¹ YE and 20 g.L⁻¹ urea (Figure 3-2).

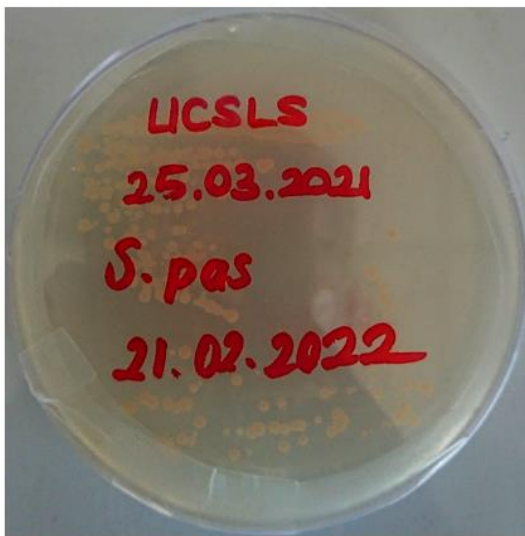


Figure 3-2. *Sporosarcina pasteurii* (DSM 33) (ureolytic axenic strain) colonies on agar medium

S. pasteurii was incubated at 30°C and kept active by replacing 90% of the liquid with fresh sterile nutrient solution in every 72 hours. At the end of each cycle, TAN measurement was conducted to determine urea hydrolysis activity.

3.7. Cultivation of Reference Nitrate Reducing Strain (*Pseudomonas aeruginosa*)

In the literature, *P. aeruginosa* was tested in most of the nitrate reduction based MICP studies [74,89,152,154,157]. Therefore, *P. aeruginosa* was preferred as the reference nitrate-reducing axenic strain.

P. aeruginosa was taken from the bacteria culture collection of Hacettepe University, Faculty of Science, Department of Biology. A *P. aeruginosa* colony was taken from the inoculated agar medium by using sterile inoculating loop and transferred into 10 ml liquid nutrient medium containing 0.6 g.L⁻¹ NaNO₃, 2.2 g.L⁻¹ NaHCOO, and 0.5 g.L⁻¹ YE (Figure 3-3). Inoculated tube was incubated at 30°C for 72 hours.



Figure 3-3. *Pseudomonas aeruginosa* (nitrate-reducing axenic strain) colonies on agar medium

P. aeruginosa was incubated at 30°C and kept active by replacing 90% of the liquid with fresh sterile nutrient solution in every 72 hours. At the end of this incubation period, a sample was taken to determine its NO₃-N measurement and confirm whether *P. aeruginosa* has the capability of nitrate-reducing activity.

3.8. Growth Curve Experiments for Isolates (WB1, WC2X, YB1, YC2), *Sporosarcina pasteurii*, and *Pseudomonas aeruginosa*

In order to observe the effect of YE on bacterial growth of the selected best performing isolates (WB1, WC2X, YB1, and YC2), *S. pasteurii*, and *P. aeruginosa*, these cultures were tested in batch reactors (200 ml). While the isolates were tested at 5 g.L⁻¹ YE concentration, *S. pasteurii* and *P. aeruginosa* were tested at various YE concentrations (0.05 g.L⁻¹, 0.5 g.L⁻¹, and 5 g.L⁻¹). Inoculated tube (20 ml) for each isolate were centrifuged at 3045 g for 5 minutes by using Nüve NF 800 centrifuge (Ankara, Türkiye),

bacteria collected at the bottom of the falcon tubes as pellets were resuspended in sterile nutrient solution.

The harvested or collected pellets were introduced into the batches. The inoculated batches were incubated at 28°C for 48 hours on a shaker at 100 rpm. Throughout the test, samples were taken at six-hour intervals to measure optical density at 600 nm via Beckman DU 530 UV/Vis Spectrophotometer (East Lyme, USA).

3.9. Preparation of Experimental Setup for Calcium Carbonate Precipitation Test Under Various Environmental Conditions

Serum bottles with 100 ml of volume were used as batches during biomineralization tests. Biomineralization tests were conducted in duplicates for biogranules, isolated strains from biogranules, *S. pasteurii*, and *P. aeruginosa* under various environmental conditions (dissolved oxygen (DO), temperature, and salinity). Test duration was set to six days in all tests. In all calcium carbonate (CaCO₃) precipitation tests (i.e. different environmental conditions), initial biogranule and bacteria concentrations were set to 0.5 g cell dry weight (CDW).L⁻¹.

In biomineralization tests, biogranules were tested in two different inoculum forms. In the first case, biogranules were taken directly from biogranule reactor and after washing with tap water, they were used as inoculum. This form of biogranules was referred as “wet biogranules” throughout the thesis. In the second case, taken biogranules were washed with tap water, and further dried before using as an inoculum in the biomineralization tests. This form of biogranules was referred as “dried biogranules” throughout the thesis. Isolated strains, *S. pasteurii* and *P. aeruginosa* were only tested in wet inoculum form.

Biogranule samples were taken from the biogranule production reactor at the end of the aeration phase and centrifuged at 3045 g for 5 minutes to separate the culture from the liquid medium. This centrifugation process was repeated 3 times by resuspending the biogranules in tap water in order to remove any residual substances coming from the

biogranule production reactor. TSS and VSS measurements were performed on the washed sample, and the amount of VSS was used to represent the cell dry weight (CDW). A portion of the washed biogranules was separated for further drying process. The remaining part of the washed biogranules was directly used as wet inoculum to set an initial bacteria concentration of 0.5 g CDW.L⁻¹ in batches. Part of the washed biogranules was dried at 60°C for 24 hours and dried biogranules were also used to set an initial inoculum concentration of 0.5 g CDW.L⁻¹ in batches.

The isolates were incubated at 28°C in the liquid nutrient medium enriched with 2 g.L⁻¹ YE, and 10 g.L⁻¹ urea. At the end of the incubation period, the isolates were centrifuged to collect as pellets. The cultivated samples were washed with fresh sterile nutrient solution to prevent any cross-contamination. After the washing process, the cultivated samples were centrifuged again and added to the test batches. Initial inoculum concentration was set to 0.5 g CDW.L⁻¹.

S. pasteurii grown in the liquid nutrient solution enriched with 10 g.L⁻¹ YE and 20 g.L⁻¹ urea was used in biomineralization tests. *P. aeruginosa* grown in liquid nutrient solution enriched with 2 g.L⁻¹ YE was used in biomineralization tests. The same centrifugation and washing process were also applied to *S. pasteurii* and *P. aeruginosa*. A minimal nutrient solution enriched with calcium ions was defined as biomineralization medium and given in Table 3-4. In the biomineralization medium, Ca(HCOO)₂, and Ca(NO₃)₂.4H₂O were used as calcium sources, and calcium formate and methanol (CH₃OH) were used as carbon sources. Initial dissolved calcium concentration was set to 2.6 g.L⁻¹ Ca²⁺. Biomineralization medium was sterilized by autoclaving at 1 bar, and 121°C for 20 minutes. In order to prevent degradation and precipitation of urea and methanol, stock solutions of these chemicals were prepared and further added to the autoclaved medium by filter sterilization. All the test equipment and test bottles were also autoclaved to ensure sterile test conditions.

Table 3-4. Composition of the biomineralization solution for tests under various environmental conditions

Chemicals	Concentration (g.L⁻¹)	Important parameters	Concentration (g.L⁻¹)
CH ₄ N ₂ O (Urea)	10	Urea	10
Ca(NO ₃) ₂ .4H ₂ O	2.11	NO ₃ -N	0.25
Ca(HCOO) ₂	7.3	COD	1.94
Yeast extract	0.05	Ca ²⁺	2.6
CH ₃ OH	0.11 ml.L ⁻¹	COD:N ratio (unitless)	7.75

Samples were taken from the batches every day and filtered through the syringe filters with a pore size of 0.45 µm. Filtered samples were stored in the refrigerator at +4°C for further analysis. Daily pH measurements were also performed. In all samples TAN, NO₃-N, NO₂-N, and Ca²⁺ concentrations were determined. At the end of the tests the amount of precipitated CaCO₃ was determined by using a carbon dioxide (CO₂) gas measurement method.

3.9.1. Oxygen

The effect of dissolved oxygen concentrations was tested in three different oxygen concentrations; (i) anoxic (<0.2 mg.L⁻¹), (ii) microaerobic (1.3 mg.L⁻¹), (iii) aerobic (4.8 mg.L⁻¹) conditions.

In order to create anoxic conditions and remove dissolved oxygen in the nutrient solution, nitrogen gas (N₂) was introduced into the batches and then the batches were tightly closed with a rubber stopper. In order to create microaerobic environment, the batches were closed by using cotton so that air could penetrate into the batches. In order to create aerobic environment, the batches were aerated by using air pumps. For all conditions, these tests lasted six days. The batches at oxygenic conditions were presented in Figure 3-4.

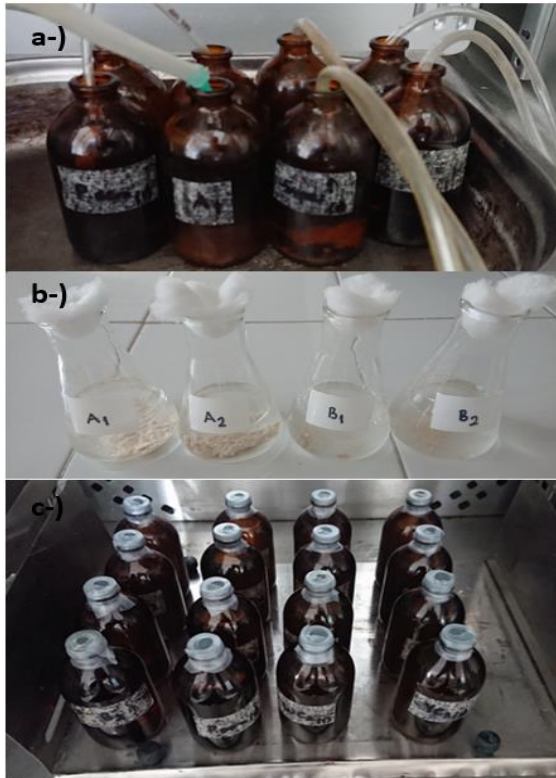


Figure 3-4. Batches in biomineralization test under different dissolved oxygen concentrations, (a) aerobic, (b) microaerobic, (c) anoxic

3.9.1.1. Assessment of Growth and Microbial Activity of *S. pasteurii* Under Anoxic Conditions

According to studies in the literature, microbial and enzymatic activity of *S. pasteurii* might be restricted under anoxic conditions. According to Martin and Mitchell et al., *S. pasteurii* did not grow under anoxic conditions and could not produce urease enzyme [123,150]. However, *S. pasteurii* grown under aerobic/microaerobic conditions produced urease enzyme [123,150]. Therefore, *S. pasteurii* could also hydrolyze urea under anoxic conditions. An experimental setup was prepared to test whether the results obtained with *S. pasteurii* in anoxic conditions were due to the aforementioned case. In this test, *S. pasteurii* was tried to be grown under anoxic conditions (in a nutrient solution enriched with 10 g.L^{-1} YE and 10 g.L^{-1} urea) instead of a microaerobic conditions.

At the same time, in order to observe a potential effect of YE on bacterial growth of *S. pasteurii* under anoxic conditions, these tests were performed in different YE

concentrations (10 g.L^{-1} YE and 0.05 g.L^{-1} YE). The bacterial growth of *S. pasteurii* could be obtained under anoxic conditions at a concentration of only 10 g.L^{-1} YE, and bacteria cells were collected by centrifuging at 3045 g for 5 minutes. After the centrifugation, cultivated bacteria was washed with a sterile nutrient solution that did not contain YE. *S. pasteurii* was prepared to be tested in wet and dry forms under anoxic conditions. The drying process was performed in a batch at 40°C for 48 hours. The test setup was demonstrated in Figure 3-5. In these tests, standard biomineralization solution was used (Table 3-4). All tests were conducted in duplicates.



Figure 3-5. *S. pasteurii* growth and tested under anoxic conditions

3.9.2. Temperature

The effect of ambient temperatures was tested in three different ambient temperatures; (i) 10°C , (ii) 22°C , (iii) 45°C . These different ambient temperatures were determined as follows; (i) 10°C to represent psychrophilic conditions, (ii) 22°C to represent mesophilic conditions, and (iii) 45°C to represent warm-climate conditions.

In order to keep temperature at 10°C , an incubator was used. In order to keep temperature at 22°C , the test conducted in a laboratory (laboratory temperature was around 22°C). In order to keep temperature at 45°C , an incubator was used. In all conditions, the test duration was six days.

3.9.3. Salinity

The effect of salt concentrations was tested in three different NaCl concentration; (i) marine water (35 g.L⁻¹ NaCl), (ii) drinking water, urban runoff, groundwater (1 g.L⁻¹ NaCl), (iii) rainwater (20 mg.L⁻¹ NaCl).

In order to create different salinity conditions, synthetic solutions with different NaCl concentrations were prepared in the laboratory. Synthetic waters were prepared according to the reported upper limits. In this thesis study, rainwater and marine water were also collected, and the conductivities of these samples were measured to confirm salt concentrations in the literature. Their conductivities were measured, and results were compared to the literature. The conductivity of collected rainwater was measured as 36 $\mu\text{S}\cdot\text{cm}^{-1}$, and the conductivity of marine water was measured as 53000 $\mu\text{S}\cdot\text{cm}^{-1}$. In the literature, it was generally mentioned that NaCl concentration of 33-35 g.L⁻¹ represented salinity of marine water [219–221]. Therefore, in the experiments, synthetic marine water with a NaCl concentration of 35 g.L⁻¹ was used to represent marine water salinity and its conductivity was measured as 51000 $\mu\text{S}\cdot\text{cm}^{-1}$. To represent tap water, urban runoff, and groundwater salinities, 1 g.L⁻¹ NaCl solution, which was the top salinity concentration in such waters, was used as the medium [222–225]. It was mentioned in the literature that salinity of rainwater was between 0-0.02 g.L⁻¹ [221,222]. Therefore, 0.02 g.L⁻¹ NaCl solution was used to represent rainwater. The prepared synthetic water samples were combined with biomineralization solution and CaCO₃ precipitation performances were performed at three different salt concentrations. For all conditions, these tests lasted six days.

3.10. Analytical and Experimental Methods

3.10.1. TAN Measurement

The amount of hydrolyzed urea was measured by TAN measurement. As a result of metabolic and microbial activity, urea transforms into NH₄⁺ as given in Table 2-1. During these reactions, two moles of ammonium are released at the end of hydrolysis of one mole of urea [26,120,226].

TAN measurements of the filtered samples were performed according to the standard method coded 4500-NH₃ Step-B, C (preliminary distillation step and titrimetric method) [227]. In the titration process, 0.02 N H₂SO₄ (sulfuric acid) was used as a titrant. TAN analysis of the samples was measured by using a BUCHI Distillation Unit K-350 (Flawil, Switzerland).

3.10.2. NO₃-N and NO₂-N Measurements

NO₃-N and NO₂-N concentrations of filtered samples were measured with HACH, LCK 340 and LCK 342 test kits, respectively. The detection ranges of the LCK 340 and LCK 342 test kits were between 5-35 mg.L⁻¹ NO₃-N and 0.6-6 mg.L⁻¹ NO₂-N, respectively. Accordingly, some samples were diluted with distilled water before the measurements to fall in the range.

3.10.3. TSS and VSS Measurement

TSS and VSS analyses were carried out according to the standard methods coded 2540-D and 2540-E [227].

3.10.4. Ca²⁺ Measurement

The dissolved calcium concentration in the samples was analyzed by using an AAS (Atomic Absorption Spectrometer) AAnalyst 800 PerkinElmer Türkiye in the Hacettepe University Environmental Engineering Department Laboratory. Samples taken from batches were diluted by using ultrapure water to measure dissolved calcium in AAS. In dissolved calcium measurements, to confirm that the AAS device made accurate measurements, standard calcium solutions (2 ppm, 4 ppm, 6 ppm, 8 ppm, and 10 ppm) were prepared, and a calibration graph was created by using the standard calcium solutions before initiating the measurements of the samples. A representative calibration curve was given in Figure 3-6.

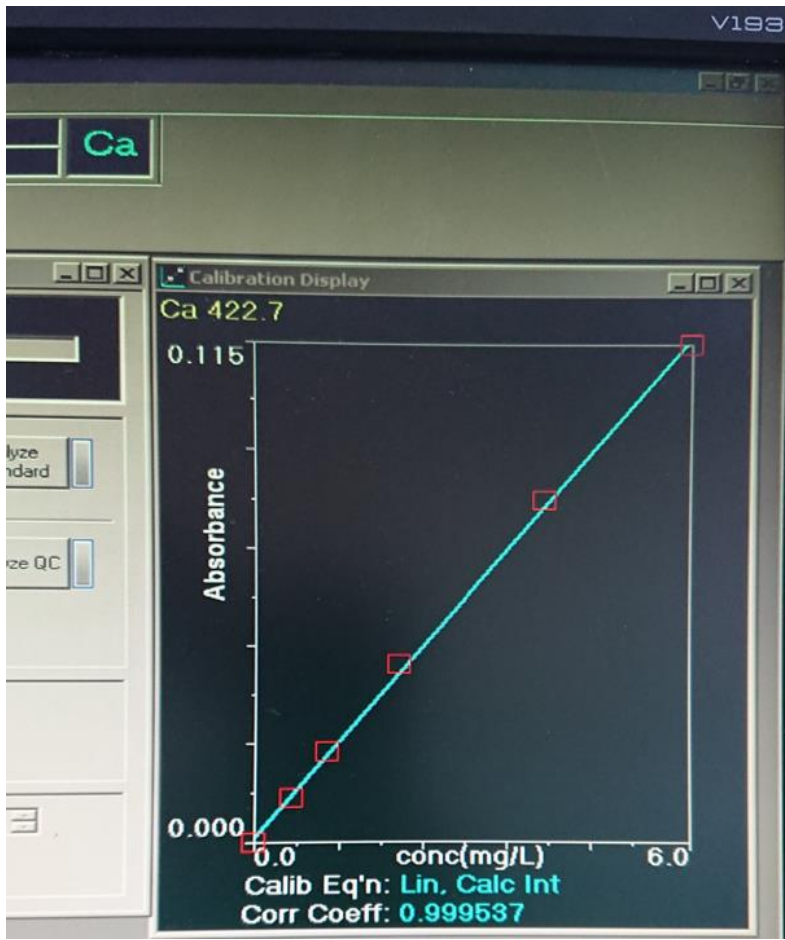


Figure 3-6. Calibration curve of standard calcium solutions

3.10.5. CaCO₃ Measurement

A carbon dioxide gas measurement method which was described in previous biomineralization studies [166,228], was used to determine the total amount of CaCO₃ precipitated under various environmental conditions in batches. In this method, the volume of CO₂ released from CaCO₃ in an acidic environment could be trapped in a water column and the amount of CO₂ could be calculated from the volumetric differences. The schematic representation and measurement setup and the details were given in Figure 3-7.

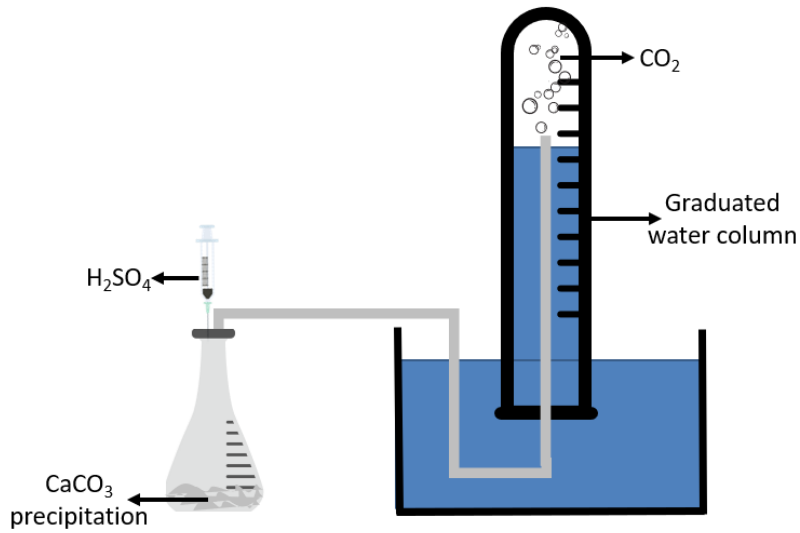


Figure 3-7. The schematic representation of CO₂ volume exchange method [166]

3.10.6. Dissolved Oxygen (DO) and pH Measurements

Dissolved oxygen (DO) measurements were made using the Hanna HI98193 DO meter device. pH measurements were performed using the Hanna HI98190 pH meter device.

4. RESULTS AND DISCUSSION

4.1. Effect of Yeast Extract (YE) on Bacterial Growth onto Solid Medium

Yeast extract (YE) was a significant nutrient substance for microorganisms. It was stated that YE provided rapid growth for bacteria due to its nutrient-rich content [229,230]. In order to detect the effects of YE on resuscitation and growth of bacteria, wet and dry biogranules were tested on agar plates. YE concentration in the agar plates was set to 0.1 g.L⁻¹ YE (at the same concentration as in the SBR bioreactor where granules were produced). It was observed that YE had a positive effect on bacterial growth and resuscitation.

In order to observe bacterial growth of undiluted samples, sample (0.2 ml) taken from the biogranule production reactor was dropped onto agar plates in the presence and in the absence of YE. The test lasted 11 days and changes between the first day and at the end of the 11th day were shown in Figure 4-1. In this test, since wet biogranules were dropped without diluting, bacterial growth is triggered within a shorter time. Bacterial growth without YE was observed encircled around the area where sample was poured. On the other hand, it was detected that bacterial growth on the solid medium enriched with YE (0.1 g.L⁻¹) was in the area where the sample was dropped and spread over a wider area (Figure 4-1).

More bacterial growth was observed in the medium enriched with YE. YE also had positive effect on bacterial growth and spread of bacteria onto solid medium Figure 4-1.

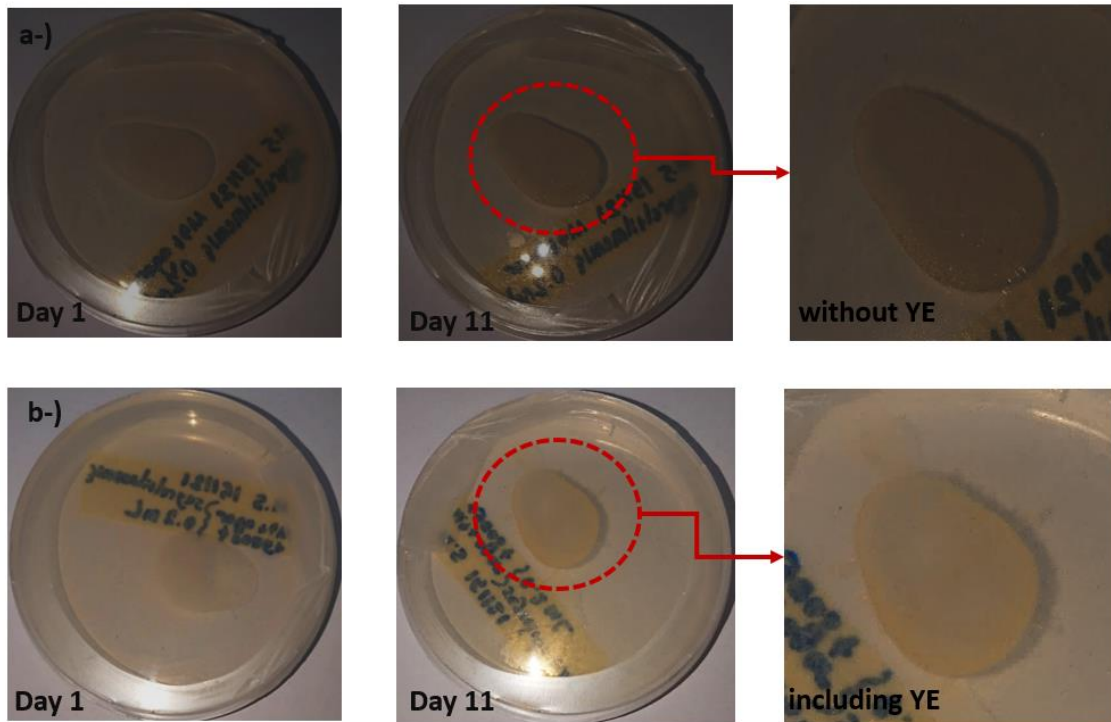


Figure 4-1. Bacterial growth of 0.2 ml biogranule in different solid medium for 11 days (a) solid medium no containing YE, (b) solid medium containing YE

4.2. Testing Biogranules for Their Resistance to Drying and The Resuscitation Performance of Inherently Present Bacteria

It was vital for MICP applications that biogranules could be stored in dried form and could be resuscitated after drying. Therefore, it was analyzed whether the microbial community in biogranules were resistant to desiccation and could be resuscitated following drying. The influence of YE on resuscitation performance of biogranules was also tested. In this test, biogranules was also tested to observe bacterial growth in the absence of YE, because YE was an undesired micronutrient in MICP applications due to its cost and its negative effects [127,152,166]. Therefore, the resuscitation of dried biogranules in the absence of YE was essential.

In this test, bacterial growth at the beginning and at the end of the experiment was observed and bacterial growth of dried biogranules were compared in the presence and absence of YE (Figure 4-2, Figure 4-3, and Figure 4-4).

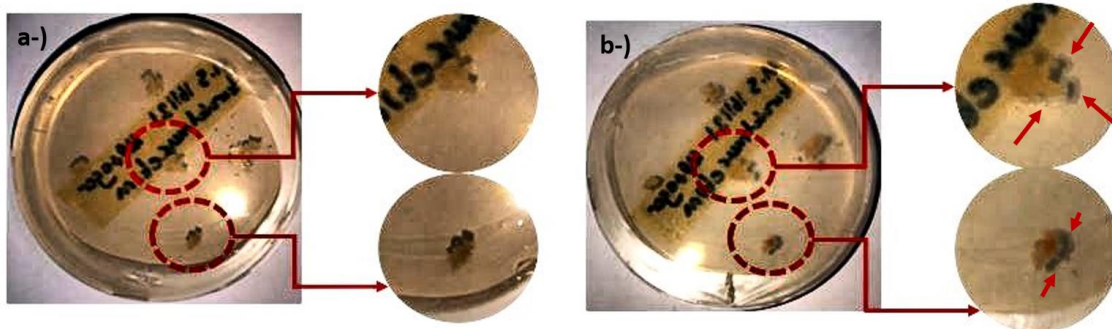


Figure 4-2. Change in the growth of biogranules dried at 60°C on agar solid medium in the absence of YE (a) 1st day, (b) at the end of the 11th day

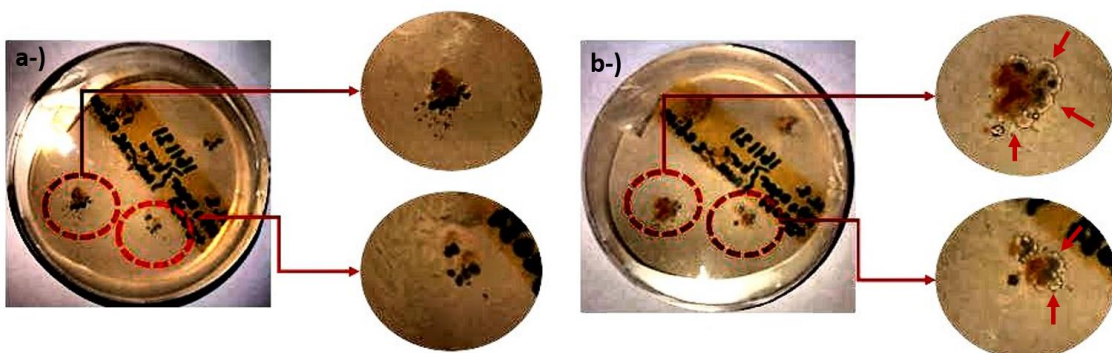


Figure 4-3. Change in the growth of biogranules dried at 60°C on agar solid medium in the presence of YE (a) 1st day, (b) at the end of the 11th day

Bacterial growth was observed around dried biogranule pieces from the second day. Bacterial growth was observed in a shorter time than on the solid medium without YE. On the one hand, this test demonstrated that YE had a positive effect on microbial growth as well as resuscitation of dried bacteria (Figure 4-3). YE also accelerated resuscitation of dried biogranules. These results were consistent with studies in the literature which investigated the positive effect of YE on microbial growth [229,230].

It was revealed that some of the inherently present bacteria in biogranules resuscitated and formed colonies on the solid medium (Figure 4-2). These results indicated that microbial community of biogranules had ability to resist dehydration and resuscitate in the absence of YE. It was revealed that biogranules could be dried and resuscitated similar to other granules in the literature [69,127,159,183].

It was stated in the literature that biogranules were more advantageous in MICP applications because they could be dried and stored in the dry form [231]. In addition, the long shelf life of dried biogranules and the preservation of their stability and structural integrity were mentioned among the advantages of the drying process [153]. Utilization of dried biogranules in MICP applications, especially in self-healing concrete applications, gained importance since it did not bring about any change in the structural properties of construction or concrete materials [92,159]. Biogranules became more resistant to environmental conditions because they produced extracellular polymeric substances (EPS) during cultivation, drying process, and spore formation [74,153,232–234]. This paved the way for dried granules to be stored for longer periods and to be used in harsh environmental conditions.

Wet biogranules were also added to the solid medium in the presence and absence of YE via the streak plate method (Figure 4-4).

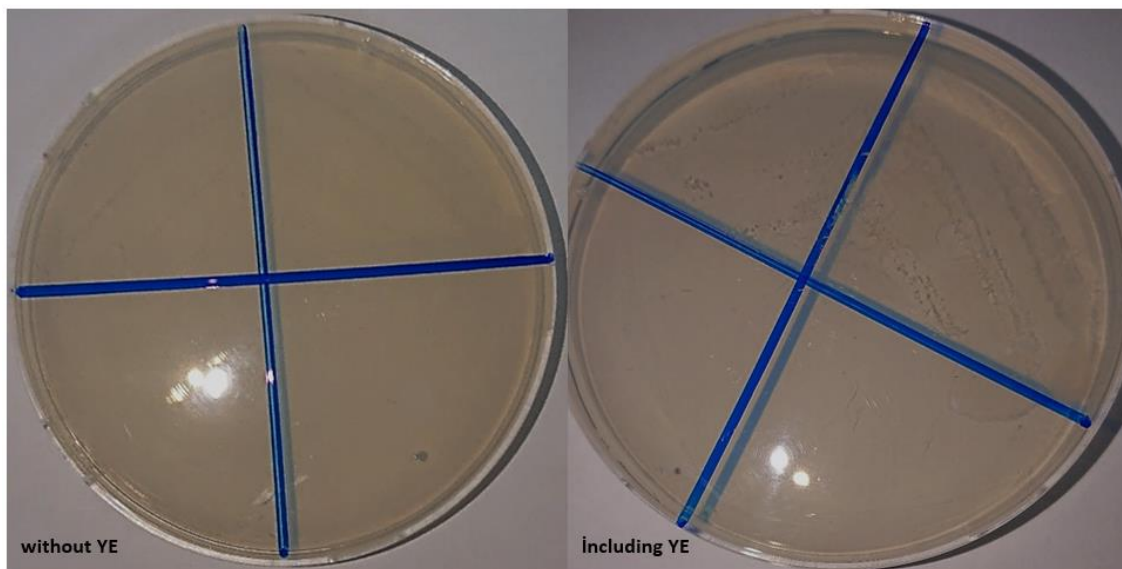


Figure 4-4. Bacterial growth on the solid medium at the end of the 11th day; (a) in the absence of YE, (b) in the presence of YE

The test performed by using the streak plate method was carried out to observe the effect of YE on bacterial growth. Bacterial growth in solid medium was monitored daily and changes between the first day and the 11th day were observed for both medium. While

bacterial growth was observed initiating from the second day in the medium containing YE, bacterial growth was observed after the fourth day in the medium without YE. It was observed that bacterial growth occurred in a shorter time and more clearly in the medium containing YE (Figure 4-4). In this test, the effect of YE on bacterial growth was also observed. As a result, YE had a positive and visible effect on bacterial growth.

4.3. Isolation of Pure Cultures and Their Selection Based on Microbial Performance

One of the objectives of this thesis was to compare biogranules with the axenic cultures inherently present in these biogranules in terms of microbial activity and biomineralization performance. This comparison was expected to reveal the advantages of the use of mixed non-axenic microbial communities over axenic communities in MICP applications. In literature, it was important that bacteria produced for biomineralization applications could be stored dry forms in terms of shelf life and ease of application [153,159,183]. It was revealed that biogranules used in this study could be dried and resuscitated in the presence and absence of YE. Therefore, the isolation was focused on isolation of the bacteria that could resist dehydration stress. To satisfy this condition, biogranules sample taken was dried at 60°C for 24 hours and the isolation process was carried out using completely dried biogranules.

4.3.1. The First Phase of The Isolation Process

In order to obtain isolates, dried biogranules were placed in different parts of the solid medium in the presence and absence of YE under sterile conditions. In this way, it was aimed to differentiate bacteria that could resuscitate in the absence and presence of YE. At the end of the incubation time, bacterial growth was observed in both solid medium, and bacterial growth were shown in the red circle (bacterial growth areas formed around biogranule pieces after 72 hours) (Figure 4-5).

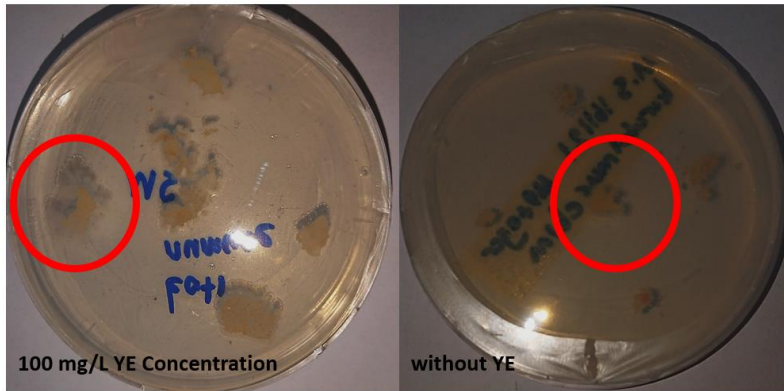


Figure 4-5. Dried biogranules into small pieces and growing them in solid medium containing or without YE

Bacterial growth observed around dried biogranule pieces was removed with a loop at the end of the third day and transferred into sterile liquid medium (Figure 4-6). Figure 4-6 presented liquid mediums which samples were grown before the isolation phase. At the end of the first phase of the isolation process, three microbial cultures were obtained.

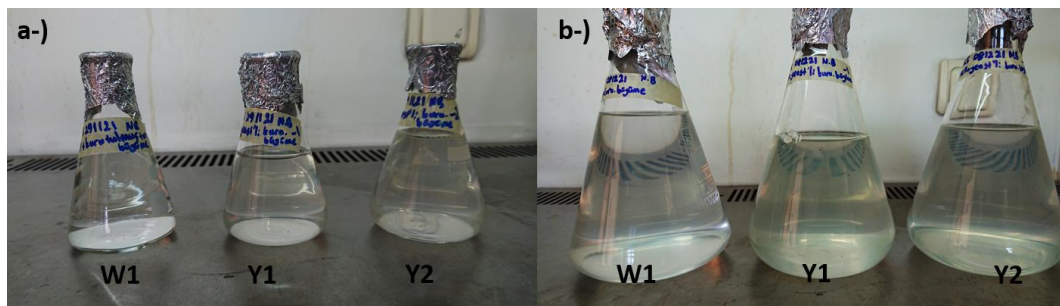


Figure 4-6. Samples transferred and grown in (a) 0.1 L and (b) 1 L

4.3.2. The Second Phase of The Isolation Process

Obtained W1, Y1, and Y2 samples were grown on solid media, and the different colonies in these cultures were detected (Figure 4-7). Since the colonies could not be seen clearly in the photographs, their contrast was improved with the ImageJ 1.53 image processing software. According to the visual examination, there were three different colony types in each bacterial culture. Therefore, a total of nine different cultures were obtained, three of which could survive and grow on the solid medium in the absence of YE, and six of which

could survive and grow on the solid medium in the presence of YE (WA, WB, WC, Y1A, Y1B, Y1C, Y2A, Y2B, Y2C).

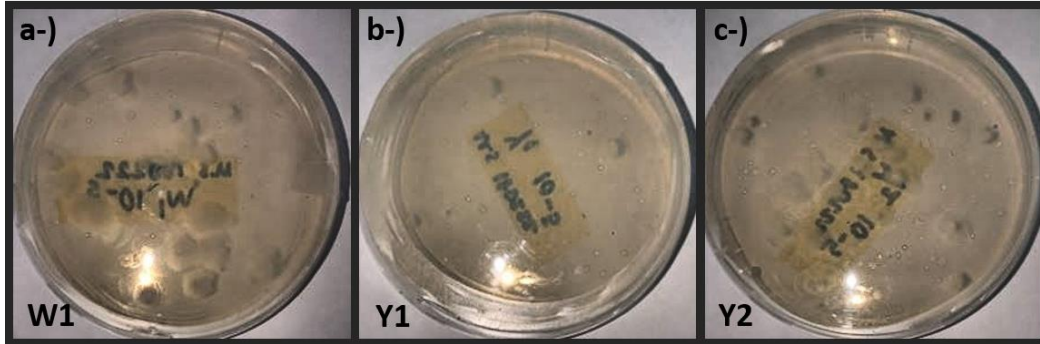


Figure 4-7. Grown in the first phase (a) W1, (b) Y1, (c) Different colonies formed by Y2 cultures on solid medium

At the end of three days, urea hydrolysis of nine bacterial cultures were compared with each other via total ammonium nitrogen (TAN) analysis. Hydrolyzed urea (%) results were given in Table 4-1. Bacterial cultures with the highest urea hydrolysis were determined as WA, WB, WC, Y1B and Y1C.

Table 4-1. TAN measurement of samples obtained in the second phase

Samples	TAN, mg.L⁻¹	Urea Hydrolysis, %
WA	302	32
WB	465	50
WC	448	48
Y1A	62	7
Y1B	314	34
Y1C	482	52
Y2A	73	8
Y2B	174	19
Y2C	101	11

4.3.3. The Third Phase of The Isolation Process

In order to test whether the selected cultures were axenic or not, these selected five cultures were further inoculated in the solid medium and the colony types were visually compared. Visual comparisons revealed that there were two different colonies in each culture. Different colony types were separately incubated again at 28°C for 72 hours. The purity of the obtained cultures was checked by the streak plate method (Figure 4-8).

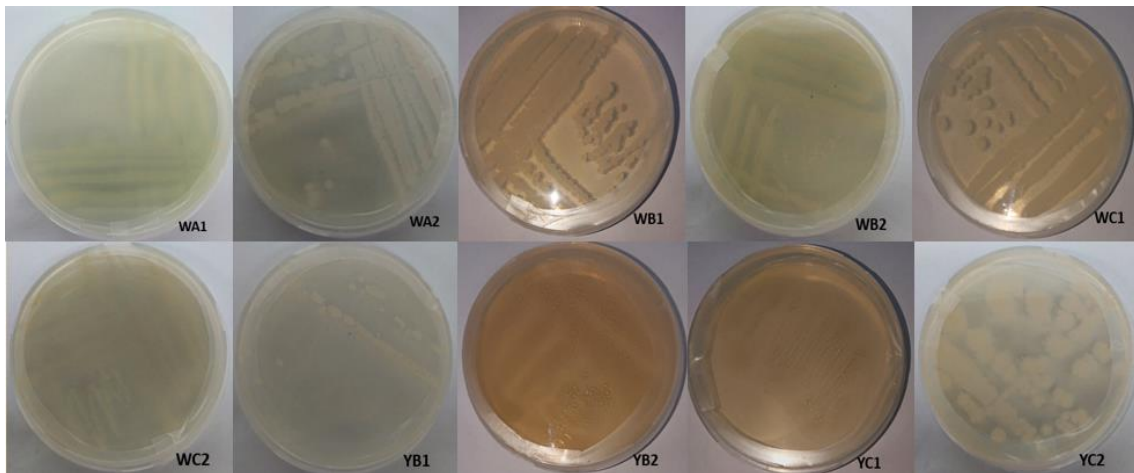


Figure 4-8. Isolates (axenic cultures) obtained from biogranules at the end of the third phase

It was determined that all cultures obtained at the end of third stage were pure cultures and the experiments were continued with these ten axenic cultures. These cultures were named as WA1, WA2, WB1, WB2, WC1, WC2, Y1B1, Y1B2, Y1C1, and Y1C2. The urea hydrolysis of 10 isolates were given in Table 4-2. According to urea hydrolysis results, top performing strains were determined as WB1, WC2, Y1B1 and Y1C2.

Table 4-2. TAN measurement results of isolates obtained after the third phase

Samples	TAN, mg.L ⁻¹	Hydrolyzed Urea, %
WA1	616	66
WA2	518	56
WB1	826	89
WB2	686	74
WC1	700	75
WC2	842	90
Y1B1	856	92
Y1B2	574	62
Y1C1	224	24
Y1C2	784	84

4.3.4. The Fourth Phase of The Isolation Process

While the purity tests for the cultivation of selected isolation were performed, it was detected that WC2 was not completely pure and formation of two different colonies was detected. The aforementioned method in previous phases was applied to obtain axenic WC2. At the end of the isolation process, WC2 was renamed as WC2X. Among the selected isolates, it was observed that the colony type of the WC2X was separate from the others (other isolates displayed colony growth similar to those of *Bacillus* genus).

At the end of the fourth phase of the isolation process, urea hydrolysis and NO₃-N was measured. WB1, YB1, and YC2 hydrolyzed urea, but WC2X did not hydrolyze urea. WB1, WC2X, YB1, and YC2 reduced 62%, 87%, 57%, and 48% of the initially provided 185 mg.L⁻¹ NO₃-N, respectively. Considering NO₃-N measurements, all isolates reduced nitrate, but the nitrate-reducing performance of WC2X was recorded to be higher than the other isolates.

4.4. Determination of 16S rRNA Gene Sequencing for Axenic Strains (Isolates)

Selected isolates were further identified via 16S rRNA gene amplification and sequencing. Obtained results were summarized in Table 4-3. Among the isolates, WB1, YB1 and YC2 revealed >99.6% similarity to ureolytic *Bacillus cereus*, which belonged to genus *Bacillus* commonly present in soil environment. Isolate WC2X showed 99.93% similarity to *P. aeruginosa* which was also known as a resilient gram-negative nitrate reducing bacteria widely present in dry and wet environments [155].

Table 4-3. Potential species of isolates according to 16s rRNA gene analysis

Samples	Nucleotide length	Taxonomic species	Similarity, %	Urease	Nitrate reductase
WB1	1406	<i>Bacillus cereus</i>	99.93	+	+
WC2X	1367	<i>Pseudomonas aeruginosa</i>	99.93	-	+
YB1	1412	<i>Bacillus cereus</i>	99.79	+	+
YC2	934	<i>Bacillus cereus</i>	99.68	+	+

In literature, there were several subspecies of *Bacillus cereus*. It was reported that the nucleotide sequences of *B. cereus* subspecies were similar to each other and thus clear distinction between subspecies of *B. cereus*, was not possible through 16S rRNA gene sequencing [235–237]. Nevertheless, distinction was still possible based on their enzymatic activities, particularly nitrate reductase and urease enzymes. In the literature, it was reported that *B. cereus* was both urease and nitrate reductase positive [238–241].

In the literature, *Bacillus paramycoides* (99.89%) and *Bacillus thuringiensis* (99.89%), were taxonomically defined as subspecies of *Bacillus cereus* and have identical 16s rRNA genes [242,243]. They were also determined to be both urease and nitrate reductase positive. Other subspecies with the same similarity, *Bacillus nitratireducens* (99.86%) and *Bacillus gaemokensis* (99.69%), were found to be positive for nitrate reductase, but there was no information about the presence of urease enzyme [244,245]. Similar to

Bacillus nitratireducens, and *Bacillus gaemokensis*, *Bacillus mycoides* (99.93%) was found to be urease positive, but there was no information about the presence of nitrate reductase enzyme [115]. These results indicated that more molecular analyses were required to distinctly define the strains and their enzymes which was beyond the scope of this master's thesis. Therefore, in this thesis study WB1, YB1, and YC2 were defined as *Bacillus cereus*, and WC2X was defined as *Pseudomonas aeruginosa*. Nonetheless, since the subspecies of *Bacillus cereus* were not clarified, the isolates were used with their coded names in the presentation of the results.

After drying process, biogranules were resuscitated and metagenome analyzes were performed on the samples taken on the first and third days of the resuscitation process. The dominant species in the resuscitated culture as a result of metagenome analysis were given in Figure 4-9. According to these results, at the end of 72 hours resuscitation period, 60% of the resuscitated community composed of *Sporosarcina* sp. and *Bacillus* sp. species. In isolation process, three of four isolates were identified as *Bacillus cereus*. This revealed that the results were consistent with each other. It was observed that *Bacillus* sp., capable of urea hydrolysis and nitrate reduction, were species that resuscitated most rapidly in dried biogranules.

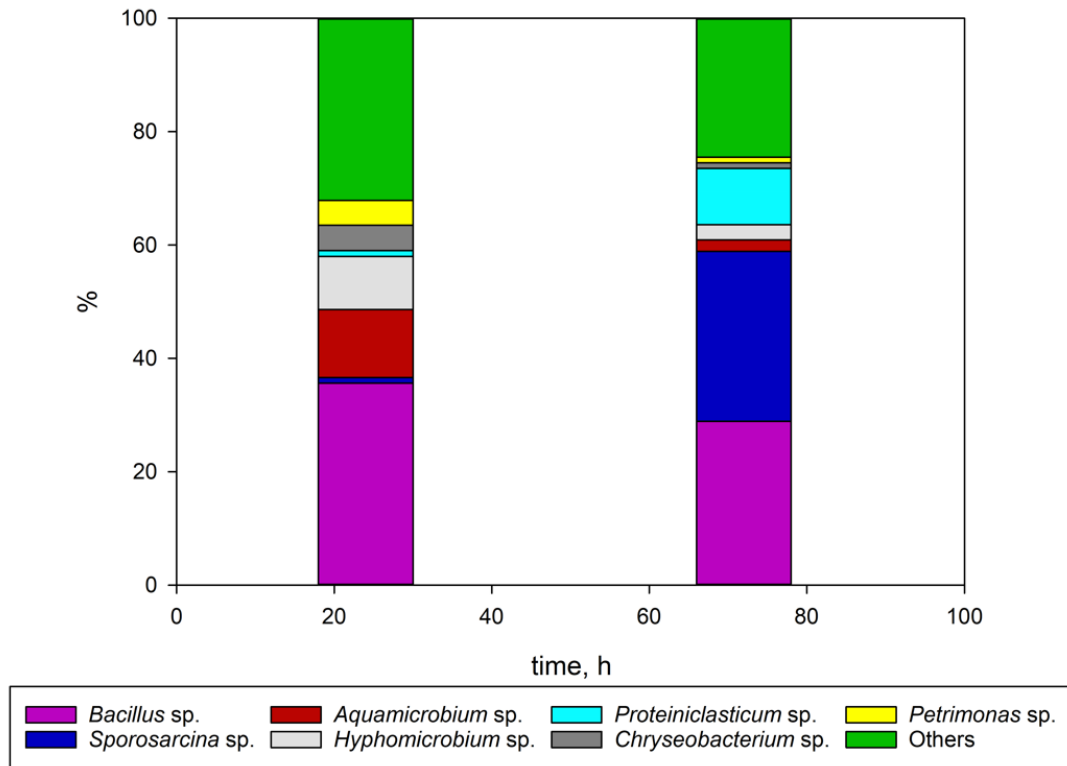


Figure 4-9. Dominant species resuscitated from dried biogranules

It was stated in the literature that *Bacillus cereus* were used in MICP applications, especially soil improvement, soil stabilization, and heavy metal removal from contaminated sites [246–249]. Identification of the isolates as *Bacillus cereus* and *Pseudomonas aeruginosa* confirmed that these isolates were potential candidates for MICP applications. Because, in the literature, *Bacillus cereus* and *Pseudomonas aeruginosa* were tested in MICP applications such as ground improvement, and self-healing concrete. Considering that biogranules were also produced for MICP applications, the comparison of biogranules with these inherently present cultures became more meaningful.

4.5. Microbial Growth Characteristics of Isolated Cultures

In order to compare bacterial growth of isolates and observe effects of YE on bacterial growth, a growth curve experiment was conducted for the isolates. The initial (t=0 h) and final (t=48 h) conditions in the growth curve experiment for pure cultures (WB1, WC2X,

YB1, YC2) were given in Figure 4-10. Bacterial growth of each isolate was expressed as optical density at 600 nm and presented in Figure 4-11.

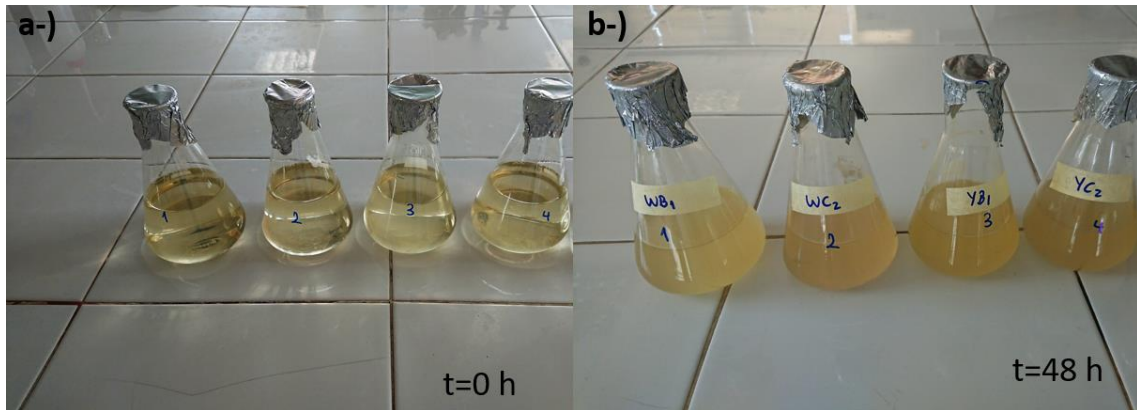


Figure 4-10. Growth related turbidity change during cultivation of axenic cultures; (a) t=0 h; (b) t=48 h

Results in Figure 4-11 revealed that the adaptation phase (lag phase) lasted less than six hours for all isolates. Exponential growth occurred between 6-24 hours. Afterward, the growth rate slowed down, and the samples reached the stationary phase at 30th hour. The highest microbial growth was recorded for WB1 and YB1. YB1 and WB1 isolates were observed to have similar growth curves. Exponential growth and adaptation phases for these isolates appeared to be similar. YC2 isolate showed less growth than YB1 and WB1 isolates. It was observed that the WC2X isolate had the lowest optical density.

According to the growth curve graph, the growth of WB1, YB1 and YC2 in the first 12 hours was similar. Growth curves began to vary after the 12th hour. After the 12th hour, WB1 and YB1 showed faster growth, while YC2 and WC2X showed less growth. As a result, according to the growth curves, while WB1 and YB1 showed similar growth rates, it was observed that YC2 and WC2X differed from them. Considering that WB1 and YB1 and YC2 isolates were *Bacillus cereus*, it was determined that similar species had similar growth curves.

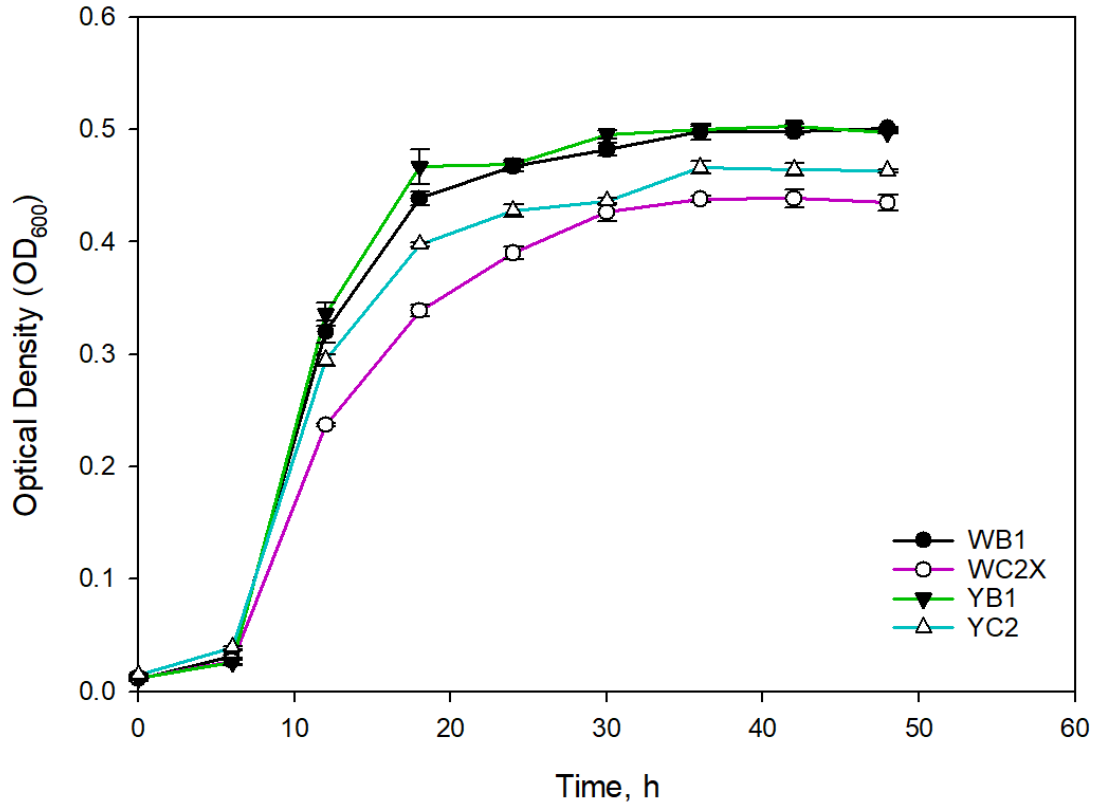


Figure 4-11. Growth curves of isolated strains in a minimal nutrient solution enriched with 5 g.L⁻¹ YE

4.6. Assessment of Ureolytic Reference Strain (*Sporosarcina pasteurii* DSM 33)

Sporosarcina pasteurii (DSM 33) is a ureolytic bacterial strain commonly used in MICP applications due to its high and non-suppressive ureolytic activity [218,250–252]. Therefore, in this thesis, *Sporosarcina pasteurii* (DSM 33) was used as a reference axenic culture to compare with wet and dried biogranules in terms of urea hydrolysis activity and biomineralization performance.

The urea hydrolyze performance of *S. pasteurii* was tested in fresh liquid medium enriched with 10 g.L⁻¹ YE and 20 g.L⁻¹ urea. *S. pasteurii* hydrolyzed 90% of 20 g.L⁻¹ initial urea in 48 hours. In the presence of high urea concentration (>20 g.L⁻¹) and high YE concentration (>10 g.L⁻¹), *S. pasteurii* hydrolyzed approximately 90% of initial urea in the environment. The obtained findings were consistent with previous studies and the literature [119,253–256].

In order to observe effects of different YE concentrations on bacterial growth, a growth curve experiment was performed for *S. pasteurii* at different YE concentrations (0.05 g.L^{-1} , 0.5 g.L^{-1} , 5 g.L^{-1}). The initial ($t=0 \text{ h}$) and final ($t=48 \text{ h}$) appearance of the *S. pasteurii* cultures were given in Figure 4-12.

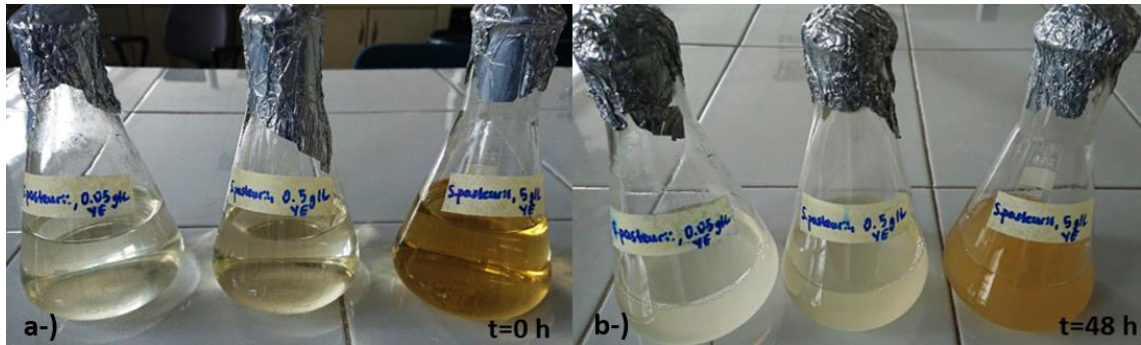


Figure 4-12. First and last hour images of the growth curve experiment performed at different YE concentrations (0.05 g.L^{-1} , 0.5 g.L^{-1} , 5 g.L^{-1})

Growth curves of *S. pasteurii* were given in Figure 4-13. According to growth curve graph, higher optical density value was detected in the batch enriched with 5 g.L^{-1} YE. It was observed that as YE concentration increased, optical density values also increased. The exponential phase ended after 24 hours for all conditions, and no growth was observed in the remaining period. The adaptation (lag phase) phase lasted less than six hours in the batch enriched with 5 g.L^{-1} YE than in other batches (Figure 4-13). The adaptation phase (lag phase) at 0.05 g.L^{-1} and 0.5 g.L^{-1} YE lasted approximately 12 hours. It was observed that YE (5 g.L^{-1}) shortened adaptation phase of *S. pasteurii*. Exponential growth was observed for this batch between 6 and 18 hours. Afterwards, the growth rate slowed down, and reached its highest level. The stationary phase of batch enriched with 5 g.L^{-1} YE started to be detected after 24 hours.

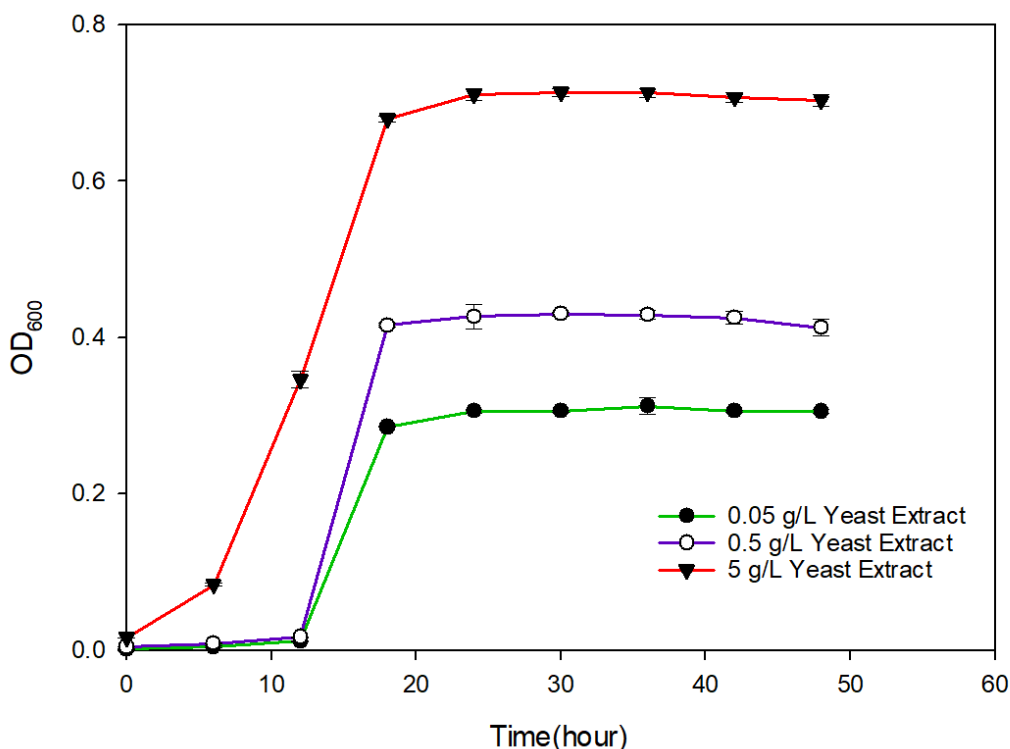


Figure 4-13. Growth curves for *S. pasteurii* (DSM 33) at different YE concentrations (0.05 g.L⁻¹, 0.5 g.L⁻¹, 5 g.L⁻¹)

Exponential growth in other batches (0.5 g.L⁻¹ and 0.05 g.L⁻¹ YE) occurred between the 12th and 18th hours. Afterwards, the growth rate slowed down, and optical density of the reactors became more stable. The effect of different YE concentration on bacterial growth was observed in this experiment. YE concentration directly affected microbial growth of *S. pasteurii*. As a result, YE had positive effect on bacterial growth and microbial activity. With this positive effect, YE changed their adaptation and exponential phase period.

Urea hydrolysis of *S. pasteurii* were given in Figure 4-14. According to this graph, urea hydrolysis performances of *S. pasteurii* at different YE concentrations altered with YE concentrations. As YE concentration in the medium increased, bacterial growth and microbial activity (urea hydrolysis) increased. It was revealed that microbial activity of *S. pasteurii* was varying with YE concentrations. Microbial activity was observed higher in the batch enriched with 5 g.L⁻¹ YE. At the end of the experiment (48th hours), *S. pasteurii* hydrolyzed %70, %36, and %16 of initial 10 g.L⁻¹ urea at 5 g.L⁻¹ YE, 0.5 g.L⁻¹ YE, and 0.05 g.L⁻¹ YE, respectively. Urea hydrolysis activity of *S. pasteurii* was stable at

all YE concentrations in the stationary phase (24th hours). After the 24th hour, urea hydrolysis of *S. pasteurii* considerably slowed down and even remained stable at three different YE concentrations. In 24 hours, *S. pasteurii* hydrolyzed %67, %33, and %14 of initial 10 g.L⁻¹ urea at 5 g.L⁻¹ YE, 0.5 g.L⁻¹ YE, and 0.05 g.L⁻¹ YE, respectively.

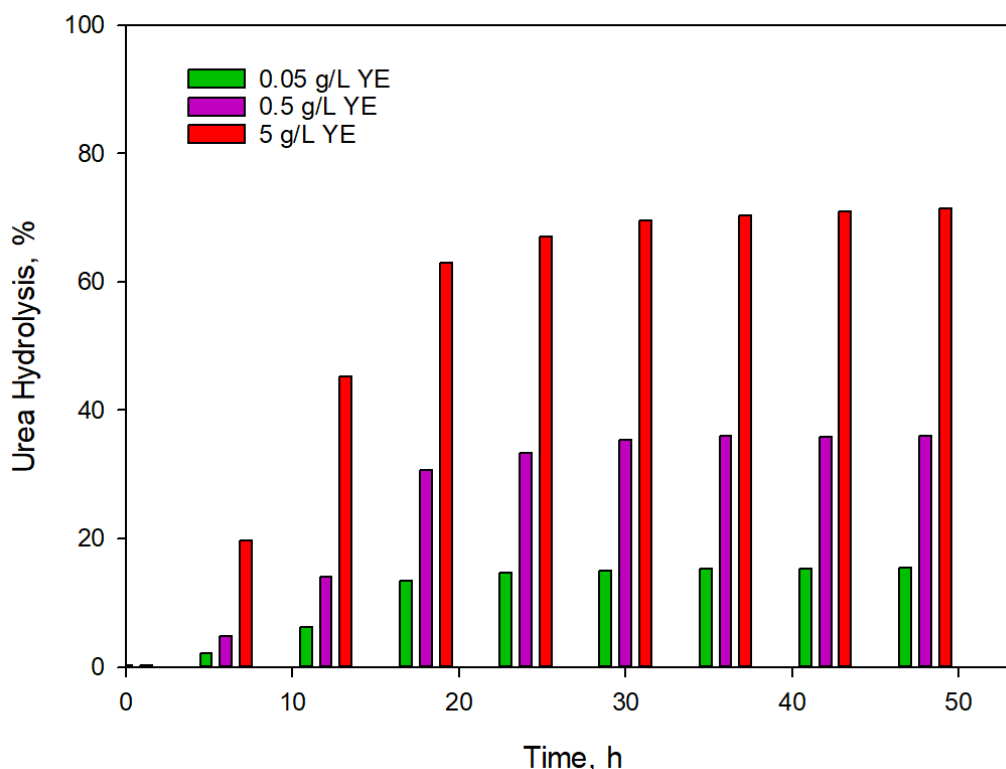


Figure 4-14. Urea hydrolysis of *S. pasteurii* (DSM 33) at different YE concentrations (0.05 g.L⁻¹, 0.5 g.L⁻¹, 5 g.L⁻¹)

4.7. Nitrate-Reducing Axenic Strain (*Pseudomonas aeruginosa*)

In this study, *P. aeruginosa* was used in the tests as a reference nitrate-reducing axenic strain in order to compare the denitrification activities of biogranules and isolates. In order to determine whether *P. aeruginosa* had nitrate reductase enzyme and whether it could denitrify, a sample was taken from the grown culture enriched with 0.5 g.L⁻¹ YE. NO₃-N measurement was made and nitrate reduction activity was determined as 0.47 mg NO₃-N.L⁻¹.h⁻¹. This result was consistent with the literature [257]. This result also indicated that nitrate reductase was positive.

In order to observe effects of different YE concentrations on bacterial growth, a growth curve experiment was performed for *P. aeruginosa* at different YE concentrations (0.05 g.L⁻¹, 0.5 g.L⁻¹, 5 g.L⁻¹). The initial (t=0 h) and final (t=60 h) conditions in the growth curve experiment for *P. aeruginosa* was given in Figure 4-15.

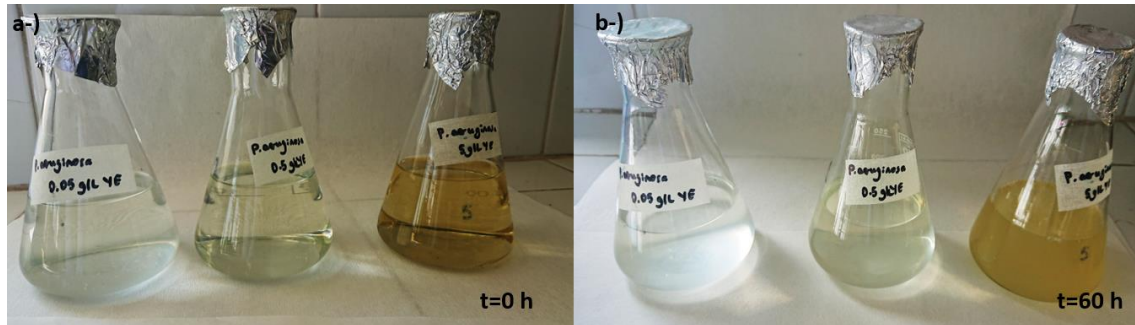


Figure 4-15. First and last hour images of the growth curve experiment for *P. aeruginosa* performed at different YE concentrations (0.05 g.L⁻¹, 0.5 g.L⁻¹, 5 g.L⁻¹)

Growth curves of *P. aeruginosa* were given in Figure 4-16. According to this graph, higher optical density value was detected in the batch enriched with 5 g.L⁻¹ YE. It was observed that as the YE concentration increased, optical density values also increased. In the literature, it was stated that OD₆₀₀ values of *P. aeruginosa* are very low when tested on low YE or no YE containing medium [154]. In this test, it was observed that the OD₆₀₀ values of *P. aeruginosa* at low YE concentration decreased significantly and were similar to the study in the literature. While the adaptation (lag phase) at 5 g.L⁻¹ YE lasted less than six hours, the adaptation phase (lag phase) at 0.05 g.L⁻¹ and 0.5 g.L⁻¹ YE lasted approximately 12 hours. As YE concentration gradually increased, the adaptation phase shortened, and microbial activity increased. Exponential growth was observed for this batch between the 6th and 48th hours. Afterwards, the growth rate slowed down, and transition to a stationary phase. The adaptation phase (between 0 and 12 hours) took longer in batches containing low YE concentrations (0.5 g.L⁻¹ and 0.05 g.L⁻¹). The growth rate was slower in these batches. Optical density was measured more stable after the 48th hour (Figure 4-16).

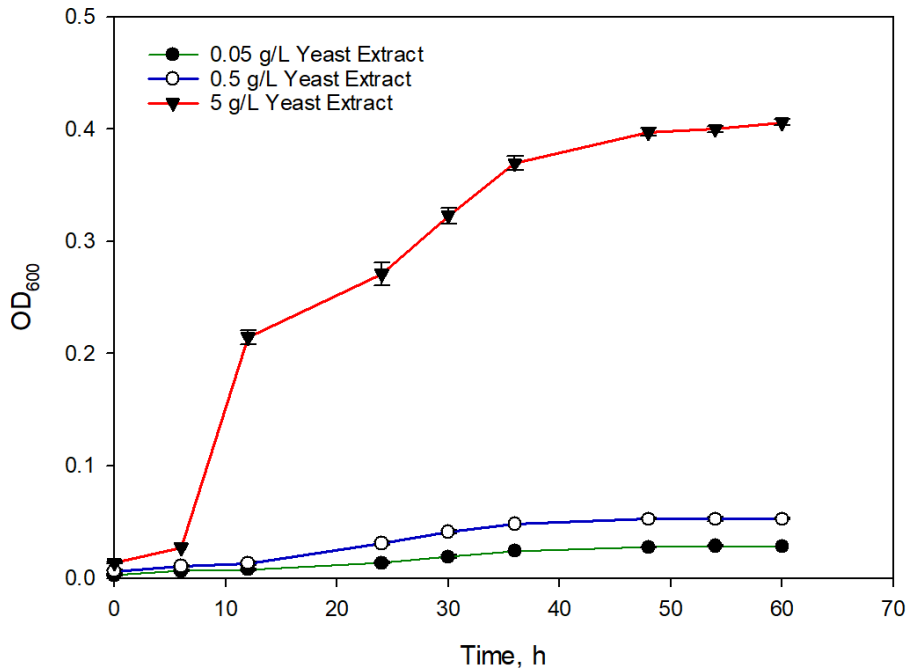


Figure 4-16. Growth curves for *Pseudomonas aeruginosa* at different YE concentrations (0.05 g.L⁻¹, 0.5 g.L⁻¹, 5 g.L⁻¹)

For different YE concentrations (0.05 g.L⁻¹, 0.5 g.L⁻¹, 5 g.L⁻¹), nitrate reduction activities measured as 0.3 mg NO₃-N.L⁻¹.h⁻¹, 0.4 mg NO₃-N.L⁻¹.h⁻¹, and 1.9 mg NO₃-N.L⁻¹.h⁻¹ respectively. YE had positive effect on the microbial growth and microbial activity of *P. aeruginosa*. It was revealed that this positive effect shortened lag phase period and increased microbial activity.

4.8. Calcium Carbonate Precipitation with Biogranules and Axenic Cultures at Different Dissolved Oxygen (DO) Concentrations

The aim of these tests was to observe effects of different DO concentrations on microbial activity and biomineralization performance and to compare biogranules with the axenic cultures and isolates in terms of microbial activity and biomineralization performance. Tests were conducted at three different DO concentrations; (i) anoxic (<0.2 mg.L⁻¹), (ii) microaerobic (1.3 mg.L⁻¹), and (iii) aerobic (4.8 mg.L⁻¹) conditions. For all conditions, test duration was set to six days.

The initial pH value of the nutrient solution was measured as 7.2 ± 0.2 at different DO concentrations (aerobic, microaerobic, and anoxic conditions). The pH values measured at the end of the sixth day of the tests were presented in Figure 4-17. At the end of the sixth day, pH elevated in all batches compared to the initial point. While the pH of dried biogranules, *P. aeruginosa*, and isolates measured stably, *S. pasteurii* and wet biogranules elevated rapidly. The pH of batches with high microbial activity increased more than those with low microbial activity (Table 4-4, Figure 4-17). The main reason for this was the generation of an alkaline environment for biomineralization. The alkalinity produced led to a higher and faster rate of CaCO_3 precipitation (Table 4-8).

Under aerobic and microaerobic conditions, the pH of dry biogranules, *P. aeruginosa*, and isolates was measured to be more stable, while the pH of *S. pasteurii* and wet biogranules swiftly raised.

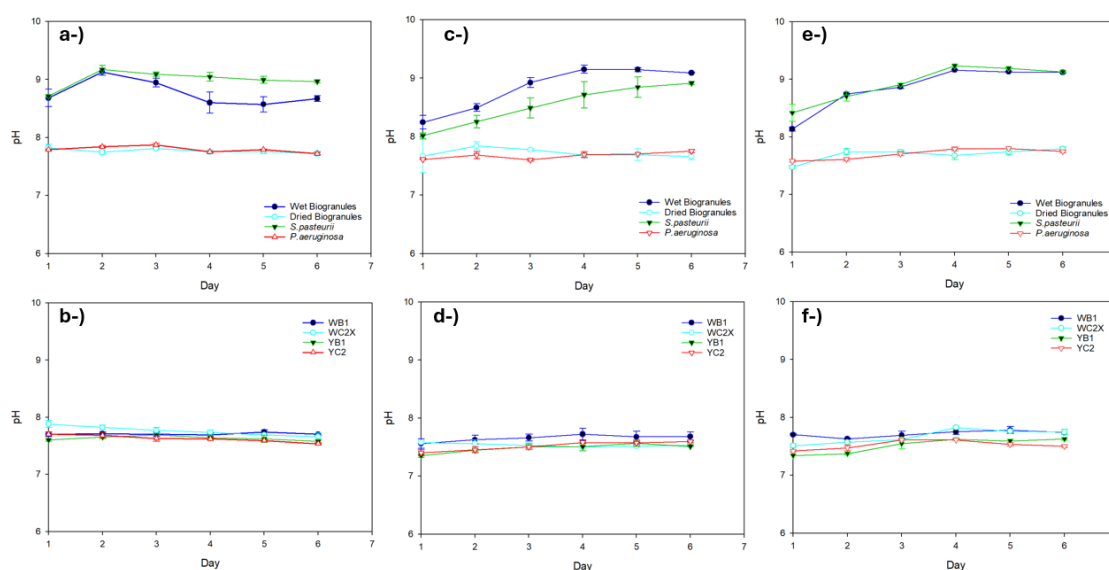


Figure 4-17. pH values at different DO concentrations; (a, b) aerobic, (c, d) microaerobic, (e, f) anoxic

4.8.1. Comparison of Urea Hydrolysis Activities at Different DO Concentrations

Urea hydrolysis was measured at different DO concentrations. The results were presented in Figure 4-18-Figure 4-23. Since *P. aeruginosa*, and WC2X did not exhibit urea

hydrolysis activity, the results were not included in the graphs. In all tests, WB1, YB1, and YC2 hydrolyzed about 4-12% of initial 10 g.L⁻¹ urea. The reason of low urea hydrolysis of the isolates under all conditions might be that they were tested at low YE concentrations in biomineralization solution (0.05 g.L⁻¹ YE). In the literature, it was mentioned that both *Bacillus* sp. and *S. pasteurii* were mostly tested at high YE concentrations (>10 g.L⁻¹) to achieve efficient urea hydrolysis and CaCO₃ precipitation in MICP applications [258]. According to previous tests, it was revealed that bacterial growth and microbial activity of *S. pasteurii* and isolates were affected by YE concentrations. YE had positive effect on their bacterial growth and microbial activity. Since it was suggested to avoid using YE in biomineralization applications, YE concentration was limited as 0.05 g.L⁻¹ in these tests, and thus the activities decreased.

Urea hydrolysis measured at the end of the sixth day of the aerobic test were calculated as 75%, 40%, and 82% for wet biogranules, dried biogranules, and *S. pasteurii*, respectively. Urea hydrolysis of the isolates (WB1, YB1, YC2) at sixth day were measured as 8%, 6%, and 5%, respectively (Figure 4-18, Figure 4-19).

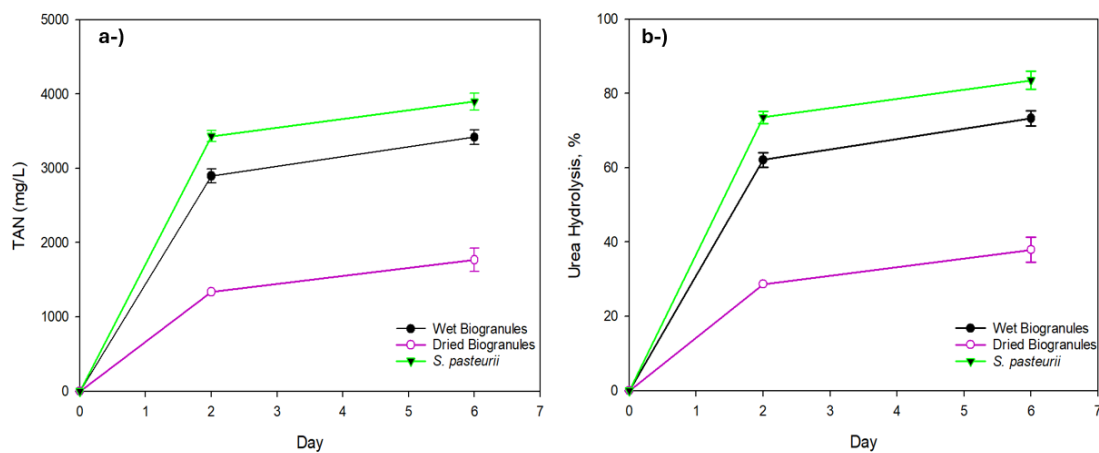


Figure 4-18. Urea hydrolysis results of wet and dried biogranules, and *S. pasteurii* in biomineralization medium with 0.05 g.L⁻¹ YE and 4.8 mg.L⁻¹ DO concentration (aerobic conditions); (a) TAN results, (b) hydrolyzed urea

It was revealed that biogranules and *S. pasteurii* rapidly hydrolyzed urea and this led to rapidly CaCO₃ precipitation. However, ammonium ions were produced as a byproduct

which was an environmental pollutant and it had harmful effects on marine habitats. This was considered as a limitation of urea hydrolysis. Therefore, determination of optimum biomineralization capacity and conditions where dominance of nitrate reduction increased was significant to minimize releasing ammonium ions.

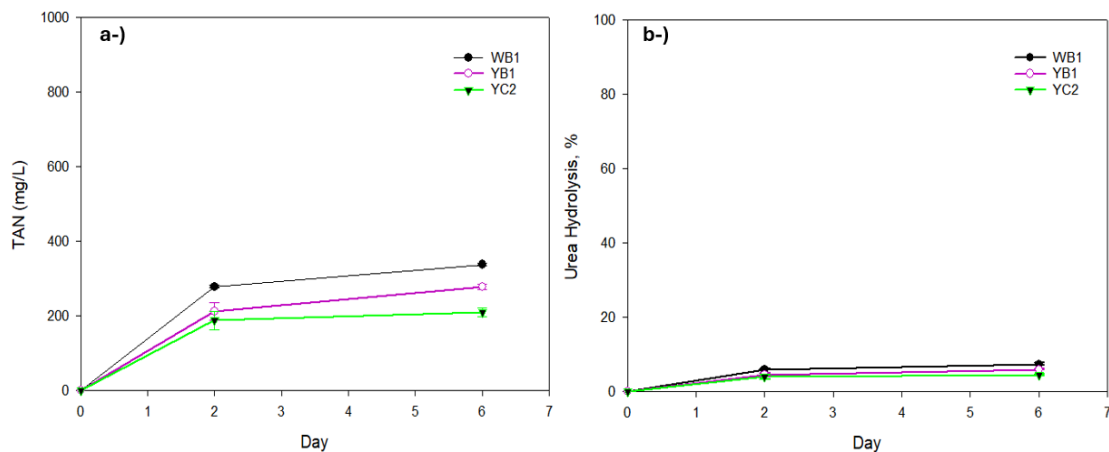


Figure 4-19. Urea hydrolysis activities of axenic strains (WB1, YB1, YC2) in biomineralization medium with 0.05 g.L^{-1} YE and 4.8 mg.L^{-1} DO concentration (aerobic conditions); (a) TAN results, (b) hydrolyzed urea

At the end of the 48 hours, *S. pasteurii* and wet granules hydrolyzed 70% and 60% of the total urea, respectively. *S. pasteurii* reached the highest urea hydrolysis activity under aerobic conditions due to its characteristics because *S. pasteurii* could produce urease enzyme under aerobic conditions. Urea hydrolysis performance of wet biogranules had lower performance than *S. pasteurii* but better performance than isolates. Since wet and dried biogranules involved ureolytic bacteria in its inherently microbial community, biogranules hydrolyzed urea. This non-axenic microbial community had higher urea hydrolysis activity than axenic cultures. However, biogranules had lower urea hydrolysis performance than *S. pasteurii*. The whole microbial community in biogranules were not ureolytic bacteria. Therefore, it was meaningful that for same initial CDW concentrations, biogranules hydrolyzed less amount of urea from *S. pasteurii* in the same test duration.

Isolates had relatively higher urea hydrolysis under aerobic conditions than under other oxygenic conditions. This could be attributed to the fact that the isolates were *Bacillus*

cereus, that was, mostly soil-borne and aerobic bacteria. It was stated in the literature that the majority of soil-borne *Bacillus* sp. were aerobic or facultative anaerobic bacteria [115,131,244]. It was calculated that the isolates reached high urea hydrolysis in previous tests (at high YE concentration) (Table 4-2). The reason for the low urea hydrolysis of the isolates under these different oxygenic concentrations might be that they were tested at low YE concentrations (0.05 g.L^{-1} instead of 2 g.L^{-1}).

Urea hydrolysis was measured under microaerobic conditions. Urea hydrolysis results were calculated as 89%, 39%, and 85% for wet biogranules, dried biogranules and *S. pasteurii*, respectively (Figure 4-20). Urea hydrolysis results were calculated as 7%, 5%, and 4% for the isolates (WB1, YB1, YC2), respectively (Figure 4-21).

Under microaerobic conditions, biogranules reached higher urea hydrolysis activity than *S. pasteurii* (at the end of the sixth day). This could be attributed to the fact that wet biogranules composed of bacteria which were not strictly aerobic and could hydrolyze urea in the presence of low oxygen. In addition, microbial activity could be restricted as CaCO_3 precipitated around *S. pasteurii* cells. Under microaerobic conditions, both slower urea hydrolysis (compared to aerobic conditions) in the first two days and the additional nitrate reduction activity increased the total amount of hydrolyzed urea.

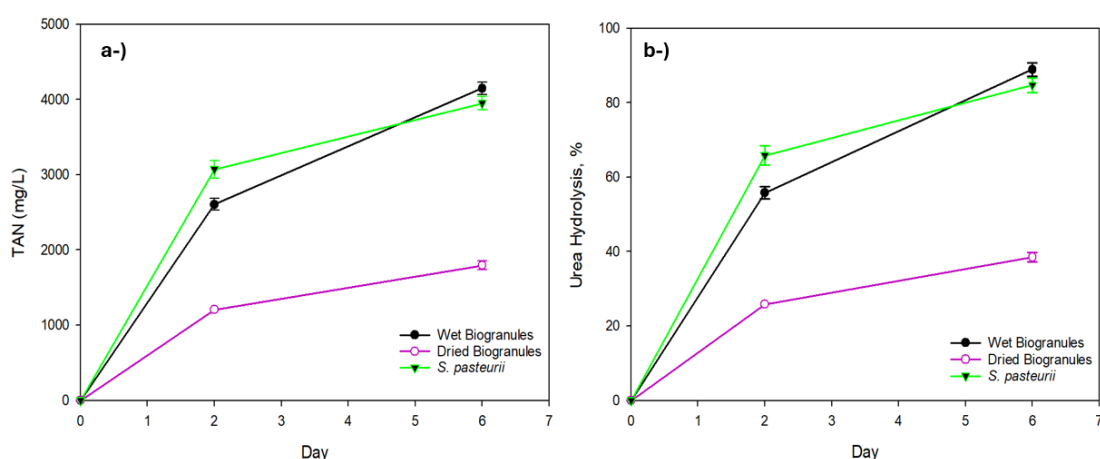


Figure 4-20. Urea hydrolysis results of wet and dried biogranules, and *S. pasteurii* in biomineralization medium with 0.05 g.L^{-1} YE and 1.3 mg.L^{-1} DO concentration (microaerobic conditions); (a) TAN results, (b) hydrolyzed urea

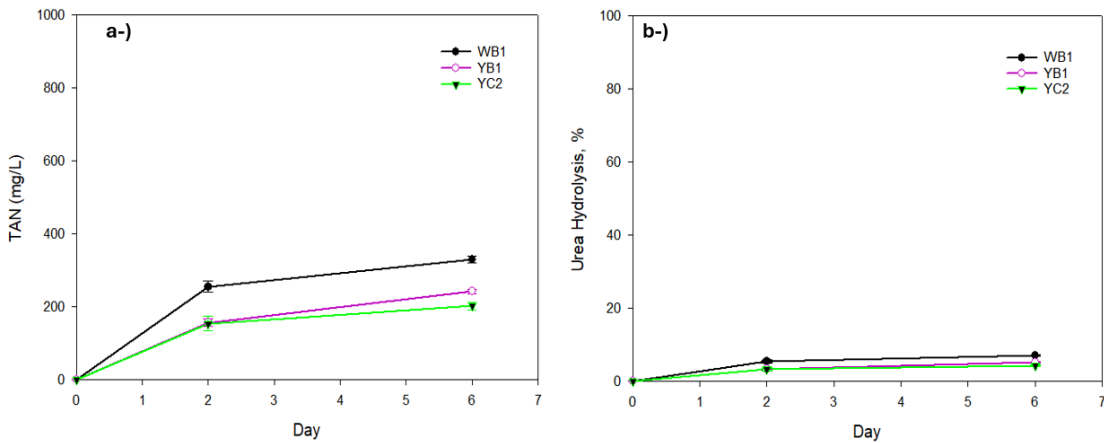


Figure 4-21. Urea hydrolysis activities of axenic strains (WB1, YB1, YC2) in biomineralization medium with 0.05 g.L^{-1} YE and 1.3 mg.L^{-1} DO concentration (microaerobic conditions); (a) TAN results, (b) hydrolyzed urea

Urea hydrolysis was measured at anoxic conditions. Urea hydrolysis results were calculated as 81%, 33%, and 79% for wet biogranules, dried biogranules and *S. pasteurii*, respectively (Figure 4-22). Urea hydrolysis results were calculated as 6%, 5%, and 3% for the isolates (WB1, YB1, YC2), respectively (Figure 4-23).

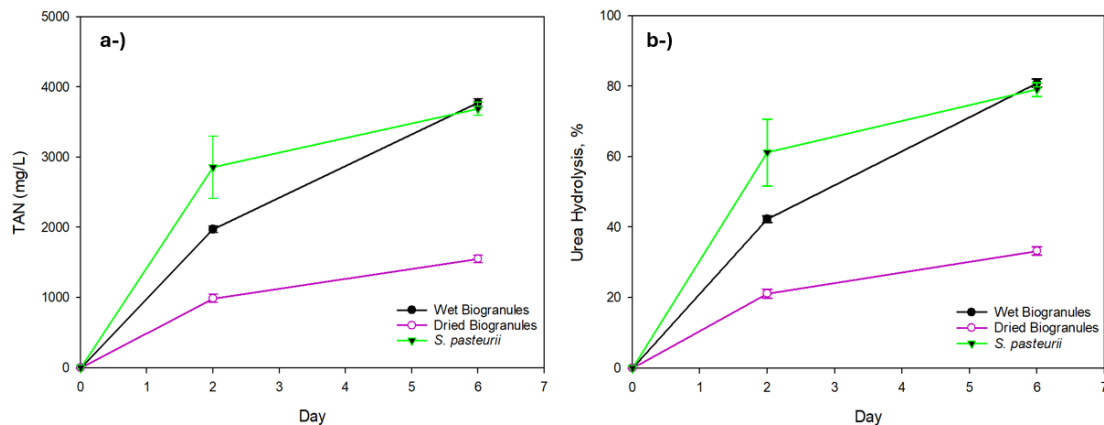


Figure 4-22. Urea hydrolysis results of wet and dried biogranules, and *S. pasteurii* in biomineralization medium with 0.05 g.L^{-1} YE and $<0.2 \text{ mg.L}^{-1}$ DO concentration (anoxic conditions); (a) TAN results, (b) hydrolyzed urea

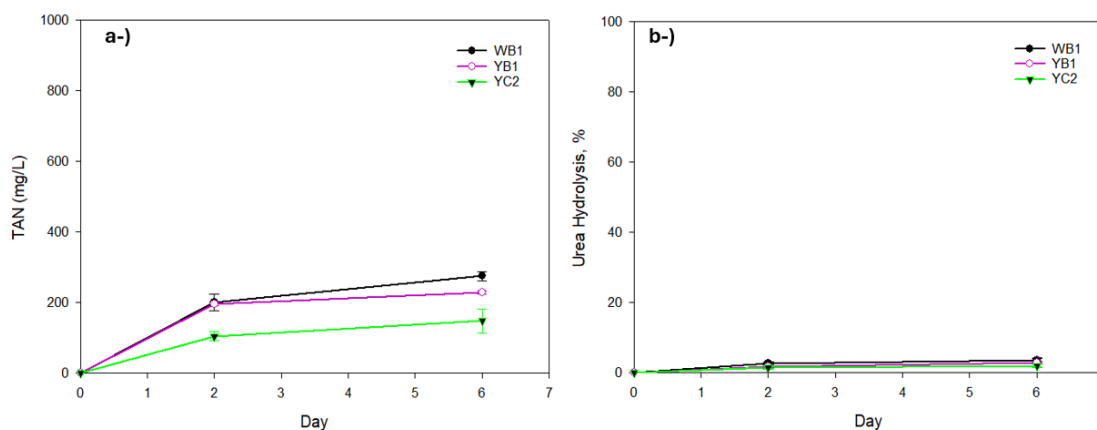


Figure 4-23. Urea hydrolysis activities of axenic strains (WB1, YB1, YC2) in biomineralization medium with 0.05 g.L^{-1} YE and $<0.2 \text{ mg.L}^{-1}$ DO concentration (anoxic conditions); (a) TAN results, (b) hydrolyzed urea

Bacteria at anoxic zone inside biogranules (at the core of biogranules) might still have microbial activity. Because microbial activity could not restrict at the core of biogranules even if CaCO_3 precipitation around biogranules [152,184,185]. Thus, biogranules could had higher urea hydrolysis activity under microaerobic and anoxic conditions.

Wet and dried biogranules, and *S. pasteurii* had higher urea hydrolysis at the end of the second day under aerobic conditions than under microaerobic and anoxic environments. At the end of the sixth day under the aerobic condition, urea hydrolysis of wet and dried biogranules, and *S. pasteurii* decreased compared to the microaerobic environment. This might be due to faster CaCO_3 precipitation under aerobic environments. Rapid CaCO_3 precipitation rate could restrict or reduce microbial activity [33]. Wet and dried biogranules, and *S. pasteurii* had high urea hydrolysis activity at three different DO concentrations (aerobic, microaerobic, anoxic).

Dried biogranules had higher urea hydrolysis under aerobic and microaerobic conditions than under anoxic conditions. This could be attributed to the fact that dried biogranules resuscitated earlier in the presence of oxygen at aerobic and microaerobic conditions.

In the literature, *S. pasteurii* was generally cultivated in high urea ($>20 \text{ g.L}^{-1}$), high YE ($>10 \text{ g.L}^{-1}$), and aerobic/microaerobic conditions [171,173,197,256,259]. As mentioned before microbial growth and microbial activity of *S. pasteurii* affected positively at high urea and high YE concentration. In addition to this, it was reported that YE had significant effect on bacterial growth and microbial activity of *S. pasteurii*.

S. pasteurii hydrolyzed 82%, 85%, and 79% of the initial urea (10 g.L^{-1}) under aerobic, microaerobic, and anoxic conditions, respectively. The amount of hydrolyzed urea of *S. pasteurii* in anoxic conditions was similar to aerobic or microaerobic conditions. According to studies in the literature, *S. pasteurii* had no microbial growth under anoxic conditions and could not produce urease enzyme [9,123,150]. However, it was stated that *S. pasteurii* grown under aerobic/microaerobic conditions could hydrolyze urea if used directly under anoxic conditions, as *S. pasteurii* produced sufficiently urease enzyme. In the literature, it was stated that urease enzyme of *S. pasteurii* was produced under aerobic/microaerobic conditions [123,150]. In these studies, *S. pasteurii* was able to grow and produce urease enzyme under microaerobic and aerobic conditions, and urease enzyme produced under aerobic/microaerobic conditions involved urea hydrolysis under anoxic conditions.

In order to verify bacterial growth and ureolytic activity under anoxic conditions, the inoculum itself was also prepared under anoxic conditions. It was tried to grow in an anoxic environment (in a nutrient solution enriched with 10 g.L^{-1} YE and 10 g.L^{-1} urea) instead of microaerobic environment. *S. pasteurii* was tested under anoxic conditions to observe whether urea hydrolysis occurred under anoxic conditions. While there was a relatively low bacterial growth at the end of the incubation period in liquid medium enriched with 10 g.L^{-1} YE, there was no microbial growth in liquid medium containing low YE (0.05 g.L^{-1}).

At the end of the sixth day under anoxic condition, TAN analysis of wet and dried *S. pasteurii* were measured. At the end of the test, urea hydrolysis results of wet and dried *S. pasteurii* were 8% and 5%, respectively. In this test, it was revealed that *S. pasteurii* did not grow sufficiently under anoxic conditions and *S. pasteurii* could not produce

enough urease enzyme to hydrolyze urea under anoxic conditions. It was also tested that *S. pasteurii* did not reach sufficient urea hydrolysis efficiency when dried and resuscitated in a biomineralization solution. With this result, it was revealed that urea hydrolysis of *S. pasteurii* at anoxic conditions led to urease enzyme produced at aerobic or microaerobic environments. As a result, *S. pasteurii* did not produce enough urease enzyme in the anoxic environment. This result was consistent with the literature [9,123,150].

When *S. pasteurii* was dried and tested in biomineralization solution under anoxic conditions, it was determined that the spores could not resuscitate, and urea hydrolysis could not occur. The results obtained from this test concluded that high urea hydrolysis obtained under anoxic conditions in the first tests was achieved by urease enzyme produced during the growth of *S. pasteurii* (in a microaerobic environment). Therefore, *S. pasteurii* did not produce significant growth and urease enzyme production in anoxic environment. These tests also confirmed the results previously reported in the literature by both Martin et al. and Mitchell et al. [123,150]. Metabolic activities of *S. pasteurii* such as bacterial growth and new enzyme production under anoxic conditions were not sufficient for biomineralization.

Specific urea hydrolysis activities of biogranules, *S. pasteurii*, and isolates at different DO concentrations were given in Table 4-4. Under aerobic conditions, wet and dried biogranules, *S. pasteurii*, and isolates (WB1, YB1, YC2) had 6.21 g Urea.d⁻¹.g⁻¹ CDW, 2.86 g Urea.d⁻¹.g⁻¹ CDW, 7.36 g Urea.d⁻¹.g⁻¹ CDW, 0.60 g Urea.d⁻¹.g⁻¹ CDW, 0.46 g Urea.d⁻¹.g⁻¹ CDW, 0.40 g Urea.d⁻¹.g⁻¹ CDW specific urea hydrolysis activity on the second day, respectively.

Table 4-4. Specific urea hydrolysis activity at different DO concentrations

Samples	Aerobic		Microaerobic		Anoxic	
	2 nd	6 th	2 nd	6 th	2 nd	6 th
	g Urea.d ⁻¹ .g ⁻¹ CDW					
Wet biogranules	6.21	2.44	5.58	2.96	4.23	2.70
Dried biogranules	2.86	1.26	2.59	1.28	2.11	1.11
<i>S. pasteurii</i>	7.36	2.79	6.59	2.63	6.12	2.63
WB1	0.60	0.25	0.55	0.24	0.43	0.20
YB1	0.46	0.20	0.34	0.17	0.42	0.16
YC2	0.40	0.15	0.33	0.15	0.23	0.11

Among specific urea hydrolysis activities on the second day, *S. pasteurii* had the highest urea hydrolysis activity. Since aerobic conditions were more suitable for urea hydrolysis activity of *S. pasteurii*, both on the second day and sixth day activities were higher than biogranules and isolates. In literature, it was reported that urea hydrolysis performance of *S. pasteurii* increased in the presence of oxygen. Wet biogranules had the highest urea hydrolysis activity, followed by *S. pasteurii*. These results indicated that the microbial activity of urease positive bacteria increased in the presence of oxygen. Among three different oxygenic conditions, all samples reached the highest specific urea hydrolysis activity under aerobic conditions. This could be due to increase in the microbial activities of bacteria that hydrolyzed urea in the presence of oxygen. Under microaerobic conditions, wet and dried biogranules, *S. pasteurii*, and isolates (WB1, YB1, YC2) had 5.58 g Urea.d⁻¹.g⁻¹ CDW, 2.59 g Urea.d⁻¹.g⁻¹ CDW, 6.59 g Urea.d⁻¹.g⁻¹ CDW, 0.55 g Urea.d⁻¹.g⁻¹ CDW, 0.34 g Urea.d⁻¹.g⁻¹ CDW, 0.33 g Urea.d⁻¹.g⁻¹ CDW specific urea hydrolysis activity on the second day, respectively.

Among specific urea hydrolysis activities on the second day, *S. pasteurii* had the highest urea hydrolysis activity. Specific urea hydrolysis activities of wet biogranules on the sixth day was calculated as 2.96 g Urea.d⁻¹.g⁻¹ CDW. Among specific urea hydrolysis activities on the sixth day, wet biogranules had the highest urea hydrolysis activity. Specific urea

hydrolysis activity of dried biogranules on the sixth day was similar to that under aerobic conditions. This could be attributed that urease positive bacteria inside dried biogranules resuscitated in two days. Specific urea hydrolysis activities of dried biogranules on the second days both aerobic and microaerobic conditions had higher than on the sixth days. Under anoxic conditions, wet and dried biogranules, *S. pasteurii*, and isolates (WB1, YB1, YC2) had 4.23 g Urea.d⁻¹.g⁻¹ CDW, 2.11 g Urea.d⁻¹.g⁻¹ CDW, 6.12 g Urea.d⁻¹.g⁻¹ CDW, 0.43 g Urea.d⁻¹.g⁻¹ CDW, 0.42 g Urea.d⁻¹.g⁻¹ CDW, 0.23 g Urea.d⁻¹.g⁻¹ CDW specific urea hydrolysis activity on the second day, respectively.

Among specific urea hydrolysis activities on the second day, *S. pasteurii* had the highest urea hydrolysis activity. It was revealed that urease enzyme of *S. pasteurii* did not inhibit under anoxic conditions. The fact that urease enzyme of *S. pasteurii* did not inhibit was consistent with the literature [150]. Specific urea hydrolysis activities of wet biogranules on the sixth day was calculated as 2.70 g Urea.d⁻¹.g⁻¹ CDW. Among specific urea hydrolysis activities on the sixth day, wet biogranules had the highest urea hydrolysis activity. Wet and dried biogranules had the lowest specific urea hydrolysis activities under anoxic conditions. These results also confirmed effects of oxygen level on urea hydrolysis activity. It could be concluded that as the oxygen level decreased in environment, specific urea hydrolysis activities decreased for all samples. Decrease in specific urea hydrolysis activity under anoxic conditions for urease positive bacteria in biogranules was minimized by using two metabolic pathways (urea hydrolysis and denitrification).

4.8.2. Nitrate Reduction Activities at Different DO Concentrations

Nitrate reduction and nitrite accumulation were measured for second and sixth days at different dissolved oxygen concentrations. NO₃-N and NO₂-N measurements of wet and dried biogranules, *S. pasteurii*, *P. aeruginosa*, and isolates (WB1, WC2X, YB1, and YC2) performed under aerobic conditions were presented in Figure 4-24, and Figure 4-25.

Nitrate reduction for sixth day under aerobic conditions were measured as 10%, 6%, 2%, and 5% for wet biogranules, dried biogranules, *S. pasteurii* and *P. aeruginosa*,

respectively. Nitrate reduction was not expected under aerobic conditions, especially for planktonic cultures. Under aerobic condition at sixth day, wet and dried biogranules, *S. pasteurii* and *P. aeruginosa* had lower nitrate reduction than under microaerobic and anoxic conditions. Under aerobic conditions, wet biogranules reached the highest nitrate reduction when compared to axenic strains. The reason for nitrate reduction in wet biogranules under aerobic conditions might be that there was an anoxic zone inside biogranules where oxygen could not penetrate [153,184,185], or CaCO₃ precipitation around biogranules limited the available to oxygen [106,151,152,201,212]. Therefore, bacteria could use nitrate which had higher concentration gradient, instead of oxygen at the end of the sixth day under aerobic conditions. Under aerobic conditions, no nitrite accumulation was observed for wet and dried biogranules, *S. pasteurii*, and *P. aeruginosa*. Nitrate reduction activity of dried biogranules was low compared to wet biogranules under aerobic conditions. This might be because nitrate-reducing spores in dried biogranules did not resuscitate under aerobic conditions.

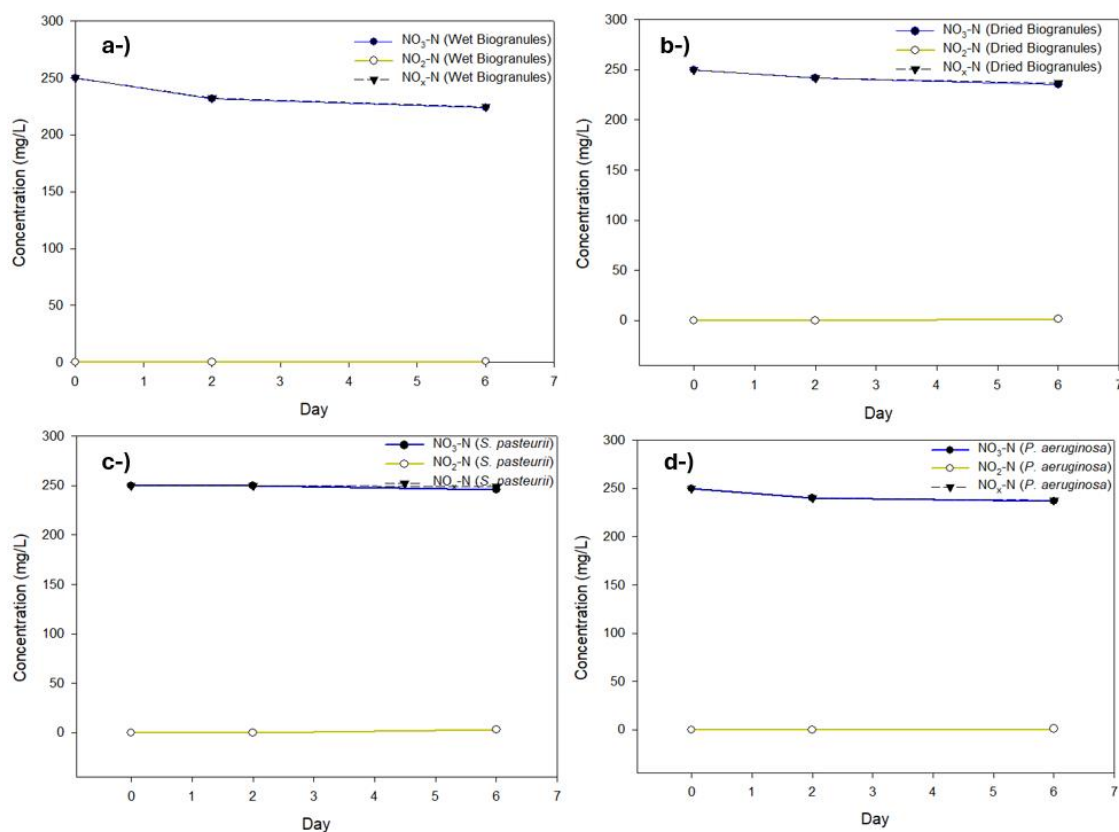


Figure 4-24. Nitrate reduction and nitrite measurements under aerobic condition, (a) wet biogranules, (b) dried biogranules, (c) *S. pasteurii*, (d) *P. aeruginosa*

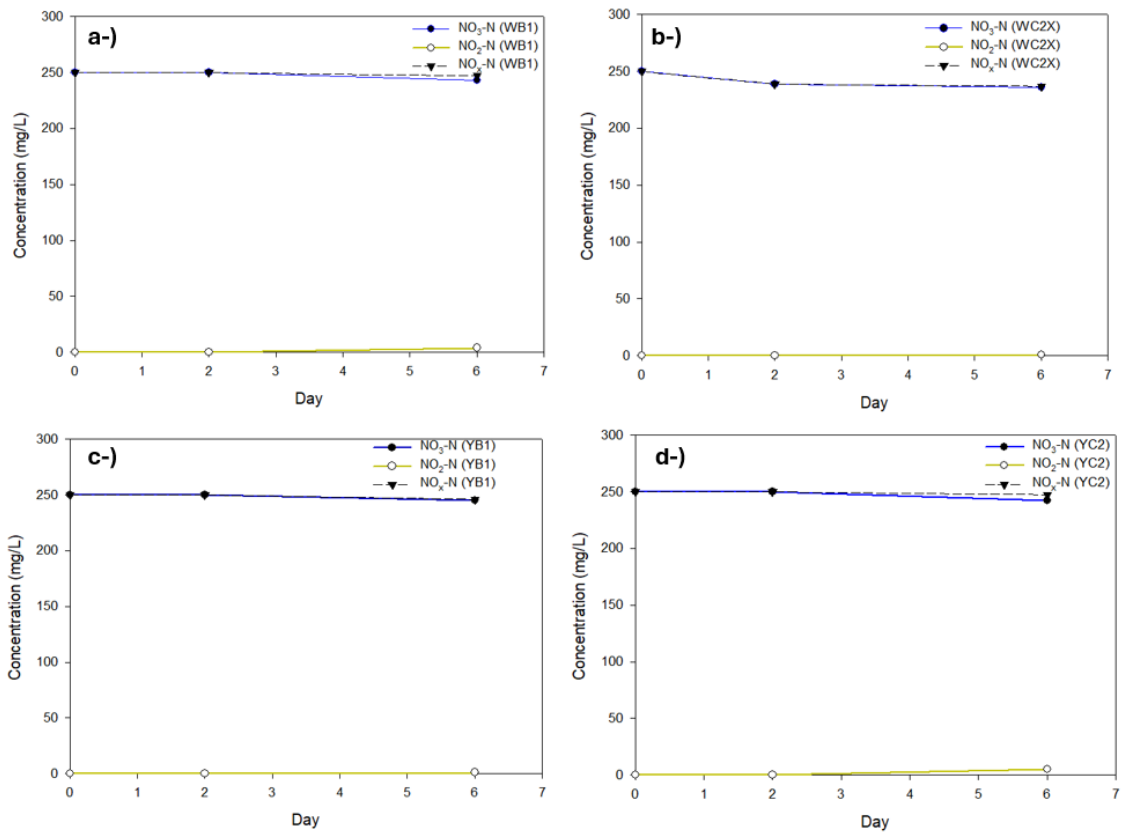


Figure 4-25. Nitrate reduction and nitrite measurements under aerobic condition, (a) WB1, (b) WC2X, (c) YB1, (d) YC2

Specific NO₃-N reducing, NO₂-N accumulation, and denitrification activity of wet and dried biogranules, *S. pasteurii*, *P. aeruginosa*, and isolates at aerobic conditions were given in Table 4-5.

Under aerobic conditions, wet and dried biogranules, *S. pasteurii*, *P. aeruginosa*, and isolates (WB1, WC2X, YB1, and YC2) had 8.40 mg NO_x-N d⁻¹.g⁻¹CDW, 4.43 mg NO_x-N d⁻¹.g⁻¹CDW, 0.33 mg NO_x-N d⁻¹.g⁻¹CDW, 4.0 mg NO_x-N d⁻¹.g⁻¹CDW, 1.0 mg NO_x-N d⁻¹.g⁻¹CDW, 4.43 mg NO_x-N d⁻¹.g⁻¹CDW, 1.27 mg NO_x-N d⁻¹.g⁻¹CDW, 0.83 mg NO_x-N d⁻¹.g⁻¹CDW specific denitrification activity on the six day, respectively.

Table 4-5. Specific NO₃-N reducing, NO₂-N accumulation, and denitrification activity at aerobic conditions

	Wet biogranules	Dried biogranules	<i>S. pasteurii</i>	<i>P. aeruginosa</i>
second day	Specific nitrate-reducing activity (mg NO ₃ -N d ⁻¹ .g ⁻¹ CDW)			
	18	8	0	10
	Specific nitrite accumulation activity (mg NO ₂ -N d ⁻¹ .g ⁻¹ CDW)			
	0.40	0	0	0
	Specific denitrification activity (mg NO _x -N d ⁻¹ .g ⁻¹ CDW)			
	17.60	8	0	10
	Wet biogranules	Dried biogranules	<i>S. pasteurii</i>	<i>P. aeruginosa</i>
sixth day	Specific nitrate-reducing activity (mg NO ₃ -N d ⁻¹ .g ⁻¹ CDW)			
	8.67	4.83	1.33	4.33
	Specific nitrite accumulation activity (mg NO ₂ -N d ⁻¹ .g ⁻¹ CDW)			
	0.27	0.40	1	0.33
	Specific denitrification activity (mg NO _x -N d ⁻¹ .g ⁻¹ CDW)			
	8.40	4.43	0.33	4.00
	WB1	WC2X	YB1	YC2
second day	Specific nitrate-reducing activity (mg NO ₃ -N d ⁻¹ .g ⁻¹ CDW)			
	0	11.20	0	0
	Specific nitrite accumulation activity (mg NO ₂ -N d ⁻¹ .g ⁻¹ CDW)			
	0	0	0	0
	Specific denitrification activity (mg NO _x -N d ⁻¹ .g ⁻¹ CDW)			
	0	11.20	0	0
	WB1	WC2X	YB1	YC2
sixth day	Specific nitrate-reducing activity (mg NO ₃ -N d ⁻¹ .g ⁻¹ CDW)			
	2.33	4.67	1.67	2.50
	Specific nitrite accumulation activity (mg NO ₂ -N d ⁻¹ .g ⁻¹ CDW)			
	1.33	0.24	0.40	1.67
	Specific denitrification activity (mg NO _x -N d ⁻¹ .g ⁻¹ CDW)			
	1	4.43	1.27	0.83

NO₃-N and NO₂-N measurements of the test performed under microaerobic conditions were presented in Figure 4-26 and Figure 4-27. Nitrate reduction on the sixth day under microaerobic conditions were measured as 65%, 49%, 25%, and 64% for wet biogranules, dried biogranules, *S. pasteurii*, and *P. aeruginosa*, respectively. Wet biogranules and *P. aeruginosa* reached higher nitrate reduction on the sixth day under microaerobic conditions. Nitrate reduction occurred under microaerobic conditions. According to NO₂-N analysis, no nitrite accumulation was detected on the sixth day for wet and dried biogranules.

Nitrate reduction on the sixth day under microaerobic conditions were measured as 35%, 64%, 30% and 27% for WB1, WC2X, YB1 and YC2, respectively. Among the isolates, WC2X had no nitrite accumulation, while other isolated strains caused NO_2^- accumulation. According to these results, isolates could reduce NO_3^- by using NO_3^- as an electron acceptor in environments where oxygen is limited. However, NO_2^- reducing activities were restricted.

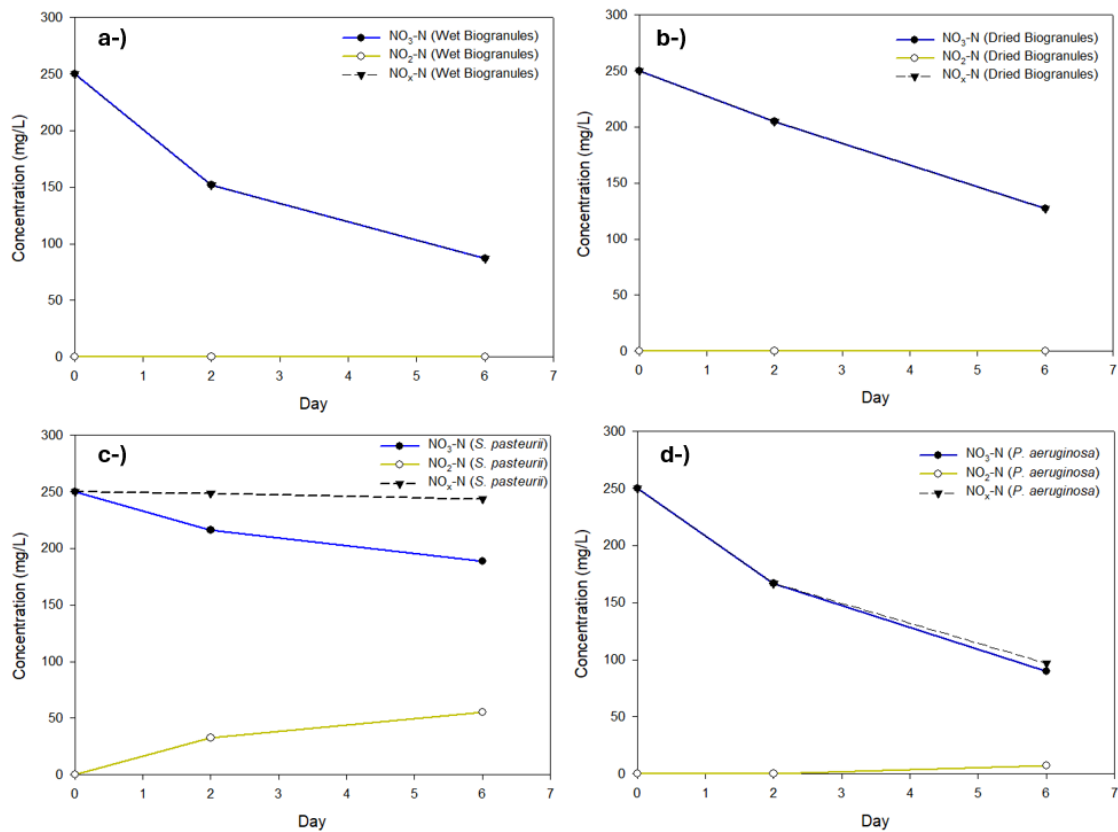


Figure 4-26. Nitrate reduction and nitrite measurements under microaerobic condition, (a) wet biogranules, (b) dried biogranules, (c) *S. pasteurii*, (d) *P. aeruginosa*

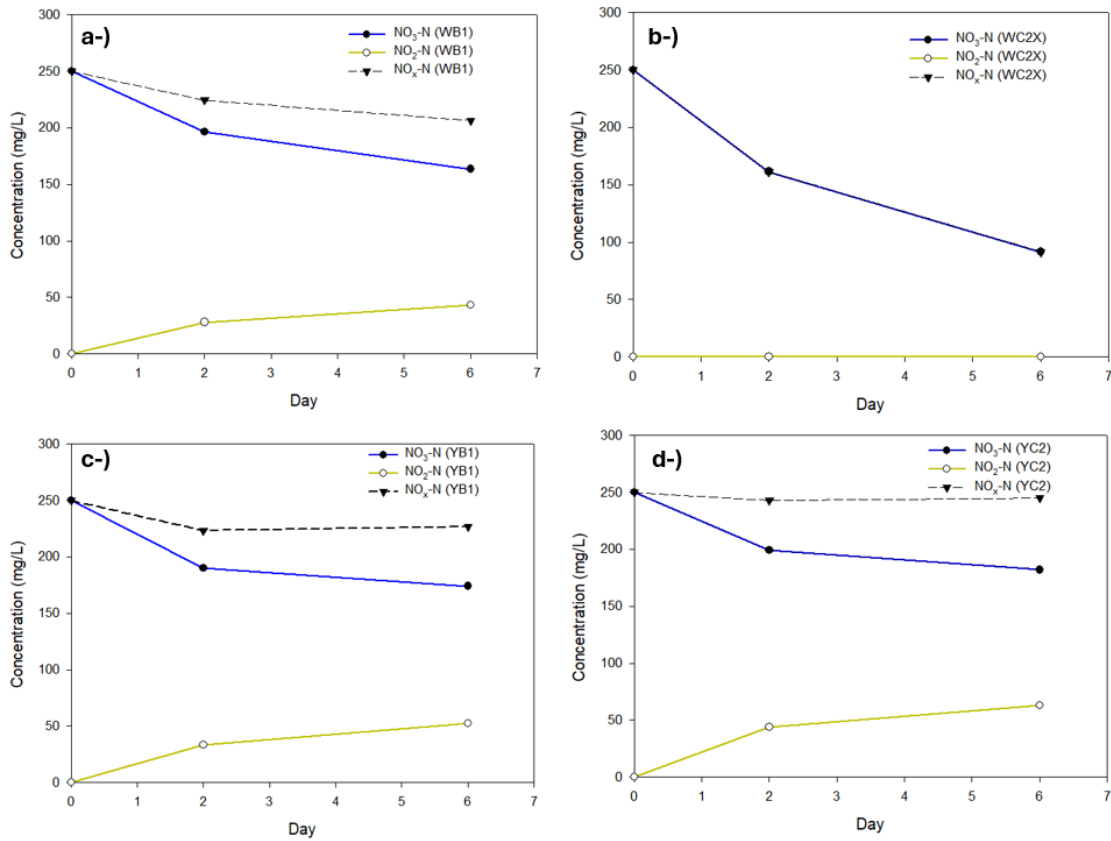


Figure 4-27. Nitrate reduction and nitrite measurements under microaerobic condition, (a) WB1, (b) WC2X, (c) YB1, (d) YC2

Specific nitrate reduction, specific nitrite accumulation, and specific denitrification activities calculated for batches under microaerobic conditions were given in Table 4-6.

According to the NO₂-N analysis performed on the sixth day, specific nitrite accumulation activity of *S. pasteurii*, and *P. aeruginosa* were measured as 55 mg.L⁻¹ NO₂-N and 7 mg.L⁻¹ NO₂-N, respectively.

Under microaerobic conditions, wet and dried biogranules, *S. pasteurii*, *P. aeruginosa*, and isolates (WB1, WC2X, YB1, and YC2) had 54 mg NO_x-N d⁻¹.g⁻¹CDW, 41 mg NO_x-N d⁻¹.g⁻¹CDW, 2 mg NO_x-N d⁻¹.g⁻¹CDW, 51 mg NO_x-N d⁻¹.g⁻¹CDW, 14 mg NO_x-N d⁻¹.g⁻¹CDW, 53 mg NO_x-N d⁻¹.g⁻¹CDW, 8 mg NO_x-N d⁻¹.g⁻¹CDW, 2 mg NO_x-N d⁻¹.g⁻¹CDW specific denitrification activity on the six day, respectively.

Table 4-6. Specific NO₃-N reducing, NO₂-N accumulation, and denitrification activity at microaerobic condition

	Wet biogranules	Dried biogranules	<i>S. pasteurii</i>	<i>P. aeruginosa</i>
second day	Specific nitrate-reducing activity (mg NO ₃ -N d ⁻¹ .g ⁻¹ CDW)			
	98	45	34	83
	Specific nitrite accumulation activity (mg NO ₂ -N d ⁻¹ .g ⁻¹ CDW)			
	0	0	32.50	0
	Specific denitrification activity (mg NO _x -N d ⁻¹ .g ⁻¹ CDW)			
	98	45	1.50	83
	Wet biogranules	Dried biogranules	<i>S. pasteurii</i>	<i>P. aeruginosa</i>
sixth day	Specific nitrate-reducing activity (mg NO ₃ -N d ⁻¹ .g ⁻¹ CDW)			
	54.33	41	20.50	53.47
	Specific nitrite accumulation activity (mg NO ₂ -N d ⁻¹ .g ⁻¹ CDW)			
	0	0	19	1.50
	Specific denitrification activity (mg NO _x -N d ⁻¹ .g ⁻¹ CDW)			
	54.33	41	1.50	51.07
	WB1	WC2X	YB1	YC2
second day	Specific nitrate-reducing activity (mg NO ₃ -N d ⁻¹ .g ⁻¹ CDW)			
	53.55	88.6	60	51
	Specific nitrite accumulation activity (mg NO ₂ -N d ⁻¹ .g ⁻¹ CDW)			
	28	0.0	33.50	44
	Specific denitrification activity (mg NO _x -N d ⁻¹ .g ⁻¹ CDW)			
	25.55	88.60	26.50	7
	WB1	WC2X	YB1	YC2
sixth day	Specific nitrate-reducing activity (mg NO ₃ -N d ⁻¹ .g ⁻¹ CDW)			
	28.8	52.8	25.27	22.67
	Specific nitrite accumulation activity (mg NO ₂ -N d ⁻¹ .g ⁻¹ CDW)			
	14.33	0	17.50	21
	Specific denitrification activity (mg NO _x -N d ⁻¹ .g ⁻¹ CDW)			
	14.47	52.80	7.77	1.67

NO₃-N and NO₂-N measurements of the test performed under anoxic conditions were presented in Figure 4-28 and Figure 4-29. Nitrate reduction at the end of the sixth day under anoxic condition were measured as 80%, 35%, 23% and 83% for wet biogranules, dried biogranules, *S. pasteurii* and *P. aeruginosa*, respectively.

Nitrate reduction at the end of the sixth day under anoxic condition were measured as 45%, 82%, 40% and 35% for WB1, WC2X, YB1 and YC2, respectively. While very low

nitrite accumulation was detected in WC2X, high nitrite accumulation was detected in other isolates (WB1, YB1, and YC2) under anoxic conditions.

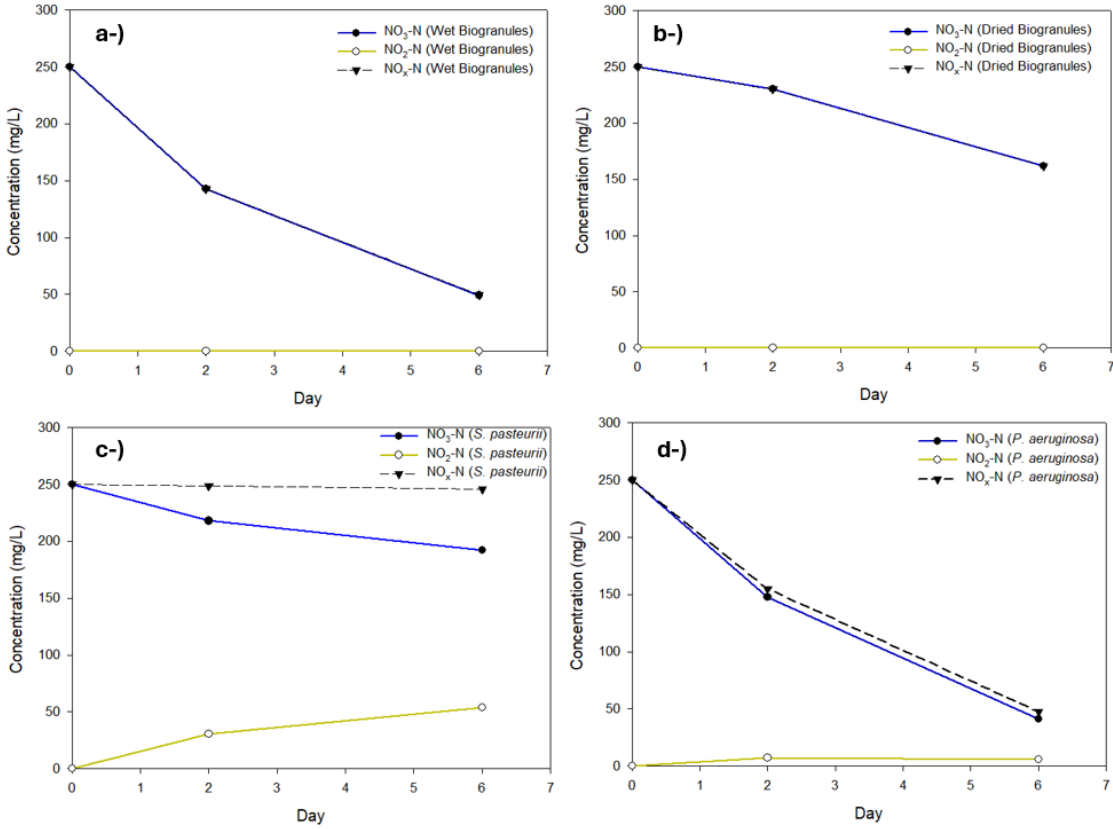


Figure 4-28. Nitrate reduction and nitrite measurements under anoxic condition, (a) wet biogranules, (b) dried biogranules, (c) *S. pasteurii*, (d) *P. aeruginosa*

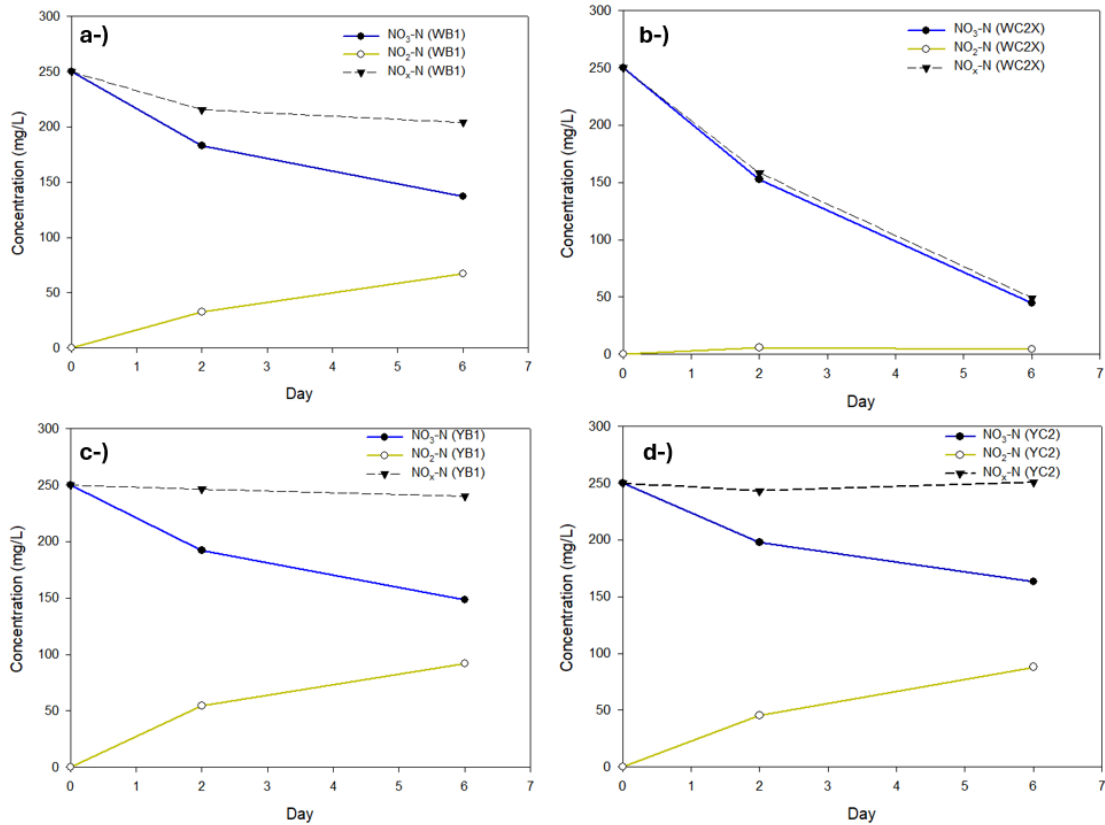


Figure 4-29. Nitrate reduction and nitrite measurements under anoxic condition, (a) WB1, (b) WC2X, (c) YB1, (d) YC2

Specific nitrate reduction, specific nitrite accumulation, and specific denitrification activities calculated for batches under anoxic conditions were given in Table 4-7.

At the end of the sixth day under anoxic condition, *P. aeruginosa* reached the highest nitrate reduction performance. Wet biogranules had almost as much nitrate reduction activity as *P. aeruginosa* at the end of the sixth day. No nitrite accumulation was detected at the end of the sixth day for the wet and dried biogranules. According to the NO₂-N analysis performed at the end of the sixth day, specific nitrite accumulation activities of *S. pasteurii* and *P. aeruginosa* were measured as 54 mg.L⁻¹ NO₂-N and 6 mg.L⁻¹ NO₂-N, respectively.

Under anoxic conditions, wet and dried biogranules, *S. pasteurii*, *P. aeruginosa* and isolates (WB1, WC2X, YB1, and YC2) had 67 mg NO_x-N d⁻¹.g⁻¹ CDW, 29 mg NO_x-N

$\text{d}^{-1} \cdot \text{g}^{-1} \text{CDW}$, $1 \text{ mg NO}_x\text{-N d}^{-1} \cdot \text{g}^{-1} \text{CDW}$, $67 \text{ mg NO}_x\text{-N d}^{-1} \cdot \text{g}^{-1} \text{CDW}$, $15 \text{ mg NO}_x\text{-N d}^{-1} \cdot \text{g}^{-1} \text{CDW}$, $67 \text{ mg NO}_x\text{-N d}^{-1} \cdot \text{g}^{-1} \text{CDW}$, $3 \text{ mg NO}_x\text{-N d}^{-1} \cdot \text{g}^{-1} \text{CDW}$, $0 \text{ mg NO}_x\text{-N d}^{-1} \cdot \text{g}^{-1} \text{CDW}$ specific denitrification activity on the six day, respectively.

Table 4-7. Specific $\text{NO}_3\text{-N}$ reducing, $\text{NO}_2\text{-N}$ accumulation, and denitrification activity at anoxic condition

	Wet biogranules	Dried biogranules	<i>S. pasteurii</i>	<i>P. aeruginosa</i>
second day	Specific nitrate-reducing activity ($\text{mg NO}_3\text{-N d}^{-1} \cdot \text{g}^{-1} \text{CDW}$)			
	98	45	34	88
	Specific nitrite accumulation activity ($\text{mg NO}_2\text{-N d}^{-1} \cdot \text{g}^{-1} \text{CDW}$)			
	0	0	30.80	7
sixth day	Specific denitrification activity ($\text{mg NO}_x\text{-N d}^{-1} \cdot \text{g}^{-1} \text{CDW}$)			
	98	45	3.20	81
	Wet biogranules			
	Dried biogranules			
second day	Specific nitrate-reducing activity ($\text{mg NO}_3\text{-N d}^{-1} \cdot \text{g}^{-1} \text{CDW}$)			
	66.93	29.33	26	69.53
	Specific nitrite accumulation activity ($\text{mg NO}_2\text{-N d}^{-1} \cdot \text{g}^{-1} \text{CDW}$)			
	0	0	24.67	2
sixth day	Specific denitrification activity ($\text{mg NO}_x\text{-N d}^{-1} \cdot \text{g}^{-1} \text{CDW}$)			
	66.93	29.33	1.33	67.53
	WB1			
	WC2X			
second day	Specific nitrate-reducing activity ($\text{mg NO}_3\text{-N d}^{-1} \cdot \text{g}^{-1} \text{CDW}$)			
	67	97.5	58	52
	Specific nitrite accumulation activity ($\text{mg NO}_2\text{-N d}^{-1} \cdot \text{g}^{-1} \text{CDW}$)			
	32.70	5.9	54.50	45.30
sixth day	Specific denitrification activity ($\text{mg NO}_x\text{-N d}^{-1} \cdot \text{g}^{-1} \text{CDW}$)			
	34.30	91.60	3.50	6.70
	WB1			
	WC2X			
second day	Specific nitrate-reducing activity ($\text{mg NO}_3\text{-N d}^{-1} \cdot \text{g}^{-1} \text{CDW}$)			
	37.67	68.4	33.93	29
	Specific nitrite accumulation activity ($\text{mg NO}_2\text{-N d}^{-1} \cdot \text{g}^{-1} \text{CDW}$)			
	22.33	1.50	30.67	29
sixth day	Specific denitrification activity ($\text{mg NO}_x\text{-N d}^{-1} \cdot \text{g}^{-1} \text{CDW}$)			
	15.33	66.93	3.27	0

4.8.3. Changes in Dissolved Ca^{2+} Concentration at Different DO Concentrations

The initial calcium, $\text{NO}_x\text{-N}$ and urea concentrations were set to $2.6 \text{ g} \cdot \text{L}^{-1} \text{ Ca}^{2+}$, $0.25 \text{ g} \cdot \text{L}^{-1} \text{ NO}_3\text{-N}$ and $10 \text{ g} \cdot \text{L}^{-1}$ urea. In tests at different DO concentrations, dissolved calcium was measured in AAS on the second and sixth days.

S. pasteurii, *P. aeruginosa*, and isolates were tested under aerobic, microaerobic and anoxic environments to compare them with wet and dried biogranules in terms of biomineralization activities. Time-dependent changes of dissolved calcium concentration in batches during six days were presented in Figure 4-30.

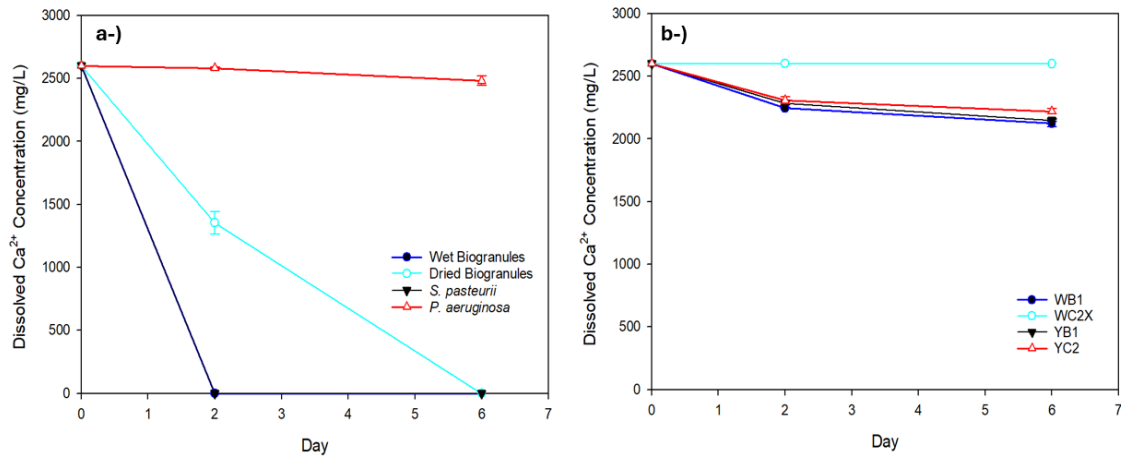


Figure 4-30. Dissolved calcium concentration results at the end of the second and sixth days under aerobic condition; (a) biogranules, *S. pasteurii*, and *P. aeruginosa*, (b) isolates

Wet biogranules and *S. pasteurii* completely precipitated dissolved calcium in biomineralization medium on the second day. Dried biogranules completely precipitated dissolved calcium on the sixth day. The amount of dissolved calcium in *P. aeruginosa* was measured as 2481 mg.L^{-1} . According to these results, *S. pasteurii* and wet biogranules under aerobic and microaerobic conditions precipitated totally dissolved calcium under aerobic conditions.

At the same time, isolates (WB1, WC2X, YB1, and YC2) precipitated dissolved calcium at lower concentrations compared to *S. pasteurii* and biogranules (Figure 4-30). Since *S. pasteurii*, wet and dried biogranules had higher microbial activity under aerobic conditions, they precipitated more calcium than isolates.

The change of dissolved calcium concentrations under microaerobic conditions was presented in Figure 4-31. Similar to under aerobic conditions, wet biogranules and *S.*

pasteurii completely precipitated dissolved calcium in biomineralization medium on the second day. The dissolved calcium concentrations of dried biogranules were measured as 1662 mg.L⁻¹, and 182 mg.L⁻¹ on the second and sixth days, respectively.

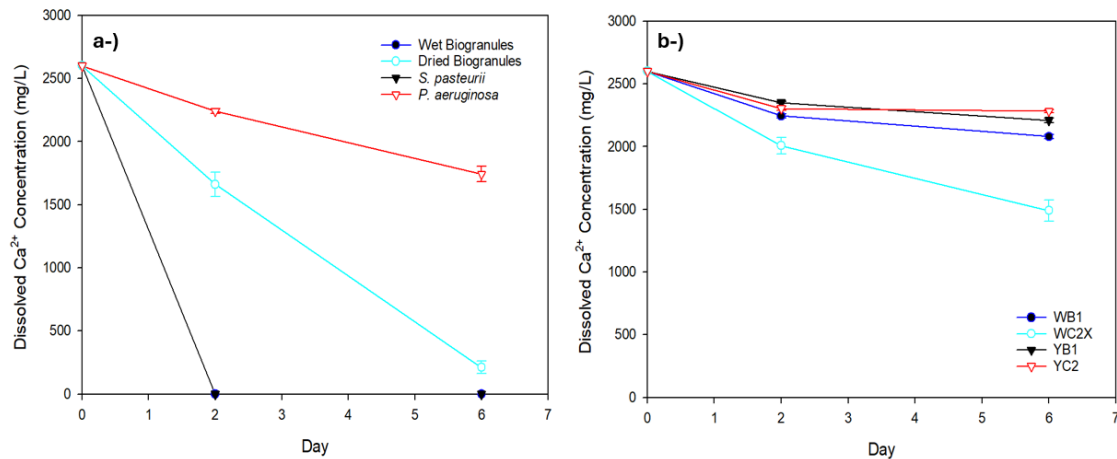


Figure 4-31. Dissolved calcium concentration results at the end of the second and sixth days under microaerobic condition; (a) biogranules, *S. pasteurii*, and *P. aeruginosa*, (b) isolates

Dried biogranules precipitated almost all amount of dissolved calcium in biomineralization solution under microaerobic conditions. The amount of dissolved calcium in *P. aeruginosa* was measured as 1743 mg.L⁻¹ on the sixth days. According to these results, *S. pasteurii*, and wet biogranules under aerobic and microaerobic conditions precipitated totally dissolved calcium in the environment. Under microaerobic conditions, *P. aeruginosa* precipitated more dissolved calcium compared to the aerobic conditions.

At the same time, isolates precipitated dissolved calcium at lower concentrations compared to *S. pasteurii*, wet and dried biogranules. Since *S. pasteurii* and biogranules had higher microbial activity under microaerobic conditions, they precipitated more dissolved calcium in the environment.

The changes of dissolved calcium concentration in anoxic condition were presented in Figure 4-32. Similar to under aerobic and microaerobic conditions, wet biogranules and

S. pasteurii completely precipitated dissolved calcium in biomineralization medium on the sixth day. Wet biogranules swiftly precipitated dissolved calcium under anoxic conditions.

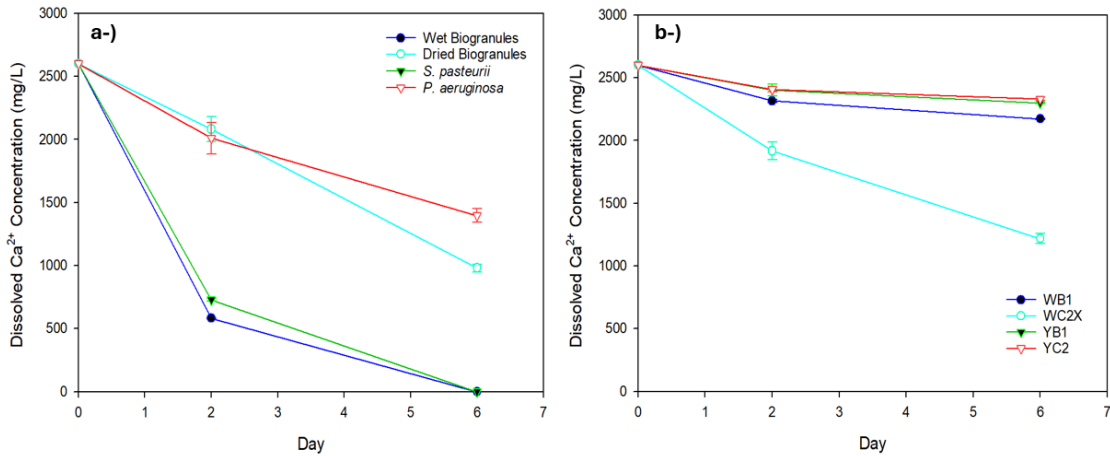


Figure 4-32. Dissolved calcium concentration results at the end of the second and sixth days under anoxic conditions; (a) biogranules, *S. pasteurii*, and *P. aeruginosa*, (b) isolates

The dissolved calcium concentrations of dried biogranules were measured as 2082 mg.L⁻¹, 980 mg.L⁻¹ on the second and sixth days, respectively. The amount of dissolved calcium in *P. aeruginosa* was measured as 1397 mg.L⁻¹ on the sixth day. According to these results, at the end of the sixth day under aerobic, microaerobic and anoxic conditions, wet biogranules and *S. pasteurii* precipitated the total amount of dissolved calcium in the environment. *P. aeruginosa* precipitated more dissolved calcium compared to aerobic and microaerobic conditions. This could be explained by its higher nitrate reduction under anoxic conditions.

At the same time, isolates precipitated dissolved calcium at lower concentrations compared to *S. pasteurii* and biogranules. Since *S. pasteurii* and biogranules showed higher microbial activity under anoxic conditions, they precipitated more dissolved calcium. Among isolates under anoxic conditions, WC2X showed better performance, while WB1, YB1, and YC2 showed lower performance. WC2X had higher microbial activity under anoxic conditions. The microbial activities of other isolates (WB1, YB1,

and YC2) were limited to urea hydrolysis. Therefore, lower amount of dissolved calcium was precipitated.

4.8.4. Comparison of CaCO₃ Precipitation Activities at Different DO Concentrations

The amounts of precipitated CaCO₃ were measured for aerobic, microaerobic, and anoxic conditions. These results were given in Figure 4-33, Figure 4-34, and Figure 4-35. Specific CaCO₃ precipitation activities were also presented in Table 4-8.

The amount of CaCO₃ precipitation was calculated by using CO₂ volume exchange method on the sixth day. Hence, the specific CaCO₃ precipitation activity was calculated according to sixth day results. However, wet biogranules and *S. pasteurii* completely precipitated dissolved calcium under aerobic and microaerobic conditions on the second day. If dissolved calcium in the biomineralization medium fully were precipitated, 650 mg of CaCO₃ would be formed. Therefore, the specific CaCO₃ precipitation activities of wet biogranules and *S. pasteurii* were calculated as 6500 mg CaCO₃.g⁻¹ CDW.d⁻¹.

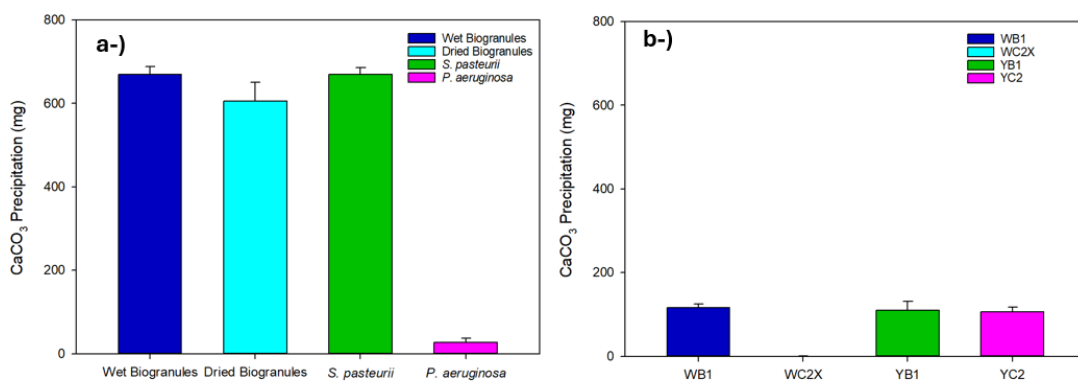


Figure 4-33. CaCO₃ precipitation under aerobic conditions; (a) biogranules, *S. pasteurii*, and *P. aeruginosa*, (b) isolates

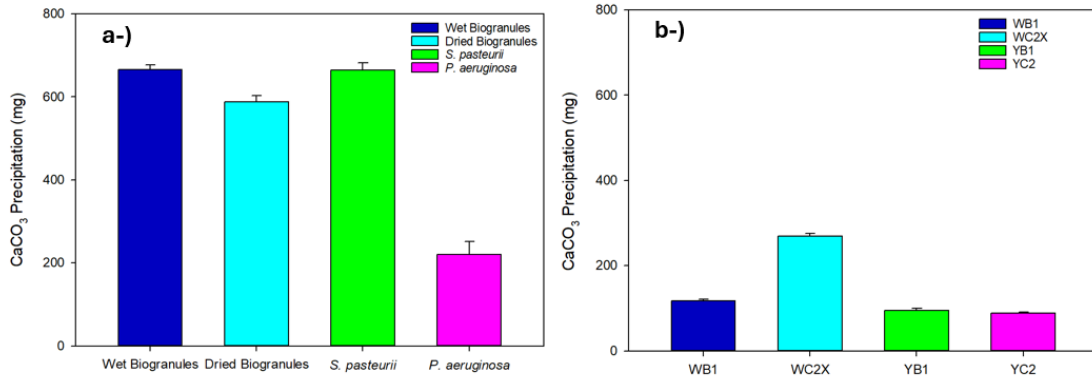


Figure 4-34. CaCO₃ precipitation under microaerobic conditions; (a) biogranules, *S. pasteurii*, and *P. aeruginosa*, (b) isolates

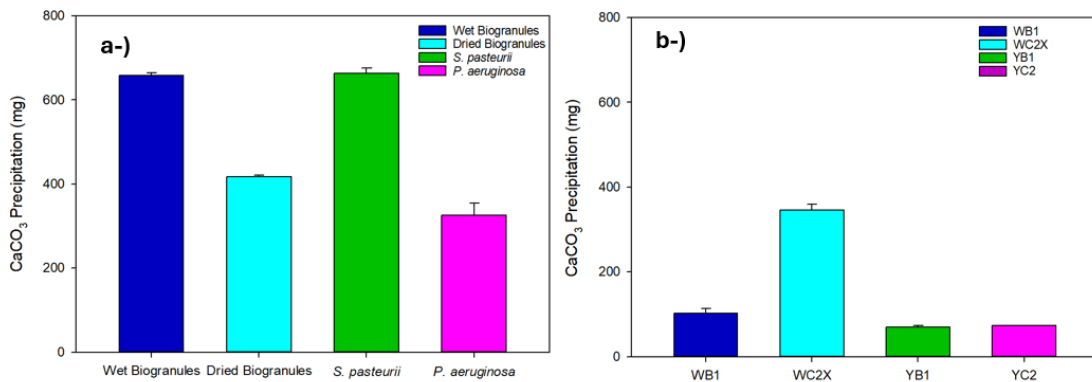


Figure 4-35. CaCO₃ precipitation under anoxic conditions; (a) biogranules, *S. pasteurii*, and *P. aeruginosa*, (b) isolates

The total amount of CaCO₃ precipitation and specific CaCO₃ precipitation activities were calculated for aerobic, microaerobic, and anoxic conditions. At the end of the sixth day under aerobic conditions, specific CaCO₃ precipitation activities for wet and dried biogranules, *S. pasteurii* and *P. aeruginosa* were calculated as 2231±63 mg CaCO₃.g⁻¹ CDW.d⁻¹, 2019±148 mg CaCO₃.g⁻¹ CDW.d⁻¹, 2233±53 mg CaCO₃.g⁻¹ CDW.d⁻¹, 90±23 mg CaCO₃.g⁻¹ CDW.d⁻¹ respectively. Under aerobic condition, specific CaCO₃ precipitation activities for WB1, WC2X, YB1 and YC2 were calculated as 385±31 mg CaCO₃.g⁻¹ CDW.d⁻¹, 0 mg CaCO₃.g⁻¹ CDW.d⁻¹, 367±71 mg CaCO₃.g⁻¹ CDW.d⁻¹, and 367±71 mg CaCO₃.g⁻¹ CDW.d⁻¹, respectively.

Under aerobic conditions, wet biogranules and *S. pasteurii* had the highest specific CaCO₃ precipitation activity. Dried biogranules reached the highest specific CaCO₃ precipitation activity under aerobic conditions. The presence of oxygen in the environment could trigger dried biogranules to resuscitate and lead to introduce microbial activity earlier. Therefore, it was measured that dried biogranules had higher specific CaCO₃ precipitation activity under aerobic conditions (compared to microaerobic and anoxic conditions). At the end of the sixth day under microaerobic conditions, specific CaCO₃ precipitation activities for wet and dried biogranules, *S. pasteurii*, and *P. aeruginosa* were calculated as 2220±38 mg CaCO₃.g⁻¹ CDW.d⁻¹, 1961±48 mg CaCO₃.g⁻¹ CDW.d⁻¹, 2215±56 mg CaCO₃.g⁻¹ CDW.d⁻¹, 733±73 mg CaCO₃.g⁻¹ CDW.d⁻¹ respectively. Under microaerobic condition, specific CaCO₃ precipitation activities for WB1, WC2X, YB1, and YC2 were calculated as 390±14 mg CaCO₃.g⁻¹ CDW.d⁻¹, 897±22 mg CaCO₃.g⁻¹ CDW.d⁻¹, 313±19 mg CaCO₃.g⁻¹ CDW.d⁻¹, and 294±8 mg CaCO₃.g⁻¹ CDW.d⁻¹, respectively.

Under microaerobic conditions, wet biogranules and *S. pasteurii* had the highest specific CaCO₃ precipitation activity. Under microaerobic conditions, *P. aeruginosa* had a higher specific CaCO₃ precipitation activity than its activity under aerobic conditions. At the end of the sixth day under anoxic conditions, specific CaCO₃ precipitation activities for wet and dried biogranules, *S. pasteurii* and *P. aeruginosa* were calculated as 2194±20 mg CaCO₃.g⁻¹ CDW.d⁻¹, 1390±14 mg CaCO₃.g⁻¹ CDW.d⁻¹, 2210±42 mg CaCO₃.g⁻¹ CDW.d⁻¹, 1083±70 mg CaCO₃.g⁻¹ CDW.d⁻¹ respectively. Under anoxic condition, specific CaCO₃ precipitation activities for WB1, WC2X, YB1, and YC2 were calculated as 341±39 mg CaCO₃.g⁻¹ CDW.d⁻¹, 1152±45 mg CaCO₃.g⁻¹ CDW.d⁻¹, 230±14 mg CaCO₃.g⁻¹ CDW.d⁻¹, and 243±1 mg CaCO₃.g⁻¹ CDW.d⁻¹, respectively.

Under anoxic conditions, wet biogranules and *S. pasteurii* had the highest specific CaCO₃ precipitation activity. Dried biogranules had the lowest specific CaCO₃ precipitation activity under anoxic conditions (compared to aerobic, and microaerobic conditions). This could be due to retarded resuscitation of dried biogranules in the absence of oxygen or decreased microbial activity.

Table 4-8. Specific CaCO₃ precipitation at different DO concentrations

Samples	Aerobic Condition	Microaerobic Condition	Anoxic Condition
	mg CaCO ₃ .g ⁻¹ CDW.d ⁻¹		
Wet biogranules	2231±63	2220±38	2194±20
Dried biogranules	2019±148	1961±48	1390±14
<i>S. pasteurii</i>	2233±53	2215±56	2210±42
<i>P. aeruginosa</i>	157±42	331±62	883±90
WB1	385±31	390±14	341±39
WC2X	0	897±22	1152±45
YB1	367±71	313±19	230±14
YC2	353±38	294±8	243±1

Under aerobic conditions, specific CaCO₃ precipitation activities for WB1, WC2X, YB1 and YC2 were calculated as 385±31 mg CaCO₃.g⁻¹ CDW.d⁻¹, 0 mg CaCO₃.g⁻¹ CDW.d⁻¹, 367±71 mg CaCO₃.g⁻¹ CDW.d⁻¹, and 353±38 mg CaCO₃.g⁻¹ CDW.d⁻¹, respectively. WB1 had the highest specific CaCO₃ precipitation activity among isolates under aerobic conditions. Under microaerobic and anoxic conditions, WC2X reached the highest activity among isolates. When compared to wet and dried biogranules, isolates were found to have lower activity at three oxygenic conditions. The potential reason of this result could be related to microbial activity. Since biogranules had the highest microbial activity (using both urea hydrolysis and denitrification metabolic pathways simultaneously), they precipitated higher CaCO₃.

Although dried biogranules precipitated less amount of CaCO₃ than *S. pasteurii*, it was determined that dried biogranules were more advantageous than *S. pasteurii* under anoxic conditions because spores could resuscitate and produce urease enzyme under anoxic

conditions. It was also determined that when nitrate was used instead of oxygen as electron acceptor in wet biogranules, specific CaCO₃ precipitation activity decreased by around 25% (Table 4-8). Under aerobic conditions, dried biogranules had the highest specific CaCO₃ precipitation activity (3070±240 mg CaCO₃.g⁻¹ CDW.d⁻¹) among different oxygenic conditions. This might be related to the fact that spores in dried biogranules resuscitated and precipitated CaCO₃ in the presence of oxygen. Since oxygen had higher redox potential than nitrate [87], which was an alternative electron acceptor, it increased resuscitation rate of facultative spores in dried biogranules and production of urease enzyme. Therefore, increase in specific CaCO₃ precipitation activity was detected. It was determined that if electron acceptor was nitrate, resuscitation of spores was retarded, and specific CaCO₃ precipitation activity decreased by 50% (Table 4-8).

The dissolved calcium concentrations and the amount of precipitated CaCO₃ in batches at different DO concentrations were compared by using mass balance method (Table 4-9). According to these results, it was determined that dissolved calcium precipitation in batches transformed into CaCO₃ minerals.

Table 4-9. Comparison of the amount of precipitated CaCO₃ and the precipitated dissolved calcium concentration at different DO concentrations

Conditions	Samples	CaCO ₃ precipitation performances, %	Precipitated Ca ²⁺ performances, %
Aerobic	Wet biogranules	100	100
	Dried biogranules	93±5	100
	<i>S. pasteurii</i>	100	100
	<i>P. aeruginosa</i>	4±1	5±1
	WB1	18±1	18±2
	WC2X	0	0
	YB1	17±3	17±1
	YC2	16±2	15±1
Microaerobic	Wet biogranules	100	100
	Dried biogranules	90±2	92±2

Conditions	Samples	CaCO ₃ precipitation performances, %	Precipitated Ca ²⁺ performances, %
	<i>S. pasteurii</i>	100	100
	<i>P. aeruginosa</i>	34±3	33±1
	WB1	18±1	20±1
	WC2X	41±1	43±5
	YB1	14±1	15±1
	YC2	14±1	12±1
Anoxic	Wet biogranules	100	100
	Dried biogranules	64±1	62±1
	<i>S. pasteurii</i>	100	100
	<i>P. aeruginosa</i>	50±3	46±2
	WB1	16±2	16±1
	WC2X	53±2	53±2
	YB1	11±1	12±1
	YC2	11±1	10±1

4.9. Calcium Carbonate Precipitation with Biogranules and Axenic Cultures at Different Ambient Temperature

The aims of these tests were to observe effects of different ambient temperatures on microbial activity and biomineralization performance and to compare biogranules with the axenic cultures and isolates in terms of microbial activity and biomineralization performance. Tests were conducted in three different ambient temperatures; (i) 10°C, (ii) 22°C, (iii) 45°C. For all conditions, these tests lasted six days.

The initial pH value of the nutrient solution was measured as 7.2±0.2 at different ambient temperature (10°C, 22°C, 45°C). Daily pH measurements were presented in Figure 4-36. At the end of the sixth day, pH elevated in all batches compared to the initial point. While the pH of dried biogranules, *P. aeruginosa*, and isolates was measured steadily, *S. pasteurii* and wet biogranules elevated rapidly.

As observed at 45°C, pH of dried biogranules, *P. aeruginosa*, and isolates were more stable, while pH of *S. pasteurii* and wet biogranules quickly raised.

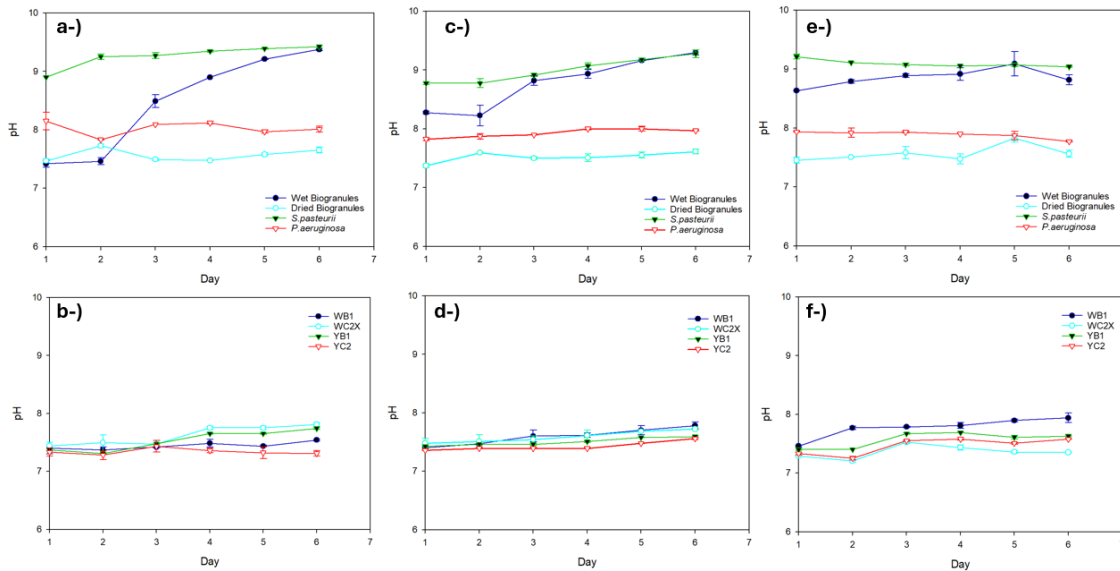


Figure 4-36. pH values at different temperatures; (a, b) 10°C, (c, d) 22°C, (e, f) 45°C

4.9.1. Comparison of Urea Hydrolysis Activities at Different Ambient Temperatures

Urea hydrolysis was measured at different ambient temperatures. The results of the measurements were presented in Figure 4-37-Figure 4-42. Since *P. aeruginosa*, and WC2X did not exhibit urea hydrolysis activity, the results were not included in the graphs. In all environmental conditions, WB1, YB1, and YC2 hydrolyzed about 4-12% of initial urea.

Urea hydrolysis results at 10°C were calculated as 55%, 20%, and 88% for wet biogranules, dried biogranules and *S. pasteurii*, respectively. Urea hydrolysis results at 10°C were calculated as 4%, 3%, and 2% for WB1, YB1, and YC2, respectively.

In the literature, *S. pasteurii* was also tested at 7-10°C [199,204]. *S. pasteurii* also showed effective urea hydrolysis activity even at 7-10°C [260].

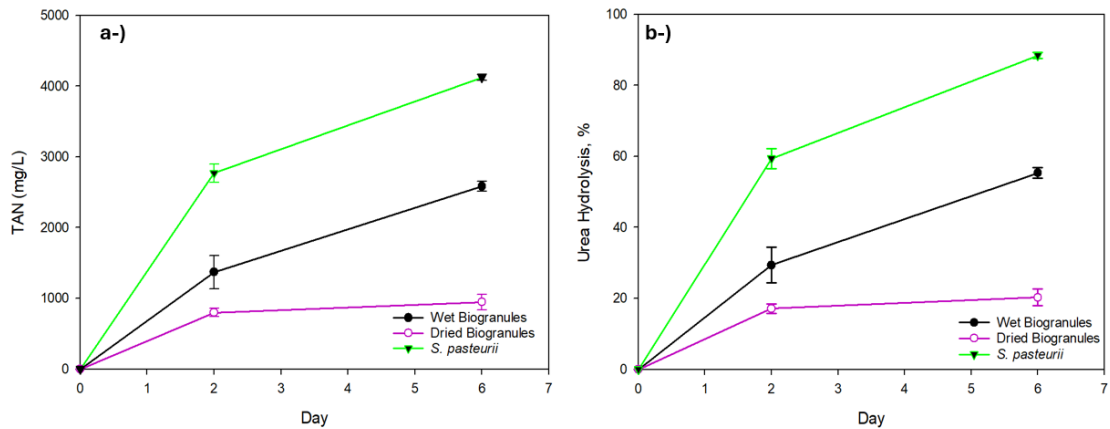


Figure 4-37. Urea hydrolysis results of wet and dried biogranules, and *S. pasteurii* in biom mineralization medium with 0.05 g.L^{-1} YE and at 10°C ; (a) TAN results, (b) hydrolyzed urea

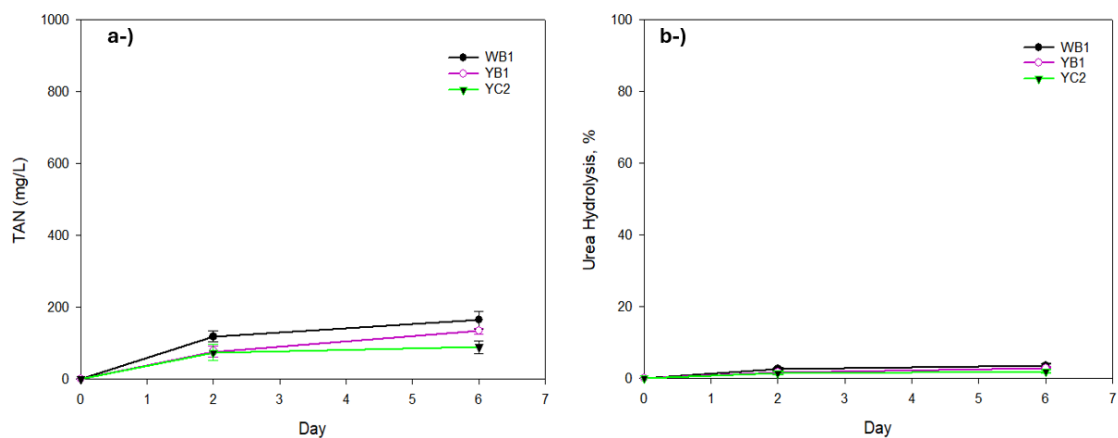


Figure 4-38. Urea hydrolysis results of axenic strains (WB1, YB1, YC2) in biom mineralization medium with 0.05 g.L^{-1} YE and at 10°C ; (a) TAN results, (b) hydrolyzed urea

The urea hydrolysis results at 22°C were presented in Figure 4-39 and Figure 4-40. Urea hydrolysis results at 22°C were calculated as 89%, 38%, and 86% for wet biogranules, dried biogranules and *S. pasteurii*, respectively. Urea hydrolysis results at 22°C were calculated as 6%, 5%, and 5% for WB1, YB1, and YC2, respectively.

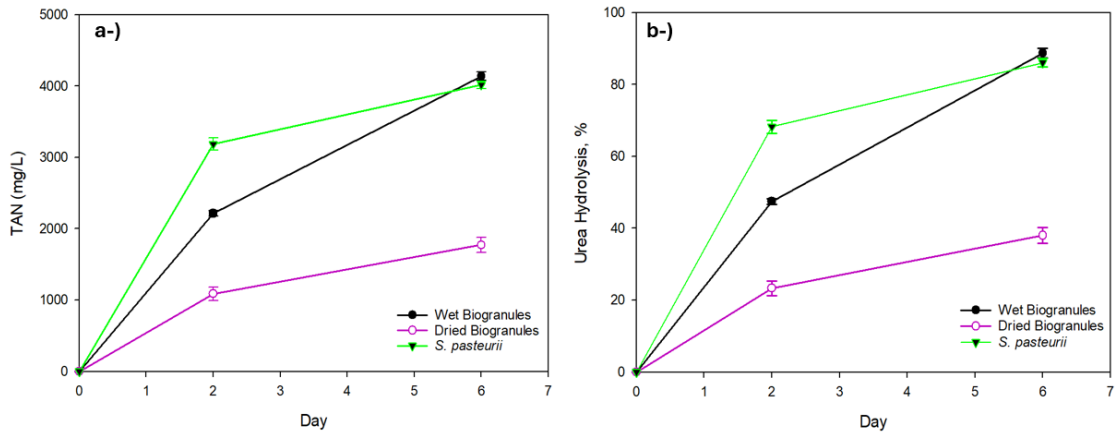


Figure 4-39. Urea hydrolysis results of wet and dried biogranules, and *S. pasteurii* in biom mineralization medium with 0.05 g.L^{-1} YE and at 22°C ; (a) TAN results, (b) hydrolyzed urea

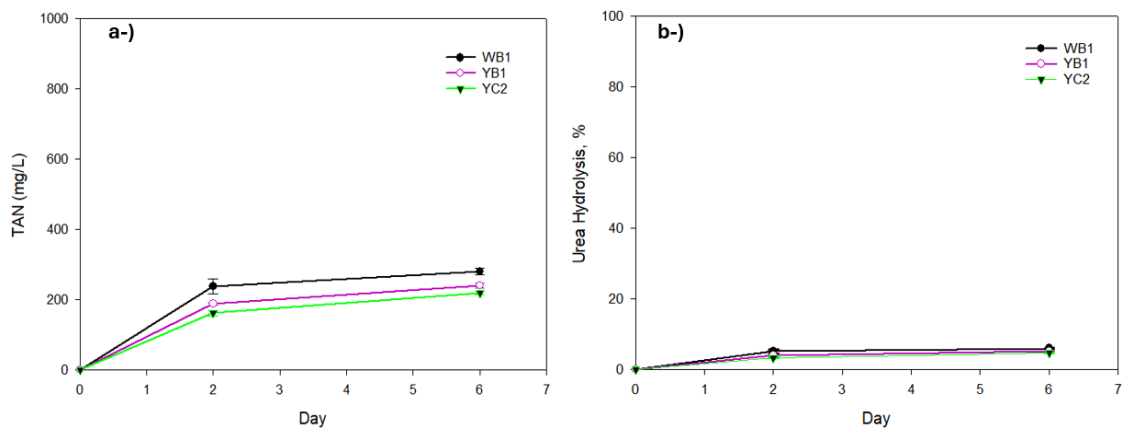


Figure 4-40. Urea hydrolysis results of axenic strains (WB1, YB1, YC2) in biom mineralization medium with 0.05 g.L^{-1} YE and at 22°C ; (a) TAN results, (b) hydrolyzed urea

The urea hydrolysis results at 45°C were presented in Figure 4-41 and Figure 4-42. Urea hydrolysis results at 45°C were calculated as 88%, 40%, and 93% for wet biogranules, dried biogranules and *S. pasteurii*, respectively. Urea hydrolysis results at 45°C were calculated as 11%, 9%, and 6% for WB1, YB1, and YC2, respectively. Wet and dried biogranules, *S. pasteurii*, and isolates had higher urea hydrolysis at 45°C when compared to at 10°C and 22°C . Their urea hydrolysis increased as temperature increased. The increase in urea hydrolysis with raising temperature was consistent with the literature [9].

The increase in temperature could trigger microbial activity of bacteria to hydrolyze urea. Urea hydrolysis of dried biogranules on the second day reached higher ratio at 45 °C. The increase in temperature could accelerate resuscitation of dried biogranules including spores.

Isolates had the highest urea hydrolysis at the highest ambient temperature (45°C). As the temperature increased, microbial activity of isolates also increased, especially WB1. Considering that isolates were of soil-origin and *Bacillus* sp., this was not an unforeseen result. *Bacillus* sp. in MICP applications were generally used in a wide temperature range. *Bacillus* sp. also have tolerant to extreme temperature. The increase in temperature also created a significant difference for isolates in terms of urea hydrolysis. Nevertheless, urea hydrolysis results of isolates were very low compared to wet and dried biogranules and *S. pasteurii*.

Wet and dried biogranules, and *S. pasteurii* had urea hydrolysis activity at three different ambient temperatures (10°C, 22°C, 45°C). *S. pasteurii* showed high urea hydrolysis activity, especially between 30-40°C. The increase in temperature also caused bacteria inside the biogranules to show higher microbial activity (in terms of urea hydrolysis). In this test, it was observed how the amount of hydrolyzed urea changed with temperature. In literature, it was revealed that as temperature increased within the range of 10°C-40°C, microbial activity of *S. pasteurii* also increased [9,260]. It could be stated that temperature range within the scope of this thesis (10°C-45°C) was suitable for *S. pasteurii* which could secrete urease enzyme up to the optimum level.

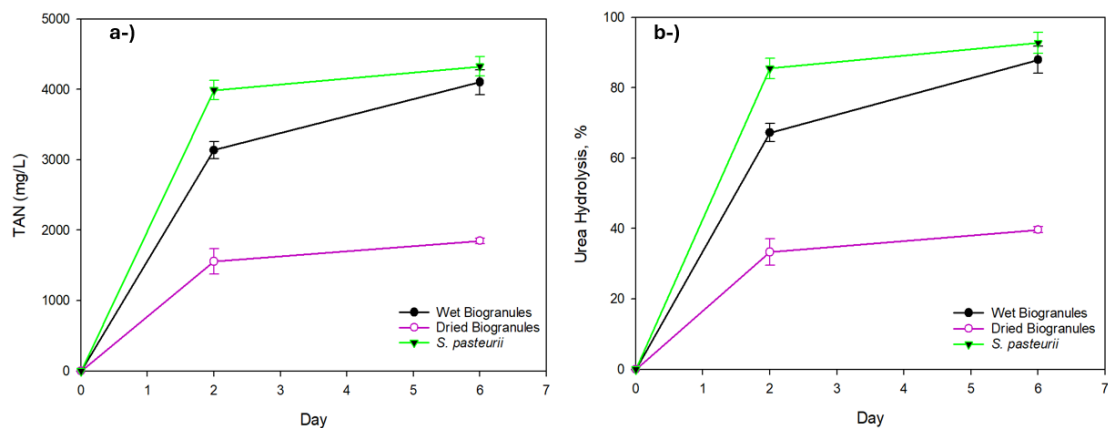


Figure 4-41. Urea hydrolysis results of wet and dried biogranules, and *S. pasteurii* in biom mineralization medium with 0.05 g.L⁻¹ YE and at 45°C; (a) TAN results, (b) hydrolyzed urea

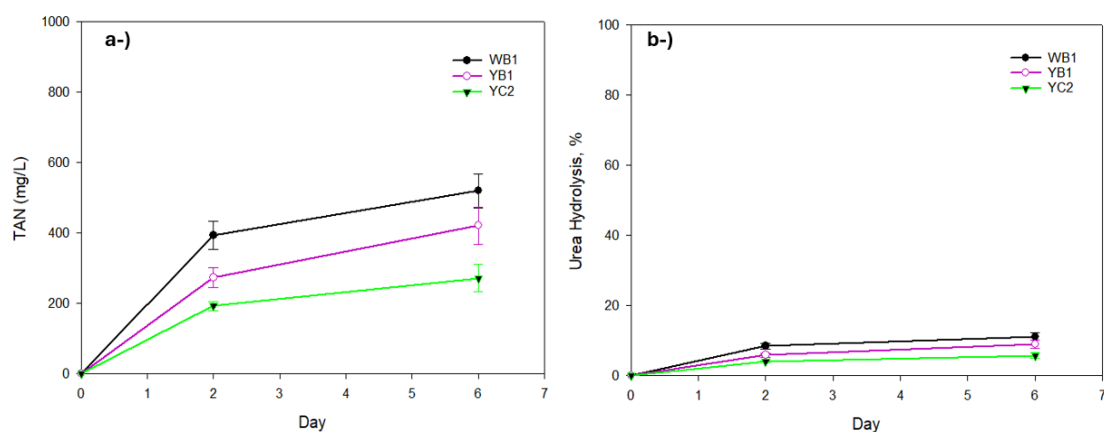


Figure 4-42. Urea hydrolysis results of axenic strains (WB1, YB1, YC2) in biom mineralization medium with 0.05 g.L⁻¹ YE and at 45°C; (a) TAN results, (b) hydrolyzed urea

Specific urea hydrolysis activities of biogranules, *S. pasteurii*, and isolates at different temperatures were given in Table 4-10. At 10°C conditions, wet and dried biogranules, *S. pasteurii*, and isolates (WB1, YB1, YC2) had 2.94 g Urea.d⁻¹.g⁻¹ CDW, 1.71 g Urea.d⁻¹.g⁻¹ CDW, 5.94 g Urea.d⁻¹.g⁻¹ CDW, 0.26 g Urea.d⁻¹.g⁻¹ CDW, 0.17 g Urea.d⁻¹.g⁻¹ CDW, 0.16 g Urea.d⁻¹.g⁻¹ CDW specific urea hydrolysis activity on the second day, respectively.

Among specific urea hydrolysis activities on the second and sixth days, *S. pasteurii* had the highest urea hydrolysis activity. *S. pasteurii* highly hydrolyzed urea even at 10°C. It was reported in the literature that *S. pasteurii* could hydrolyze urea at low temperatures [204]. Wet biogranules had the highest urea hydrolysis activity, followed by *S. pasteurii*. Specific urea hydrolysis activity of dried biogranules at 10°C had the lowest performance compared to other temperatures on the second days. The reason of this might be attributed that resuscitation of dried biogranules could retard at 10°C. Similar to dried biogranules, specific urea hydrolysis activity of isolates at 10°C had the lowest performance compared to other temperatures on the second days.

Table 4-10. Specific urea hydrolysis activity at different temperatures

Samples	10°C		22°C		45°C	
	2 nd	6 th	2 nd	6 th	2 nd	6 th
	g Urea.d ⁻¹ .g ⁻¹ CDW					
Wet biogranules	2.94	1.85	4.75	2.96	6.73	2.93
Dried biogranules	1.71	0.68	2.33	1.27	3.33	1.32
<i>S. pasteurii</i>	5.94	2.95	6.83	2.87	8.55	3.09
WB1	0.26	0.12	0.52	0.20	0.85	0.37
YB1	0.17	0.10	0.41	0.17	0.59	0.30
YC2	0.16	0.06	0.35	0.16	0.41	0.19

At 22°C conditions, wet and dried biogranules, *S. pasteurii*, and isolates (WB1, YB1, YC2) had 4.75 g Urea.d⁻¹.g⁻¹ CDW, 2.33 g Urea.d⁻¹.g⁻¹ CDW, 6.83 g Urea.d⁻¹.g⁻¹ CDW, 0.52 g Urea.d⁻¹.g⁻¹ CDW, 0.41 g Urea.d⁻¹.g⁻¹ CDW, 0.35 g Urea.d⁻¹.g⁻¹ CDW specific urea hydrolysis activity on the second day, respectively.

Specific urea hydrolysis activities of wet biogranules on the sixth day was calculated as 2.96 g Urea.d⁻¹.g⁻¹ CDW. Among specific urea hydrolysis activities on the sixth day, wet biogranules had the highest urea hydrolysis activity. Specific urea hydrolysis activity of

dried biogranules on the sixth day was 1.27 g Urea.d⁻¹.g⁻¹ CDW. Specific urea hydrolysis activity of dried biogranules at 22°C was superior to 10°C of temperature. At 45°C conditions, wet and dried biogranules, *S. pasteurii*, and isolates (WB1, YB1, YC2) had 6.73 g Urea.d⁻¹.g⁻¹ CDW, 3.33 g Urea.d⁻¹.g⁻¹ CDW, 8.55 g Urea.d⁻¹.g⁻¹ CDW, 0.85 g Urea.d⁻¹.g⁻¹ CDW, 0.59 g Urea.d⁻¹.g⁻¹ CDW, 0.41 g Urea.d⁻¹.g⁻¹ CDW specific urea hydrolysis activity on the second day, respectively.

As in previous conditions (at 10°C and 22°C), *S. pasteurii* had the highest urea hydrolysis activity compared to biogranules and isolates. According to these results, as the temperature increased from 10°C to 45°C, specific urea hydrolysis activities of all samples increased. Increase in temperature caused to increase in microbial activity and urea hydrolysis performances of wet and dried biogranules, *S. pasteurii*, and isolates. Specific urea hydrolysis activities of isolates at 45°C were superior to other conditions (10°C and 22°C). WB1 had the highest specific urea hydrolysis activity compared to YB1 and YC2.

4.9.2. Nitrate Reduction Activities at Different Ambient Temperatures

Nitrate reduction and nitrite accumulation were measured at the end of the second and sixth days in tests at different ambient temperatures. NO₃-N and NO₂-N measurements performed at 10°C were presented in Figure 4-43 and Figure 4-44.

Nitrate reduction results on the sixth day at 10°C were measured as 40%, 10%, 20%, and 10% for wet biogranules, dried biogranules, *S. pasteurii* and *P. aeruginosa*, respectively. At 10°C, wet and dried biogranules, *S. pasteurii*, and *P. aeruginosa* had low nitrate reduction. At 10°C, wet biogranules reached the highest nitrate reduction. Nitrate reduction of wet and dried biogranules, *S. pasteurii*, and *P. aeruginosa* decreased at 10°C. As in previous tests, *S. pasteurii* was found to be only able to reduce NO₃⁻ to NO₂⁻.

Isolates had low nitrate reduction at 10°C. It was observed that microbial activities of isolates decreased as temperature decreased. Nitrate-reducing axenic cultures (*P. aeruginosa* and WC2X) also had lower nitrate reduction as the temperature decreased.

Nitrite accumulation was not detected for dried biogranules and *P. aeruginosa*, while it was measured as 4 mg.L⁻¹ NO₂-N and 44 mg.L⁻¹ NO₂-N for wet biogranules and *S. pasteurii*, respectively.

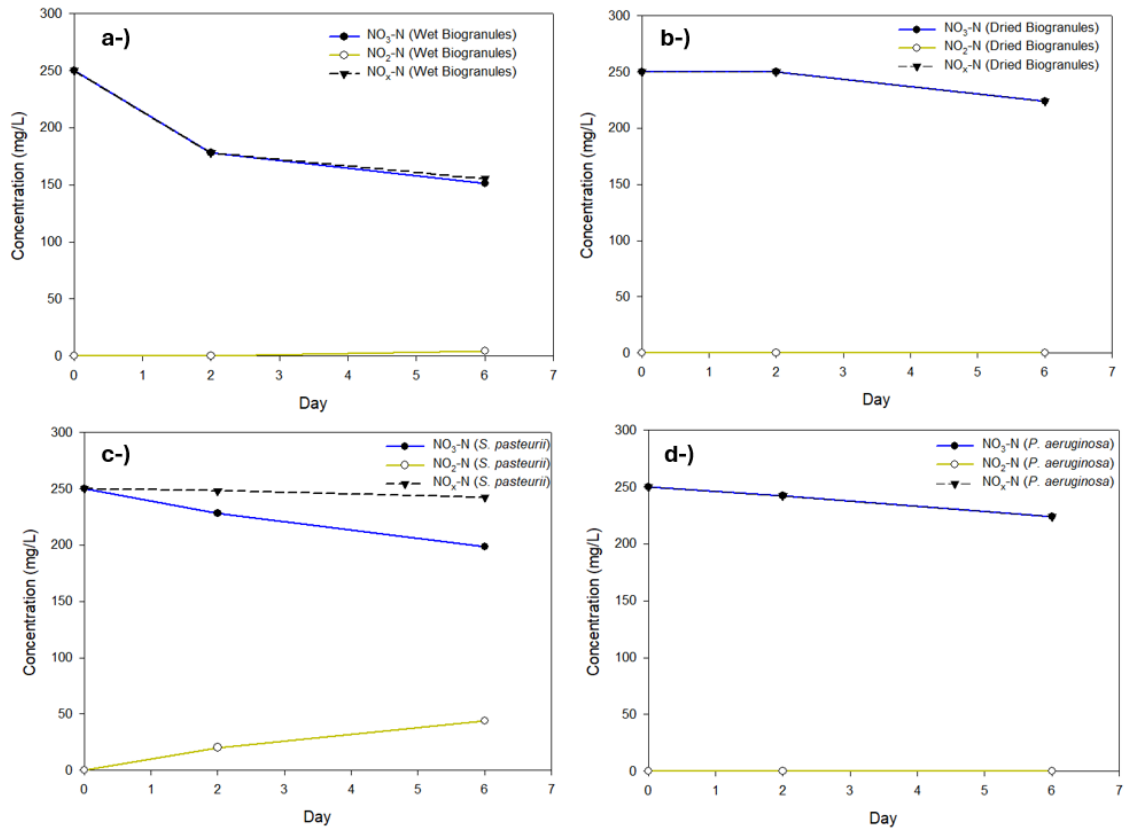


Figure 4-43. Nitrate reduction and nitrite measurements at 10°C, (a) wet biogranules, (b) dried biogranules, (c) *S. pasteurii*, (d) *P. aeruginosa*

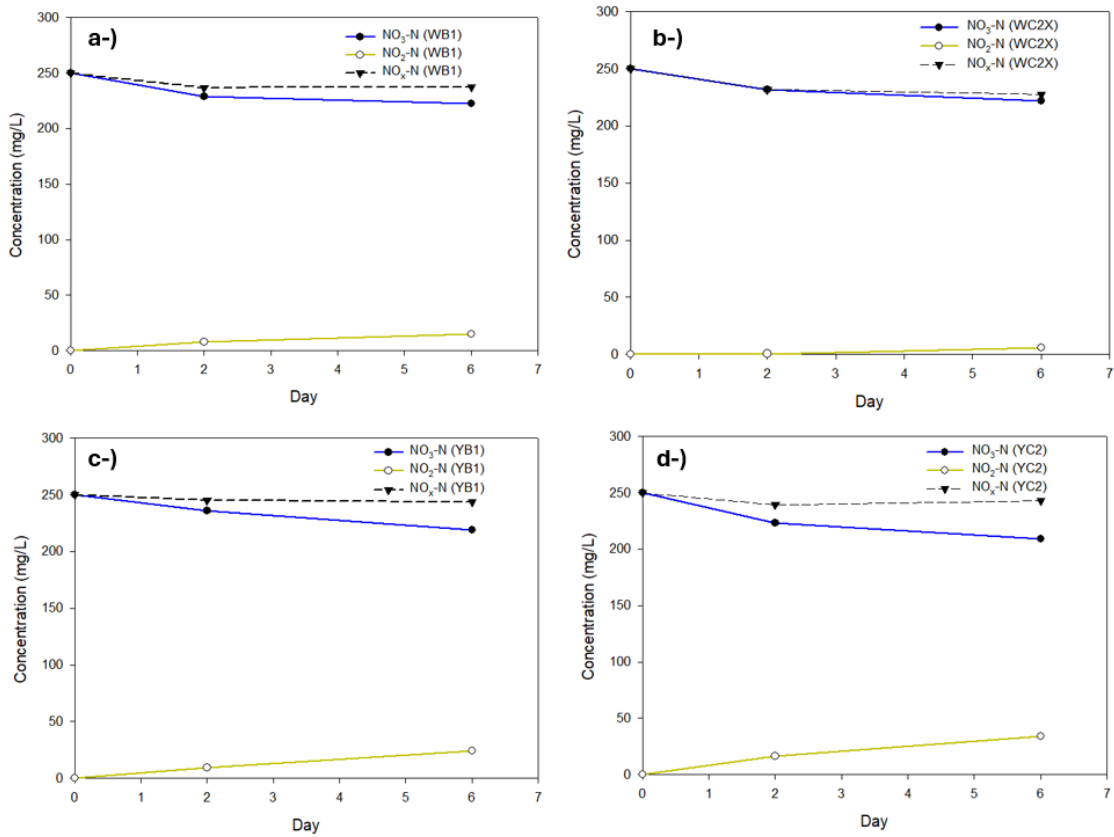


Figure 4-44. Nitrate reduction and nitrite measurements at 10°C, (a) WB1, (b) WC2X, (c) YB1, (d) YC2

Specific nitrate reduction, specific nitrite accumulation, and specific denitrification activities for batches at 10°C were given in Table 4-11.

At 10°C conditions, wet and dried biogranules, *S. pasteurii*, *P. aeruginosa* and isolates (WB1, WC2X, YB1, and YC2) had 32 mg NO_x-N d⁻¹.g⁻¹CDW, 9 mg NO_x-N d⁻¹.g⁻¹CDW, 2 mg NO_x-N d⁻¹.g⁻¹CDW, 9 mg NO_x-N d⁻¹.g⁻¹CDW, 4 mg NO_x-N d⁻¹.g⁻¹CDW, 7 mg NO_x-N d⁻¹.g⁻¹CDW, 2 mg NO_x-N d⁻¹.g⁻¹CDW, 2 mg NO_x-N d⁻¹.g⁻¹CDW specific denitrification activity on the six day, respectively. It was revealed that resuscitation period of dried biogranules retarded under psychrophilic conditions and their specific denitrification activities decreased under psychrophilic conditions.

Table 4-11. Specific NO₃-N reducing, NO₂-N accumulation, and denitrification activity at 10°C

	Wet biogranules	Dried biogranules	<i>S. pasteurii</i>	<i>P. aeruginosa</i>
second day	Specific nitrate-reducing activity (mg NO ₃ -N d ⁻¹ .g ⁻¹ CDW)			
	72	0	22	8
	Specific nitrite accumulation activity (mg NO ₂ -N d ⁻¹ .g ⁻¹ CDW)			
	0	0	20.30	0.00
	Specific denitrification activity (mg NO _x -N d ⁻¹ .g ⁻¹ CDW)			
	72.00	0	1.70	8.00
	Wet biogranules			
	Dried biogranules			
sixth day	Specific nitrate-reducing activity (mg NO ₃ -N d ⁻¹ .g ⁻¹ CDW)			
	33	8.67	17.17	8.67
	Specific nitrite accumulation activity (mg NO ₂ -N d ⁻¹ .g ⁻¹ CDW)			
	1.43	0	15.33	0.00
	Specific denitrification activity (mg NO _x -N d ⁻¹ .g ⁻¹ CDW)			
	31.57	8.67	1.83	8.67
	WB1			
	WC2X			
second day	Specific nitrate-reducing activity (mg NO ₃ -N d ⁻¹ .g ⁻¹ CDW)			
	21	18.5	14	27
	Specific nitrite accumulation activity (mg NO ₂ -N d ⁻¹ .g ⁻¹ CDW)			
	8	0.50	9.40	16.30
	Specific denitrification activity (mg NO _x -N d ⁻¹ .g ⁻¹ CDW)			
	13	18	4.60	10.70
	WB1			
	WC2X			
sixth day	Specific nitrate-reducing activity (mg NO ₃ -N d ⁻¹ .g ⁻¹ CDW)			
	9.17	9.43	10.25	13.67
	Specific nitrite accumulation activity (mg NO ₂ -N d ⁻¹ .g ⁻¹ CDW)			
	5.03	2.00	8.10	11.33
	Specific denitrification activity (mg NO _x -N d ⁻¹ .g ⁻¹ CDW)			
	4.13	7.43	2.15	2.33

NO₃-N and NO₂-N measurements of the test performed at 22°C were presented in Figure 4-45 and Figure 4-46. Nitrate reduction on the sixth day at 22°C were measured as 86%, 58%, 37%, and 88% for wet biogranules, dried biogranules, *S. pasteurii* and *P. aeruginosa*, respectively. At 22°C, wet and dried biogranules, *S. pasteurii*, and *P. aeruginosa* had higher nitrate reduction compared to 10°C. Wet biogranules and *P. aeruginosa* reached the highest nitrate reduction at 22°C. The increase in ambient temperature (from 10°C to 22°C) led to increase nitrate reduction of wet and dried biogranules, *S. pasteurii*, and *P. aeruginosa*. Nitrate reduction activities of all samples at 22°C were superior to psychrophilic conditions. No nitrite accumulation was detected for

wet and dried biogranules, and *P. aeruginosa*, while 83 mg.L⁻¹ NO₂-N was accumulated in *S. pasteurii* at 22°C.

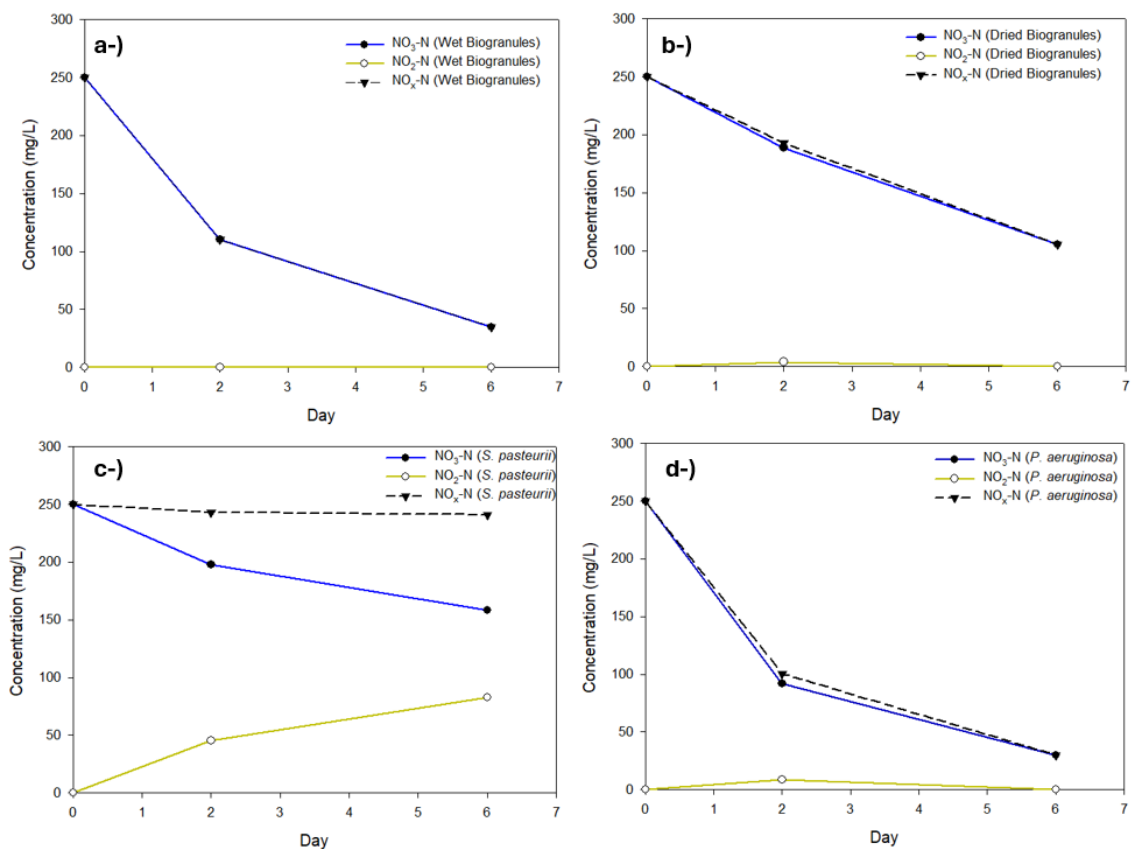


Figure 4-45. Nitrate reduction and nitrite measurements at 22°C, (a) wet biogranules, (b) dried biogranules, (c) *S. pasteurii*, (d) *P. aeruginosa*

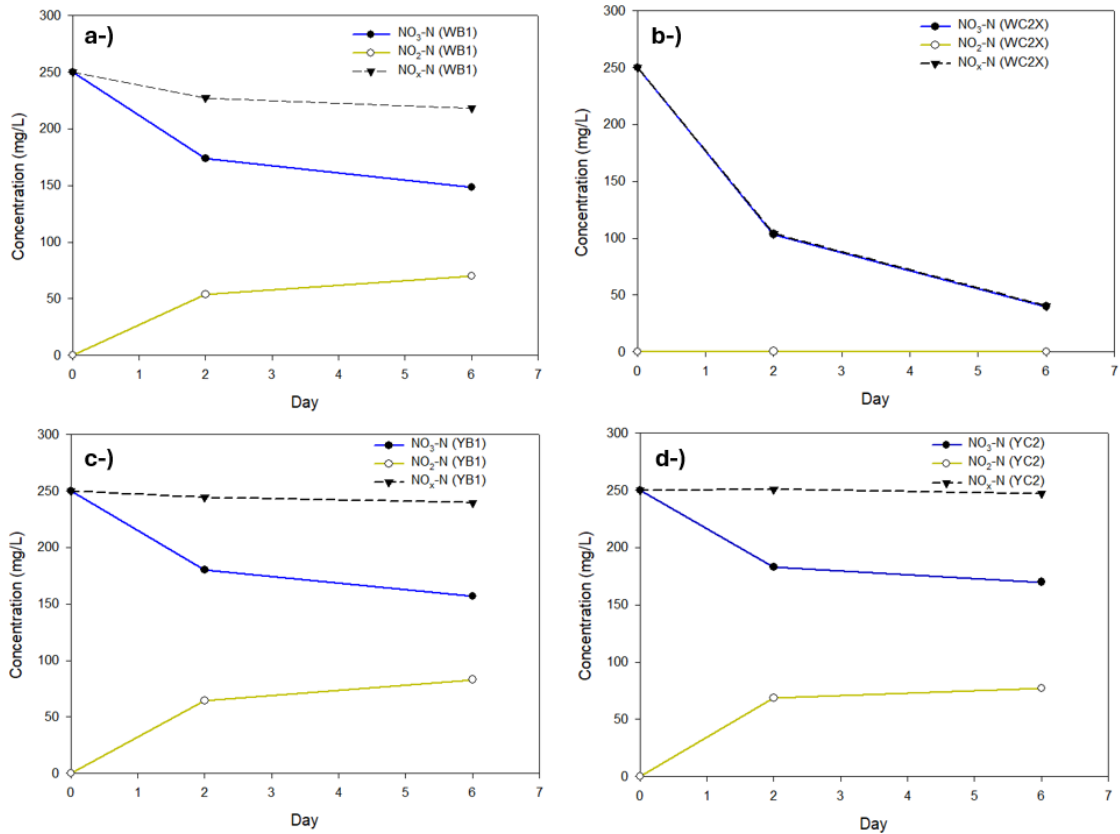


Figure 4-46. Nitrate reduction and nitrite measurements at 22°C, (a) WB1, (b) WC2X, (c) YB1, (d) YC2

Specific nitrate reduction, specific nitrite accumulation, and specific denitrification activities for batches at 22°C were given in Table 4-12.

At 22°C conditions, wet and dried biogranules, *S. pasteurii*, *P. aeruginosa* and isolates (WB1, WC2X, YB1, and YC2) had 72 mg NO_x-N d⁻¹.g⁻¹CDW, 48 mg NO_x-N d⁻¹.g⁻¹CDW, 3 mg NO_x-N d⁻¹.g⁻¹CDW, 73 mg NO_x-N d⁻¹.g⁻¹CDW, 11 mg NO_x-N d⁻¹.g⁻¹CDW, 70 mg NO_x-N d⁻¹.g⁻¹CDW, 3 mg NO_x-N d⁻¹.g⁻¹CDW, 1 mg NO_x-N d⁻¹.g⁻¹CDW specific denitrification activity on the six day, respectively.

Table 4-12. Specific NO₃-N reducing, NO₂-N accumulation, and denitrification activity at 22°C

	Wet biogranules	Dried biogranules	<i>S. pasteurii</i>	<i>P. aeruginosa</i>
second day	Specific nitrate-reducing activity (mg NO ₃ -N d ⁻¹ .g ⁻¹ CDW)			
	140	61	52	158
	Specific nitrite accumulation activity (mg NO ₂ -N d ⁻¹ .g ⁻¹ CDW)			
	0	4	45.30	8.60
	Specific denitrification activity (mg NO _x -N d ⁻¹ .g ⁻¹ CDW)			
	140	57	6.70	149.40
	Wet biogranules	Dried biogranules	<i>S. pasteurii</i>	<i>P. aeruginosa</i>
sixth day	Specific nitrate-reducing activity (mg NO ₃ -N d ⁻¹ .g ⁻¹ CDW)			
	71.67	48.17	30.5	73.33
	Specific nitrite accumulation activity (mg NO ₂ -N d ⁻¹ .g ⁻¹ CDW)			
	0	0	27.57	0
	Specific denitrification activity (mg NO _x -N d ⁻¹ .g ⁻¹ CDW)			
	71.67	48.17	2.93	73.33
	WB1	WC2X	YB1	YC2
second day	Specific nitrate-reducing activity (mg NO ₃ -N d ⁻¹ .g ⁻¹ CDW)			
	76.25	146.5	70	67
	Specific nitrite accumulation activity (mg NO ₂ -N d ⁻¹ .g ⁻¹ CDW)			
	54	0.5	64.40	67
	Specific denitrification activity (mg NO _x -N d ⁻¹ .g ⁻¹ CDW)			
	22.25	146	5.60	0
	WB1	WC2X	YB1	YC2
sixth day	Specific nitrate-reducing activity (mg NO ₃ -N d ⁻¹ .g ⁻¹ CDW)			
	33.93	70	31.07	26.67
	Specific nitrite accumulation activity (mg NO ₂ -N d ⁻¹ .g ⁻¹ CDW)			
	23.33	0.1	27.67	25.67
	Specific denitrification activity (mg NO _x -N d ⁻¹ .g ⁻¹ CDW)			
	10.60	69.87	3.40	1

NO₃-N and NO₂-N measurements at 45°C were presented in Figure 4-47 and Figure 4-48. Nitrate reduction on the sixth day at 45°C were measured as 49%, 16%, 29%, and 31% for wet biogranules, dried biogranules, *S. pasteurii* and *P. aeruginosa*, respectively. Nitrate reduction of wet and dried biogranules, *S. pasteurii*, and *P. aeruginosa* at 45°C were lower compared to 22°C. Wet biogranules and *P. aeruginosa* reached the highest nitrate reduction at 45°C. The increase in ambient temperature (from 22°C to 45°C) decreased nitrate reduction of wet and dried biogranules, *S. pasteurii*, and *P. aeruginosa*. Nitrate reduction was measured to be higher at 22°C. While no nitrite accumulation was detected for dried biogranules at the end of the sixth day at 45°C, it was measured as 2

mg.L⁻¹ NO₂-N, 66 mg.L⁻¹ NO₂-N, 13 mg.L⁻¹ NO₂-N for wet biogranules, *S. pasteurii* and *P. aeruginosa*, respectively.

Isolates had a similar nitrate reduction compared to results occurred at 22°C. However, YB1 and YC2 had higher nitrite accumulation than other isolates (WB1 and WC2X). Isolates also showed microbial activity at 45°C.

When these results were assessed in terms of nitrate and nitrite reduction performance, it was determined that denitrification activity of wet biogranules was less affected by temperature changes. The ambient temperature was found to have a significant effect on both nitrate-reducing activity and resuscitation of spores in dried biogranules. Although decrease in denitrification activities was detected, biogranules could be used in dried form. This led to make biogranules more advantageous compared to *P. aeruginosa* in MICP applications. *S. pasteurii* could only use NO₃-N and performed partial denitrification (only reduce NO₃⁻ to NO₂⁻). Therefore, biomineralization via denitrification put *S. pasteurii* at a disadvantage under anoxic conditions compared to wet biogranules.

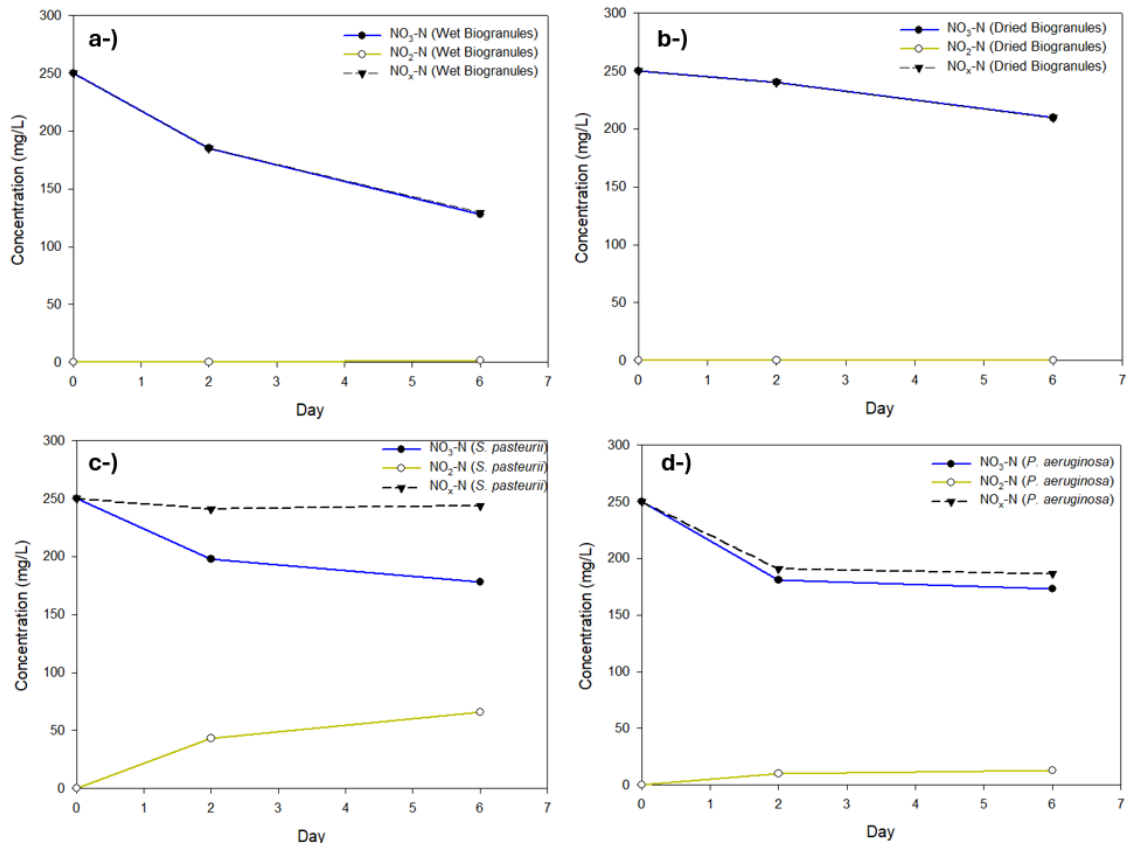


Figure 4-47. Nitrate reduction and nitrite measurements at 45°C, (a) wet biogranules, (b) dried biogranules, (c) *S. pasteurii*, (d) *P. aeruginosa*

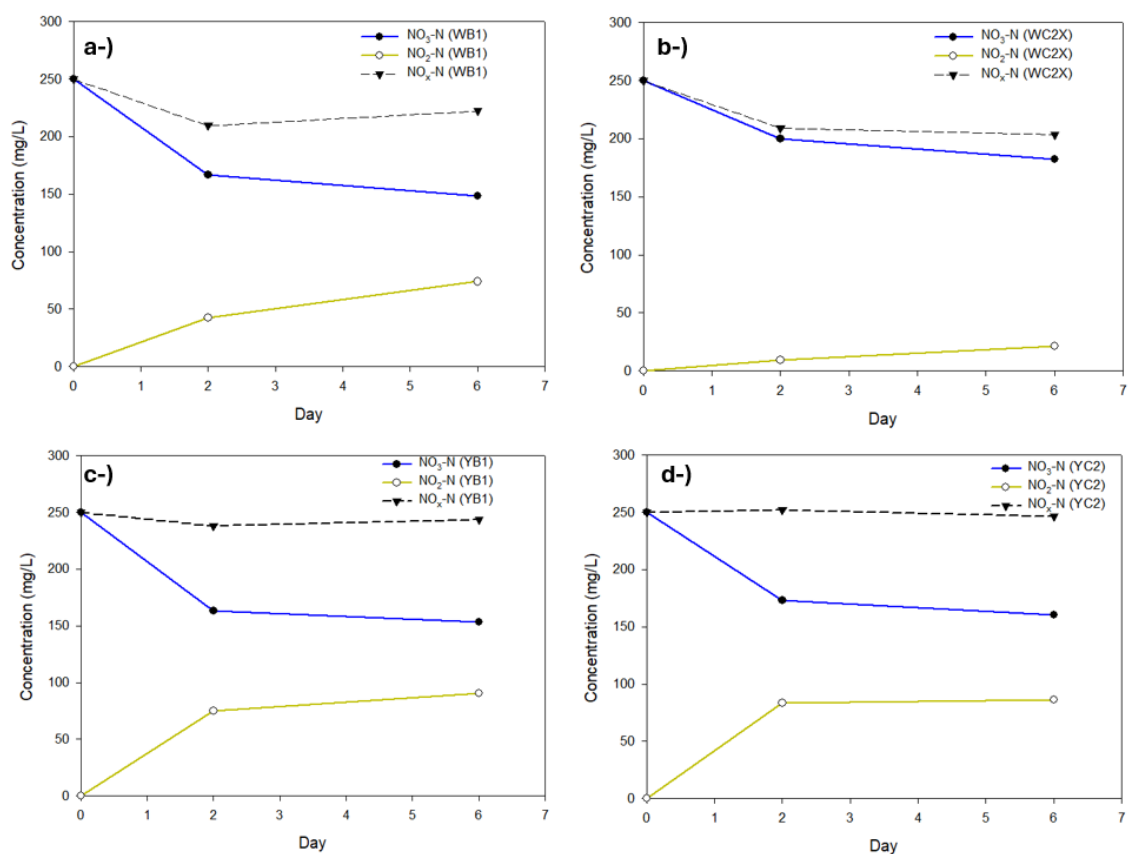


Figure 4-48. Nitrate reduction and nitrite measurements at 45°C, (a) WB1, (b) WC2X, (c) YB1, (d) YC2

Specific nitrate reduction, specific nitrite accumulation, and specific denitrification activities for batches at 45°C were given in Table 4-13.

At 45°C conditions, wet and dried biogranules, *S. pasteurii*, *P. aeruginosa* and isolates (WB1, WC2X, YB1, and YC2) had 40 mg NO_x-N d⁻¹.g⁻¹CDW, 14 mg NO_x-N d⁻¹.g⁻¹CDW, 2 mg NO_x-N d⁻¹.g⁻¹CDW, 21 mg NO_x-N d⁻¹.g⁻¹CDW, 9 mg NO_x-N d⁻¹.g⁻¹CDW, 15 mg NO_x-N d⁻¹.g⁻¹CDW, 2 mg NO_x-N d⁻¹.g⁻¹CDW, 1 mg NO_x-N d⁻¹.g⁻¹CDW specific denitrification activity on the six day, respectively.

It was determined that resuscitation period and nitrate reduction activity of dried biogranules affected by changing temperature. The decrease in denitrification activity with rising temperature (from 22°C to 45°C) was detected. However, this decrease in denitrification activity of dried biogranules was compensated for urea hydrolysis which

increased by temperature. Therefore, biomineralization performance of biogranules did not negatively affect. Using simultaneous urea hydrolysis and nitrate reduction metabolic pathways in biogranules was an advantage to maintain biomineralization performance under varying environmental conditions.

Table 4-13. Specific NO₃-N reducing, NO₂-N accumulation, and denitrification activity at 45°C

	Wet biogranules	Dried biogranules	<i>S. pasteurii</i>	<i>P. aeruginosa</i>
second day	Specific nitrate-reducing activity (mg NO ₃ -N d ⁻¹ .g ⁻¹ CDW)			
	65	10	52	69
	Specific nitrite accumulation activity (mg NO ₂ -N d ⁻¹ .g ⁻¹ CDW)			
	0.30	0	43.20	9.80
	Specific denitrification activity (mg NO _x -N d ⁻¹ .g ⁻¹ CDW)			
	64.70	10	8.80	59.20
	Wet biogranules	Dried biogranules	<i>S. pasteurii</i>	<i>P. aeruginosa</i>
sixth day	Specific nitrate-reducing activity (mg NO ₃ -N d ⁻¹ .g ⁻¹ CDW)			
	40.75	13.5	24	25.58
	Specific nitrite accumulation activity (mg NO ₂ -N d ⁻¹ .g ⁻¹ CDW)			
	0.60	0	22	4.33
	Specific denitrification activity (mg NO _x -N d ⁻¹ .g ⁻¹ CDW)			
	40.15	13.50	2	21.25
	WB1	WC2X	YB1	YC2
second day	Specific nitrate-reducing activity (mg NO ₃ -N d ⁻¹ .g ⁻¹ CDW)			
	83	50	87	77
	Specific nitrite accumulation activity (mg NO ₂ -N d ⁻¹ .g ⁻¹ CDW)			
	42.50	9.10	75.20	77
	Specific denitrification activity (mg NO _x -N d ⁻¹ .g ⁻¹ CDW)			
	40.50	40.90	11.80	0
	WB1	WC2X	YB1	YC2
sixth day	Specific nitrate-reducing activity (mg NO ₃ -N d ⁻¹ .g ⁻¹ CDW)			
	33.92	22.58	32.27	29.87
	Specific nitrite accumulation activity (mg NO ₂ -N d ⁻¹ .g ⁻¹ CDW)			
	24.67	7.10	30.13	28.67
	Specific denitrification activity (mg NO _x -N d ⁻¹ .g ⁻¹ CDW)			
	9.25	15.47	2.14	1.20

4.9.3. Changes in Dissolved Ca²⁺ Concentration at Different Ambient Temperatures

In tests at different temperatures, the changes of dissolved Ca²⁺ concentration were measured in AAS on the second and sixth days. The initial calcium concentration was adjusted to 2.6 g.L⁻¹ Ca²⁺ and the NO_x-N concentration was adjusted to 0.25 g.L⁻¹ NO₃-N. The ureolytic axenic culture *S. pasteurii* and the nitrate-reducing *P. aeruginosa* and isolates, were tested at different ambient temperature (10°C, 22°C, 45°C) to compare them with wet and dried biogranules in terms of biomineralization performances. Time-dependent changes of dissolved calcium concentration in batches during the test period (sixth day) were presented in Figure 4-49, Figure 4-50, and Figure 4-51.

The time-dependent changes of dissolved calcium concentrations at 10°C were presented in Figure 4-49. Wet biogranules and *S. pasteurii* completely precipitated dissolved calcium in the biomineralization medium at the end of the second day. The dissolved calcium concentrations of dried biogranules on the second and sixth days were measured as 2500 mg.L⁻¹, 1373 mg.L⁻¹, respectively. The amount of dissolved calcium in *P. aeruginosa* measured at the end of the sixth day was measured as 2309 mg.L⁻¹. Since the microbial activities of the isolates were low, precipitated dissolved calcium was low.

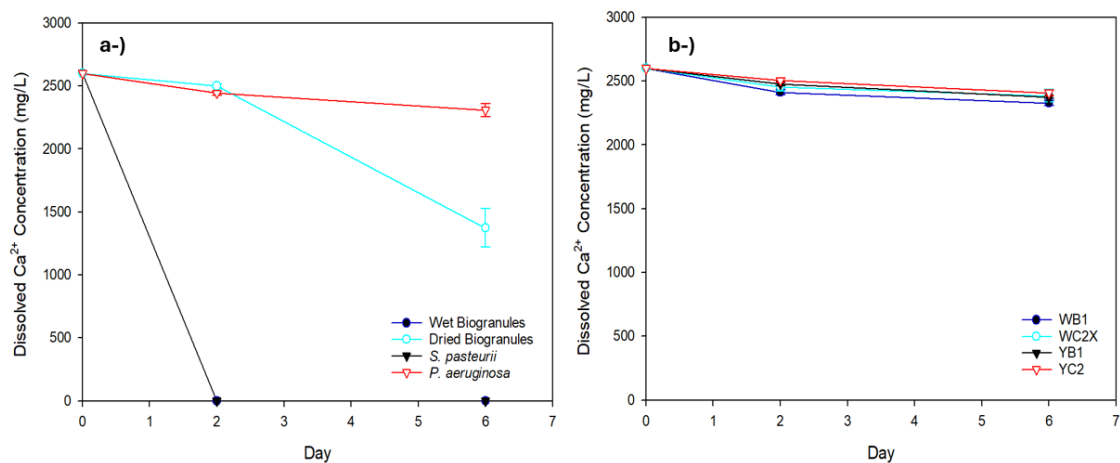


Figure 4-49. Dissolved calcium concentration results at the end of the second and sixth days at 10°C; (a) biogranules, *S. pasteurii*, and *P. aeruginosa*, (b) isolates

The time-dependent changes of dissolved calcium concentration at 22°C were presented in Figure 4-50. While wet biogranules totally precipitated dissolved calcium in the medium at the end of the second day, *S. pasteurii* totally precipitated dissolved calcium in the medium at the end of the sixth day. The dissolved calcium concentration of *S. pasteurii* at the end of the sixth day was measured as 59 mg.L⁻¹. At 22°C, *S. pasteurii* also precipitated almost all dissolved calcium in the environment at the end of the second day. The dissolved calcium concentrations of dried biogranules on the second and sixth days were measured as 1280 mg.L⁻¹, 47 mg.L⁻¹, respectively. The amount of dissolved calcium in *P. aeruginosa* on the sixth day was measured as 1299 mg.L⁻¹. Although changes in dissolved calcium concentration of isolates increased when compared to 10°C, it did not reach a certain level that could cope with biogranules and *S. pasteurii*. Except for WC2X, changes in dissolved calcium concentration of isolates had low microbial activity.

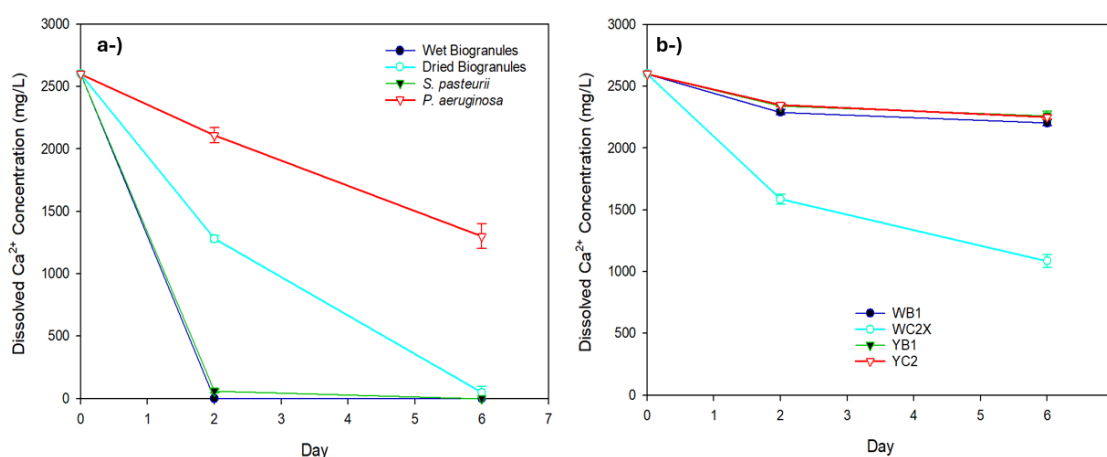


Figure 4-50. Dissolved calcium concentration results at the end of the second and sixth days at 22°C; (a) biogranules, *S. pasteurii*, and *P. aeruginosa*, (b) isolates

The time-dependent changes of dissolved calcium concentration at 45°C were presented in Figure 4-51. While *S. pasteurii* completely precipitated dissolved calcium in biomineralization medium at the end of the second day, wet and dried biogranules completely precipitated dissolved calcium at the end of the sixth day. The dissolved calcium concentration of wet biogranules on the second day was measured as 131 mg.L⁻¹. Wet biogranules precipitated almost all the dissolved calcium in the environment on the second day. The dissolved calcium concentration of dried biogranules was measured as 761 mg.L⁻¹ at the end of the second day. The dissolved calcium concentration

in *P. aeruginosa* on the sixth day was measured as 2207 mg.L⁻¹. At 22°C, *P. aeruginosa* precipitated the highest amount of dissolved calcium, while *P. aeruginosa* precipitated similar amounts of dissolved calcium at 10°C and 45°C. As microbial activity of isolates increased at 45°C, precipitation of dissolved calcium concentration also increased. While dissolved calcium precipitation of WC2X decreased, dissolved calcium precipitation of other three isolates (WB1, YB1, and YC2) increased. These isolates had lower microbial activity and calcium precipitation compared to biogranules and *S. pasteurii*.

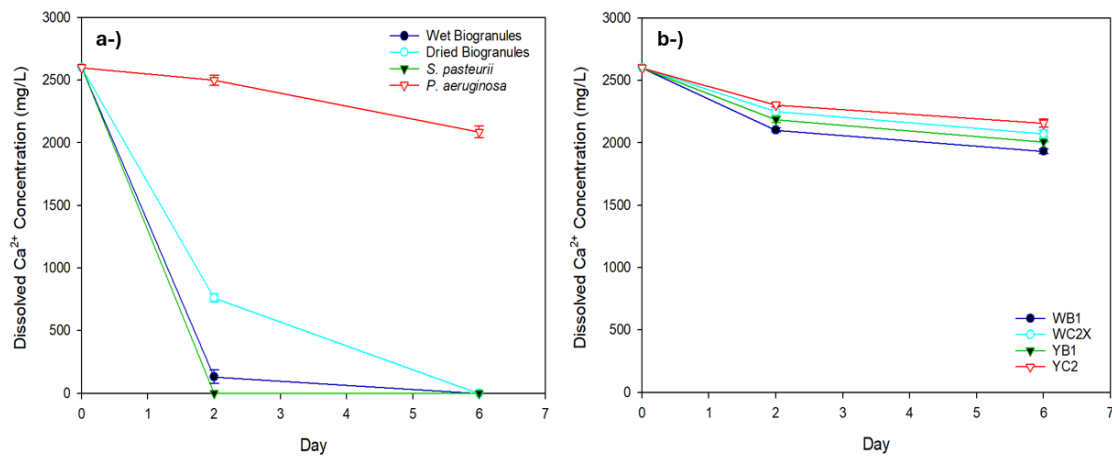


Figure 4-51. Dissolved calcium concentration results at the end of the second and sixth days at 45°C; (a) biogranules, *S. pasteurii*, and *P. aeruginosa*, (b) isolates

4.9.4. Comparison of CaCO₃ Precipitation Activities at Different Ambient Temperatures

The amounts of precipitated CaCO₃ were measured for 10°C, 22°C, and 45°C conditions. CaCO₃ precipitation results were given in Figure 4-52, Figure 4-53, and Figure 4-54. Specific CaCO₃ precipitation activities were given in Table 4-14.

Wet biogranules and *S. pasteurii* completely precipitated dissolved calcium at 10°C, 22°C, and 45°C conditions on the second day. Therefore, the specific CaCO₃ precipitation activities of wet biogranules and *S. pasteurii* were calculated as 6500 mg CaCO₃.g⁻¹ CDW.d⁻¹ on the second day.

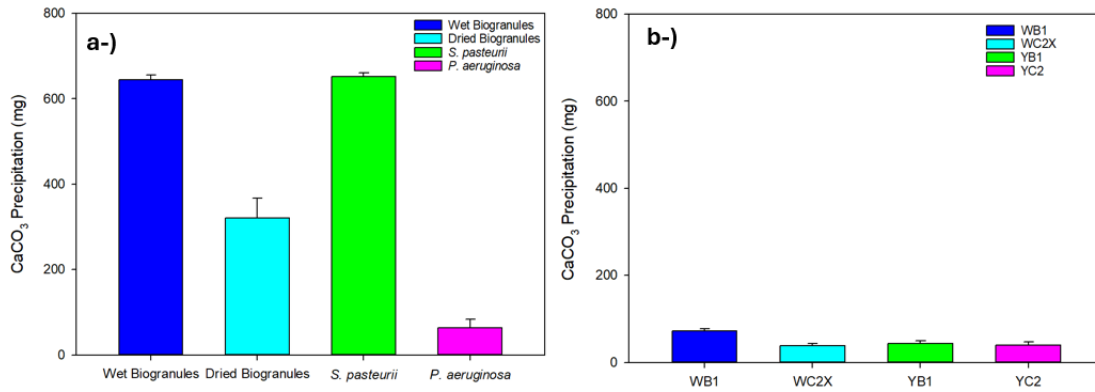


Figure 4-52. CaCO₃ precipitation at 10°C; (a) biogranules, *S. pasteurii*, and *P. aeruginosa*, (b) isolates

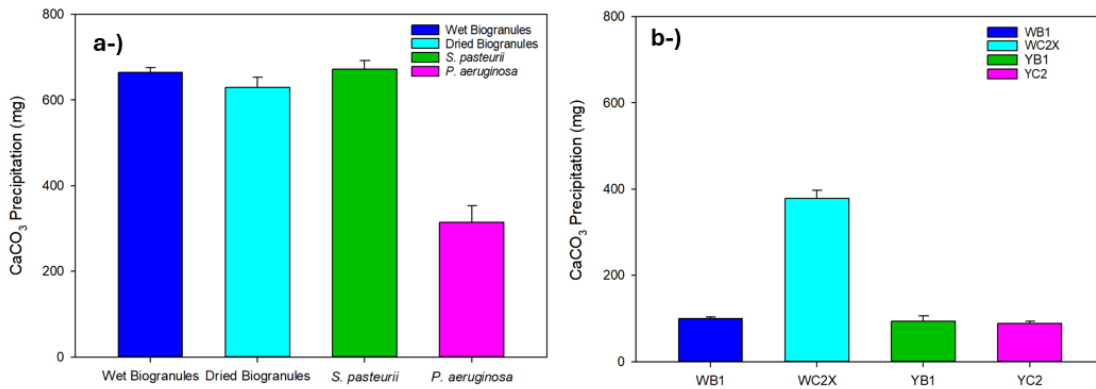


Figure 4-53. CaCO₃ precipitation at 22°C; (a) biogranules, *S. pasteurii*, and *P. aeruginosa*, (b) isolates

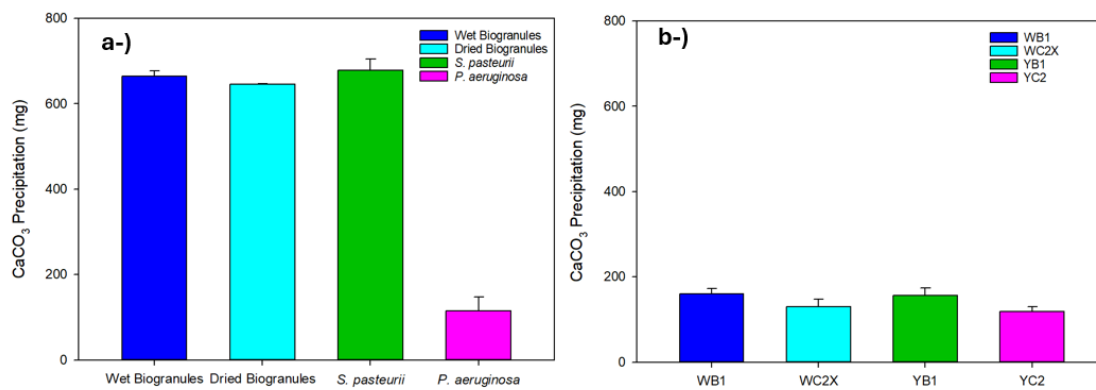


Figure 4-54. CaCO₃ precipitation at 45°C; (a) biogranules, *S. pasteurii*, and *P. aeruginosa*, (b) isolates

At the end of the sixth day at 10°C, specific CaCO₃ precipitation activities for wet and dried biogranules, *S. pasteurii* and *P. aeruginosa* were calculated as 2148±36 mg CaCO₃.g⁻¹ CDW.d⁻¹, 1066±158 mg CaCO₃.g⁻¹ CDW.d⁻¹, 2174±28 mg CaCO₃.g⁻¹ CDW.d⁻¹, 199±59 mg CaCO₃.g⁻¹ CDW.d⁻¹, respectively. Wet biogranules and *S. pasteurii* had the highest specific CaCO₃ precipitation activity at 10°C.

Specific CaCO₃ precipitation activities for WB1, WC2X, YB1 and YC2 were calculated as 239±16 mg CaCO₃.g⁻¹ CDW.d⁻¹, 93±28 mg CaCO₃.g⁻¹ CDW.d⁻¹, 143±20 mg CaCO₃.g⁻¹ CDW.d⁻¹, and 132±26 mg CaCO₃.g⁻¹ CDW.d⁻¹, respectively at 10°C. WB1 had the highest specific CaCO₃ precipitation activity among isolates at 10°C.

At the end of the sixth day at 22°C, specific CaCO₃ precipitation activities for wet and dried biogranules, *S. pasteurii* and *P. aeruginosa* were calculated as 2215±38 mg CaCO₃.g⁻¹ CDW.d⁻¹, 2097±81 mg CaCO₃.g⁻¹ CDW.d⁻¹, 2239±67 mg CaCO₃.g⁻¹ CDW.d⁻¹, 548±104 mg CaCO₃.g⁻¹ CDW.d⁻¹, respectively. Wet biogranules and *S. pasteurii* had the highest specific CaCO₃ precipitation activity at 22°C. *S. pasteurii* reached the highest specific CaCO₃ precipitation activity at 22°C.

Specific CaCO₃ precipitation activities at 22°C for WB1, WC2X, YB1 and YC2 were calculated as 331±13 mg CaCO₃.g⁻¹ CDW.d⁻¹, 1262±61 mg CaCO₃.g⁻¹ CDW.d⁻¹, 312±42 mg CaCO₃.g⁻¹ CDW.d⁻¹, and 294±18 mg CaCO₃.g⁻¹ CDW.d⁻¹, respectively. WC2X had the highest specific CaCO₃ precipitation activity among isolates at 22°C.

At the end of the sixth day at 45°C, specific CaCO₃ precipitation activities wet and dried biogranules, *S. pasteurii* and *P. aeruginosa* were calculated as 2213±43 mg CaCO₃.g⁻¹ CDW.d⁻¹, 1648±66 mg CaCO₃.g⁻¹ CDW.d⁻¹, 2262±87 mg CaCO₃.g⁻¹ CDW.d⁻¹, 901±38 mg CaCO₃.g⁻¹ CDW.d⁻¹, respectively. Wet biogranules and *S. pasteurii* had the highest specific CaCO₃ precipitation activity. *S. pasteurii* reached the highest specific CaCO₃ precipitation activity at 45°C.

Specific CaCO₃ precipitation activities at 45°C for WB1, WC2X, YB1 and YC2 were calculated as 534±39 mg CaCO₃.g⁻¹ CDW.d⁻¹, 433±57 mg CaCO₃.g⁻¹ CDW.d⁻¹, 521±58 mg CaCO₃.g⁻¹ CDW.d⁻¹, and 395±39 mg CaCO₃.g⁻¹ CDW.d⁻¹, respectively. WB1 had the highest specific CaCO₃ precipitation activity among isolates at 45°C.

Table 4-14. Specific CaCO₃ precipitation at different ambient temperature

Samples	10°C	22°C	45°C
	mg CaCO ₃ .g ⁻¹ CDW.d ⁻¹		
Wet biogranules	2148±36	2215±38	2213±43
Dried biogranules	1066±158	2097±81	1648±66
<i>S. pasteurii</i>	2239±67	2239±67	2262±87
<i>P. aeruginosa</i>	400±57	548±104	901±38
WB1	239±16	331±13	534±39
WC2X	93±28	1262±61	433±57
YB1	143±20	312±42	521±58
YC2	132±26	294±18	395±39

Since *P. aeruginosa* only had denitrification activity and its denitrification activity was low under psychrophilic conditions, the amount of CaCO₃ precipitation was also quite low. Although denitrification activities of dried biogranules and *P. aeruginosa* were similar under psychrophilic conditions (~9 mg NO_x-N.d⁻¹.g⁻¹ CDW) (Table 4-11), dried biogranules also precipitated more CaCO₃ via urea hydrolysis. While biomineralization under psychrophilic conditions was mainly due to urea hydrolysis, there was less CaCO₃ precipitation via denitrification. Biomineralization performances via denitrification was less at lower temperatures. The effect of decrease in denitrification activities on biomineralization performance with the increase in temperature from 22°C to 45°C was not observed in the amount of precipitated CaCO₃ (Figure 4-53, Figure 4-54). In addition,

the effect of decrease on biomineralization performances of wet biogranules and *S. pasteurii* at 45°C was not observed. (Table 4-14, Figure 4-54).

There might be two main reasons for these two situations. The first and main reason was that initial amount of urea in biomineralization solution (10 g. L⁻¹) was sufficient to precipitate all of the dissolved calcium in the environment (2.6 g.L⁻¹). Therefore, as long as there was no significant decrease in urea hydrolysis activity, the whole amount of dissolved calcium in the medium could be precipitated after six days. The second reason was that urea hydrolysis activities of all urease-positive cultures increased with the increase in temperature. In this case, even if denitrification activity decreased, no decrease in CaCO₃ precipitation was observed. Therefore, although there was a decrease in nitrate reduction activities of all samples, there was no substantial change in the total amount of CaCO₃ precipitated by biogranules and *S. pasteurii*, but only a decrease was observed in the total amount of CaCO₃ precipitated by *P. aeruginosa*. Specific CaCO₃ precipitation activity of dried biogranules at 45°C was superior to other temperature conditions. This might be due to the fact that resuscitation of urease-positive spores in dried biogranules and production of urease enzyme increased with temperature.

It was also determined that nitrate-reducing spores resuscitated more rapidly at 22°C. Hence, only urea hydrolysis occurred in the first 48 hours and no nitrate reduction activity was observed in dried biogranules at 10°C (Figure 4-37, Figure 4-43). It was determined that increase in activities was quite slow in the next 96 hours. Although nitrate reduction activity of spores was higher at 22°C, increase in urea hydrolysis was greater at 45°C, so biomineralization activity was also higher at 45°C (Figure 4-41, Figure 4-45, Figure 4-54). Although biomineralization activities of dried biogranules at different ambient temperature were lower compared to wet biogranules and *S. pasteurii*, spores which were capable of both urea hydrolysis and denitrification resuscitated at three different ambient temperatures. In this way, it was revealed that biogranules could be used as dried form and dried biogranules were more advantageous than axenic cultures.

The dissolved calcium concentrations and the amount of precipitated CaCO₃ in batches at different ambient temperatures were compared by using mass balance method (Table

4-15). According to these results, it was determined that dissolved calcium precipitation in batches transformed into CaCO₃ minerals.

Table 4-15. Comparison of the amount of precipitated CaCO₃ and the precipitated dissolved calcium concentration at different ambient temperatures

Conditions	Samples	CaCO ₃ precipitation performances, %	Precipitated Ca ²⁺ performances, %
10°C	Wet biogranules	99	100
	Dried biogranules	49±5	47±6
	<i>S. pasteurii</i>	100	100
	<i>P. aeruginosa</i>	11±1	9±2
	WB1	11±1	10±1
	WC2X	6±1	8±3
	YB1	7±1	9±1
	YC2	6±1	7±1
22°C	Wet biogranules	100	100
	Dried biogranules	97±2	98±2
	<i>S. pasteurii</i>	100	100
	<i>P. aeruginosa</i>	50±2	48±4
	WB1	15±1	15±1
	WC2X	55±4	58±3
	YB1	14±2	13±2
	YC2	14±1	14±1
45°C	Wet biogranules	100	100
	Dried biogranules	99±1	100
	<i>S. pasteurii</i>	100	100
	<i>P. aeruginosa</i>	18±4	15±3
	WB1	25±2	26±1
	WC2X	20±3	20±1
	YB1	24±3	23±1
	YC2	18±2	17±2

4.10. Calcium Carbonate Precipitation with Biogranules and Axenic Cultures at Different Salt Concentrations

The aim of these tests was to observe effects of different salt concentrations on bacterial activity and biomineralization performance and to compare biogranules with the axenic cultures and isolates in terms of microbial activity and biomineralization performance. Tests were conducted at three different salinity; (i) marine water (35 g.L⁻¹ NaCl), (ii) drinking water, urban runoff, groundwater (1 g.L⁻¹ NaCl), (iii) rainwater (20 mg.L⁻¹ NaCl). For all conditions, these tests lasted six days. The initial pH value of the biomineralization solution was measured as 7.2±0.2 at different salt concentrations. The pH values measured at the end of the sixth day of the tests were presented in Figure 4-55. At the end of the sixth day, pH elevated in all batches compared to the initial point. The pH of batches with high microbial activity increased more than those with low microbial activity. The main reason for this was formation of an alkaline environment for biomineralization. The alkalinity production led to a higher and faster rate of CaCO₃ precipitation. As observed at 1 g.L⁻¹ NaCl concentration, the pH of *P. aeruginosa*, and isolates were measured to be more stable, while the pH of *S. pasteurii* and wet biogranules quickly raised. While the pH of wet biogranules and *S. pasteurii*, *P. aeruginosa*, and isolates were measured steadily, *S. pasteurii* and wet biogranules elevated rapidly at 0.02 g.L⁻¹ NaCl.

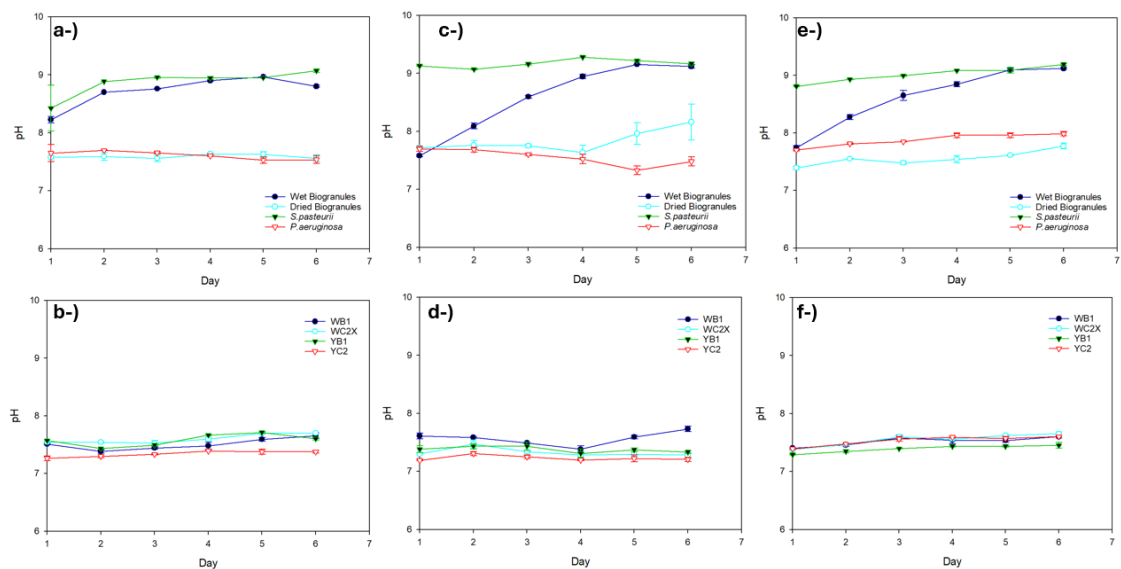


Figure 4-55. pH values at different salinity conditions; (a, b) marine water conditions, (c, d) 1 g.L⁻¹ NaCl, (e, f) rainwater conditions

4.10.1. Comparison of Urea Hydrolysis Activities at Different Salt Concentrations

Urea hydrolysis was measured at the end of the second and sixth days in tests at different salt concentrations. The results of the measurements were presented in Figure 4-56-Figure 4-61. Since *P. aeruginosa* and WC2X did not show urea hydrolysis activity, the results were not included in the graphs.

Urea hydrolysis on the sixth day of marine water conditions were calculated as 86%, 42%, and 87% for wet biogranules, dried biogranules, and *S. pasteurii*, respectively. Urea hydrolysis on the sixth day of marine water condition were calculated as 5%, 4%, and 3% for WB1, YB1, and YC2, respectively. Wet biogranules and *S. pasteurii* had similar urea hydrolysis performances at three different salt concentrations. Wet and dried biogranules and *S. pasteurii* had urea hydrolysis performances under marine water conditions. They could adapt to an environment containing high salt concentrations such as marine water [113,261]. Therefore, this could pave the way for using in MICP applications.

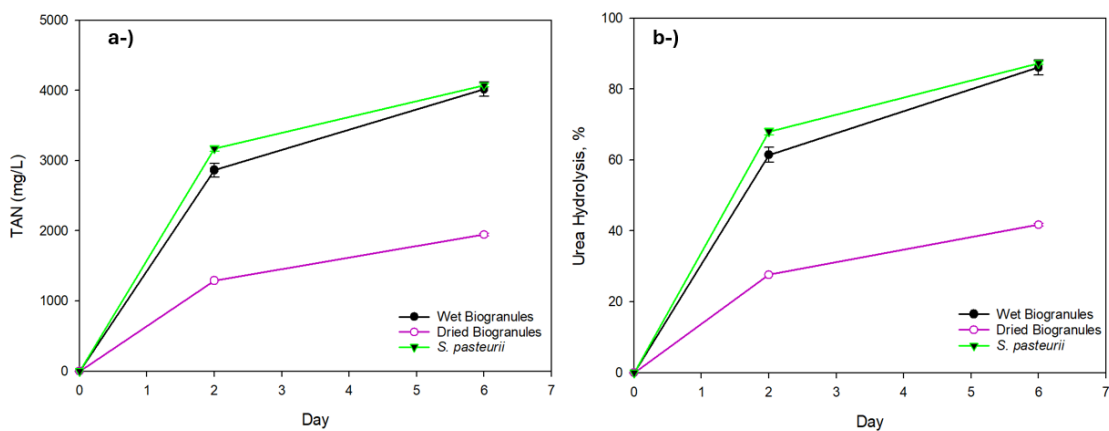


Figure 4-56. Urea hydrolysis activities of wet and dried biogranules and *S. pasteurii* in biom mineralization medium with 0.05 g.L⁻¹ YE and 35 g.L⁻¹ NaCl concentration (marine water conditions); (a) TAN results, (b) hydrolyzed urea

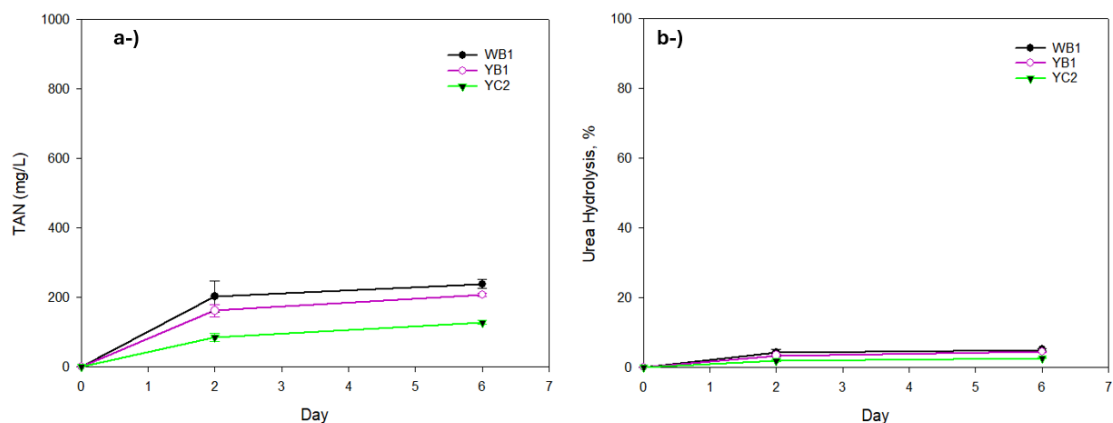


Figure 4-57. Urea hydrolysis activities of axenic strains (WB1, YB1, YC2) in biom mineralization medium with 0.05 g.L^{-1} YE and 35 g.L^{-1} NaCl concentration (marine water conditions); (a) TAN results, (b) hydrolyzed urea

Urea hydrolysis on the sixth day at 1 g.L^{-1} NaCl test were calculated as 88%, 47%, and 92% for wet biogranules, dried biogranules, and *S. pasteurii*, respectively. Urea hydrolysis on the sixth day at 1 g.L^{-1} NaCl were calculated as 5%, 4%, and 4% for WB1, YB1, and YC2, respectively. Dried biogranules showed the highest urea hydrolysis performances at 1 g.L^{-1} NaCl concentration.

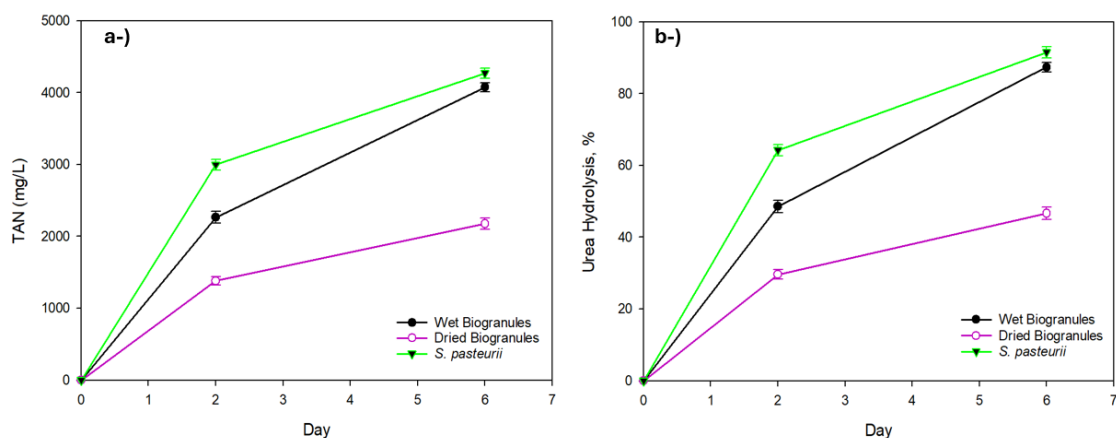


Figure 4-58. Urea hydrolysis activities of wet and dried biogranules and *S. pasteurii* in biom mineralization medium with 0.05 g.L^{-1} YE and 1 g.L^{-1} NaCl concentration (tap water, urban runoff); (a) TAN results, (b) hydrolyzed urea

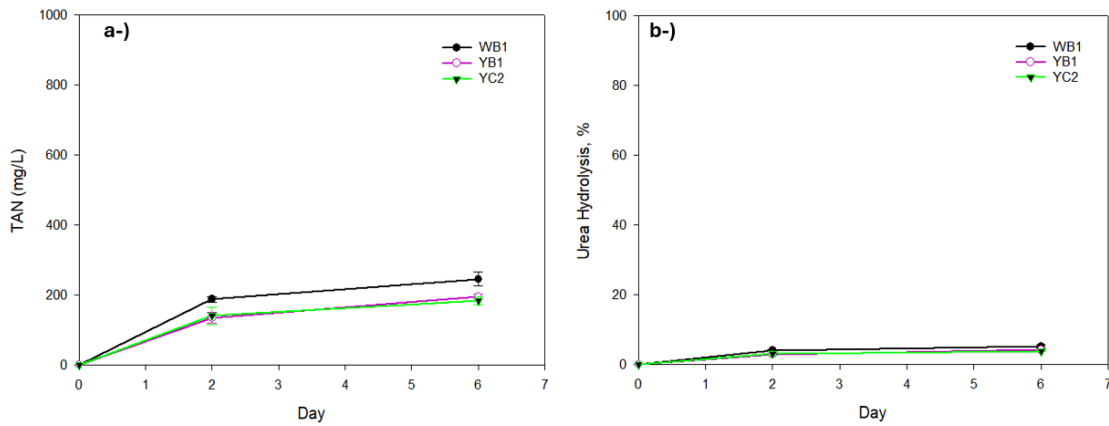


Figure 4-59. Urea hydrolysis activities of axenic strains (WB1, YB1, YC2) in biomineralization medium with 0.05 g.L⁻¹ YE and 1 g.L⁻¹ NaCl concentration (tap water, urban runoff conditions); (a) TAN results, (b) hydrolyzed urea

Urea hydrolysis on the sixth day of rainwater conditions were calculated as 88%, 36%, and 89% for wet biogranules, dried biogranules, and *S. pasteurii*, respectively. Urea hydrolysis on the sixth day of rainwater condition were calculated as 6%, 5%, and 4% for WB1, YB1, and YC2, respectively.

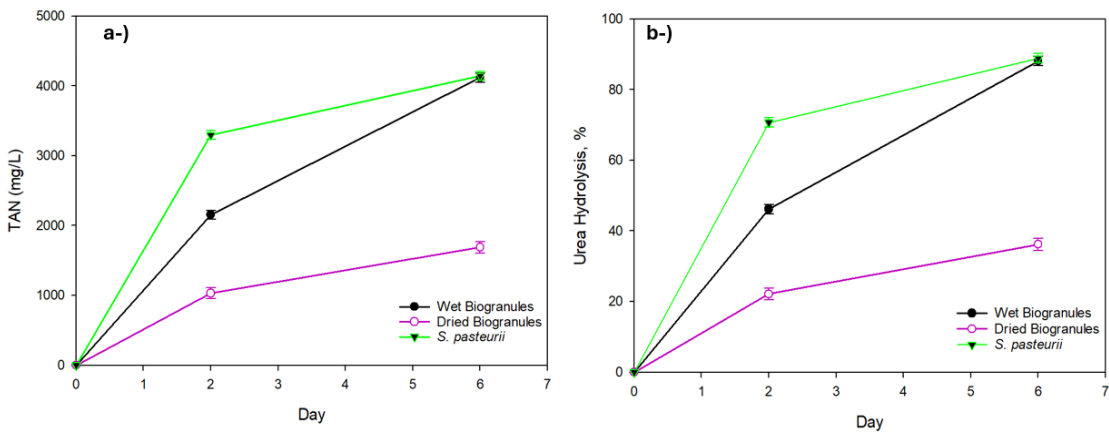


Figure 4-60. Urea hydrolysis activities of wet and dried biogranules and *S. pasteurii* in biomineralization medium with 0.05 g.L⁻¹ YE and 0.02 g.L⁻¹ NaCl concentration (rainwater conditions); (a) TAN results, (b) hydrolyzed urea

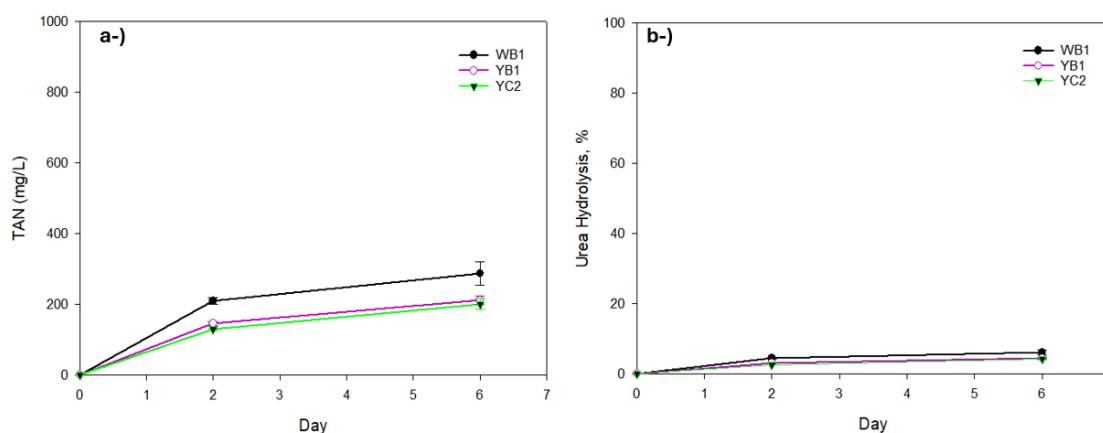


Figure 4-61. Urea hydrolysis activities of axenic strains (WB1, YB1, YC2) in biomineralization medium with 0.05 g.L^{-1} YE and 0.02 g.L^{-1} NaCl concentration (rainwater conditions); (a) TAN results, (b) hydrolyzed urea

Specific urea hydrolysis activities of biogranules, *S. pasteurii*, and isolates at different salinity concentrations were given in Table 4-16. At marine water (35 g.L^{-1} NaCl) conditions, wet and dried biogranules, *S. pasteurii*, and isolates (WB1, YB1, YC2) had $6.14 \text{ g Urea.d}^{-1}.\text{g}^{-1}$ CDW, $2.76 \text{ g Urea.d}^{-1}.\text{g}^{-1}$ CDW, $6.80 \text{ g Urea.d}^{-1}.\text{g}^{-1}$ CDW, $0.44 \text{ g Urea.d}^{-1}.\text{g}^{-1}$ CDW, $0.35 \text{ g Urea.d}^{-1}.\text{g}^{-1}$ CDW, $0.19 \text{ g Urea.d}^{-1}.\text{g}^{-1}$ CDW specific urea hydrolysis activity on the second day, respectively. At marine water (35 g.L^{-1} NaCl) conditions, wet and dried biogranules, *S. pasteurii*, and isolates (WB1, YB1, YC2) had $2.87 \text{ g Urea.d}^{-1}.\text{g}^{-1}$ CDW, $1.39 \text{ g Urea.d}^{-1}.\text{g}^{-1}$ CDW, $2.91 \text{ g Urea.d}^{-1}.\text{g}^{-1}$ CDW, $0.17 \text{ g Urea.d}^{-1}.\text{g}^{-1}$ CDW, $0.15 \text{ g Urea.d}^{-1}.\text{g}^{-1}$ CDW, $0.09 \text{ g Urea.d}^{-1}.\text{g}^{-1}$ CDW specific urea hydrolysis activity on the sixth day, respectively. Among specific urea hydrolysis activities on the second and sixth days, *S. pasteurii* had the highest urea hydrolysis activity. Wet biogranules and *S. pasteurii* highly hydrolyzed urea even at marine water conditions. It was reported in the literature that *S. pasteurii* could hydrolyze urea at high NaCl conditions (3-5% w/v) [113,261].

Table 4-16. Specific urea hydrolysis activity at different salinity concentrations (marine water (35 g.L⁻¹ NaCl), drinking water, urban runoff, groundwater (1 g.L⁻¹ NaCl), rainwater (0.02 g.L⁻¹ NaCl)

Samples	35 g.L ⁻¹ NaCl		1 g.L ⁻¹ NaCl		0.02 g.L ⁻¹ NaCl	
	2 nd	6 th	2 nd	6 th	2 nd	6 th
	g Urea.d ⁻¹ .g ⁻¹ CDW					
Wet biogranules	6.14	2.87	4.86	2.91	4.62	2.94
Dried biogranules	2.76	1.39	2.96	1.55	2.21	1.21
<i>S. pasteurii</i>	6.80	2.91	6.42	3.05	7.07	2.96
WB1	0.44	0.17	0.41	0.18	0.45	0.21
YB1	0.35	0.15	0.29	0.14	0.31	0.15
YC2	0.19	0.09	0.31	0.13	0.28	0.14

Wet biogranules had the highest urea hydrolysis activity, followed by *S. pasteurii*. At 1 g.L⁻¹ NaCl concentration, wet and dried biogranules, *S. pasteurii*, and isolates (WB1, YB1, YC2) had 4.86 g Urea.d⁻¹.g⁻¹ CDW, 2.96 g Urea.d⁻¹.g⁻¹ CDW, 6.42 g Urea.d⁻¹.g⁻¹ CDW, 0.41 g Urea.d⁻¹.g⁻¹ CDW, 0.29 g Urea.d⁻¹.g⁻¹ CDW, 0.31 g Urea.d⁻¹.g⁻¹ CDW specific urea hydrolysis activity on the second day, respectively. Specific urea hydrolysis activities on the sixth day at 1 g.L⁻¹ NaCl were calculated as 2.91 g Urea.d⁻¹.g⁻¹ CDW, 1.55 g Urea.d⁻¹.g⁻¹ CDW, 3.05 g Urea.d⁻¹.g⁻¹ CDW, 0.18 g Urea.d⁻¹.g⁻¹ CDW, 0.14 g Urea.d⁻¹.g⁻¹ CDW, 0.13 g Urea.d⁻¹.g⁻¹ CDW for wet and dried biogranules, *S. pasteurii*, and isolates (WB1, YB1, YC2), respectively. Among specific urea hydrolysis activities on the sixth day, *S. pasteurii* and wet biogranules had higher urea hydrolysis activity compared to dried biogranules and isolates. Dried biogranules had higher specific urea hydrolysis activity than marine water conditions. At rainwater (0.02 g.L⁻¹ NaCl) conditions, wet and dried biogranules, *S. pasteurii*, and isolates (WB1, YB1, YC2) had 4.62 g Urea.d⁻¹.g⁻¹ CDW, 2.21 g Urea.d⁻¹.g⁻¹ CDW, 7.07 g Urea.d⁻¹.g⁻¹ CDW, 0.45 g Urea.d⁻¹.g⁻¹ CDW, 0.31 g Urea.d⁻¹.g⁻¹ CDW, 0.28 g Urea.d⁻¹.g⁻¹ CDW specific urea hydrolysis activity on the second day, respectively. At rainwater (0.02 g.L⁻¹ NaCl) conditions, wet and dried biogranules, *S. pasteurii*, and isolates (WB1, YB1, YC2) had

2.94 g Urea.d⁻¹.g⁻¹ CDW, 1.21 g Urea.d⁻¹.g⁻¹ CDW, 2.96 g Urea.d⁻¹.g⁻¹ CDW, 0.21 g Urea.d⁻¹.g⁻¹ CDW, 0.15 g Urea.d⁻¹.g⁻¹ CDW, 0.14 g Urea.d⁻¹.g⁻¹ CDW specific urea hydrolysis activity on the second day, respectively. As in previous conditions (at 35 g.L⁻¹ NaCl and 1 g.L⁻¹ NaCl concentrations), *S. pasteurii* had the highest urea hydrolysis activity compared to biogranules and isolates. WB1 had the highest specific urea hydrolysis activity compared to YB1 and YC2.

4.10.2. Nitrate Reduction Activities at Different Salt Concentrations

Nitrate reduction and nitrite accumulation were measured at the end of the second and sixth days in tests at different environmental salinities. NO₃-N and NO₂-N measurements of wet and dried biogranules, *S. pasteurii*, *P. aeruginosa*, and isolates (WB1, WC2X, YB1, and YC2) at 35 g.L⁻¹ NaCl were presented in Figure 4-64 and Figure 4-65. Under marine water conditions, nitrate reduction at the end of the sixth day were measured as 25%, 16%, 33%, and 38% for wet biogranules, dried biogranules, *S. pasteurii* and *P. aeruginosa*, respectively. Under marine water conditions, *S. pasteurii* and *P. aeruginosa* reached the highest nitrate reduction performance at the end of the sixth day. Wet and dried biogranules and *P. aeruginosa* showed the lowest nitrate reduction performance under marine water conditions when compared to other salinity environments.

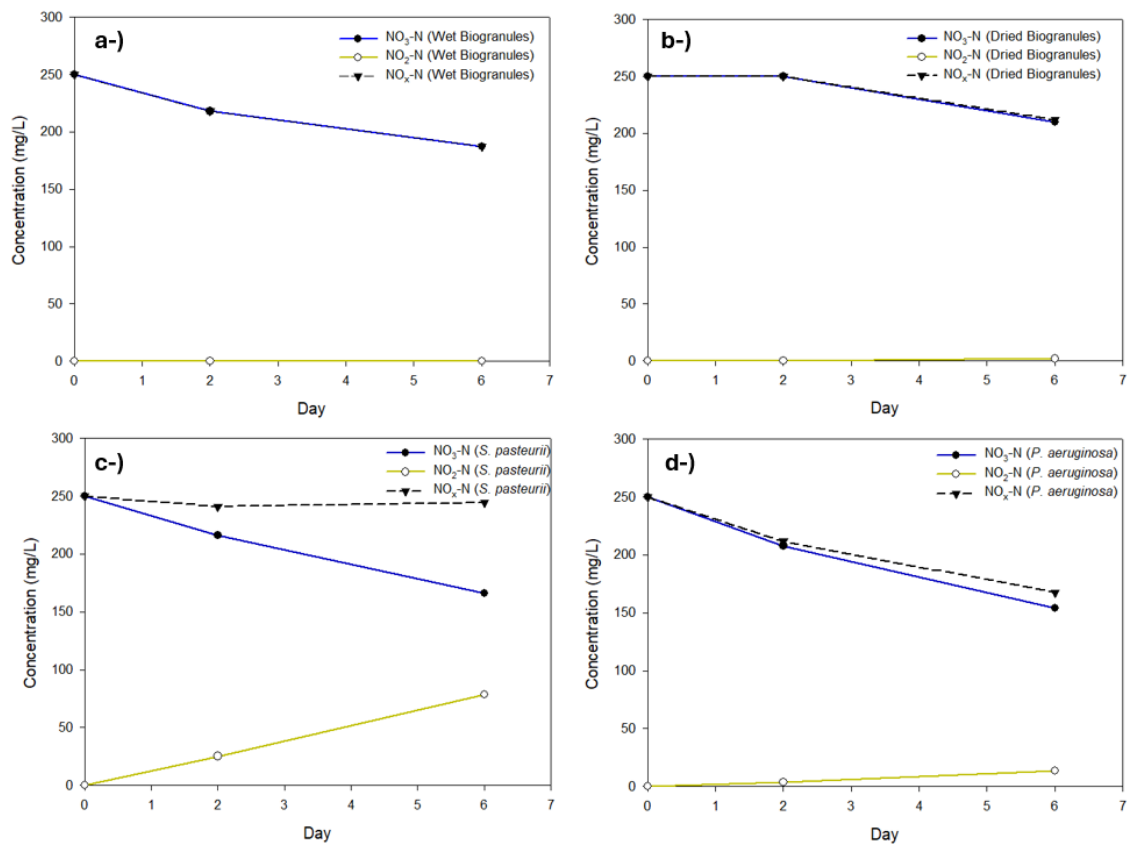


Figure 4-62. Nitrate reduction and nitrite measurements at marine water, (a) wet biogranules, (b) dried biogranules, (c) *S. pasteurii*, (d) *P. aeruginosa*

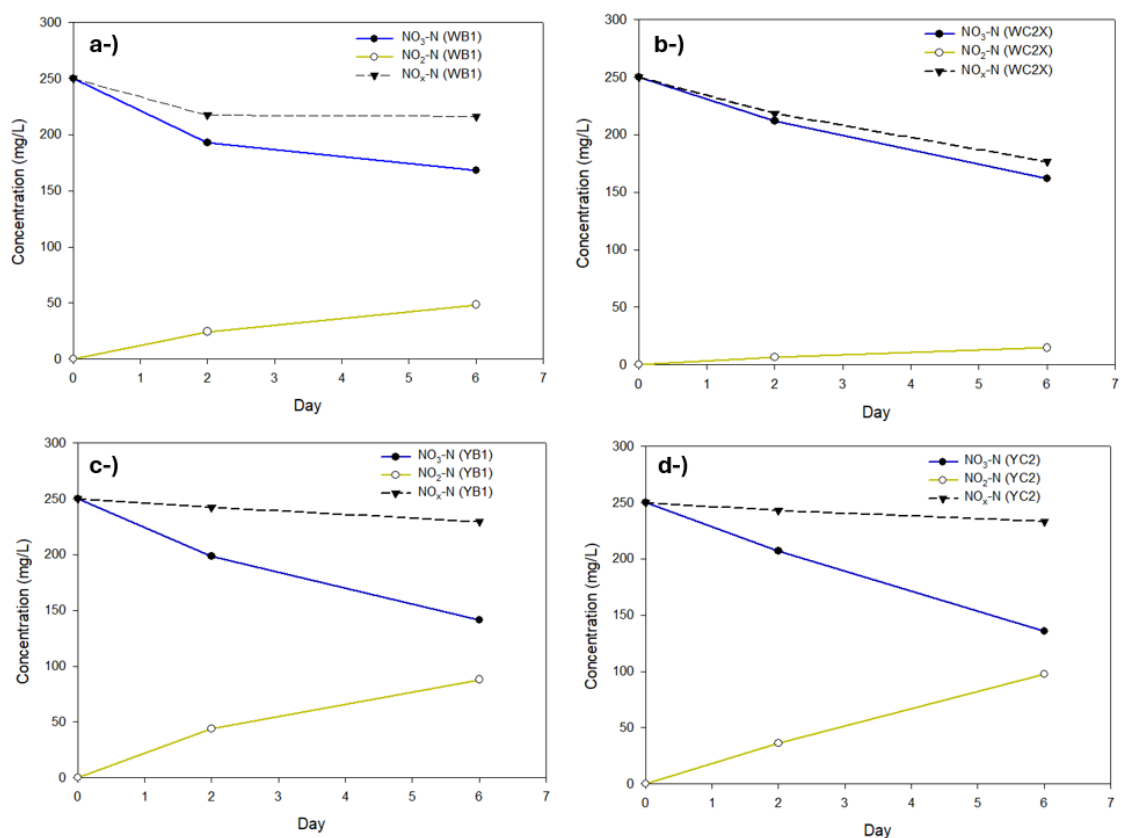


Figure 4-63. Nitrate reduction and nitrite measurements at marine water, (a) WB1, (b) WC2X, (c) YB1, (d) YC2

Specific nitrate reduction, specific nitrite accumulation, and specific denitrification activities for batches at 35 g.L⁻¹ NaCl were given in Table 4-17.

At marine water (35 g.L⁻¹ NaCl) conditions, wet and dried biogranules, *S. pasteurii*, *P. aeruginosa* and isolates (WB1, WC2X, YB1, and YC2) had 21 mg NO_x-N d⁻¹.g⁻¹CDW, 13 mg NO_x-N d⁻¹.g⁻¹CDW, 2 mg NO_x-N d⁻¹.g⁻¹CDW, 27 mg NO_x-N d⁻¹.g⁻¹CDW, 11 mg NO_x-N d⁻¹.g⁻¹CDW, 24 mg NO_x-N d⁻¹.g⁻¹CDW, 2 mg NO_x-N d⁻¹.g⁻¹CDW, 0 mg NO_x-N d⁻¹.g⁻¹CDW specific denitrification activity on the six day, respectively.

It was revealed that resuscitation of nitrate reducing bacteria in dried biogranules, and their specific nitrate reduction activities were negatively affected under marine water conditions. Under marine water conditions, although microbial activities slightly decreased due to retardation of resuscitation of bacteria in dried biogranules, similar

biomineralization performances were detected compared to other salt concentrations (fresh water and rainwater conditions).

Table 4-17. Specific NO₃-N reducing, NO₂-N accumulation, and denitrification activity at marine water condition

	Wet biogranules	Dried biogranules	<i>S. pasteurii</i>	<i>P. aeruginosa</i>
second day	Specific nitrate-reducing activity (mg NO ₃ -N d ⁻¹ .g ⁻¹ CDW)			
	32	0	32	42
	Specific nitrite accumulation activity (mg NO ₂ -N d ⁻¹ .g ⁻¹ CDW)			
	0.30	0	27.20	3.80
	Specific denitrification activity (mg NO _x -N d ⁻¹ .g ⁻¹ CDW)			
	31.70	0	4.80	38.20
	Wet biogranules	Dried biogranules	<i>S. pasteurii</i>	<i>P. aeruginosa</i>
sixth day	Specific nitrate-reducing activity (mg NO ₃ -N d ⁻¹ .g ⁻¹ CDW)			
	21	13.33	28	32
	Specific nitrite accumulation activity (mg NO ₂ -N d ⁻¹ .g ⁻¹ CDW)			
	0.13	0.70	26.17	4.60
	Specific denitrification activity (mg NO _x -N d ⁻¹ .g ⁻¹ CDW)			
	20.87	12.67	1.83	27.40
	WB1	WC2X	YB1	YC2
second day	Specific nitrate-reducing activity (mg NO ₃ -N d ⁻¹ .g ⁻¹ CDW)			
	57	38	51.50	43
	Specific nitrite accumulation activity (mg NO ₂ -N d ⁻¹ .g ⁻¹ CDW)			
	24.50	6.70	44	36
	Specific denitrification activity (mg NO _x -N d ⁻¹ .g ⁻¹ CDW)			
	32.50	31.30	7.50	7
	WB1	WC2X	YB1	YC2
sixth day	Specific nitrate-reducing activity (mg NO ₃ -N d ⁻¹ .g ⁻¹ CDW)			
	27.33	29.33	30.83	24.73
	Specific nitrite accumulation activity (mg NO ₂ -N d ⁻¹ .g ⁻¹ CDW)			
	16.17	4.9	29.33	24.73
	Specific denitrification activity (mg NO _x -N d ⁻¹ .g ⁻¹ CDW)			
	11.17	24.43	1.50	0

NO₃-N and NO₂-N measurements of wet and dried biogranules, *S. pasteurii*, *P. aeruginosa*, and isolates (WB1, WC2X, YB1, and YC2) at 1 g.L⁻¹ NaCl were presented in Figure 4-64 and Figure 4-65.

Nitrate reduction on the sixth day at 1 g.L⁻¹ NaCl concentration were measured as 83%, 53%, 31%, and 49% for wet biogranules, dried biogranules, *S. pasteurii* and *P. aeruginosa*, respectively. Wet biogranules and *P. aeruginosa* reached the highest nitrate reduction at 1 g.L⁻¹ NaCl. At the end of this test, no nitrite accumulation was detected for wet and dried biogranules and *P. aeruginosa*. For *S. pasteurii*, 72 mg.L⁻¹ NO₂-N was accumulated as of sixth days.

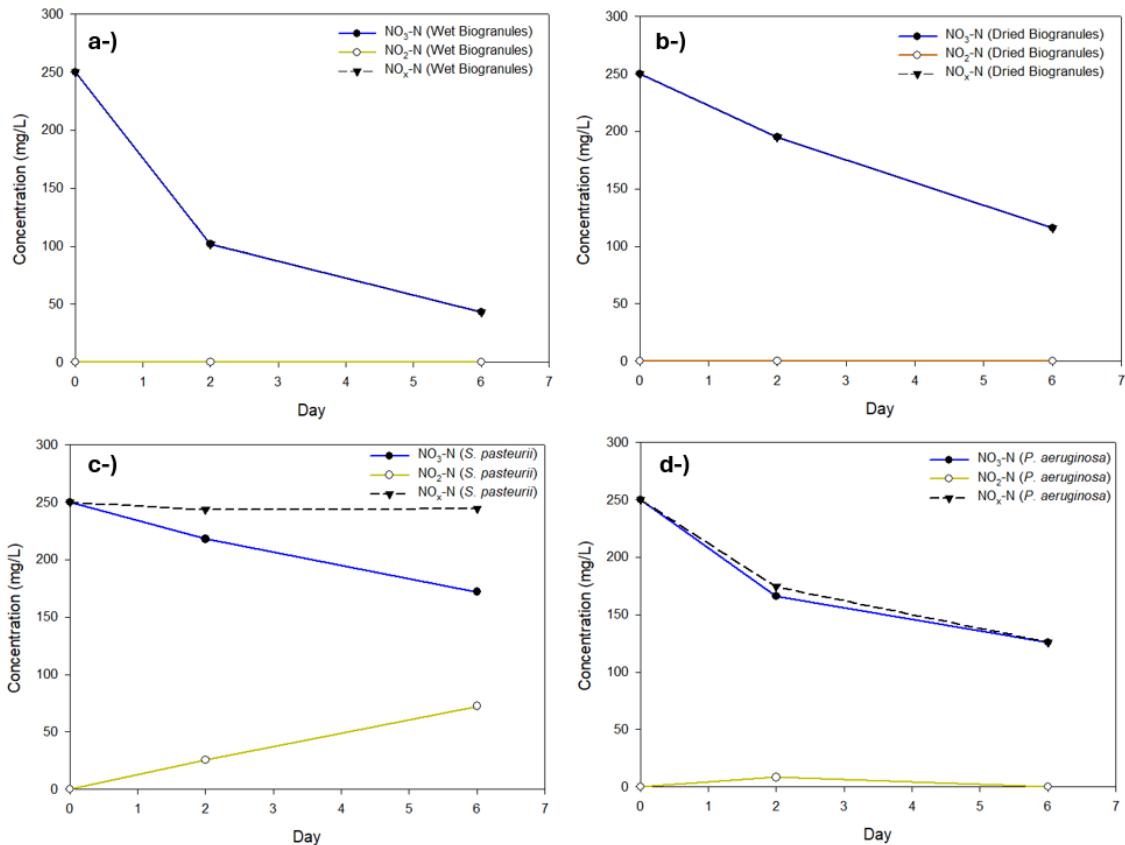


Figure 4-64. Nitrate reduction and nitrite measurements at 1 g.L⁻¹ NaCl, (a) wet biogranules, (b) dried biogranules, (c) *S. pasteurii*, (d) *P. aeruginosa*

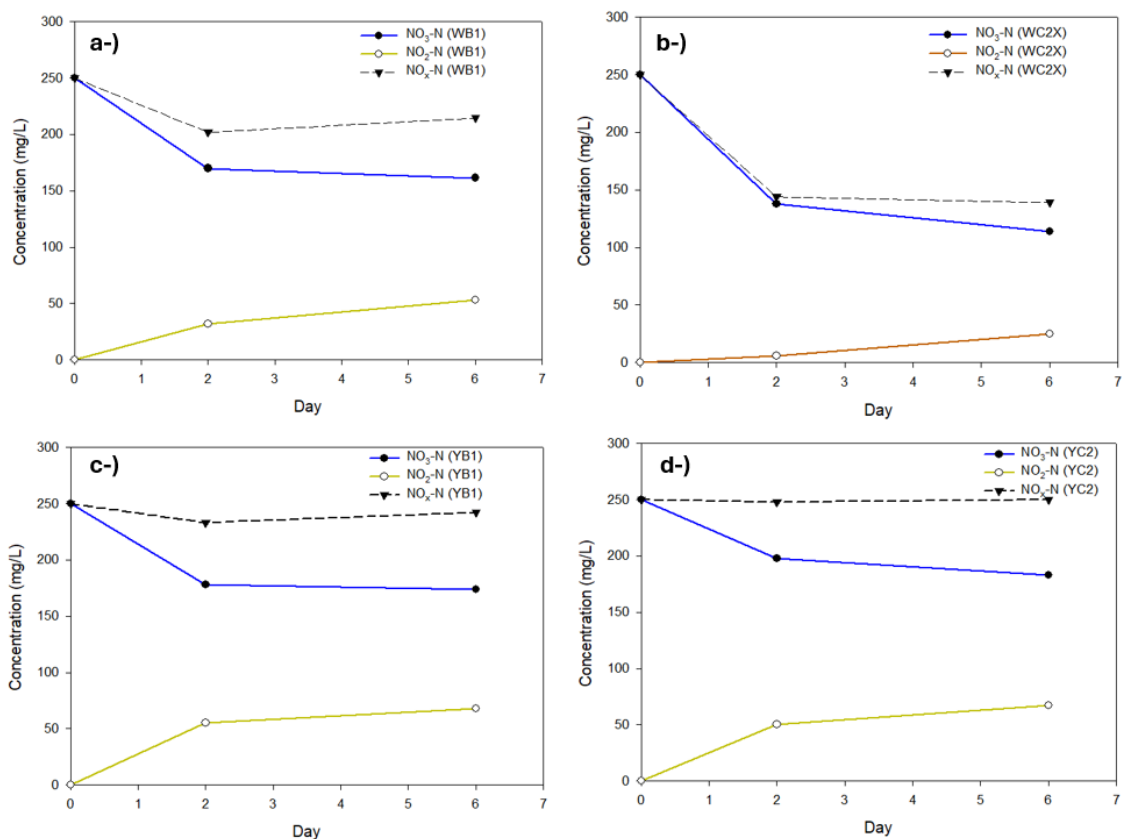


Figure 4-65. Nitrate reduction and nitrite measurements at 1 g.L⁻¹ NaCl, (a) WB1, (b) WC2X, (c) YB1, (d) YC2

Specific nitrate reduction, specific nitrite accumulation, and specific denitrification activities for batches at 1 g.L⁻¹ NaCl were given in Table 4-18.

At 1 g.L⁻¹ NaCl concentration, wet and dried biogranules, *S. pasteurii*, *P. aeruginosa* and isolates (WB1, WC2X, YB1, and YC2) had 69 mg NO_x-N d⁻¹.g⁻¹CDW, 45 mg NO_x-N d⁻¹.g⁻¹CDW, 2 mg NO_x-N d⁻¹.g⁻¹CDW, 41 mg NO_x-N d⁻¹.g⁻¹CDW, 12 mg NO_x-N d⁻¹.g⁻¹CDW, 37 mg NO_x-N d⁻¹.g⁻¹CDW, 3 mg NO_x-N d⁻¹.g⁻¹CDW, 0 mg NO_x-N d⁻¹.g⁻¹CDW specific denitrification activity on the six day, respectively.

Table 4-18. Specific NO₃-N reducing, NO₂-N accumulation, and denitrification activity at 1 g.L⁻¹ NaCl condition

	Wet biogranules	Dried biogranules	<i>S. pasteurii</i>	<i>P. aeruginosa</i>
second day	Specific nitrate-reducing activity (mg NO ₃ -N d ⁻¹ .g ⁻¹ CDW)			
	148	55	32	84
	Specific nitrite accumulation activity (mg NO ₂ -N d ⁻¹ .g ⁻¹ CDW)			
	0.20	0	25.40	8.30
	Specific denitrification activity (mg NO _x -N d ⁻¹ .g ⁻¹ CDW)			
	147.80	55	6.60	75.70
	Wet biogranules	Dried biogranules	<i>S. pasteurii</i>	<i>P. aeruginosa</i>
sixth day	Specific nitrate-reducing activity (mg NO ₃ -N d ⁻¹ .g ⁻¹ CDW)			
	69	44.67	26	41.33
	Specific nitrite accumulation activity (mg NO ₂ -N d ⁻¹ .g ⁻¹ CDW)			
	0	0	24.13	0
	Specific denitrification activity (mg NO _x -N d ⁻¹ .g ⁻¹ CDW)			
	69	44.67	1.87	41.33
	WB1	WC2X	YB1	YC2
second day	Specific nitrate-reducing activity (mg NO ₃ -N d ⁻¹ .g ⁻¹ CDW)			
	80	112	72	52
	Specific nitrite accumulation activity (mg NO ₂ -N d ⁻¹ .g ⁻¹ CDW)			
	32	6	55.30	50
	Specific denitrification activity (mg NO _x -N d ⁻¹ .g ⁻¹ CDW)			
	48	106	16.70	2
	WB1	WC2X	YB1	YC2
sixth day	Specific nitrate-reducing activity (mg NO ₃ -N d ⁻¹ .g ⁻¹ CDW)			
	29.5	45.33	25.33	22.33
	Specific nitrite accumulation activity (mg NO ₂ -N d ⁻¹ .g ⁻¹ CDW)			
	17.67	8.3	22.70	22.33
	Specific denitrification activity (mg NO _x -N d ⁻¹ .g ⁻¹ CDW)			
	11.83	37	2.63	0

NO₃-N and NO₂-N measurements of wet and dried biogranules, *S. pasteurii*, *P. aeruginosa*, and isolates (WB1, WC2X, YB1, and YC2) at 0.02 g.L⁻¹ NaCl (rainwater condition) were presented in Figure 4-66 and Figure 4-67. Nitrate reduction on the sixth day of rainwater condition were measured as 79%, 54%, 39%, and 81% for wet biogranules, dried biogranules, *S. pasteurii* and *P. aeruginosa*, respectively. Wet biogranules and *P. aeruginosa* reached the highest nitrate reduction performance. In tests conducted in rainwater and 1 g.L⁻¹ NaCl concentration, nitrate reduction performances were found to be lower when compared to marine water conditions. At the end of this test, no nitrite accumulation was detected for wet and dried biogranules and *P.*

aeruginosa. For *S. pasteurii*, 92 mg.L⁻¹ NO₂-N was accumulated at the end of the sixth day.

Nitrate reduction on the sixth day of rainwater conditions were measured as 39%, 78%, 33%, and 29% for isolates (WB1, WC2X, YB1, YC2), respectively. WC2X had the highest nitrate reducing performance among isolates.

It was determined that salt concentration had an effect on both the resuscitation period and denitrification activity of nitrate-reducing spores in dried biogranules. The fact that the lowest denitrification activity of wet and dried biogranules, and *P. aeruginosa* at marine water conditions showed negative effect of marine water conditions on denitrification activity. When these results were assessed in terms of denitrification performance, it was determined that salt concentrations affected denitrification activity of all samples except *S. pasteurii*. It was determined that *S. pasteurii* showed similar activity to aforementioned tests at three salinity conditions, but *S. pasteurii* could only reduce nitrate to nitrite. It was determined that *P. aeruginosa* showed higher activity at marine water conditions compared to wet and dried biogranules. It was stated that wet and dried biogranules had similar or higher denitrification activity to *P. aeruginosa* in surface water and groundwater salinity. Wet biogranules and *P. aeruginosa* had similar denitrification activity and they outperformed dried biogranules at rainwater conditions.

According to the results, it was determined that biogranules were capable of denitrification under three different salinity conditions and had denitrification activity comparable to axenic cultures that only denitrify. The fact that dried biogranules did not show denitrification activity on the second day under marine water conditions depended on resuscitation of spores inside dried biogranules. Nitrate-reducing spores were affected by salt concentrations. Studies in the literature indicated that osmotic stress conditions triggered spore formation, and as salinity increased, especially nitrite reduction activity decreased [262,263]. This situation led to nitrite accumulation in the medium. However, it was reported that high salinity did not have a negative effect on resuscitation of spores [135]. Therefore, the fact that the spores inside dried biogranules resuscitated and

denitrified under high salt concentrations was important for the applicability of dried biogranules in such environments.

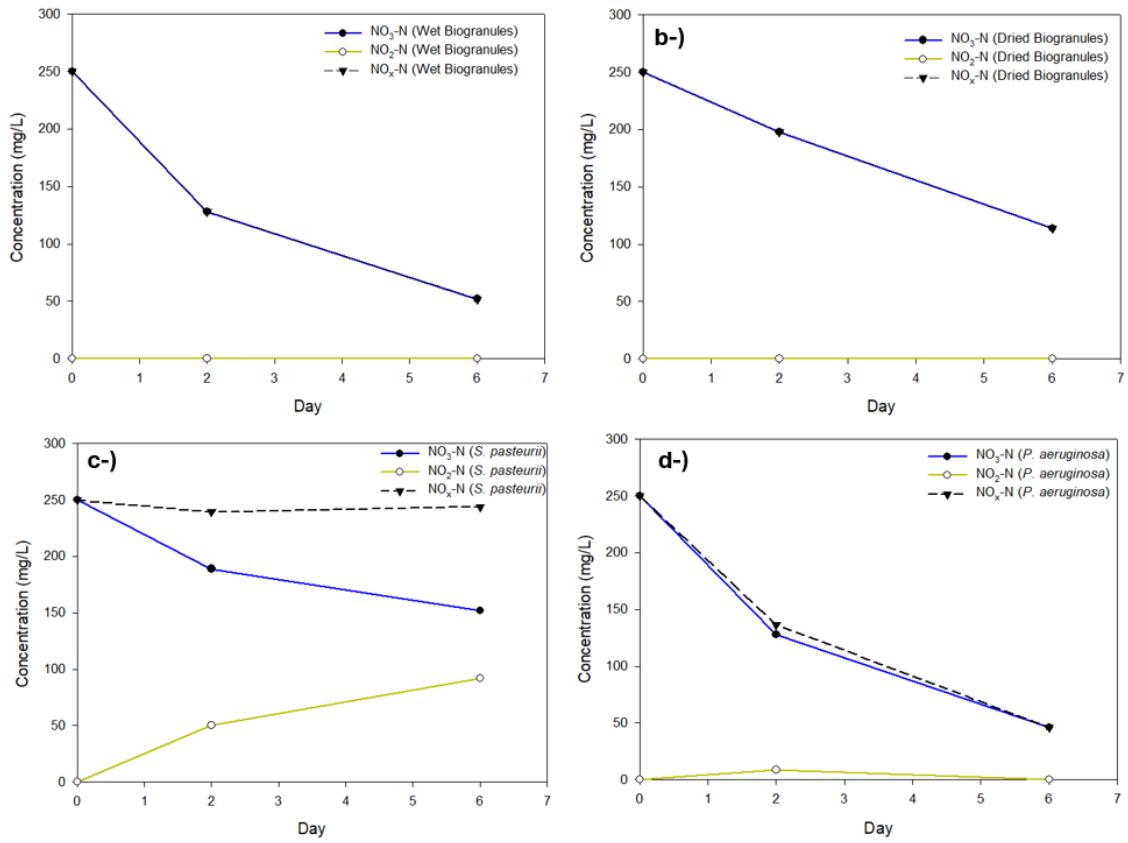


Figure 4-66. Nitrate reduction and nitrite measurements at rainwater, (a) wet biogranules, (b) dried biogranules, (c) *S. pasteurii*, (d) *P. aeruginosa*

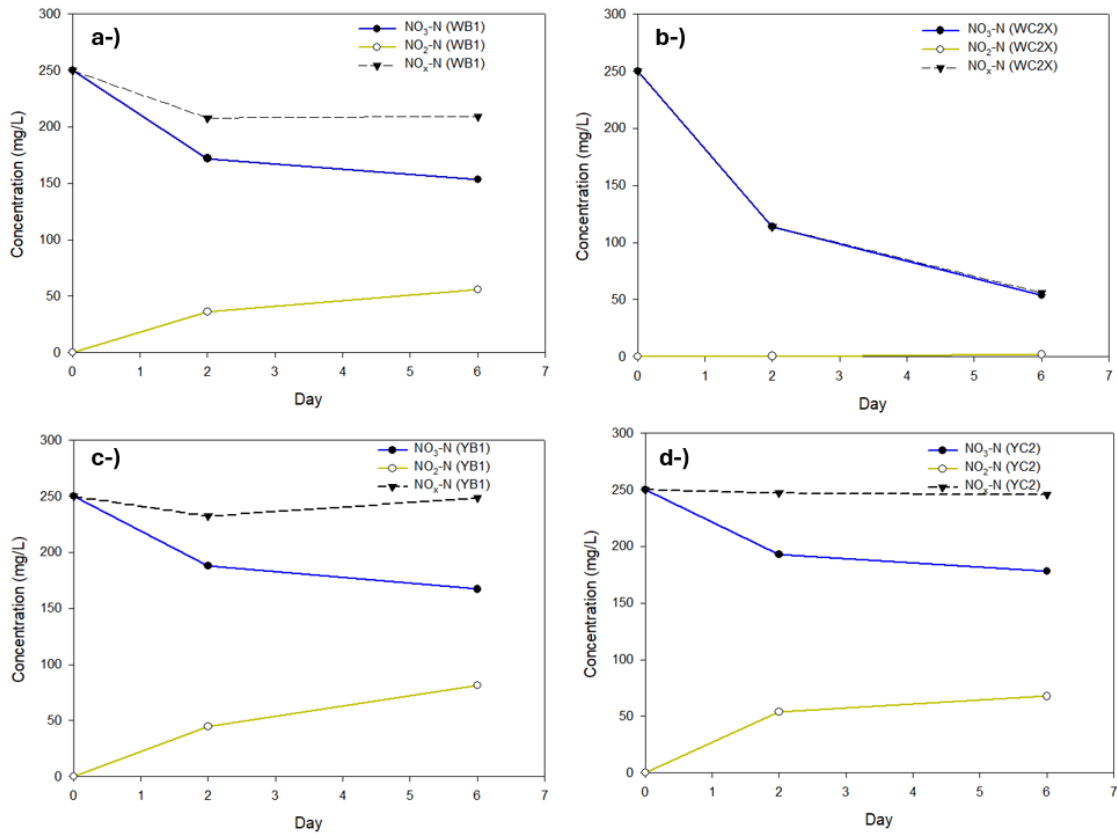


Figure 4-67. Nitrate reduction and nitrite measurements at rainwater, (a) WB1, (b) WC2X, (c) YB1, (d) YC2

Specific nitrate reduction, specific nitrite accumulation, and specific denitrification activities for batches at 0.02 g.L⁻¹ NaCl were given in Table 4-19.

At rainwater (0.02 g.L⁻¹ NaCl) conditions, wet and dried biogranules, *S. pasteurii*, *P. aeruginosa* and isolates (WB1, WC2X, YB1, and YC2) had 66 mg NO_x-N d⁻¹.g⁻¹CDW, 45 mg NO_x-N d⁻¹.g⁻¹CDW, 2 mg NO_x-N d⁻¹.g⁻¹CDW, 68 mg NO_x-N d⁻¹.g⁻¹CDW, 14 mg NO_x-N d⁻¹.g⁻¹CDW, 65 mg NO_x-N d⁻¹.g⁻¹CDW, 1 mg NO_x-N d⁻¹.g⁻¹CDW, 1 mg NO_x-N d⁻¹.g⁻¹CDW specific denitrification activity on the six day, respectively.

Table 4-19. Specific NO₃-N reducing, NO₂-N accumulation, and denitrification activity at rainwater condition

	Wet biogranules	Dried biogranules	<i>S. pasteurii</i>	<i>P. aeruginosa</i>
second day	Specific nitrate-reducing activity (mg NO ₃ -N d ⁻¹ .g ⁻¹ CDW)			
	122	52	61	122
	Specific nitrite accumulation activity (mg NO ₂ -N d ⁻¹ .g ⁻¹ CDW)			
	0	0	50.30	8.60
	Specific denitrification activity (mg NO _x -N d ⁻¹ .g ⁻¹ CDW)			
	122	52	10.70	113.40
	Wet biogranules	Dried biogranules	<i>S. pasteurii</i>	<i>P. aeruginosa</i>
sixth day	Specific nitrate-reducing activity (mg NO ₃ -N d ⁻¹ .g ⁻¹ CDW)			
	66	45.33	32.67	68
	Specific nitrite accumulation activity (mg NO ₂ -N d ⁻¹ .g ⁻¹ CDW)			
	0	0	30.67	0
	Specific denitrification activity (mg NO _x -N d ⁻¹ .g ⁻¹ CDW)			
	66	45.33	2	68
	WB1	WC2X	YB1	YC2
second day	Specific nitrate-reducing activity (mg NO ₃ -N d ⁻¹ .g ⁻¹ CDW)			
	78	136.5	62	57
	Specific nitrite accumulation activity (mg NO ₂ -N d ⁻¹ .g ⁻¹ CDW)			
	36	0.5	44.40	54
	Specific denitrification activity (mg NO _x -N d ⁻¹ .g ⁻¹ CDW)			
	42	136	17.60	3
	WB1	WC2X	YB1	YC2
sixth day	Specific nitrate-reducing activity (mg NO ₃ -N d ⁻¹ .g ⁻¹ CDW)			
	32.27	65.33	27.6	24
	Specific nitrite accumulation activity (mg NO ₂ -N d ⁻¹ .g ⁻¹ CDW)			
	18.73	0.7	27.13	22.53
	Specific denitrification activity (mg NO _x -N d ⁻¹ .g ⁻¹ CDW)			
	13.53	64.67	0.47	1.47

4.10.3. Changes in Dissolved Ca²⁺ Concentration at Different Salt Concentrations

The initial calcium, NO_x-N and urea concentrations were set to 2.6 g.L⁻¹ Ca²⁺, 0.25 g.L⁻¹ NO₃-N and 10 g.L⁻¹ urea. In tests at different salt concentrations, dissolved calcium concentrations were measured in AAS on the second and sixth days. *S. pasteurii*, *P. aeruginosa*, and isolates were tested in marine water (35 g.L⁻¹ NaCl), drinking water, urban runoff, groundwater (1 g.L⁻¹ NaCl), rainwater (20 mg.L⁻¹ NaCl) condition to compare them with wet and dried biogranules in terms of biomineralization activities.

Time-dependent changes of dissolved calcium concentration in batches during six days were presented in Figure 4-68, Figure 4-69, and Figure 4-70.

Dissolved calcium concentrations in the biomineralization medium of wet and dried biogranules, *S. pasteurii*, and *P. aeruginosa* were measured as 131 mg.L⁻¹, 666 mg.L⁻¹, 261 mg.L⁻¹ and 2116 mg.L⁻¹, respectively at 35 g.L⁻¹ NaCl. Marine water affected dissolved calcium precipitation performances of biogranules and axenic cultures.

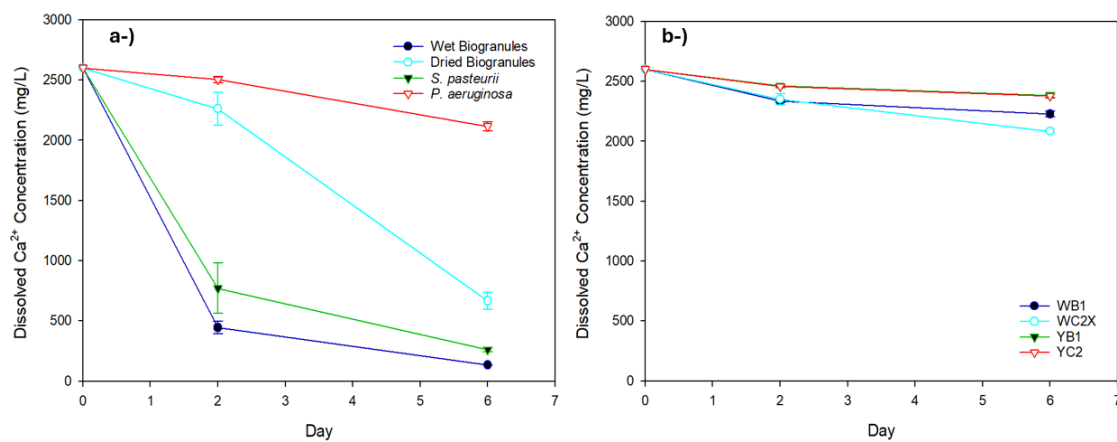


Figure 4-68. Dissolved calcium concentration results at the end of the second and sixth days under marine water condition; (a) biogranules, *S. pasteurii*, and *P. aeruginosa*, (b) isolates

The time-dependent change of dissolved calcium concentration at 1 g.L⁻¹ NaCl concentration was presented in Figure 4-69. Wet biogranules and *S. pasteurii* totally precipitated the amount of dissolved calcium in biomineralization medium at the end of the second day. At the end of the sixth day of dried biogranules, dissolved calcium concentration in biomineralization medium was measured as 124 mg.L⁻¹. At the end of the sixth day, *P. aeruginosa* precipitated 600 mg.L⁻¹ dissolved Ca²⁺ at 1 g.L⁻¹ NaCl. *P. aeruginosa* precipitated more dissolved calcium at 1 g.L⁻¹ NaCl than in marine water.

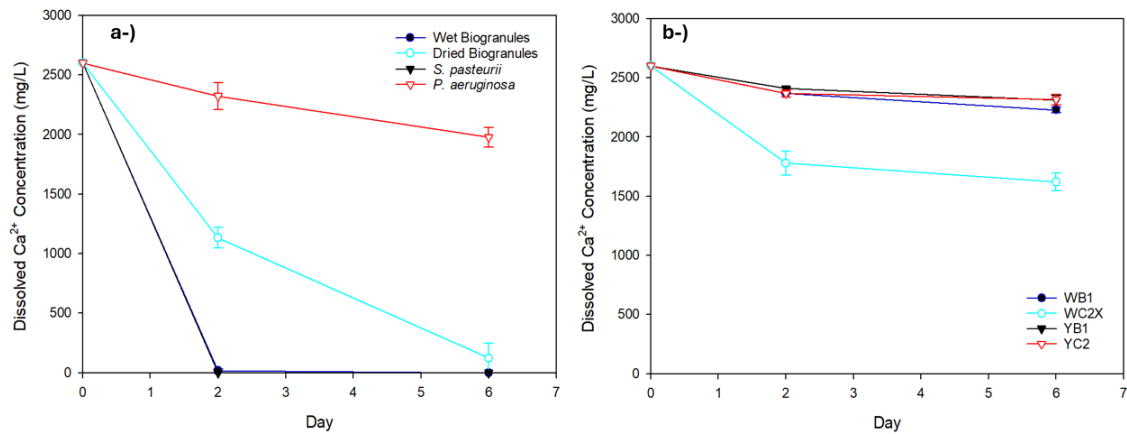


Figure 4-69. Dissolved calcium concentration results at the end of the second and sixth days at 1 g.L⁻¹ NaCl; (a) biogranules, *S. pasteurii*, and *P. aeruginosa*, (b) isolates

The time-dependent changes of dissolved calcium concentration in rainwater conditions were presented in Figure 4-70. Wet biogranules and *S. pasteurii* completely precipitated dissolved calcium in biomineralization medium at the end of the second day. Dried biogranules precipitated 2410 mg.L⁻¹ dissolved Ca²⁺. At the end of the sixth day, dissolved calcium concentration of *P. aeruginosa* at 0.02 g.L⁻¹ NaCl was measured as 1424 mg.L⁻¹. *P. aeruginosa* precipitated more dissolved calcium in rainwater than in marine water.

For isolates, WC2X had the highest dissolved calcium precipitation performance among isolates. WC2X was similar to *P. aeruginosa* in terms of dissolved calcium precipitation performance. Compared to marine water conditions, microbial activity, and dissolved calcium precipitation performance of *P. aeruginosa* was increased. While an extremely salty environment inhibited bacterial cells, a low salty environment could contribute to the growth of bacteria.

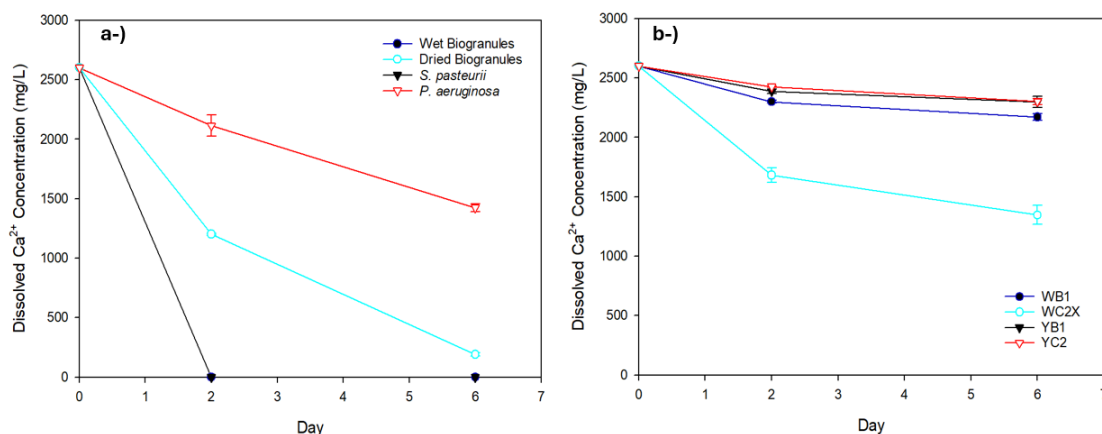


Figure 4-70. Dissolved calcium concentration results at the end of the second and sixth days under rainwater condition; (a) biogranules, *S. pasteurii*, and *P. aeruginosa*, (b) isolates

4.10.4. Comparison of CaCO₃ Precipitation Activities at Different Salt Concentrations

The amounts of precipitated CaCO₃ were measured for in marine water (35 g.L⁻¹ NaCl), drinking water, urban runoff, groundwater (1 g.L⁻¹ NaCl), rainwater (20 mg.L⁻¹ NaCl). These results were given in Figure 4-71, Figure 4-72, and Figure 4-73. Specific CaCO₃ precipitation activities were also presented in Table 4-20.

Wet biogranules and *S. pasteurii* completely precipitated dissolved calcium at 1 g.L⁻¹ NaCl, 0.02 g.L⁻¹ NaCl concentration on the second day. Therefore, the specific CaCO₃ precipitation activities of wet biogranules and *S. pasteurii* were calculated as 6500 mg CaCO₃.g⁻¹ CDW.d⁻¹ on the second day.

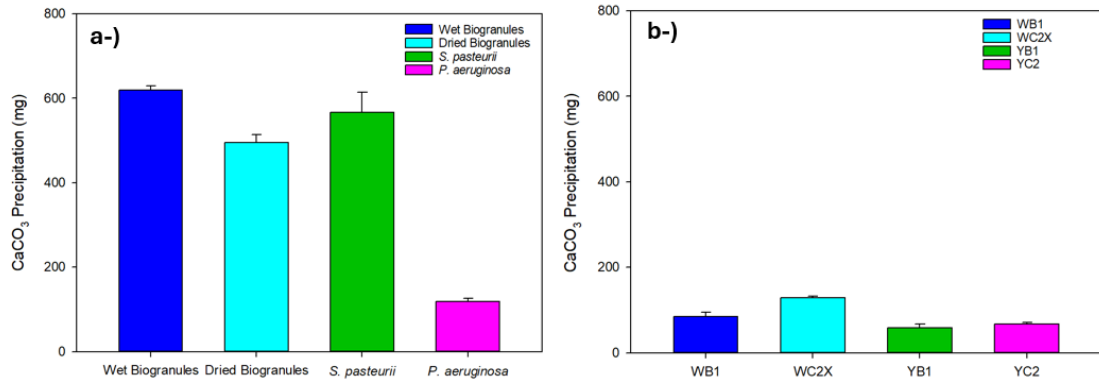


Figure 4-71. CaCO₃ Precipitation at 35 g.L⁻¹ NaCl (marine water conditions); (a) biogranules, *S. pasteurii*, and *P. aeruginosa*, (b) isolates

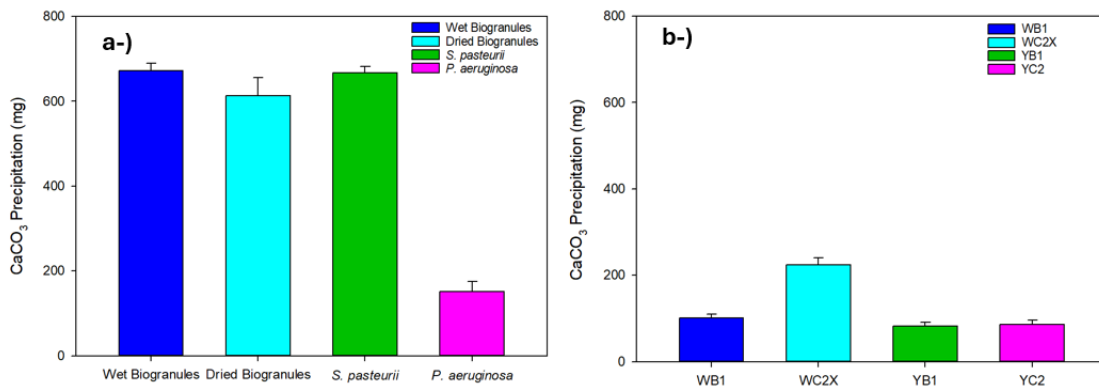


Figure 4-72. CaCO₃ precipitation at 1 g.L⁻¹ NaCl (tap water/groundwater condition); (a) biogranules, *S. pasteurii*, and *P. aeruginosa*, (b) isolates

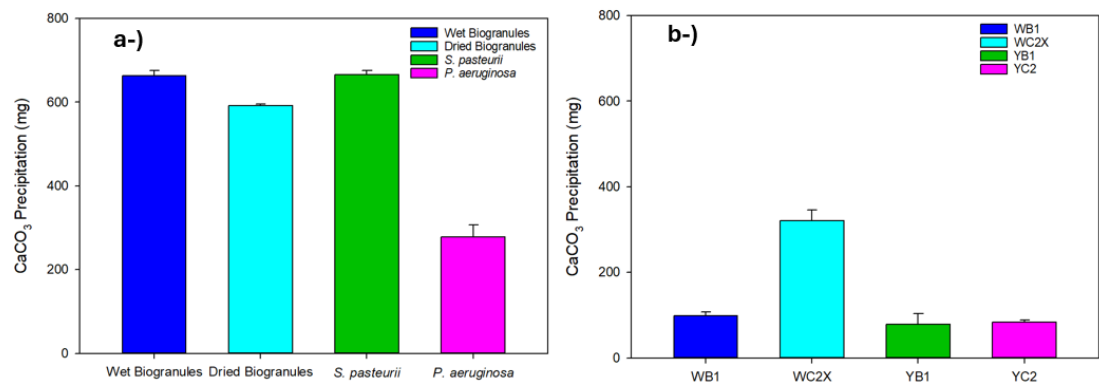


Figure 4-73. CaCO₃ precipitation at 0.02 g.L⁻¹ NaCl (rainwater condition); (a) biogranules, *S. pasteurii*, and *P. aeruginosa*, (b) isolates

Under marine water conditions, at the end of the sixth day, specific CaCO₃ precipitation activities for wet and dried biogranules, *S. pasteurii*, and *P. aeruginosa* were calculated as 2065±31 mg CaCO₃.g⁻¹ CDW.d⁻¹, 1648±66 mg CaCO₃.g⁻¹ CDW.d⁻¹, 1887±159 mg CaCO₃.g⁻¹ CDW.d⁻¹, 394±27 mg CaCO₃.g⁻¹ CDW.d⁻¹ respectively. Specific CaCO₃ precipitation activities for WB1, WC2X, YB1 and YC2 were calculated as 282±35 mg CaCO₃.g⁻¹ CDW.d⁻¹, 430±12 mg CaCO₃.g⁻¹ CDW.d⁻¹, 194±27 mg CaCO₃.g⁻¹ CDW.d⁻¹, and 224±14 mg CaCO₃.g⁻¹ CDW.d⁻¹, respectively at 35 g.L⁻¹ NaCl.

Under marine water conditions, wet biogranules and *S. pasteurii* had the highest specific CaCO₃ precipitation activity. Specific CaCO₃ precipitation activities for wet and dried biogranules, *S. pasteurii*, and *P. aeruginosa* were calculated as 2239±58 mg CaCO₃.g⁻¹ CDW.d⁻¹, 2043±144 mg CaCO₃.g⁻¹ CDW.d⁻¹, 2224±51 mg CaCO₃.g⁻¹ CDW.d⁻¹, 505±80 mg CaCO₃.g⁻¹ CDW.d⁻¹ respectively at 1 g.L⁻¹ NaCl. Specific CaCO₃ precipitation activities for WB1, WC2X, YB1 and YC2 were calculated as 337±29 mg CaCO₃.g⁻¹ CDW.d⁻¹, 745±57 mg CaCO₃.g⁻¹ CDW.d⁻¹, 274±27 mg CaCO₃.g⁻¹ CDW.d⁻¹, and 285±34 mg CaCO₃.g⁻¹ CDW.d⁻¹, respectively at 1 g.L⁻¹ NaCl.

Wet biogranules and *S. pasteurii* had the highest specific CaCO₃ precipitation activity. Specific CaCO₃ precipitation activities for wet and dried biogranules, *S. pasteurii*, and *P. aeruginosa* were calculated as 2210±42 mg CaCO₃.g⁻¹ CDW.d⁻¹, 1972±13 mg CaCO₃.g⁻¹ CDW.d⁻¹, 2218±33 mg CaCO₃.g⁻¹ CDW.d⁻¹, 927±67 mg CaCO₃.g⁻¹ CDW.d⁻¹, respectively at 0.02 g.L⁻¹ NaCl. Specific CaCO₃ precipitation activities for WB1, WC2X, YB1 and YC2 were calculated as 329±30 mg CaCO₃.g⁻¹ CDW.d⁻¹, 1070±80 mg CaCO₃.g⁻¹ CDW.d⁻¹, 259±86 mg CaCO₃.g⁻¹ CDW.d⁻¹, and 277±18 mg CaCO₃.g⁻¹ CDW.d⁻¹, respectively at 0.02 g.L⁻¹ NaCl.

Wet biogranules and *S. pasteurii* had the highest specific CaCO₃ precipitation activity at 1 g.L⁻¹ NaCl concentration. Wet and dried biogranules precipitated calcium carbonate at three different salt concentrations.

Table 4-20. Specific CaCO₃ precipitation at different salt concentrations

Samples	35 g.L ⁻¹ NaCl	1 g.L ⁻¹ NaCl	0.02 g.L ⁻¹ NaCl
	mg CaCO ₃ .g ⁻¹ CDW.d ⁻¹		
Wet biogranules	2065±31	2239±58	2210±42
Dried biogranules	1648±66	2043±144	1972±13
<i>S. pasteurii</i>	1887±159	2224±51	2218±33
<i>P. aeruginosa</i>	394±27	505±80	600±57
WB1	282±35	337±29	329±30
WC2X	430±12	745±57	1070±80
YB1	194±27	274±27	259±86
YC2	224±14	285±34	277±18

Resuscitation of spores in dried biogranules increased time required for CaCO₃ precipitation of all dissolved calcium in the environment to six days. The amount of CaCO₃ precipitation in three different salt concentrations was obtained similarly for *S. pasteurii*, wet and dried biogranules. Specific CaCO₃ precipitation activity of biogranules was found to be less affected by salinity than axenic cultures. Salt concentrations affected both resuscitation period and denitrification activity of spores in dried biogranules. As a result, it was determined that specific CaCO₃ precipitation activity decreased by 40% at 35 g.L⁻¹ NaCl concentration. Because salt concentration provoked sporulation by causing osmotic stress, and nitrite reduction activity decreased as salt concentration increased, spores in dried biogranules resuscitated and had both urea hydrolysis and denitrification activities, resulting in CaCO₃ precipitation.

The dissolved calcium concentrations and the amount of precipitated CaCO₃ in batches at different salt concentrations were compared by using mass balance method (Table 4-21). According to these results, it was determined that dissolved calcium precipitation in batches transformed into CaCO₃ minerals.

Table 4-21. Comparison of the amount of precipitated CaCO₃ and the precipitated dissolved calcium concentration at different salt concentrations

Conditions	Samples	CaCO ₃ precipitation performances, %	Precipitated Ca ²⁺ performances, %
35 g.L ⁻¹ NaCl	Wet biogranules	95±1	95±1
	Dried biogranules	76±2	74±3
	<i>S. pasteurii</i>	87±5	90±1
	<i>P. aeruginosa</i>	18±1	15±1
	WB1	13±2	14±1
	WC2X	22±1	20±1
	YB1	9±1	8±1
	YC2	10±1	9±1
1 g.L ⁻¹ NaCl	Wet biogranules	100	100
	Dried biogranules	94±5	95±4
	<i>S. pasteurii</i>	100	100
	<i>P. aeruginosa</i>	23±2	23±3
	WB1	16±1	14±1
	WC2X	34±3	38±4
	YB1	13±1	11±2
	YC2	13±2	11±2
0.02 g.L ⁻¹ NaCl	Wet biogranules	100	100
	Dried biogranules	91±1	93±1
	<i>S. pasteurii</i>	100	100
	<i>P. aeruginosa</i>	43±3	44±2
	WB1	15±1	16±1
	WC2X	49±4	48±4
	YB1	12±4	12±3
	YC2	13±1	12±1

4.11. Analysis and Comparison of Microbial Activities of Biogranules and Axenic Cultures Under Varying Environmental Conditions

Microbial activities (urea hydrolysis and denitrification) in biomineralization tests of biogranules, isolated strains and reference axenic cultures were presented in Figure 4-74 and Figure 4-75. These figures included results for all tested environmental conditions.

Urea hydrolysis percentage of wet biogranules changed between 55-90% (Figure 4-74). While wet biogranules showed the lowest urea hydrolysis activity at 10°C, they reached the highest urea hydrolysis activity under microaerobic and warm-climate conditions (45°C). Urea hydrolysis activities of wet biogranules were not significantly affected by different salt concentrations and oxygenic conditions, but their urea hydrolysis activities were highly affected by temperatures. It was revealed that urea hydrolysis of wet biogranules had high sensitivity to temperature, especially at low temperatures such as 10°C. Urea hydrolysis of dried biogranules changed between 20-45%. Similar to wet biogranules, dried biogranules also showed the lowest urea hydrolysis activity at 10°C. But dried biogranules reached the highest urea hydrolysis activity under marine water, freshwater, and warm-climate conditions (45°C). Dissimilar to wet biogranules, dried biogranules were not significantly affected by salt concentrations. Urea hydrolysis activities of dried biogranules were similar under oxygenic and salinity conditions.

Urea hydrolysis of isolated strains (WB1, YB1, and YC2) changed between 4-12%. Isolated strains reached the highest urea hydrolysis activity under warm-climate conditions (45°C). Similar to biogranules, isolated strains showed the lowest urea hydrolysis activity at 10°C and had high sensitivity to temperature changing. Urea hydrolysis of *S. pasteurii* changed between 80-95%. Dissimilar to biogranules and isolated strains, *S. pasteurii* had lowest urea hydrolysis activity under anoxic conditions. In biomineralization test, *S. pasteurii* hydrolyzed urea under anoxic conditions. But it was revealed that when *S. pasteurii* were growth and cultivated under anoxic conditions, its urea hydrolysis activity and microbial growth were substantially restricted.

Considering all tested environmental conditions, urea hydrolysis activity was highly affected by oxygenic conditions and temperature. Ureolytic bacteria had high sensitivity to varying oxygenic conditions and temperatures.

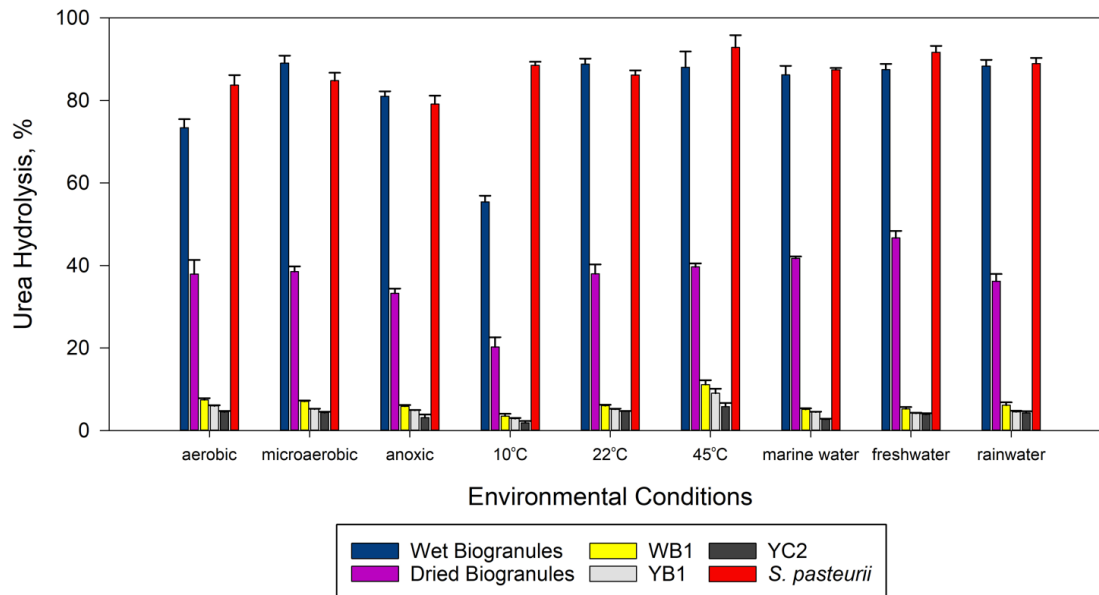


Figure 4-74. Comparison of urea hydrolysis of biogranules and axenic cultures under varying environmental conditions

Denitrification rate of biogranules, isolated strains and reference axenic cultures were given in Figure 4-75. Since denitrification occurred under anoxic conditions, biogranules and axenic cultures had lowest denitrification activity under aerobic conditions. Denitrification activity of wet and dried biogranules negatively affected by psychrophilic, warm-climate and marine water conditions. It was revealed that their denitrification activities were highly depended on varying environmental conditions. Denitrification rate of wet biogranules changed between 10-86%. Wet biogranules reached the highest denitrification activity under mesophilic and freshwater conditions, 86%, and 83%, respectively. Denitrification rate of dried biogranules changed between 5-60%. Dried biogranules reached the highest denitrification activity under mesophilic and rainwater conditions, approximately 60%, and 55%, respectively.

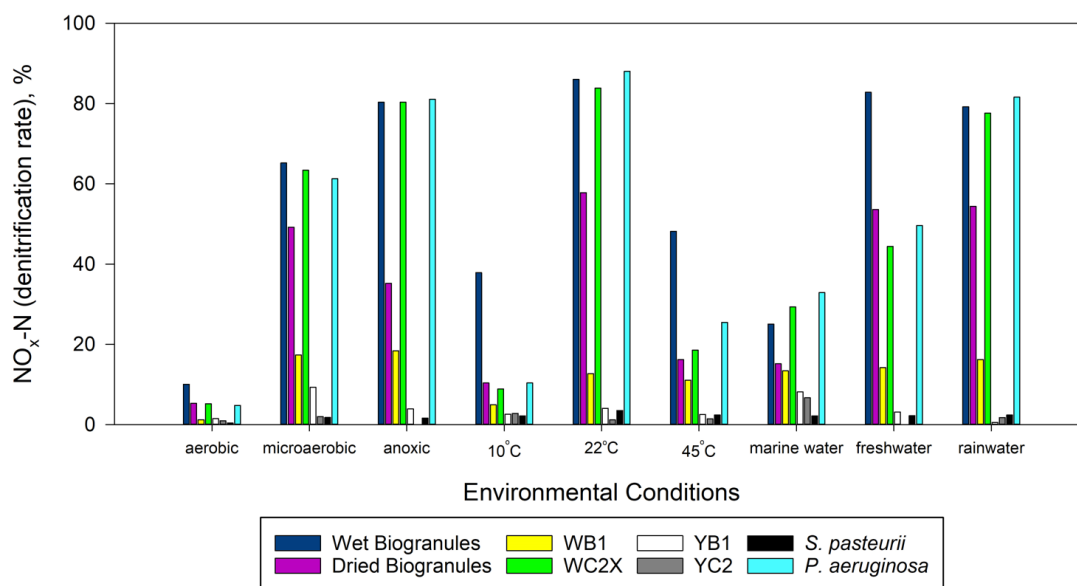


Figure 4-75. Comparison of denitrification rate of biogranules and axenic cultures under varying environmental conditions

Denitrification activity of WC2X and *P. aeruginosa* were similar under varying environmental conditions. Denitrification activities of other isolated strains (WB1, YB1, and YC2) were low compared to biogranules, WC2X, and *P. aeruginosa*. These isolates also negatively affected by varying environmental conditions. Denitrification activity of *S. pasteurii* was quite low because *S. pasteurii* did not completely reduce nitrate to nitrogen.

Denitrification was high sensitivity to varying environmental conditions. Fluctuations in denitrification activities was frequently detected. In addition, denitrification activity had more affected by varying environmental conditions compared to urea hydrolysis activity.

5. CONCLUSION

In conclusion, firstly, the following tests were performed within the scope of this thesis: (i) sensitivity of dried biogranules and axenic cultures to YE, (ii) effects of YE on microbial activity and resuscitation performance of biogranules and their resistance to dehydration stress. It was revealed that YE had positive effects on microbial growth and resuscitation of dried biogranules. According to the results, sensitivity of YE to axenic cultures was higher compared to dried biogranules. Microbial community of biogranules had ability to resist dehydration and resuscitate in the absence of YE.

It was concluded that under favor of biogranules' ability to use simultaneously more than one metabolic pathway (urea hydrolysis and denitrification) and their low sensitivity to YE, limitations in MICP applications could not suppress non-axenic cultures and CaCO_3 was precipitated more efficiently. In this way, use of dried biogranules in the absence of YE at industrial scale could pave the way for MICP applications because YE was defined as undesired substances in MICP applications due to negative effects, especially in self-healing concrete application.

The second part of the thesis based on comparison of biogranules (wet and dried form) with isolated strains and reference axenic cultures in terms of microbial activity and biomineralization performance. The findings indicated that wet biogranules had the highest urea hydrolysis and denitrification activities among axenic cultures and isolates. But urea hydrolysis activity of *S. pasteurii* was similar to wet biogranules under varying environmental conditions. The CaCO_3 precipitation rate of wet biogranules and *S. pasteurii* were superior to dried biogranules and axenic cultures. *P. aeruginosa* and WC2X had as high nitrate reduction activities as biogranules but *P. aeruginosa* and WC2X precipitated less amount of CaCO_3 . Because their metabolic activities were mainly governed by nitrate reduction and reaction rate of nitrate reduction was slower than urea hydrolysis reaction rate. Isolated strains (WB1, YB1, and YC2) hydrolyzed about 4-12% of initial 10 g.L^{-1} urea under varying environmental conditions. The reason of low urea hydrolysis of the isolates was that they were tested at low YE concentrations in biomineralization solution (0.05 g.L^{-1} YE). Therefore, isolated strains could not easily adopt to varying environmental conditions at 0.05 g.L^{-1} YE concentration. The all-

isolated strains (WB1, WC2X, YB1, and YC2) under varying environmental conditions were inferior to biogranules in terms of both microbial activity (urea hydrolysis and denitrification activities) and biomineralization performance.

Biomineralization performances of wet biogranules under varying environmental conditions were affected by at most 10%. These results indicated that wet biogranules could easily adopt to varying environmental conditions. Biomineralization performances of dried biogranules under varying environmental conditions were affected by at most 50%. Biomineralization performances of dried biogranules decreased by 20%, 30%, and 50% under marine water, anoxic, and psychrophilic conditions, respectively. These conditions were also retarded resuscitation period of dried biogranules. In addition, ureolytic and nitrate reducing bacteria in dried biogranules' microbial community were negatively affected due to exposure to these environmental conditions.

As a result, it was revealed that using simultaneous more than one metabolic pathway (urea hydrolysis and denitrification) in non-axenic granular cultures were not only advantageous in oxygen availability but also advantageous in minimizing negative effects of varying environmental conditions on biomineralization performances. The fact that biogranules were dried and resuscitated could extend shelf life. Dried biogranules could hold potential to using in MICP applications. However, since microbial activity and biomineralization performance of wet biogranules were superior to dried biogranules, the determination of shelf-life of wet biogranules was important. Further efforts are needed to conduct studies on optimizing storage conditions of wet biogranules and determining their shelf life.

Within the scope of this thesis, biogranules were not tested in high alkali environments (pH 12-13). In order to increase efficacy of biogranules for MICP applications, biogranules should be tested in high alkali environments. Biogranules were only tested at temperature range of 10°C-45°C. In order to determine whether enzymatic activity and biomineralization performance maintain at very low or high temperatures, biogranules should be tested at extreme temperatures such as between at 0-10°C and 50-60°C. It was suggested that biomineralization-oriented biogranules should be tested in MICP

applications such as heavy metal removal from contaminated sites, soil stabilization, self-healing concrete, and metal recovery. Further efforts are needed to conduct studies on biomineralization performance of biogranules under harsh environmental conditions. These suggestions for future work may contribute to increase potential of using simultaneous more than one metabolic pathway through biogranules and optimize biomineralization performances of biogranules for many MICP applications in environmental, civil, and geotechnical engineering.

6. REFERENCES

- [1] A. Saif, A. Cuccurullo, D. Gallipoli, C. Perlot, A.W. Bruno, Advances in Enzyme Induced Carbonate Precipitation and Application to Soil Improvement: A Review, *Materials* 15 (2022) 950. <https://doi.org/10.3390/ma15030950>.
- [2] S. Hinderer, L. Brändle, A. Kuckertz, Transition to a Sustainable Bioeconomy, *Sustainability* 13 (2021) 8232. <https://doi.org/10.3390/su13158232>.
- [3] K. Stefaniak, J. Wierzbicki, B. Ksist, A. Szymczak-Graczyk, Biocementation as a Pro-Ecological Method of Stabilizing Construction Subsoil, *Energies (Basel)* 16 (2023) 2849. <https://doi.org/10.3390/en16062849>.
- [4] G. Liobikienė, A. Miceikienė, Contribution of the European Bioeconomy Strategy to the Green Deal Policy: Challenges and Opportunities in Implementing These Policies, *Sustainability* 15 (2023) 7139. <https://doi.org/10.3390/su15097139>.
- [5] M. Avramenko, K. Nakashima, S. Kawasaki, State-of-the-Art Review on Engineering Uses of Calcium Phosphate Compounds: An Eco-Friendly Approach for Soil Improvement, *Materials* 15 (2022) 6878. <https://doi.org/10.3390/ma15196878>.
- [6] H. Porter, A. Mukherjee, R. Tuladhar, N.K. Dhama, Life Cycle Assessment of Biocement: An Emerging Sustainable Solution?, *Sustainability* 13 (2021) 13878. <https://doi.org/10.3390/su132413878>.
- [7] M.A. Jarwar, S. Dumontet, R.A. Nastro, M.E. Sanz-Montero, V. Pasquale, Global Scientific Research and Trends Regarding Microbial Induced Calcite Precipitation: A Bibliometric Network Analysis, *Sustainability* 14 (2022) 16114. <https://doi.org/10.3390/su142316114>.
- [8] X. Feng, H. Guo, X. Feng, Y. Yin, Z. Li, Z. Huang, M. Urynowicz, Denitrification induced calcium carbonate precipitation by indigenous microorganisms in coal seam and its application potential in CO₂ geological storage, *Fuel* 365 (2024) 131276. <https://doi.org/10.1016/j.fuel.2024.131276>.
- [9] T. Fu, A.C. Saracho, S.K. Haigh, Microbially induced carbonate precipitation (MICP) for soil strengthening: A comprehensive review, *Biogeotechnics* 1 (2023) 100002. <https://doi.org/10.1016/j.bgtech.2023.100002>.

- [10] W. Mwandira, M. Mavroulidou, M.J. Gunn, D. Purchase, H. Garelick, J. Garelick, Concurrent Carbon Capture and Biocementation through the Carbonic Anhydrase (CA) Activity of Microorganisms -a Review and Outlook, *Environmental Processes* 10 (2023) 56. <https://doi.org/10.1007/s40710-023-00667-2>.
- [11] W. Pungrasmi, J. Intarasontron, P. Jongvivatsakul, S. Likitlersuang, Evaluation of Microencapsulation Techniques for MICP Bacterial Spores Applied in Self-Healing Concrete, *Sci Rep* 9 (2019) 12484. <https://doi.org/10.1038/s41598-019-49002-6>.
- [12] A.S. Fouladi, A. Arulrajah, J. Chu, S. Horpibulsuk, Application of Microbially Induced Calcite Precipitation (MICP) technology in construction materials: A comprehensive review of waste stream contributions, *Constr Build Mater* 388 (2023) 131546. <https://doi.org/10.1016/j.conbuildmat.2023.131546>.
- [13] C. Konstantinou, Y. Wang, Unlocking the Potential of Microbially Induced Calcium Carbonate Precipitation (MICP) for Hydrological Applications: A Review of Opportunities, Challenges, and Environmental Considerations, *Hydrology* 10 (2023). <https://doi.org/10.3390/hydrology10090178>.
- [14] Y. Wang, C. Konstantinou, S. Tang, H. Chen, Applications of microbial-induced carbonate precipitation: A state-of-the-art review, *Biogeotechnics* 1 (2023). <https://doi.org/10.1016/j.bgtech.2023.100008>.
- [15] A. Almajed, M.A. Lateef, A.A.B. Moghal, K. Lemboye, State-of-the-Art Review of the Applicability and Challenges of Microbial-Induced Calcite Precipitation (MICP) and Enzyme-Induced Calcite Precipitation (EICP) Techniques for Geotechnical and Geoenvironmental Applications, *Crystals (Basel)* 11 (2021) 370. <https://doi.org/10.3390/cryst11040370>.
- [16] Q. Jia, Y. Wang, Study on Calcium Carbonate Deposition of Microorganism Bottom Grouting to Repair Concrete Cracks, *Sustainability* 15 (2023) 3723. <https://doi.org/10.3390/su15043723>.
- [17] Z. Song, C. Wu, Z. Li, D. Shen, Fracture sealing based on microbially induced carbonate precipitation and its engineering applications: A review, *Biogeotechnics* (2024) 100100. <https://doi.org/10.1016/j.bgtech.2024.100100>.

- [18] T. Kariminia, M.A. Rowshanzamir, S.M. Abtahi, S. Soleimanian-Zad, H.M. Bak, A. Baghbanan, Soil microbial improvement using enriched vinasse as a new abundant waste, *Sci Rep* 13 (2023) 22279. <https://doi.org/10.1038/s41598-023-49401-w>.
- [19] A.I. Omoregie, K. Muda, D.E.L. Ong, O.O. Ojuri, M.K. Bin Bakri, M.R. Rahman, H.F. Basri, Y.E. Ling, Soil bio-cementation treatment strategies: state-of-the-art review, *Geotechnical Research* 11 (2024) 3–27. <https://doi.org/10.1680/jgere.22.00051>.
- [20] K. Zhang, C.S. Tang, N.J. Jiang, X.H. Pan, B. Liu, Y.J. Wang, B. Shi, Microbial-induced carbonate precipitation (MICP) technology: a review on the fundamentals and engineering applications, *Environ Earth Sci* 82 (2023). <https://doi.org/10.1007/s12665-023-10899-y>.
- [21] L.A. Van Paassen, Biogrout, ground improvement by microbial induced carbonate precipitation, TU Delft, 2009.
- [22] S. Mondal, A. (Dey) Ghosh, Review on microbial induced calcite precipitation mechanisms leading to bacterial selection for microbial concrete, *Constr Build Mater* 225 (2019) 67–75. <https://doi.org/10.1016/j.conbuildmat.2019.07.122>.
- [23] M. Seifan, A. Berenjian, Microbially induced calcium carbonate precipitation: a widespread phenomenon in the biological world, *Appl Microbiol Biotechnol* 103 (2019) 4693–4708. <https://doi.org/10.1007/s00253-019-09861-5>.
- [24] C. Zhao, V. Toufigh, J. Zhang, Y. Liu, W. Fan, X. He, B. Cao, Y. Xiao, Enhancing biomineralization process efficiency with trained bacterial strains: A technical perspective, *Biogeotechnics* 1 (2023) 100017. <https://doi.org/10.1016/j.bgtech.2023.100017>.
- [25] L. Addadi, S. Weiner, Biomineralization: mineral formation by organisms, *Phys Scr* 89 (2014) 98003. <https://doi.org/10.1088/0031-8949/89/9/098003>.
- [26] D. Kumari, X.Y. Qian, X. Pan, V. Achal, Q. Li, G.M. Gadd, Microbially-induced Carbonate Precipitation for Immobilization of Toxic Metals, *Adv Appl Microbiol* 94 (2016) 79–108. <https://doi.org/10.1016/bs.aambs.2015.12.002>.

- [27] N.K. Dhama, M.S. Reddy, A. Mukherjee, Biomineralization of calcium carbonates and their engineered applications: a review, *Front Microbiol* 4 (2013). <https://doi.org/10.3389/fmicb.2013.00314>.
- [28] A. Liang, C. Paulo, Y. Zhu, M. Dittrich, CaCO₃ biomineralization on cyanobacterial surfaces: Insights from experiments with three *Synechococcus* strains, *Colloids Surf B Biointerfaces* 111 (2013) 600–608. <https://doi.org/10.1016/j.colsurfb.2013.07.012>.
- [29] S. Jain, C. Fang, V. Achal, A critical review on microbial carbonate precipitation via denitrification process in building materials, *Bioengineered* 12 (2021) 7529–7551. <https://doi.org/10.1080/21655979.2021.1979862>.
- [30] T.D. Hoffmann, B.J. Reeksting, S. Gebhard, Bacteria-induced mineral precipitation: a mechanistic review, *Microbiology (N Y)* 167 (2021). <https://doi.org/10.1099/mic.0.001049>.
- [31] P. Ye, F. Xiao, S. Wei, Biomineralization and Characterization of Calcite and Vaterite Induced by the Fungus *Cladosporium* sp. YPLJS-14, *Minerals* 13 (2023) 1344. <https://doi.org/10.3390/min13101344>.
- [32] C. Dupraz, P.T. Visscher, L.K. Baumgartner, R.P. Reid, Microbe-mineral interactions: Early carbonate precipitation in a hypersaline lake (Eleuthera Island, Bahamas), *Sedimentology* 51 (2004) 745–765. <https://doi.org/10.1111/j.1365-3091.2004.00649.x>.
- [33] P. Anbu, C.-H. Kang, Y.-J. Shin, J.-S. So, Formations of calcium carbonate minerals by bacteria and its multiple applications, *Springerplus* 5 (2016) 250. <https://doi.org/10.1186/s40064-016-1869-2>.
- [34] T. Zhao, H. Du, R. Shang, The Effect of Bacteria-to-Calcium Ratio on Microbial-Induced Carbonate Precipitation (MICP) under Different Sequences of Calcium-Source Introduction, *Materials* 17 (2024) 1881. <https://doi.org/10.3390/ma17081881>.
- [35] A. Robles-Fernández, C. Areias, D. Daffonchio, V. Vahrenkamp, M. Sánchez-Román, The Role of Microorganisms in the Nucleation of Carbonates, Environmental Implications and Applications, *Minerals* 12 (2022) 1562. <https://doi.org/10.3390/min12121562>.

- [36] M.J. Castro-Alonso, L.E. Montañez-Hernandez, M.A. Sanchez-Muñoz, M.R. Macias Franco, R. Narayanasamy, N. Balagurusamy, Microbially induced calcium carbonate precipitation (MICP) and its potential in bioconcrete: Microbiological and molecular concepts, *Front Mater* 6 (2019). <https://doi.org/10.3389/fmats.2019.00126>.
- [37] M. Vert, Y. Doi, K.H. Hellwich, M. Hess, P. Hodge, P. Kubisa, M. Rinaudo, F. Schué, Terminology for biorelated polymers and applications (IUPAC recommendations 2012), *Pure and Applied Chemistry* 84 (2012) 377–410. <https://doi.org/10.1351/PAC-REC-10-12-04>.
- [38] T. Zhu, M. Dittrich, Carbonate precipitation through microbial activities in natural environment, and their potential in biotechnology: A review, *Front Bioeng Biotechnol* 4 (2016). <https://doi.org/10.3389/fbioe.2016.00004>.
- [39] C. Dupraz, R.P. Reid, O. Braissant, A.W. Decho, R.S. Norman, P.T. Visscher, Processes of carbonate precipitation in modern microbial mats, *Earth Sci Rev* 96 (2009) 141–162. <https://doi.org/10.1016/j.earscirev.2008.10.005>.
- [40] G.K. Hunter, Interfacial aspects of biomineralization, *Curr Opin Solid State Mater Sci* 1 (1996) 430–435. [https://doi.org/10.1016/S1359-0286\(96\)80036-2](https://doi.org/10.1016/S1359-0286(96)80036-2).
- [41] J. W. Morse, The kinetics of calcium carbonate dissolution and precipitation, *Carbonates: Mineralogy and Chemistry* (1983).
- [42] E. SIRT ÇIPLAK, K. BİLECEN, K.G. AKOĞLU, N. ŞAHİN GÜÇHAN, POTENTIAL OF BIOLOGICAL MORTAR FOR MICRO-CRACK REMEDIATION OF CALCAREOUS STONES IN HISTORICAL MONUMENTS, *Türkiye Bilimler Akademisi Kültür Envanteri Dergisi* (2022). <https://doi.org/10.22520/tubaked2021.24.012>.
- [43] K.R. Hendry, A.O. Marron, F. Vincent, D.J. Conley, M. Gehlen, F.M. Ibarbalz, B. Quéguiner, C. Bowler, Competition between silicifiers and non-silicifiers in the past and present ocean and its evolutionary impacts, *Front Mar Sci* 5 (2018). <https://doi.org/10.3389/fmars.2018.00022>.
- [44] K.H. Caesar, J.R. Kyle, T.W. Lyons, A. Tripathi, S.J. Loyd, Carbonate formation in salt dome cap rocks by microbial anaerobic oxidation of methane, *Nat Commun* 10 (2019) 808. <https://doi.org/10.1038/s41467-019-08687-z>.

- [45] G. Nadson, Beitrag zur Kenntnis der bakteriogenen Kalkablagerung, *Arch. Für Hydrobiol* 19 (1928) 154–164.
- [46] G. Nadson, Microorganisms as geologic agents, I. Tr Komissii Issled Min Vodg (1903).
- [47] H.L., and N.D. Ehrlich, *Geomicrobiology*, 5th ed., New York: CRC Press, 2008.
- [48] M.M. Rahman, R.N. Hora, I. Ahenkorah, S. Beecham, M.R. Karim, A. Iqbal, State-of-the-Art Review of Microbial-Induced Calcite Precipitation and Its Sustainability in Engineering Applications, *Sustainability* 12 (2020) 6281. <https://doi.org/10.3390/su12156281>.
- [49] V. Achal, X. Pan, Influence of Calcium Sources on Microbially Induced Calcium Carbonate Precipitation by *Bacillus* sp. CR2, *Appl Biochem Biotechnol* 173 (2014) 307–317. <https://doi.org/10.1007/s12010-014-0842-1>.
- [50] P. Cacchio, M. Del Gallo, A novel approach to isolation and screening of calcifying bacteria for biotechnological applications, *Geosciences (Switzerland)* 9 (2019). <https://doi.org/10.3390/geosciences9110479>.
- [51] Y. Jung, W. Kim, W. Kim, W. Park, Complete Genome and Calcium Carbonate Precipitation of Alkaliphilic *Bacillus* sp. AK13 for Self-Healing Concrete, *J Microbiol Biotechnol* 30 (2020) 404–416. <https://doi.org/10.4014/jmb.1908.08044>.
- [52] F. Hammes, W. Verstraete*, Key roles of pH and calcium metabolism in microbial carbonate precipitation, *Rev Environ Sci Biotechnol* 1 (2002) 3–7. <https://doi.org/10.1023/A:1015135629155>.
- [53] N.K. Dhama, Biomineralization of Calcium Carbonate Polymorphs by the Bacterial Strains Isolated from Calcareous Sites, *J Microbiol Biotechnol* 23 (2013) 707–714. <https://doi.org/10.4014/jmb.1212.11087>.
- [54] J. Zhang, C. Zhao, A. Zhou, C. Yang, L. Zhao, Z. Li, Aragonite formation induced by open cultures of microbial consortia to heal cracks in concrete: Insights into healing mechanisms and crystal polymorphs, *Constr Build Mater* 224 (2019) 815–822. <https://doi.org/10.1016/j.conbuildmat.2019.07.129>.
- [55] M. Nodehi, T. Ozbakkaloglu, A. Gholampour, A systematic review of bacteria-based self-healing concrete: Biomineralization, mechanical, and durability

- properties, *Journal of Building Engineering* 49 (2022) 104038. <https://doi.org/10.1016/j.jobe.2022.104038>.
- [56] M. Gao, J. Guo, H. Cao, H. Wang, X. Xiong, R. Krastev, K. Nie, H. Xu, L. Liu, Immobilized bacteria with pH-response hydrogel for self-healing of concrete, *J Environ Manage* 261 (2020) 110225. <https://doi.org/10.1016/j.jenvman.2020.110225>.
- [57] H.M. Jonkers, A. Thijssen, G. Muyzer, O. Copuroglu, E. Schlangen, Application of bacteria as self-healing agent for the development of sustainable concrete, *Ecol Eng* 36 (2010) 230–235. <https://doi.org/10.1016/j.ecoleng.2008.12.036>.
- [58] S. Wang, L. Fang, M.F. Dapaah, Q. Niu, L. Cheng, Bio-Remediation of Heavy Metal-Contaminated Soil by Microbial-Induced Carbonate Precipitation (MICP)—A Critical Review, *Sustainability* 15 (2023) 7622. <https://doi.org/10.3390/su15097622>.
- [59] J. Chen, B. Liu, M. Zhong, C. Jing, B. Guo, Research status and development of microbial induced calcium carbonate mineralization technology, *PLoS One* 17 (2022) e0271761. <https://doi.org/10.1371/journal.pone.0271761>.
- [60] V. Wiktor, H.M. Jonkers, Quantification of crack-healing in novel bacteria-based self-healing concrete, *Cem Concr Compos* 33 (2011) 763–770. <https://doi.org/10.1016/j.cemconcomp.2011.03.012>.
- [61] T. Zhu, M. Dittrich, Carbonate Precipitation through Microbial Activities in Natural Environment, and Their Potential in Biotechnology: A Review, *Front Bioeng Biotechnol* 4 (2016). <https://doi.org/10.3389/fbioe.2016.00004>.
- [62] Z. Wang, J. Su, A. Ali, Z. Gao, R. Zhang, Y. Li, W. Yang, Microbially induced calcium precipitation driven by denitrification: Performance, metabolites, and molecular mechanisms, *J Environ Manage* 338 (2023) 117826. <https://doi.org/10.1016/j.jenvman.2023.117826>.
- [63] W. Lin, W. Lin, X. Cheng, G. Chen, Y.C. Ersan, Microbially Induced Desaturation and Carbonate Precipitation through Denitrification: A Review, *Applied Sciences* 11 (2021) 7842. <https://doi.org/10.3390/app11177842>.

- [64] V. Achal, A. Mukherjee, D. Kumari, Q. Zhang, Biomineralization for sustainable construction – A review of processes and applications, *Earth Sci Rev* 148 (2015) 1–17. <https://doi.org/10.1016/j.earscirev.2015.05.008>.
- [65] J.M. Minto, Q. Tan, R.J. Lunn, G. El Mountassir, H. Guo, X. Cheng, ‘Microbial mortar’-restoration of degraded marble structures with microbially induced carbonate precipitation, *Constr Build Mater* 180 (2018) 44–54. <https://doi.org/10.1016/j.conbuildmat.2018.05.200>.
- [66] D. Gat, M. Tsesarsky, D. Shamir, Z. Ronen, Accelerated microbial-induced CaCO₃ precipitation in a defined coculture of ureolytic and non-ureolytic bacteria, *Biogeosciences* 11 (2014) 2561–2569. <https://doi.org/10.5194/bg-11-2561-2014>.
- [67] M. Song, T. Ju, Y. Meng, S. Han, L. Lin, J. Jiang, A review on the applications of microbially induced calcium carbonate precipitation in solid waste treatment and soil remediation, *Chemosphere* 290 (2022). <https://doi.org/10.1016/j.chemosphere.2021.133229>.
- [68] I.S. Muhammad, B.B. Kurna, B.S. U Ibn Abubakar, APPLICATION OF MICROBIAL INDUCED CALCITE PRECIPITATION (MICP) TECHNOLOGY IN GEOTECHNICAL AND GEO-ENVIRONMENTAL ENGINEERING: A REVIEW, 17 (2021) 185–196. www.azojete.com.ng.
- [69] Y.Ç. Erşan, Self-Healing Performance of Biogranule Containing Microbial Self-Healing Concrete Under Intermittent Wet/Dry Cycles, *Politeknik Dergisi* 24 (2021) 323–332. <https://doi.org/10.2339/politeknik.742210>.
- [70] J. Wang, K. Van Tittelboom, N. De Belie, W. Verstraete, Use of silica gel or polyurethane immobilized bacteria for self-healing concrete, *Constr Build Mater* 26 (2012) 532–540. <https://doi.org/10.1016/j.conbuildmat.2011.06.054>.
- [71] H. Kim, H.M. Son, J. Seo, H.K. Lee, Recent advances in microbial viability and self-healing performance in bacterial-based cementitious materials: A review, *Constr Build Mater* 274 (2021). <https://doi.org/10.1016/j.conbuildmat.2020.122094>.
- [72] F. Martirena, Y. Rodriguez-Rodriguez, A. Callico, Y. Diaz, G. Bracho, A. Hereira, J.O. Guerra de Leon, L. Sorelli, Y. Alvarado-Capó, Microorganism-based

- bioplasticizer for cementitious materials, in: *Biopolymers and Biotech Admixtures for Eco-Efficient Construction Materials*, Elsevier, 2016: pp. 151–171. <https://doi.org/10.1016/B978-0-08-100214-8.00008-7>.
- [73] J.T. DeJong, B.M. Mortensen, B.C. Martinez, D.C. Nelson, Bio-mediated soil improvement, *Ecol Eng* 36 (2010) 197–210. <https://doi.org/10.1016/j.ecoleng.2008.12.029>.
- [74] Y.Ç. Erşan, H. Verbruggen, I. De Graeve, W. Verstraete, N. De Belie, N. Boon, Nitrate reducing CaCO₃ precipitating bacteria survive in mortar and inhibit steel corrosion, *Cem Concr Res* 83 (2016) 19–30. <https://doi.org/10.1016/j.cemconres.2016.01.009>.
- [75] N. De Belie, Application of bacteria in concrete: a critical evaluation of the current status, *RILEM Technical Letters* 1 (2016) 56–61. <https://doi.org/10.21809/rilemtechlett.2016.14>.
- [76] M.E. Espitia Nery, D.E. Corredor Pulido, P.A. Castaño Oliveros, J.A. Rodriguez Medina, Q.Y. Ordoñez Bello, M.S. Perez Fuentes, Mechanisms of encapsulation of bacteria in self-healing concrete: review, *Dyna (Medellin)* 86 (2019) 17–22. <https://doi.org/10.15446/dyna.v86n210.75343>.
- [77] J. Li, W. Bi, Y. Yao, Z. Liu, State-of-the-Art Review of Utilization of Microbial-Induced Calcite Precipitation for Improving Moisture-Dependent Properties of Unsaturated Soils, *Applied Sciences* 13 (2023) 2502. <https://doi.org/10.3390/app13042502>.
- [78] L. Chen, Y. Song, J. Huang, C. Lai, H. Jiao, H. Fang, J. Zhu, X. Song, Critical Review of Solidification of Sandy Soil by Microbially Induced Carbonate Precipitation (MICP), *Crystals (Basel)* 11 (2021) 1439. <https://doi.org/10.3390/cryst11121439>.
- [79] Y. Wu, H. Li, Y. Li, Biomineralization induced by cells of *Sporosarcina pasteurii*: Mechanisms, applications and challenges, *Microorganisms* 9 (2021). <https://doi.org/10.3390/microorganisms9112396>.
- [80] E. Kalkan, A Review on the Microbial Induced Carbonate Precipitation (MICP) for Soil Stabilization, (2020).

- [81] M. Li, X. Cheng, H. Guo, Heavy metal removal by biomineralization of urease producing bacteria isolated from soil, *Int Biodeterior Biodegradation* 76 (2013) 81–85. <https://doi.org/10.1016/j.ibiod.2012.06.016>.
- [82] F. Hammes, N. Boon, J. de Villiers, W. Verstraete, S.D. Siciliano, Strain-Specific Ureolytic Microbial Calcium Carbonate Precipitation, *Appl Environ Microbiol* 69 (2003) 4901–4909. <https://doi.org/10.1128/AEM.69.8.4901-4909.2003>.
- [83] R. Andalib, M.Z. Abd Majid, M.W. Hussin, M. Ponraj, A. Keyvanfar, J. Mirza, H.-S. Lee, Optimum concentration of *Bacillus megaterium* for strengthening structural concrete, *Constr Build Mater* 118 (2016) 180–193. <https://doi.org/10.1016/j.conbuildmat.2016.04.142>.
- [84] P. Ednie-Brown, bioMASON and the Speculative Engagements of Biotechnical Architecture, *Architectural Design* 83 (2013) 84–91. <https://doi.org/10.1002/ad.1529>.
- [85] T. Zhu, C. Paulo, M.L. Merroun, M. Dittrich, Potential application of biomineralization by *Synechococcus* PCC8806 for concrete restoration, *Ecol Eng* 82 (2015) 459–468. <https://doi.org/10.1016/j.ecoleng.2015.05.017>.
- [86] I.A. Bundeleva, L.S. Shirokova, P. Bénézeth, O.S. Pokrovsky, E.I. Kompantseva, S. Balor, Calcium carbonate precipitation by anoxygenic phototrophic bacteria, *Chem Geol* 291 (2012) 116–131. <https://doi.org/10.1016/j.chemgeo.2011.10.003>.
- [87] A. Kumar, H.W. Song, S. Mishra, W. Zhang, Y.L. Zhang, Q.R. Zhang, Z.G. Yu, Application of microbial-induced carbonate precipitation (MICP) techniques to remove heavy metal in the natural environment: A critical review, *Chemosphere* 318 (2023). <https://doi.org/10.1016/j.chemosphere.2023.137894>.
- [88] R. Ramanan, K. Kannan, A. Deshkar, R. Yadav, T. Chakrabarti, Enhanced algal CO₂ sequestration through calcite deposition by *Chlorella* sp. and *Spirulina platensis* in a mini-raceway pond, *Bioresour Technol* 101 (2010) 2616–2622. <https://doi.org/10.1016/j.biortech.2009.10.061>.
- [89] Y.Ç. Erşan, K. Van Tittelboom, N. Boon, N. De Belie, Nitrite producing bacteria inhibit reinforcement bar corrosion in cementitious materials, *Sci Rep* 8 (2018) 14092. <https://doi.org/10.1038/s41598-018-32463-6>.

- [90] Y.C. Ersan, D. Palin, S.B. Yengec Tasdemir, K. Tasdemir, H.M. Jonkers, N. Boon, N. De Belie, Volume Fraction, Thickness, and Permeability of the Sealing Layer in Microbial Self-Healing Concrete Containing Biogranules, *Front Built Environ* 4 (2018). <https://doi.org/10.3389/fbuil.2018.00070>.
- [91] Y.Ç. Erşan, E. Hernandez-Sanabria, N. Boon, N. de Belie, Enhanced crack closure performance of microbial mortar through nitrate reduction, *Cem Concr Compos* 70 (2016) 159–170. <https://doi.org/10.1016/j.cemconcomp.2016.04.001>.
- [92] Y.Ç. Erşan, F.B. Da Silva, N. Boon, W. Verstraete, N. De Belie, Screening of bacteria and concrete compatible protection materials, *Constr Build Mater* 88 (2015) 196–203. <https://doi.org/10.1016/j.conbuildmat.2015.04.027>.
- [93] D. Martin, K. Dodds, I.B. Butler, B.T. Ngwenya, Carbonate Precipitation under Pressure for Bioengineering in the Anaerobic Subsurface via Denitrification, *Environ Sci Technol* (2013) 130709154540005. <https://doi.org/10.1021/es401270q>.
- [94] V.P. Pham, A. Nakano, W.R.L. van der Star, T.J. Heimovaara, L.A. van Paassen, Applying MICP by denitrification in soils: a process analysis, *Environmental Geotechnics* 5 (2018) 79–93. <https://doi.org/10.1680/jenge.15.00078>.
- [95] N. Dopffel, F. Kögler, H. Hartmann, P.I. Costea, E. Mahler, A. Herold, H. Alkan, Microbial induced mineral precipitations caused by nitrate treatment for souring control during microbial enhanced oil recovery (MEOR), *Int Biodeterior Biodegradation* 135 (2018) 71–79. <https://doi.org/10.1016/j.ibiod.2018.09.004>.
- [96] Y. Song, K. Chetty, U. Garbe, J. Wei, H. Bu, L. O'moore, X. Li, Z. Yuan, T. McCarthy, G. Jiang, A novel granular sludge-based and highly corrosion-resistant bio-concrete in sewers, *Science of The Total Environment* 791 (2021) 148270. <https://doi.org/10.1016/j.scitotenv.2021.148270>.
- [97] M. Seifan, A.K. Samani, A. Berenjian, Bioconcrete: next generation of self-healing concrete, *Appl Microbiol Biotechnol* 100 (2016) 2591–2602. <https://doi.org/10.1007/s00253-016-7316-z>.
- [98] R. Garg, R. Garg, N.O. Eddy, Microbial induced calcite precipitation for self-healing of concrete: a review, *J Sustain Cem Based Mater* 12 (2023) 317–330. <https://doi.org/10.1080/21650373.2022.2054477>.

- [99] X. Zhu, J. Wang, N. De Belie, N. Boon, Complementing urea hydrolysis and nitrate reduction for improved microbially induced calcium carbonate precipitation, *Appl Microbiol Biotechnol* 103 (2019) 8825–8838. <https://doi.org/10.1007/s00253-019-10128-2>.
- [100] C. Fang, V. Achal, Enhancing carbon neutrality: A perspective on the role of Microbially Induced Carbonate Precipitation (MICP), *Biogeotechnics* (2024). <https://doi.org/10.1016/j.bgtech.2024.100083>.
- [101] J. He, J. Chu, S. fan Wu, J. Peng, Mitigation of soil liquefaction using microbially induced desaturation, *Journal of Zhejiang University: Science A* 17 (2016) 577–588. <https://doi.org/10.1631/jzus.A1600241>.
- [102] S. Al-Thawadi, S.M. Al-Thawadi, A. Info, Ureolytic Bacteria and Calcium Carbonate Formation as a Mechanism of Strength Enhancement of Sand, 2011. <https://www.researchgate.net/publication/230603500>.
- [103] J.J. Sigurdarson, S. Svane, H. Karring, The molecular processes of urea hydrolysis in relation to ammonia emissions from agriculture, *Rev Environ Sci Biotechnol* 17 (2018) 241–258. <https://doi.org/10.1007/s11157-018-9466-1>.
- [104] F. Su, Y.Y. Yang, soil treatment ability of MICP technology, (n.d.).
- [105] C. Konstantinou, Y. Wang, G. Biscontin, K. Soga, The role of bacterial urease activity on the uniformity of carbonate precipitation profiles of bio-treated coarse sand specimens, *Sci Rep* 11 (2021) 6161. <https://doi.org/10.1038/s41598-021-85712-6>.
- [106] V.S. Whiffin, L.A. Van Paassen, M.P. Harkes, Microbial Carbonate Precipitation as a Soil Improvement Technique, *Geomicrobiol J* 24 (2007) 417–423. <https://doi.org/10.1080/01490450701436505>.
- [107] J.T. DeJong, M.G. Gomez, State of the Art: MICP soil improvement and its application to liquefaction hazard mitigation, (n.d.).
- [108] R.J. Burdalski, B.G.O. Ribeiro, M.G. Gomez, D. Gorman-Lewis, Mineralogy, morphology, and reaction kinetics of ureolytic bio-cementation in the presence of seawater ions and varying soil materials, *Sci Rep* 12 (2022) 17100. <https://doi.org/10.1038/s41598-022-21268-3>.

- [109] M. Wu, X. Hu, Q. Zhang, D. Xue, Y. Zhao, Growth environment optimization for inducing bacterial mineralization and its application in concrete healing, *Constr Build Mater* 209 (2019) 631–643. <https://doi.org/10.1016/j.conbuildmat.2019.03.181>.
- [110] L. Jiang, G. Jia, C. Jiang, Z. Li, Sugar-coated expanded perlite as a bacterial carrier for crack-healing concrete applications, *Constr Build Mater* 232 (2020) 117222. <https://doi.org/10.1016/j.conbuildmat.2019.117222>.
- [111] J. Zhang, Y. Liu, T. Feng, M. Zhou, L. Zhao, A. Zhou, Z. Li, Immobilizing bacteria in expanded perlite for the crack self-healing in concrete, *Constr Build Mater* 148 (2017) 610–617. <https://doi.org/10.1016/j.conbuildmat.2017.05.021>.
- [112] Y. Yang, J. Chu, B. Cao, H. Liu, L. Cheng, Biocementation of soil using non-sterile enriched urease-producing bacteria from activated sludge, *J Clean Prod* 262 (2020) 121315. <https://doi.org/10.1016/j.jclepro.2020.121315>.
- [113] F. Qionglin, Y. Wu, S. Liu, L. Lu, J. Wang, The adaptability of *Sporosarcina pasteurii* in marine environments 3 and the feasibility of its application in mortar crack repair 4 5, n.d. <https://ssrn.com/abstract=4030248>.
- [114] A.D. Aliyu, M. Mustafa, N.A.A. Aziz, Y.C. Kong, N.S. Hadi, Assessing Indigenous Soil Ureolytic Bacteria as Potential Agents for Soil Stabilization, *J Trop Biodivers Biotechnol* 8 (2023) 75128. <https://doi.org/10.22146/jtbb.75128>.
- [115] E.F. Öztürk K, Determination of biocalcification properties of bacillus species isolated from soil, *Erciyes Üniversitesi Fen Bilim. Enstitüsü Dergisi* (2022) 147–154.
- [116] J. Wang, H.M. Jonkers, N. Boon, N. De Belie, *Bacillus sphaericus* LMG 22257 is physiologically suitable for self-healing concrete, *Appl Microbiol Biotechnol* 101 (2017) 5101–5114. <https://doi.org/10.1007/s00253-017-8260-2>.
- [117] E.G. Lauchnor, D.M. Topp, A.E. Parker, R. Gerlach, Whole cell kinetics of ureolysis by *Sporosarcina pasteurii*, *J Appl Microbiol* 118 (2015) 1321–1332. <https://doi.org/10.1111/jam.12804>.
- [118] S. Bhaduri, N. Debnath, S. Mitra, Y. Liu, A. Kumar, Microbiologically induced calcite precipitation mediated by *sporosarcina pasteurii*, *Journal of Visualized Experiments* 2016 (2016). <https://doi.org/10.3791/53253>.

- [119] B.M. Mortensen, M.J. Haber, J.T. DeJong, L.F. Caslake, D.C. Nelson, Effects of environmental factors on microbial induced calcium carbonate precipitation, *J Appl Microbiol* 111 (2011) 338–349. <https://doi.org/10.1111/j.1365-2672.2011.05065.x>.
- [120] D.J. Tobler, M.O. Cuthbert, R.B. Greswell, M.S. Riley, J.C. Renshaw, S. Handley-Sidhu, V.R. Phoenix, Comparison of rates of ureolysis between *Sporosarcina pasteurii* and an indigenous groundwater community under conditions required to precipitate large volumes of calcite, *Geochim Cosmochim Acta* 75 (2011) 3290–3301. <https://doi.org/10.1016/j.gca.2011.03.023>.
- [121] N.K. Prajapati, A.K. Agnihotri, N. Basak, Microbial induced calcite precipitation (MICP) a sustainable technique for stabilization of soil: A review, in: *Mater Today Proc*, Elsevier Ltd, 2023: pp. 357–361. <https://doi.org/10.1016/j.matpr.2023.07.303>.
- [122] G.D.O. Okwadha, J. Li, Optimum conditions for microbial carbonate precipitation, *Chemosphere* 81 (2010) 1143–1148. <https://doi.org/10.1016/j.chemosphere.2010.09.066>.
- [123] A.C. Mitchell, E.J. Espinosa-Ortiz, S.L. Parks, A.J. Phillips, A.B. Cunningham, R. Gerlach, Kinetics of calcite precipitation by ureolytic bacteria under aerobic and anaerobic conditions, *Biogeosciences* 16 (2019) 2147–2161. <https://doi.org/10.5194/bg-16-2147-2019>.
- [124] D.J. Skorupa, A. Akyel, M.W. Fields, R. Gerlach, Facultative and anaerobic consortia of haloalkaliphilic ureolytic micro-organisms capable of precipitating calcium carbonate, *J Appl Microbiol* 127 (2019) 1479–1489. <https://doi.org/10.1111/jam.14384>.
- [125] C. Liu, X. Xu, Z. Lv, L. Xing, Self-healing of Concrete Cracks by Immobilizing Microorganisms in Recycled Aggregate, *Journal of Advanced Concrete Technology* 18 (2020) 168–178. <https://doi.org/10.3151/jact.18.168>.
- [126] J. Xu, X. Wang, Self-healing of concrete cracks by use of bacteria-containing low alkali cementitious material, *Constr Build Mater* 167 (2018) 1–14. <https://doi.org/10.1016/j.conbuildmat.2018.02.020>.

- [127] F.B. da Silva, N. De Belie, N. Boon, W. Verstraete, Production of non-axenic ureolytic spores for self-healing concrete applications, *Constr Build Mater* 93 (2015) 1034–1041. <https://doi.org/10.1016/j.conbuildmat.2015.05.049>.
- [128] S. Al-Thawadi, R. Cord-Ruwisch, A. Info, Calcium Carbonate Crystals Formation by Ureolytic Bacteria Isolated from Australian Soil and Sludge, *Journal of Advanced Science and Engineering Research* 2 (2012) 12–26. <https://www.researchgate.net/publication/230603445>.
- [129] J.Y. Wang, D. Snoeck, S. Van Vlierberghe, W. Verstraete, N. De Belie, Application of hydrogel encapsulated carbonate precipitating bacteria for approaching a realistic self-healing in concrete, *Constr Build Mater* 68 (2014) 110–119. <https://doi.org/10.1016/j.conbuildmat.2014.06.018>.
- [130] X. Zhu, A. Mignon, S.D. Nielsen, S.E. Zieger, K. Koren, N. Boon, N. De Belie, Viability determination of *Bacillus sphaericus* after encapsulation in hydrogel for self-healing concrete via microcalorimetry and in situ oxygen concentration measurements, *Cem Concr Compos* 119 (2021). <https://doi.org/10.1016/j.cemconcomp.2021.104006>.
- [131] R. Biermann, S. Beutel, Endospore production of *Bacillus* spp. for industrial use, *Eng Life Sci* 23 (2023). <https://doi.org/10.1002/elsc.202300013>.
- [132] T. Abee, M.N. Groot, M. Tempelaars, M. Zwietering, R. Moezelaar, M. van der Voort, Germination and outgrowth of spores of *Bacillus cereus* group members: Diversity and role of germinant receptors, *Food Microbiol* 28 (2011) 199–208. <https://doi.org/10.1016/j.fm.2010.03.015>.
- [133] T.F. El-Arabi, M.W. Griffiths, *Bacillus cereus*, in: *Foodborne Infections and Intoxications*, Elsevier, 2021: pp. 431–437. <https://doi.org/10.1016/B978-0-12-819519-2.00011-6>.
- [134] L. Delbrassinne, J. Mahillon, *Bacillus*: Occurrence, in: *Encyclopedia of Food and Health*, Elsevier, 2016: pp. 307–311. <https://doi.org/10.1016/B978-0-12-384947-2.00050-7>.
- [135] K. Nagler, P. Setlow, K. Reineke, A. Driks, R. Moeller, Involvement of Coat Proteins in *Bacillus subtilis* Spore Germination in High-Salinity Environments,

Appl Environ Microbiol 81 (2015) 6725–6735.
<https://doi.org/10.1128/AEM.01817-15>.

- [136] S.A. Kadapure, U.B. Deshannavar, B.G. Katageri, P.S. Kadapure, A systematic review on MICP technique for developing sustainability in concrete, *European Journal of Environmental and Civil Engineering* 27 (2023) 4581–4597. <https://doi.org/10.1080/19648189.2023.2194942>.
- [137] R. Marrollo, *Microbiology of Bacillus cereus*, in: *The Diverse Faces of Bacillus Cereus*, Elsevier, 2016: pp. 1–13. <https://doi.org/10.1016/B978-0-12-801474-5.00001-3>.
- [138] S.-G. Choi, I. Chang, M. Lee, J.-H. Lee, J.-T. Han, T.-H. Kwon, Review on geotechnical engineering properties of sands treated by microbially induced calcium carbonate precipitation (MICP) and biopolymers, *Constr Build Mater* 246 (2020) 118415. <https://doi.org/10.1016/j.conbuildmat.2020.118415>.
- [139] N. Shaheen, R.A. Khushnood, W. Khaliq, H. Murtaza, R. Iqbal, M.H. Khan, Synthesis and characterization of bio-immobilized nano/micro inert and reactive additives for feasibility investigation in self-healing concrete, *Constr Build Mater* 226 (2019) 492–506. <https://doi.org/10.1016/j.conbuildmat.2019.07.202>.
- [140] S.C. Chuo, S.F. Mohamed, S.H.M. Setapar, A. Ahmad, M. Jawaid, W.A. Wani, A.A. Yaqoob, M.N.M. Ibrahim, Insights into the current trends in the utilization of bacteria for microbially induced calcium carbonate precipitation, *Materials* 13 (2020) 1–28. <https://doi.org/10.3390/ma13214993>.
- [141] W. Khaliq, M.B. Ehsan, Crack healing in concrete using various bio influenced self-healing techniques, *Constr Build Mater* 102 (2016) 349–357. <https://doi.org/10.1016/j.conbuildmat.2015.11.006>.
- [142] R.A. Khushnood, Z.A. Qureshi, N. Shaheen, S. Ali, Bio-mineralized self-healing recycled aggregate concrete for sustainable infrastructure, *Science of The Total Environment* 703 (2020) 135007. <https://doi.org/10.1016/j.scitotenv.2019.135007>.
- [143] S. Mondal, A. (Dey) Ghosh, Investigation into the optimal bacterial concentration for compressive strength enhancement of microbial concrete, *Constr Build Mater* 183 (2018) 202–214. <https://doi.org/10.1016/j.conbuildmat.2018.06.176>.

- [144] N.-J. Jiang, H. Yoshioka, K. Yamamoto, K. Soga, Ureolytic activities of a urease-producing bacterium and purified urease enzyme in the anoxic condition: Implication for subseafloor sand production control by microbially induced carbonate precipitation (MICP), *Ecol Eng* 90 (2016) 96–104. <https://doi.org/10.1016/j.ecoleng.2016.01.073>.
- [145] H.W. Kua, S. Gupta, A.N. Aday, W. V. Srubar, Biochar-immobilized bacteria and superabsorbent polymers enable self-healing of fiber-reinforced concrete after multiple damage cycles, *Cem Concr Compos* 100 (2019) 35–52. <https://doi.org/10.1016/j.cemconcomp.2019.03.017>.
- [146] J. Wang, A. Mignon, G. Trensou, S. Van Vlierberghe, N. Boon, N. De Belie, A chitosan based pH-responsive hydrogel for encapsulation of bacteria for self-sealing concrete, *Cem Concr Compos* 93 (2018) 309–322. <https://doi.org/10.1016/j.cemconcomp.2018.08.007>.
- [147] J.Y. Wang, N. De Belie, W. Verstraete, Diatomaceous earth as a protective vehicle for bacteria applied for self-healing concrete, *J Ind Microbiol Biotechnol* 39 (2012) 567–577. <https://doi.org/10.1007/s10295-011-1037-1>.
- [148] J.Y. Wang, H. Soens, W. Verstraete, N. De Belie, Self-healing concrete by use of microencapsulated bacterial spores, *Cem Concr Res* 56 (2014) 139–152. <https://doi.org/10.1016/j.cemconres.2013.11.009>.
- [149] J. Wang, J. Dewanckele, V. Cnudde, S. Van Vlierberghe, W. Verstraete, N. De Belie, X-ray computed tomography proof of bacterial-based self-healing in concrete, *Cem Concr Compos* 53 (2014) 289–304. <https://doi.org/10.1016/j.cemconcomp.2014.07.014>.
- [150] D. Martin, K. Dodds, B.T. Ngwenya, I.B. Butler, S.C. Elphick, Inhibition of *Sporosarcina pasteurii* under Anoxic Conditions: Implications for Subsurface Carbonate Precipitation and Remediation via Ureolysis, *Environ Sci Technol* 46 (2012) 8351–8355. <https://doi.org/10.1021/es3015875>.
- [151] L.A. van Paassen, C.M. Daza, M. Staal, D.Y. Sorokin, W. van der Zon, Mark.C.M. van Loosdrecht, Potential soil reinforcement by biological denitrification, *Ecol Eng* 36 (2010) 168–175. <https://doi.org/10.1016/j.ecoleng.2009.03.026>.

- [152] Y.Ç. Erşan, N. de Belie, N. Boon, Microbially induced CaCO₃ precipitation through denitrification: An optimization study in minimal nutrient environment, *Biochem Eng J* 101 (2015) 108–118. <https://doi.org/10.1016/j.bej.2015.05.006>.
- [153] Y.Ç. Erşan, E. Gruyaert, G. Louis, C. Lors, N. De Belie, N. Boon, Self-protected nitrate reducing culture for intrinsic repair of concrete cracks, *Front Microbiol* 6 (2015). <https://doi.org/10.3389/fmicb.2015.01228>.
- [154] Y.C. Ersan, *Microbial nitrate reduction induced autonomous self-healing in concrete*, 2016.
- [155] S.P. Diggle, M. Whiteley, *Microbe Profile: Pseudomonas aeruginosa: opportunistic pathogen and lab rat: This article is part of the Microbe Profiles collection.*, *Microbiology (N Y)* 166 (2020) 30–33. <https://doi.org/10.1099/mic.0.000860>.
- [156] S.W. Miranda, K.L. Asfahl, A.A. Dandekar, E.P. Greenberg, *Pseudomonas aeruginosa Quorum Sensing*, in: 2022: pp. 95–115. https://doi.org/10.1007/978-3-031-08491-1_4.
- [157] Y. Bai, X. Guo, Y. Li, T. Huang, Experimental and visual research on the microbial induced carbonate precipitation by *Pseudomonas aeruginosa*, *AMB Express* 7 (2017) 57. <https://doi.org/10.1186/s13568-017-0358-5>.
- [158] Y.Ç. Erşan, [Yusuf, C. Ersan, N. De Belie, N. Boon, Resilient Denitrifiers Wink at Microbial Self-Healing Concrete, *International Journal of Environmental Engineering-IJEE* 2 (2015). <https://www.researchgate.net/publication/271906572>.
- [159] M. Sonmez, Y.Ç. Erşan, Production and compatibility assessment of denitrifying biogranules tailored for self-healing concrete applications, *Cem Concr Compos* 126 (2022) 104344. <https://doi.org/10.1016/j.cemconcomp.2021.104344>.
- [160] G., M.M., T.I., Z.E., and S.C. Ranalli, *Bioremediation of cultural heritage: Removal of sulphates, nitrates and organic substances*, in: O. Ciferri, P. Tiano, G. Mastromei (Eds.), *Of Microbes and Art*, Springer US, 2000: pp. 231–245.
- [161] X. Li, D.L. Chopp, W.A. Russin, P.T. Brannon, M.R. Parsek, A.I. Packman, Spatial Patterns of Carbonate Biomineralization in Biofilms, *Appl Environ Microbiol* 81 (2015) 7403–7410. <https://doi.org/10.1128/AEM.01585-15>.

- [162] N. Hamdan, E. Kavazanjian, B.E. Rittmann, I. Karatas, Carbonate Mineral Precipitation for Soil Improvement Through Microbial Denitrification, *Geomicrobiol J* 34 (2017) 139–146. <https://doi.org/10.1080/01490451.2016.1154117>.
- [163] Z. Al Disi, E. Attia, M.I. Ahmad, N. Zouari, Immobilization of heavy metals by microbially induced carbonate precipitation using hydrocarbon-degrading ureolytic bacteria, *Biotechnology Reports* 35 (2022) e00747. <https://doi.org/10.1016/j.btre.2022.e00747>.
- [164] C.M.R. Graddy, M.G. Gomez, J.T. DeJong, D.C. Nelson, Native Bacterial Community Convergence in Augmented and Stimulated Ureolytic MICP Biocementation, *Environ Sci Technol* 55 (2021) 10784–10793. <https://doi.org/10.1021/acs.est.1c01520>.
- [165] W. De Muynck, K. Verbeken, N. De Belie, W. Verstraete, Influence of temperature on the effectiveness of a biogenic carbonate surface treatment for limestone conservation, *Appl Microbiol Biotechnol* 97 (2013) 1335–1347. <https://doi.org/10.1007/s00253-012-3997-0>.
- [166] F.B. Silva, Up-scaling the production of bacteria for self-healing concrete application, (2013).
- [167] V.S. Whiffin, Microbial CaCO₃ precipitation for the production of biocement, Murdoch University, 2004.
- [168] L. Cheng, R. Cord-Ruwisch, Upscaling Effects of Soil Improvement by Microbially Induced Calcite Precipitation by Surface Percolation, *Geomicrobiol J* 31 (2014) 396–406. <https://doi.org/10.1080/01490451.2013.836579>.
- [169] F.B. Silva, N. Boon, N. De Belie, W. Verstraete, Industrial Application of Biological Self-healing Concrete: Challenges and Economical Feasibility, *J Commer Biotechnol* 21 (2015). <https://doi.org/10.5912/jcb662>.
- [170] Silva F, ; Boon, ; Verstraete, P ublis he d b y: S out h A s i a n A c a d e m i c R e s e a r c h J o u r n a l s ACADEMICIA: THE INDUSTRIAL MARKETS OF SPORULATING BACTERIA, *ACADEMICIA The South Asian Academic Research Journals* 4 (2014) 2249–7137. <http://www.saarj.com><http://www.saarj.com>.

- [171] S.L. Williams, M.J. Kirisits, R.D. Ferron, Optimization of growth medium for *Sporosarcina pasteurii* in bio-based cement pastes to mitigate delay in hydration kinetics, *J Ind Microbiol Biotechnol* 43 (2016) 567–575. <https://doi.org/10.1007/s10295-015-1726-2>.
- [172] F. Wang, X. Jin, S. Yang, Y. Liu, X. Chen, A control strategy for promoting the stability of denitrifying granular sludge in upflow sludge blankets, *Environ Technol* 35 (2014) 52–59. <https://doi.org/10.1080/09593330.2013.808250>.
- [173] A.I. Omoregie, L.H. Ngu, D.E.L. Ong, P.M. Nissom, Low-cost cultivation of *Sporosarcina pasteurii* strain in food-grade yeast extract medium for microbially induced carbonate precipitation (MICP) application, *Biocatal Agric Biotechnol* 17 (2019) 247–255. <https://doi.org/10.1016/j.bcab.2018.11.030>.
- [174] V. Achal, A. Mukherjee, P.C. Basu, M.S. Reddy, Lactose mother liquor as an alternative nutrient source for microbial concrete production by *Sporosarcina pasteurii*, *J Ind Microbiol Biotechnol* 36 (2009) 433–438. <https://doi.org/10.1007/s10295-008-0514-7>.
- [175] N.S.A. Ali, K. Muda, M.F. Mohd Amin, M.Z.M. Najib, E.H. Ezechi, M.S.J. Darwish, Initialization, enhancement and mechanisms of aerobic granulation in wastewater treatment, *Sep Purif Technol* 260 (2021). <https://doi.org/10.1016/j.seppur.2020.118220>.
- [176] K. Chetty, S. Xie, Y. Song, T. McCarthy, U. Garbe, X. Li, G. Jiang, Self-healing bioconcrete based on non-axenic granules: A potential solution for concrete wastewater infrastructure, *Journal of Water Process Engineering* 42 (2021) 102139. <https://doi.org/10.1016/j.jwpe.2021.102139>.
- [177] Y. Tang, J. Xu, Application of microbial precipitation in self-healing concrete: A review on the protection strategies for bacteria, *Constr Build Mater* 306 (2021) 124950. <https://doi.org/10.1016/j.conbuildmat.2021.124950>.
- [178] J. Zhang, C. Zhao, A. Zhou, C. Yang, L. Zhao, Z. Li, Aragonite formation induced by open cultures of microbial consortia to heal cracks in concrete: Insights into healing mechanisms and crystal polymorphs, *Constr Build Mater* 224 (2019) 815–822. <https://doi.org/10.1016/j.conbuildmat.2019.07.129>.

- [179] M. Sonmez, H. Ilcan, B. Dundar, G. Yildirim, Y.C. Ersan, M. Sahmaran, The effect of chemical- versus microbial-induced calcium carbonate mineralization on the enhancement of fine recycled concrete aggregate: A comparative study, *Journal of Building Engineering* 44 (2021) 103316. <https://doi.org/10.1016/j.jobe.2021.103316>.
- [180] Y.C. Ersan, D. Palin, S.B. Yengec Tasdemir, K. Tasdemir, H.M. Jonkers, N. Boon, N. De Belie, Volume Fraction, Thickness, and Permeability of the Sealing Layer in Microbial Self-Healing Concrete Containing Biogranules, *Front Built Environ* 4 (2018). <https://doi.org/10.3389/fbuil.2018.00070>.
- [181] K. Chetty, T. McCarthy, F. Hai, S. Zhang, Y. Song, G. Jiang, Physiological suitability of sulfate-reducing granules for the development of bioconcrete, *Biotechnol Bioeng* 119 (2022) 2743–2756. <https://doi.org/10.1002/bit.28184>.
- [182] D. de la Broise, M. Ventura, L. Chauchat, M. Guerreiro, T. Michez, T. Vinet, N. Gautron, F. Le Grand, A. Bideau, N. Le Goïc, A. Bidault, C. Lambert, P. Soudant, Scale-Up to Pilot of a Non-Axenic Culture of Thraustochytrids Using Digestate from Methanization as Nitrogen Source, *Mar Drugs* 20 (2022) 499. <https://doi.org/10.3390/md20080499>.
- [183] M. Sonmez, Y.C. Ersan, Production of concrete compatible biogranules for self-healing concrete applications, *MATEC Web of Conferences* 289 (2019) 1002. <https://doi.org/10.1051/matecconf/201928901002>.
- [184] G. Yilmaz, R. Lemaire, J. Keller, Z. Yuan, Simultaneous nitrification, denitrification, and phosphorus removal from nutrient-rich industrial wastewater using granular sludge, *Biotechnol Bioeng* 100 (2008) 529–541. <https://doi.org/10.1002/bit.21774>.
- [185] J. Wang, X. Wang, Z. Zhao, J. Li, Organics and nitrogen removal and sludge stability in aerobic granular sludge membrane bioreactor, *Appl Microbiol Biotechnol* 79 (2008) 679–685. <https://doi.org/10.1007/s00253-008-1466-6>.
- [186] D. Gao, L. Liu, H. Liang, W.-M. Wu, Aerobic granular sludge: characterization, mechanism of granulation and application to wastewater treatment, *Crit Rev Biotechnol* 31 (2011) 137–152. <https://doi.org/10.3109/07388551.2010.497961>.

- [187] Y.Ç. Erşan, T.H. Erguder, The effects of aerobic/anoxic period sequence on aerobic granulation and COD/N treatment efficiency, *Bioresour Technol* 148 (2013) 149–156. <https://doi.org/10.1016/j.biortech.2013.08.096>.
- [188] J. De Vrieze, T. De Mulder, S. Matassa, J. Zhou, L.T. Angenent, N. Boon, W. Verstraete, Stochasticity in microbiology: managing unpredictability to reach the Sustainable Development Goals, *Microb Biotechnol* 13 (2020) 829–843. <https://doi.org/10.1111/1751-7915.13575>.
- [189] K. Milferstedt, J. Hamelin, C. Park, J. Jung, Y. Hwang, S.-K. Cho, K.-W. Jung, D.-H. Kim, Biogranules applied in environmental engineering, *Int J Hydrogen Energy* 42 (2017) 27801–27811. <https://doi.org/10.1016/j.ijhydene.2017.07.176>.
- [190] C.L. Amorim, M. Alves, P.M.L. Castro, I. Henriques, Bacterial community dynamics within an aerobic granular sludge reactor treating wastewater loaded with pharmaceuticals, *Ecotoxicol Environ Saf* 147 (2018) 905–912. <https://doi.org/10.1016/j.ecoenv.2017.09.060>.
- [191] T.H. Ergüder, G.N. Demirer, Investigation of granulation of a mixture of suspended anaerobic and aerobic cultures under alternating anaerobic/microaerobic/aerobic conditions, *Process Biochemistry* 40 (2005) 3732–3741. <https://doi.org/10.1016/j.procbio.2005.05.005>.
- [192] Y.-M. Zheng, H.-Q. Yu, S.-J. Liu, X.-Z. Liu, Formation and instability of aerobic granules under high organic loading conditions, *Chemosphere* 63 (2006) 1791–1800. <https://doi.org/10.1016/j.chemosphere.2005.08.055>.
- [193] Y.-C. Juang, S.S. Adav, D.-J. Lee, J.-Y. Lai, Biodiversity in aerobic granule membrane bioreactor at high organic loading rates, *Appl Microbiol Biotechnol* 85 (2009) 383–388. <https://doi.org/10.1007/s00253-009-2227-x>.
- [194] X. Li, Y. Li, H. Liu, Z. Hua, G. Du, J. Chen, Characteristics of aerobic biogranules from membrane bioreactor system, *J Memb Sci* 287 (2007) 294–299. <https://doi.org/10.1016/j.memsci.2006.11.005>.
- [195] K.-Y. Show, D.-J. Lee, J.-H. Tay, Aerobic Granulation: Advances and Challenges, *Appl Biochem Biotechnol* 167 (2012) 1622–1640. <https://doi.org/10.1007/s12010-012-9609-8>.

- [196] B. Arrojo, A. Mosquera-Corral, J.M. Garrido, R. Méndez, Aerobic granulation with industrial wastewater in sequencing batch reactors, *Water Res* 38 (2004) 3389–3399. <https://doi.org/10.1016/j.watres.2004.05.002>.
- [197] V.L. Pacheco, L. Bragagnolo, C. Reginatto, A. Thomé, Microbially Induced Calcite Precipitation (MICP): Review from an Engineering Perspective, *Geotechnical and Geological Engineering* (2022). <https://doi.org/10.1007/s10706-021-02041-1>.
- [198] J. Zhang, X. Shi, X. Chen, X. Huo, Z. Yu, Microbial-Induced Carbonate Precipitation: A Review on Influencing Factors and Applications, *Advances in Civil Engineering* 2021 (2021) 1–16. <https://doi.org/10.1155/2021/9974027>.
- [199] G. Kim, J. Kim, H. Youn, Effect of Temperature, pH, and Reaction Duration on Microbially Induced Calcite Precipitation, *Applied Sciences* 8 (2018) 1277. <https://doi.org/10.3390/app8081277>.
- [200] T. Yu, H. Souli, Y. Péchaud, J.-M. Fleureau, Optimizing protocols for microbial induced calcite precipitation (MICP) for soil improvement—a review, *European Journal of Environmental and Civil Engineering* 26 (2022) 2218–2233. <https://doi.org/10.1080/19648189.2020.1755370>.
- [201] M.P. Harkes, L.A. Van Paassen, J.L. Booster, V.S. Whiffin, M.C.M. Van Loosdrecht, Fixation and distribution of bacterial activity in sand to induce carbonate precipitation for ground reinforcement, *Ecol Eng* 36 (2010) 112–117. <https://doi.org/10.1016/j.ecoleng.2009.01.004>.
- [202] J. Tourney, B.T. Ngwenya, Bacterial extracellular polymeric substances (EPS) mediate CaCO₃ morphology and polymorphism, *Chem Geol* 262 (2009) 138–146. <https://doi.org/10.1016/j.chemgeo.2009.01.006>.
- [203] A.J. Phillips, R. Gerlach, E. Lauchnor, A.C. Mitchell, A.B. Cunningham, L. Spangler, Engineered applications of ureolytic biomineralization: A review, *Biofouling* 29 (2013) 715–733. <https://doi.org/10.1080/08927014.2013.796550>.
- [204] F.G. Ferris, V. Phoenix, Y. Fujita, R.W. Smith, Kinetics of calcite precipitation induced by ureolytic bacteria at 10 to 20°C in artificial groundwater, *Geochim Cosmochim Acta* 68 (2004) 1701–1710. [https://doi.org/10.1016/S0016-7037\(03\)00503-9](https://doi.org/10.1016/S0016-7037(03)00503-9).

- [205] Y. Yuan, Z. Yuan, Y. Xi, Z. Wen, H. Leilei, X. Defeng, H. Fuxing, Effect of Microbially Induced Carbonate Precipitation (MICP) in the Highly Saline Silty Soil of the Cold Plateau Area of the Qinghai-Tibetan Plateau, *KSCE Journal of Civil Engineering* 26 (2022) 4407–4418. <https://doi.org/10.1007/s12205-022-1695-8>.
- [206] E. Peng, X. Hu, Y. Chou, Y. Sheng, S. Liu, F. Zhou, J. Wu, W. Cao, Study of microbially-induced carbonate precipitation for improving coarse-grained salty soil, *J Clean Prod* 365 (2022). <https://doi.org/10.1016/j.jclepro.2022.132788>.
- [207] J. Do, T.-H. Kwon, Effect of Salt Water on the Process of Microbially Induced Carbonate Precipitation, in: *Geo-Congress 2022*, American Society of Civil Engineers, Reston, VA, 2022: pp. 318–325. <https://doi.org/10.1061/9780784484012.033>.
- [208] S. Liu, B. Dong, J. Yu, Y. Cai, X. Peng, X. Zhou, Effect of Different Mineralization Modes on Strengthening Calcareous Sand under Simulated Seawater Conditions, *Sustainability* 13 (2021) 8265. <https://doi.org/10.3390/su13158265>.
- [209] A.L. Ibarra-Villarreal, A. Gándara-Ledezma, A.D. Godoy-Flores, A. Herrera-Sepúlveda, A.M. Díaz-Rodríguez, F.I. Parra-Cota, S. de los Santos-Villalobos, Salt-tolerant *Bacillus* species as a promising strategy to mitigate the salinity stress in wheat (*Triticum turgidum* subsp. *durum*), *J Arid Environ* 186 (2021) 104399. <https://doi.org/10.1016/j.jaridenv.2020.104399>.
- [210] S. Fazelikia, S.A. Abtahi, M. Kargar, M. Jafarinaia, Microbial Induced Calcite Precipitation (MICP) Potential of Ureolytic *Bacillus* sp. Isolated from the Soil of Eroded Ecosystems for Stabilizing and Improving the Fertility of Eroded Soils, *Geomicrobiol J* 40 (2023) 569–581. <https://doi.org/10.1080/01490451.2023.2211077>.
- [211] S. Stocks-Fischer, J.K. Galinat, S.S. Bang, Microbiological precipitation of CaCO₃, *Soil Biol Biochem* 31 (1999) 1563–1571. [https://doi.org/10.1016/S0038-0717\(99\)00082-6](https://doi.org/10.1016/S0038-0717(99)00082-6).
- [212] S. Dupraz, M. Parmentier, B. Ménez, F. Guyot, Experimental and numerical modeling of bacterially induced pH increase and calcite precipitation in saline aquifers, *Chem Geol* 265 (2009) 44–53. <https://doi.org/10.1016/j.chemgeo.2009.05.003>.

- [213] J. Peng, T. Cao, J. He, D. Dai, Y. Tian, Improvement of Coral Sand With MICP Using Various Calcium Sources in Sea Water Environment, *Front Phys* 10 (2022). <https://doi.org/10.3389/fphy.2022.825409>.
- [214] Y. Zhang, H.X. Guo, X.H. Cheng, Influences of calcium sources on microbially induced carbonate precipitation in porous media, *Materials Research Innovations* 18 (2014) S2-79-S2-84. <https://doi.org/10.1179/1432891714Z.0000000000384>.
- [215] K. Şekercioğlu, ABSTRACT INVESTIGATION OF NICKEL RECOVERY BY BIOGRANULES TAILORED FOR METAL RECOVERY THROUGH BIOMINERALIZATION, n.d.
- [216] B. Ozbay, Complementing urea hydrolysis and nitrate reduction metabolisms to enhance microbial self-healing performance in cementitious composites, 2023.
- [217] Z. Basaran Bundur, M.J. Kirisits, R.D. Ferron, Biomineralized cement-based materials: Impact of inoculating vegetative bacterial cells on hydration and strength, *Cem Concr Res* 67 (2015) 237–245. <https://doi.org/10.1016/j.cemconres.2014.10.002>.
- [218] S. Botusharova, D. Gardner, M. Harbottle, Augmenting Microbially Induced Carbonate Precipitation of Soil with the Capability to Self-Heal, *Journal of Geotechnical and Geoenvironmental Engineering* 146 (2020). [https://doi.org/10.1061/\(asce\)gt.1943-5606.0002214](https://doi.org/10.1061/(asce)gt.1943-5606.0002214).
- [219] W., and M.J. Stumm, *Aquatic Chemistry, Chemical Equilibria and Rates in Natural Waters Environmental Science and Technology*, 3rd ed., Wiley, New York, USA, 1996.
- [220] <https://www.lenntech.com/composition-seawater.htm>, Composition of seawater- LennTech, *Water Cond. Purif. Mag.* (2024).
- [221] S.A.M. Al Dahaan, N. Al-Ansari, S. Knutsson, Influence of Groundwater Hypothetical Salts on Electrical Conductivity Total Dissolved Solids, *Engineering* 08 (2016) 823–830. <https://doi.org/10.4236/eng.2016.811074>.
- [222] Q. Zhang, X. Wang, P. Hou, W. Wan, R. Li, Y. Ren, Z. Ouyang, Quality and seasonal variation of rainwater harvested from concrete, asphalt, ceramic tile and green roofs in Chongqing, China, *J Environ Manage* 132 (2014) 178–187. <https://doi.org/10.1016/j.jenvman.2013.11.009>.

- [223] B. Tutmez, Z. Hatipoglu, U. Kaymak, Modelling electrical conductivity of groundwater using an adaptive neuro-fuzzy inference system, *Comput Geosci* 32 (2006) 421–433. <https://doi.org/10.1016/j.cageo.2005.07.003>.
- [224] P. Göbel, C. Dierkes, W.G. Coldewey, Storm water runoff concentration matrix for urban areas, *J Contam Hydrol* 91 (2007) 26–42. <https://doi.org/10.1016/j.jconhyd.2006.08.008>.
- [225] A. Bozdağ, G. Göçmez, Evaluation of groundwater quality in the Cihanbeyli basin, Konya, Central Anatolia, Turkey, *Environ Earth Sci* 69 (2013) 921–937. <https://doi.org/10.1007/s12665-012-1977-4>.
- [226] J. Wang, H. Mitrani, A. Wipat, P. Moreland, J. Haystead, M. Zhang, M.D. Robertson, A Numerical Bio-Geotechnical Model of Pressure-Responsive Microbially Induced Calcium Carbonate Precipitation, *Applied Sciences* 14 (2024) 2854. <https://doi.org/10.3390/app14072854>.
- [227] A.W. APHA, Standard Methods for Examination of water and wastewater, 22nd ed., APHA Press, Washington DC, 2012.
- [228] B. Kardogan, K. Sekercioglu, Y.Ç. Erşan, Compatibility and Biomineralization Oriented Optimization of Nutrient Content in Nitrate-Reducing-Biogranelles-Based Microbial Self-Healing Concrete, *Sustainability* 13 (2021) 8990. <https://doi.org/10.3390/su13168990>.
- [229] M. Li, X. Liao, D. Zhang, G. Du, J. Chen, Yeast Extract Promotes Cell Growth and Induces Production of Polyvinyl Alcohol-Degrading Enzymes, *Enzyme Res* 2011 (2011) 1–8. <https://doi.org/10.4061/2011/179819>.
- [230] M. Leclerc, L. Elfoul-Bensaid, A. Bernalier, Effect of Yeast Extract on Growth and Metabolism of H₂-Utilizing Acetogenic Bacteria from the Human Colon, *Curr Microbiol* 37 (1998) 166–171. <https://doi.org/10.1007/s002849900358>.
- [231] Y. Lv, C. Wan, X. Liu, Y. Zhang, D.-J. Lee, J.-H. Tay, Drying and re-cultivation of aerobic granules, *Bioresour Technol* 129 (2013) 700–703. <https://doi.org/10.1016/j.biortech.2012.12.178>.
- [232] H.-C. Xu, P.-J. He, G.-Z. Wang, G.-H. Yu, L.-M. Shao, Enhanced storage stability of aerobic granules seeded with pellets, *Bioresour Technol* 101 (2010) 8031–8037. <https://doi.org/10.1016/j.biortech.2010.05.062>.

- [233] B.Y.-P. Moy, J.-H. Tay, S.-K. Toh, Y. Liu, S.T.-L. Tay, High organic loading influences the physical characteristics of aerobic sludge granules, *Lett Appl Microbiol* 34 (2002) 407–412. <https://doi.org/10.1046/j.1472-765X.2002.01108.x>.
- [234] Y.Ç. Erşan, T.H. Erguder, The effect of seed sludge type on aerobic granulation via anoxic–aerobic operation, *Environ Technol* 35 (2014) 2928–2939. <https://doi.org/10.1080/09593330.2014.925513>.
- [235] Y. Liu, Q. Lai, M. Göker, J.P. Meier-Kolthoff, M. Wang, Y. Sun, L. Wang, Z. Shao, Genomic insights into the taxonomic status of the *Bacillus cereus* group, *Sci Rep* 5 (2015). <https://doi.org/10.1038/srep14082>.
- [236] K. Oliwa-Stasiak, C.I. Molnar, K. Arshak, M. Bartoszcze, C.C. Adley, Development of a PCR assay for identification of the *Bacillus cereus* group species, *J Appl Microbiol* 108 (2010) 266–273. <https://doi.org/10.1111/j.1365-2672.2009.04419.x>.
- [237] Y. Cui, E. Märtlbauer, R. Dietrich, H. Luo, S. Ding, K. Zhu, Multifaceted toxin profile, an approach toward a better understanding of probiotic *Bacillus cereus*, *Crit Rev Toxicol* 49 (2019) 342–356. <https://doi.org/10.1080/10408444.2019.1609410>.
- [238] M. Mols, T. Abee, Role of Ureolytic Activity in *Bacillus cereus* Nitrogen Metabolism and Acid Survival, *Appl Environ Microbiol* 74 (2008) 2370–2378. <https://doi.org/10.1128/AEM.02737-07>.
- [239] S. Maruthamuthu, P. Dhandapani, S. Kamalasekaran, A.S. Siddarth, S.P. Manoharan, K. Muthuraman, G. Narayanan, Role of ureolytic bacteria on corrosion behavior of fretted grade 880mild steel rail, *Eng Fail Anal* 33 (2013) 315–326. <https://doi.org/10.1016/j.engfailanal.2013.05.021>.
- [240] Y. Huang, M. Liang, S. Zhao, S. Chen, J. Liu, D. Liu, Y. Lu, Isolation, expression, and biochemical characterization: nitrite reductase from *Bacillus cereus* LJ01, *RSC Adv* 10 (2020) 37871–37882. <https://doi.org/10.1039/D0RA06129H>.
- [241] J. Dou, A. Ding, X. Liu, Y. Du, D. Deng, J. Wang, Anaerobic benzene biodegradation by a pure bacterial culture of *Bacillus cereus* under nitrate reducing conditions, *Journal of Environmental Sciences* 22 (2010) 709–715. [https://doi.org/10.1016/S1001-0742\(09\)60167-4](https://doi.org/10.1016/S1001-0742(09)60167-4).

- [242] E. Mekonnen, A. Kebede, A. Nigussie, G. Kebede, M. Tafesse, Isolation and Characterization of Urease-Producing Soil Bacteria, *Int J Microbiol* 2021 (2021) 1–11. <https://doi.org/10.1155/2021/8888641>.
- [243] T.S. Ghosh, S. Chatterjee, S.A. Azmi, A. Mazumdar, T.K. Dangar, Virulence assay and role of *Bacillus thuringiensis* TS110 as biocontrol agent against the larval stages of rice leafhopper *Cnaphalocrocis medinalis*, *Journal of Parasitic Diseases* 41 (2017) 491–495. <https://doi.org/10.1007/s12639-016-0835-9>.
- [244] Y. Liu, J. Du, Q. Lai, R. Zeng, D. Ye, J. Xu, Z. Shao, Proposal of nine novel species of the *Bacillus cereus* group, *Int J Syst Evol Microbiol* 67 (2017) 2499–2508. <https://doi.org/10.1099/ijsem.0.001821>.
- [245] M.-Y. Jung, W.K. Paek, I.-S. Park, J.-R. Han, Y. Sin, J. Paek, M.-S. Rhee, H. Kim, H.S. Song, Y.-H. Chang, *Bacillus gaemokensis* sp. nov., isolated from foreshore tidal flat sediment from the Yellow Sea, *The Journal of Microbiology* 48 (2010) 867–871. <https://doi.org/10.1007/s12275-010-0148-0>.
- [246] J. Zhang, D. Kumari, C. Fang, V. Achal, Combining the microbial calcite precipitation process with biochar in order to improve nickel remediation, *Applied Geochemistry* 103 (2019) 68–71. <https://doi.org/10.1016/j.apgeochem.2019.02.011>.
- [247] H.J. Kim, H.J. Eom, C. Park, J. Jung, B. Shin, W. Kim, N. Chung, I.-G. Choi, W. Park, Calcium Carbonate Precipitation by *Bacillus* and *Sporosarcina* Strains Isolated from Concrete and Analysis of the Bacterial Community of Concrete, *J Microbiol Biotechnol* 26 (2016) 540–548. <https://doi.org/10.4014/jmb.1511.11008>.
- [248] H. Do, Y. Wang, Z. Long, T. Ketehouli, X. Li, Z. Zhao, M. Li, A psychrotolerant Ni-resistant *Bacillus cereus* D2 induces carbonate precipitation of nickel at low temperature, *Ecotoxicol Environ Saf* 198 (2020) 110672. <https://doi.org/10.1016/j.ecoenv.2020.110672>.
- [249] V. Anitha, *Bacillus cereus* KLUVAA Mediated Biocement Production Using Hard Water and Urea, *Chem Biochem Eng Q* 32 (2018) 257–266. <https://doi.org/10.15255/CABEQ.2017.1096>.

- [250] N. Hosseini Balam, D. Mostofinejad, M. Eftekhari, Use of carbonate precipitating bacteria to reduce water absorption of aggregates, *Constr Build Mater* 141 (2017) 565–577. <https://doi.org/10.1016/j.conbuildmat.2017.03.042>.
- [251] A.M. Grabiec, J. Klama, D. Zawal, D. Krupa, Modification of recycled concrete aggregate by calcium carbonate biodeposition, *Constr Build Mater* 34 (2012) 145–150. <https://doi.org/10.1016/j.conbuildmat.2012.02.027>.
- [252] N. Chahal, R. Siddique, A. Rajor, Influence of bacteria on the compressive strength, water absorption and rapid chloride permeability of concrete incorporating silica fume, *Constr Build Mater* 37 (2012) 645–651. <https://doi.org/10.1016/j.conbuildmat.2012.07.029>.
- [253] A.I. Omoregie, E.A. Palombo, D.E.L. Ong, P.M. Nissom, A feasible scale-up production of *Sporosarcina pasteurii* using custom-built stirred tank reactor for in-situ soil biocementation, *Biocatal Agric Biotechnol* 24 (2020). <https://doi.org/10.1016/j.bcab.2020.101544>.
- [254] A.I. Omoregie, G. Khoshdelnezamiha, N. Senian, D.E.L. Ong, P.M. Nissom, Experimental optimisation of various cultural conditions on urease activity for isolated *Sporosarcina pasteurii* strains and evaluation of their biocement potentials, *Ecol Eng* 109 (2017) 65–75. <https://doi.org/10.1016/j.ecoleng.2017.09.012>.
- [255] S. Jain, D.N. Arnepalli, Biochemically Induced Carbonate Precipitation in Aerobic and Anaerobic Environments by *Sporosarcina pasteurii*, *Geomicrobiol J* 36 (2019) 443–451. <https://doi.org/10.1080/01490451.2019.1569180>.
- [256] H. Behzadipour, A. Sadrekarimi, Biochar-assisted bio-cementation of a sand using native bacteria, (n.d.). <https://doi.org/10.1007/s10064-021-02235-0/Published>.
- [257] L. Line, M. Alhede, M. Kolpen, M. Kähler, O. Ciofu, T. Bjarnsholt, C. Moser, M. Toyofuku, N. Nomura, N. Håiby, P.Å. Jensen, Physiological levels of nitrate support anoxic growth by denitrification of *Pseudomonas aeruginosa* at growth rates reported in cystic fibrosis lungs and sputum, *Front Microbiol* 5 (2014). <https://doi.org/10.3389/fmicb.2014.00554>.
- [258] S. Vučetić, D. Čjepa, B. Miljević, J.M. van der Bergh, O. Šovljanski, A. Tomić, E. Nikolić, S. Markov, H. Hiršenberger, J. Ranogajec, Bio-Stimulated Surface

- Healing of Historical and Compatible Conservation Mortars, *Materials* 16 (2023) 642. <https://doi.org/10.3390/ma16020642>.
- [259] D. Pei, Z. Liu, W. Wu, B. Hu, Transcriptome analyses reveal the utilization of nitrogen sources and related metabolic mechanisms of *Sporosarcina pasteurii*, *PLoS One* 16 (2021). <https://doi.org/10.1371/journal.pone.0246818>.
- [260] L. Li, T. Liu, G. Jiang, C. Fang, B. Qu, S. Zheng, G. Yang, C. Tang, Insight into the temperature stimulation on the self-healing properties of cement-based materials, *Constr Build Mater* 361 (2022) 129704. <https://doi.org/10.1016/j.conbuildmat.2022.129704>.
- [261] Z. Wang, W. Chen, Z. Tong, W. Wu, X. Chen, X. Deng, Y. Xie, Research on the Effect of Natural Seawater in Domesticating *Bacillus pasteurii* and Reinforcing Calcareous Sand, *J Mar Sci Eng* 12 (2024) 542. <https://doi.org/10.3390/jmse12040542>.
- [262] C., and S.J. Glass, Denitrification of high-nitrate, high-salinity wastewater, *Water Res.* (1999) 223–229.
- [263] H. Nguyen Thi Minh, J.-M. Perrier-Cornet, P. Gervais, Effect of the osmotic conditions during sporulation on the subsequent resistance of bacterial spores, *Appl Microbiol Biotechnol* 80 (2008) 107. <https://doi.org/10.1007/s00253-008-1519-x>.

APPENDIX

ANNEX 1 – Publications Derived from The Thesis (Conference Paper)

Suluk M., Kardođan B., and Erřan Y. . (2022). "Biogranules Simultaneously Hydrolysing Urea and Reducing Nitrate and Their Biomineralization Performance." 6th Eurasia Waste Management Symposium, İstanbul, Türkiye, pp.665-672.